Aspects of Topology in Quantum Phases of Matter:
A Journey through Lands both Flat and Not

by

Abhinav Prem

B.S., University of Southern California, 2013

B.A., University of Southern California, 2013

M.S., University of Colorado Boulder, 2015

A thesis submitted to the

Faculty of the Graduate School of the

University of Colorado in partial fulfillment

of the requirements for the degree of

Doctor of Philosophy

Department of Physics

2018

This thesis entitled:
Aspects of Topology in Quantum Phases of Matter:
A Journey through Lands both Flat and Not
written by Abhinav Prem
has been approved for the Department of Physics

_____

Prof. Victor Gurarie

_____

Prof. Rahul Nandkishore

Date _____

The final copy of this thesis has been examined by the signatories, and we find that both the
content and the form meet acceptable presentation standards of scholarly work in the above
mentioned discipline.

Prem, Abhinav (Ph.D., Physics)

Aspects of Topology in Quantum Phases of Matter:

　A Journey through Lands both Flat and Not

Thesis directed by Prof. Victor Gurarie

Topological quantum phases of matter are often characterized by the presence of fractionalized quasiparticles, which exhibit non-trivial braiding statistics or carry fractional quantum numbers, or of protected gapless surface states. In this thesis, we study topological phases in two and three spatial dimensions, from the perspective of searching for new exotic quantum phases and of characterizing their experimental signatures.

We first study topological defects in fermionic paired superfluids and discover that in the presence of a multiply quantized vortex, such a state hosts unpaired fermions in the BCS regime. We predict that these unpaired fermions will result in an experimentally measurable deviation of the system's angular momentum from its value in the BEC regime. Focusing on two-dimensions, we then study superconductors coupled to dynamically fluctuating electromagnetism, and establish a universal framework for studying the low-energy physics of such systems. We derive topological field theories describing all spin-singlet superconductors which naturally capture the interplay of symmetry and topology in these gapped states.

The remainder of this thesis is focused on a novel class of long-range entangled states of matter, known as "fracton" phases, in both two– and three-dimensions. These phases exhibit an intriguing phenomenology, most surprising of which is the presence of excitations which are immobile in isolation. Studying the non-equilibrium dynamics of gapped fracton phases, we discover that they naturally exhibit glassy quantum dynamics in the absence of quenched disorder, and hence may have potential technological applications as robust quantum memories. Finally, we conclude with a description of fracton phases as higher-rank tensor gauge theories and discuss the emergent phases of matter in which a finite density of fractons or their bound states may exist.

To my parents,

for never warning me about getting lost in libraries,

and to $\mathcal{K}$,

for petrichoral waundrings.

Acknowledgements

"Thou shalt not do as the dean pleases,

Thou shalt not write thy doctor's thesis."

—W. H. Auden, *Under Which Lyre*

It is a pleasure to thank the many people who have made the past decade an absolute joy and without whose support each of the following pages would have been intentionally left blank.

It has been my exceedingly good fortune to have had Victor Gurarie as my advisor, the extent of which is clear only in retrospect. My sensibilities as a physicist have been profoundly shaped by his insightful guidance and by the extraordinary time and care he has invested in my development. Working with Victor is always enjoyable and inspiring, and he has been a constant source of encouragement. His remarkable ability to tease out the essential physics from seemingly mundane calculations, and to explain complicated phenomena clearly, have constantly pushed me to expand the boundaries of my understanding. Victor has something interesting and unexpected to say about almost anything (be it physics, politics, or life in general) with keen insight and wit, which has made for many engaging hours at the blackboard. I am deeply indebted to Victor for his advice and counsel through the years, and I am grateful that he knew when to leave me to my own devices, and even more so that he sensed when I could not.

I have been fortunate to have spent most of my academic life in a place where sauntering up to the 6th floor deposits one at the doorsteps of the finest mentors one could hope for. I am especially grateful to Rahul Nandkishore for working closely with me over the past few years. Rahul's clarity of thought and his uncanny ability to identify exciting new ideas is truly extraordinary and has

deeply impacted my approach to physics. I am also extremely grateful to him for introducing me to fractons and for being more patient with me than I deserved as I floundered my way through our first project together; working with him gave me the courage to be curious about problems in which I had no particular expertise. I am incredibly lucky to have had the opportunity to work with Leo Radzihovsky, whose knack for cutting through superfluous mathematical distractions and quickly arriving at key insights has imbued in me the sense that much can often be said about a system on general grounds. It has been an equally invaluable learning experience working with Mike Hermele, with whom each conversation seems to broaden my knowledge. The care and precision with which he discusses physics is truly remarkable and has indubitably helped me mature scientifically. I cannot overstate the extent to which I am thankful to Victor, Rahul, Leo, and Mike for always having their doors open for discussions of physics (amongst other things!) and for treating me like an adult physicist when I was probably little more than an adolescent.

Half of the work presented in this thesis stems from collaborations with Sergej Moroz, from whom I have learned most of what I know about superfluids and superconductors, and whose care and attention to detail is truly aspirational. Much of my appreciation for the balance between elegant mathematics and physical systems comes from Sergej, and I also thank him for inviting me to München in what turned out to be a fun and productive week. Michael Pretko has been a wellspring of enthusiasm and brilliant ideas over the past year, and has informed much of how I now think about gapless topological phases. I am also grateful to Jeongwan Haah for his lucid elucidation of the Cubic Code, which led to one of the results contained in this thesis.

I am equally grateful for ongoing collaborations not documented in this thesis. Sheng-Jie Huang, my officemate of four years, has been especially generous with his time and conversations with him have taught me much about topologically ordered phases. Our many discussions have contributed greatly to my understanding and I am also grateful to him for instantly alleviating all of my trivial confusions and for tolerating all of my distracting questions over this long period! I remain in awe of Hao Song's mathematical prowess and thank him for his patience in explaining his truly elegant framework for studying non-Abelian fractons. Yang-Zhi Chou has been a dependable

resource of knowledge for all matters non-fractonic, and despite his best protestations, fractonic.

I would be remiss to not thank those from whom I've learned much about condensed matter physics and with whom I've had many valuable discussions. While I cannot possibly thank all those from whose insights I've benefited, even the most partial of such lists must include Sarang Gopalakrishnan, Vadim Oganesyan, and Rahul Roy. I will be forever indebted to them for their generosity in sponsoring my post-doctoral applications and for taking a genuine interest in my work. I have likewise learned much from my conversations with Victor Albert, Jason Alicea, Barry Bradlyn, Daniel Bulmash, Jennifer Cano, Xie Chen, Trithep Devakul, Andrey Gromov, Fenner Harper, David Huse, Vedika Khemani, Wilbur Shirley, Kevin Slagle, Shivaji Sondhi, Ryan Thorngren, Sagar Vijay, and Yizhi You.

The physics department at Boulder has been a stimulating environment thanks to the many current and previous members of the condensed matter group and of CTQM, including Dan Hackett, Yi-Ping Huang, Han Ma, Karl Mayer, Albert Schmitz, and Xiao Yin. Thanks are also due to Oliver DeWolfe and Ana Maria Rey for serving on my Comps III committee, and to Tom DeGrand for his fantastic graduate quantum courses. I am also grateful to Prof. Markus Pflaum for serving on my thesis committee and agreeing to read the following many pages. I would like to thank the administrators who've made dealing with bureaucratic matters as painless as possible: Jeanne Nijhowne, Jason Hopkins, and Kirsten Apodaca. I would also like to acknowledge my funding sources over the course of my graduate career, without whom many of my experiences would not have been possible: the University of Colorado Boulder and the Center for Theory of Quantum Matter; the National Science Foundation through grants to Victor Gurarie; and the Sloan Foundation and the U.S. Air Force Office of Sponsored Research through grants to Rahul Nandkishore.

I owe a great deal to my undergraduate professors: To Gene Bickers, to whom a paean is in order but is beyond my abilities. Suffice it to say that I would not be a physicist if not for his course on mechanics. To Vitaly Kresin, my undergraduate advisor, who taught me how to be a physicist and whose support and encouragement convinced me to pursue research. And to Clifford Johnson, for showing me that a physicist needn't be just that. Also to David Treuer, Aimee Bender, and
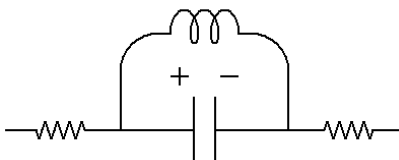
Susan Segal, for teaching me to read, write, and re-write.

Now for those whose friendship has helped retain any remnants of sanity which remain towards the end of my time in Boulder. I cannot imagine how I would have managed without my weekly lunches with Will Jay, which have been a constant source of enjoyable discussions on things literary, cinematic, and often, philosophical. Being able to knock on his door and reliably have my questions on abstract mathematics answered has been a privilege. Annie Jay's baked goods have likewise sustained me through many a long week. Raghavendra Srinivas has been the greatest of accomplices in cheering loudly while watching tennis. My house mates—William Cairncross, Allison Duh, Pattilyn McLaughlin, Helen Strnad, and Luna—have been a constant source of company, rides to Trader Joes, board games, and all around good cheer. I thank them for indulging in all of my shenanigans.

To all purveyors of caffeine, who understand that drinking two cups of coffee daily is vital to any intellectual endeavour, and of sugar, which is nothing if not granular happiness, I say thank you. The same goes for Vivian Darkbloom and Kilgore Trout, those finest of writers.

Above all else, I am grateful to my family: mother, father, sister, Beagle. My sister Shreya is a constant source of inspiration and is responsible for all the (amazing!) non-scientific figures in this thesis. My parents, Archana and Sunil, explained everything to me before I learned how to learn and taught me to try again, fail again, fail better, and most of all, to read.

Finally, I remain ineffably grateful to Katie, who has all this while been holding the universe together, and without whom this wouldn't quite matter as much.

This thesis is brought to you by Kilroy who, as always, was here.

Contents

Tables

Table

Figures

Figure

Prologue

know the place for the first time," as V became fond of saying in her later years. Unbeknownst to most, concurrent with the events recounted in A. Square's memoir *Flatland* [1]—for which he was imprisoned under the false pretext of heresy—another challenge to the cultural hegemony was emerging. It began with Vera Ball Stevens (or V), who, keen of mind and intent on escaping Flatland's Code, embarked on a voyage. Her reasoning was simple—since Flatland was unbounded, a realm without end, eventually she would reach the hinterlands, beyond the purview of the Code. Before starting, she tied one end of a long elastic rope to her house so as to leave behind a trail in case she ever decided to return. Since this is not an account of her long and arduous journey, we travel forwards in time to when she found herself back at her house. Convinced she had followed a straight path throughout, her bewilderment soon gave way to the conviction that she was living on a closed surface. Armed with this startling revelation, V put together a team, with whom she devised a series of tests designed to unearth the nature of this surface. They found that no matter how much they wiggled V's rope (keeping the two ends fixed to her house), they could not reel it in, proving they were not living on a 2-sphere. They then connected each (two-dimensional) tree with rope, with each tree forming the vertex of a triangle, to find that # Trees + # Triangles - # Pieces of Rope used = 0, firm evidence that Flatland was a torus. Thus began an unprecedented age of enlightenment, leading eventually to the formation of the Republic of Flatland. This is an account of the years following that eventful chapter in Flatland's history, in which we follow the attempts of Benny Square to follow in the footsteps of his academic ancestor.

Caveat Lector: This thesis satisfies periodic boundary conditions.

Chapter 1

Introduction: *Flatland* in the Global Era

In which Benny Square,

having mastered theorems egregious,

discovers his degenerate twins.

Consider the following sentence from Thomas Pynchon's *Gravity's Rainbow*:

"Decisions are never really made—at best they manage to emerge,

from a chaos of peeves, whims, and hallucinations."

Broken into its most fundamental constituents, this sentence is comprised of 53 consonants, 38 vowels, and 5 punctuations. Taking a reductionist's point of view, in which the behaviour of all complex structures can be inferred from their fundamental building blocks, we should then be able to recreate all aspects of this particular sentence simply by knowing the rules governing letters and how they combine (interact) to form words. While this is sufficient information for us to understand how the word "emerge" forms from the letters e, m, e, r, g, and e, in order to reproduce the entire sentence we require a new set of rules—those governing words. We are thus examining the sentence at a larger scale now, one at which the rules governing letters cease to be relevant and at which it is more instructive to think not in terms of the fundamental constituents, but rather a different set of objects—in this case, words. In this sense, the semantic information contained within a sentence emerges from the words and sounds contained within it, and on their organisation in relation to each other. Even though the sentence may be broken into its fundamental parts, taken as a whole

it contains more information than those parts combined; there is a rhythm to the sentence that would be lost when described in reductionist terms[1] .

If literature isn't quite your speed, consider as Laughlin does (in *A Different Universe* [3]) a painting by your favourite French impressionist. While "daubs of paint" comprising the painting lack any structure, the painting remains interesting as a whole; like Pynchon's sentence, its essence is its organization. Or take for instance the biological complexity of living organisms, once thought to be encoded entirely in DNA. Instead, as it turns out, DNA does not encode emergent properties, which instead switch on at the scale of proteins[2] .

At first glance, it would appear that physics at the very least would take kindly to a reductionist point of view, since much of the 20th century played witness to a remarkable number of developments: in the understanding of elementary particles and their interactions with light, the structure of atoms and molecules, and most spectacularly, the development of the Standard Model, which provides a unified framework for all forces excluding gravity. Quantum electrodynamics, which codifies interactions between light and matter by marrying together quantum mechanics and special relativity, allows one to calculate to astonishing precision the properties of elementary particles or small groups thereof, remaining to this day the most quantitatively accurate theory ever developed.

In our every day lives, however, one simply does not encounter the elementary particles governed by the principles of quantum mechanics—developed by Heisenberg, Schrödinger, Dirac, Pauli, amongst others—or of quantum electrodynamics, or the massive astrophysical objects governed by Einstein's theory of General Relativity. Instead, we are faced with macroscopic objects comprised of a truly enormous number of interacting particles[3] . Yet, given how well our current understanding of the laws governing the fundamental particles and their interactions seems to work, deciphering the behaviour of electrons interacting in a crystal shouldn't really be that complicated. In fact,

---

[1] In philosophical circles, a great deal has been made about the distinction between weak and strong emergence [2], with this linguistic example displaying the former. Such distinctions have no place in this thesis.

[2] This is a relief for the author, who was dismayed on learning that a tomato possesses more genes than him.

[3] For context, the number of electrons in a copper penny $\sim 10^{24}$ while the number of stars in the Milky Way galaxy $\sim 10^{11}$.

taking a reductionist point of view, the study of anything that doesn't inform the study of the "fundamental" laws is merely "applied" physics as once the fundamental laws governing the fundamental constituents are known, we have established a theory governing all known things. So the laws governing electrons beget the laws governing many-body physics and thermodynamics beget the laws of chemistry beget the laws of molecular biology and so proceed *ad infinitum*. All one has to do then is to feed the fundamental laws into a computer, wait for the desired computation to finish running, and call it a night.

Thus Spake Anderson

There is much that is appealing about reductionism; after all, it seems to fit well with our everyday experiences. Fortunately, common sense does not provide a blueprint for how nature seems to behave. One obvious problem with a reductionist approach has to do with the limits of human comprehension and of computational power, and with the inherent complexity of quantum mechanics. Suppose we wish to simulate a system comprised of n quantum mechanical particles, each of which can be in one of two states, such as the spin of an electron or the polarization of a photon. The dimension of the total Hilbert space for such a system is 2^n, such that each state of the system is described by a 2^n-dimensional vector. In other words, the number of classical bits required simply to store a single state is 2^n while to implement any unitary operations on this state would require storing a matrix with 2^{2n} elements. With a classical computer made up of every atom in the universe, we would still not be able to store a single state, let alone operate on it, when $n = 100$. There are $\sim 10^{23}$ electrons in a macroscopic solid and therein lies the inherent difficulty of taking a reductionist approach for studying many-particle systems. Even if some higher dimensional beings could, in principle, compute on these gigantic Hilbert spaces and provide us with a solution, the limits of human cognition would render any such solution incomprehensible. Even in the event that we could fathom these large dimensional Hilbert spaces, it is unclear how much, if any, physical insight could be gleaned from such a perspective. Besides, such an inefficient description of nature seems unsatisfying, especially when physics at smaller scales tends to admit

elegant mathematical descriptions.

Where does this leave those of us who are wont to study condensed matter physics, a field whose primary goal is, broadly, understanding the organizational principles underlying the collective behaviour of complex assemblies of particles? Thankfully, contrary to what that ancient philosopher Democritus would have you believe, the truth is emphatically not all atoms and the void. Instead, the modern point of view, espoused by most physicists today and encapsulated by the title of Phil Anderson's beautiful article, is that "More is Different" [4]. The underlying concept behind this is that of *emergence*, the idea that the "whole becomes not merely more, but very different from the sum of its parts [4]". In other words, in systems with large numbers of degrees of freedom interacting with each other, complex collective behaviour may arise from the constituent parts, often leading to qualitatively new phenomena at macroscopic scales.

$$\text{Scale} + \text{Complexity} = \text{Emergence}.$$

At these larger scales, new degrees of freedom emerge which obey their own set of rules, which often look drastically different from those obeyed by the microscopic degrees of freedom. In terms of these emergent degrees of freedom, the system often admits a simple description, with the macroscopic behaviour governed by a simple set of rules. All this despite the seemingly insurmountable complexity of a many-body system!

The simplest example of a complex system admitting a simple description in terms of emergent quantities is that of liquid water. There is no real sense in which we can associate a notion of fluidity with single molecule of H_2O or of viscosity, and yet, these are terms one regularly uses when describing the behaviour of a macroscopic number of these molecules, which are violently colliding with each other. The key insight from emergence here is to coarse-grain away the complicated behaviour of the microscopic molecules and to instead focus on macroscopic quantities, described by averaging over large numbers of molecules. The appropriate quantity in this context is the average velocity field, which obeys the Navier-Stokes equation. In this sense, we can describe the macroscopic behaviour of water through a set of *effective* hydrodynamic rules governing the

continuous fluid into which the molecules have collectively organised. Such an effective description allows us to capture phenomenon such as viscosity, turbulence, and vorticity, which were invisible at the scale of individual water molecules.

This coarse-graining procedure is behind one of the most profound ideas of modern physics— the renormalisation group (RG) approach developed by Wilson [5] and others (see [6] for an excellent review). RG encodes the notion of coarse-graining in a precise sense, providing insights into why, at large distance scales, complex microscopic behaviour gives way to relatively simple macroscopic systems, which can only behave in ways determined by the fixed points of the RG flow. Studying these RG flows and their fixed points has proven to be one of most powerful methods for investigating phases of matter and the transitions between them. Within this framework, effective field theoretic descriptions of complex interacting systems emerge from the collective behaviour of large numbers of degrees of freedom, leading to phenomena which are not manifest in the rules governing the fundamental constituents of the system. These effective descriptions provide simple models defined in terms of the relevant degrees of freedom at low energies, allowing us to delineate the key features governing that system.

Leapfrogging from Landau ...

While water provided a simple and familiar example for understanding the nature of emergence in many-body systems, there is another familiar phase of matter which, unlike liquid water, is governed by the principles of quantum mechanics—the metallic state. Electrons, being fermions, obey the Pauli exclusion principle which prohibits any two electrons from occupying the same quantum mechanical state. In a metal, the microscopic degrees of freedom are the conduction electrons, which are forced to occupy higher and higher energy levels sequentially, forming a Fermi sea at low temperatures. When interactions between the electrons are weak, only the states near the Fermi surface are affected, leaving us with a simple description of the metallic state.

In cases when the interactions between the constituent electrons are strong compared to their kinetic energy, one would naïvely expect that the emergent macroscopic properties would be

significantly altered from the non-interacting Fermi sea of electrons. Remarkably, the properties of such systems are experimentally found to closely resemble those of non-interacting electrons. This seeming discrepancy is resolved by Landau's celebrated Fermi liquid theory [7], wherein the macroscopic properties of such materials are described in terms of weakly interacting quasi-particles, which behave much in the way that electrons do (albeit with an effective mass which may differ from an electron's by several orders of magnitude). A quasi-particle may be thought of as an electron dressed by the quantum fluctuations of its neighbouring electrons, allowing us to effectively describe the system of strongly interacting electrons as one of weakly interacting quasi-particles with Fermi liquid behaviour.

An even more striking example of emergent phenomena is that of spontaneous symmetry breaking, amongst the most important concepts in the physics of many-body systems. The fundamental laws governing elementary particles have a high degree of symmetry, being invariant under translations, rotations, reflections, and time-reversal amongst others. Yet, many of the macroscopic structures we encounter every day break these symmetries. Ice, the solid phase of water, breaks translational and rotational symmetries. Similarly, crystals break the continuous translational symmetry of space. As it turns out, most of the well-known phases in condensed matter physics, such as superconductivity, magnetism, and Bose-Einstein condensation, are explained by the fact that the thermal or ground state of the system does not obey its full symmetry.

Strictly speaking, spontaneous symmetry breaking (SSB) is only well defined in the thermodynamic limit i.e. a system can only break a symmetry spontaneously when the number of constituent particles becomes infinite. It is in this sense that SSB is an emergent phenomenon, since it does not occur for any system with finite degrees of freedom but emerges in the macroscopic limit. A particle moving in a one-dimensional double-well potential provides a good example for this—this system admits two degenerate ground states, with tunnelling between the two states resulting in a unique ground state given by the superposition of the degenerate states. However, the tunnelling probabilities vanish in the thermodynamic limit, thus partitioning the Hilbert space into mutually inaccessible sectors and leaving the system stuck in one of the two degenerate minima.

More generally, for any finite system size, the free energy for a quantum statistical system is an analytic function. Since all thermodynamic quantities, such as the entropy or heat capacity, are given by derivatives of the free energy, they too do not display any non-analyticities. It is only the thermodynamic limit that these quantities can diverge, signalling a phase transition.

The task of classifying various phases of matter is hence aided greatly by the concepts of emergence and symmetry, since we can now simply categorize quantum phases in terms of the symmetries they break. A standard tool in investigations of SSB is that of the order parameter, a *local* phenomenological quantity which emerges from the complex collective behaviour of the constituent degrees of freedom. In the thermodynamic limit, the order parameter vanishes in the symmetric (disordered) state and acquires a non-vanishing value in the symmetry broken (ordered) phase. In what has since become a cornerstone of modern condensed matter physics, Landau proposed a classification scheme for different phases of matter based on the unbroken symmetry of the dynamics governing the system and the residual symmetry of the ground state in the symmetry broken state. Within this framework, the macroscopic properties of the phase, along with phase transitions between phases with different patterns of symmetry breaking, are captured by the order parameter field, which is a simply a mapping from physical space to order parameter space. The rules governing this behaviour are vastly simpler than those describing the complicated interactions between the microscopic particles, a simplification which has allowed us to understand a whole zoo of quantum phases. For instance, a Bose-Einstein condensate spontaneously breaks U(1) particle number conservation, with the corresponding order parameter a complex number with unit modulus; a nematic liquid crystal, on the other hand, spontaneously breaks rotational symmetry and is described by a rank-2 symmetric tensor order parameter. In this elegant formalism, superconductivity is simply the result of spontaneous breaking of U(1) charge conservation[4] .

---

[4] In the BCS theory of superconductivity, the electron charge is effectively screened such that the response functions of the charged system are argued to be qualitatively similar to those of a neutral superfluid, such that the fluctuations of the electromagnetic gauge field are irrelevant at long distances. The novel physics that arises when considering a system of charged electrons coupled to dynamically fluctuating electromagnetism is the subject of § 3.

...to Laughlin

Symmetry as an organisational principle is a theoretically elegant concept, one which has been vindicated by several decades of experiments. And yet, despite the remarkable success of this theory, there remained those brave enough to venture forth into the theoretical hinterlands and ask, "Who else goes there?" Could there be heretofore undiscovered principles by which nature assembles, insensitive to the local probes launched so far?

The first hints of physics beyond the symmetry breaking paradigm appeared with the discovery of the Berezinksii-Kosterlitz-Thouless (BKT) transition in two-dimensional superfluids [8, 9]. A superfluid is a low-temperature state formed by a many-body quantum system comprised of electrically neutral particles, characterised by the absence of dissipation and the presence of irrotational flow (neglecting quantum vortices). According to the Mermin-Wagner-Hohenberg theorem [10, 11], which states that continuous global symmetries cannot be spontaneously broken below three dimensions at finite temperatures, any breaking of the global U(1) symmetry will be restored by the gapless Goldstone mode, destroying the spontaneous order. In other words, based on symmetry arguments alone, there is no reason to expect a finite temperature phase transition in a two-dimensional system of neutral particles with a conserved U(1) symmetry. What BKT found instead was a novel transition separating a high temperature phase from one at low temperatures. A characteristic feature of superfluids is that they host quantised vortices (point defects in two-dimensions), around which the phase of the order parameter winds by an integer multiple of 2π, in response to external rotation. The BKT transition is a result of the proliferation of these topological defects in the superfluid phase, resulting from a delicate balance between the energy and entropy of the system. Below a critical temperature, it is too energetically costly to produce isolated vortices, which remain bound in vortex-antivortex pairs; at temperatures above the critical, the system can lower its free energy by proliferating vortices, and the BKT transition is precisely the temperature driven transition from bound vortex-antivortex pairs to unbound vortices. We have just encountered our first example of a phase (albeit classical) distinguished not in terms of
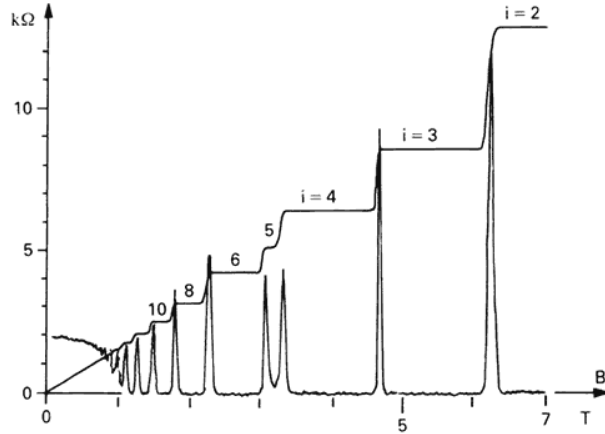
Figure 1.1: Resistivity measurements for the Integer Quantum Hall state.

its symmetry properties, but rather by the nature of its topologically non-trivial excitations.

Not long after the description of the BKT transition, the fundamental role played by topology in the physics of interacting quantum many-body systems came to the fore with the dramatic discovery of new quantum phases of matter, profoundly distinct from anything previously observed in nature and unforeseen by any theory. The discovery of the Quantum Hall effect (QHE) by von Klitzing et al [12], followed shortly thereafter by that of the Fractional Quantum Hall effect (FQHE) by Tsui et al [13], unearthed emergent macroscopic phenomena which evade any classical descriptions and hence require an intrinsically quantum description.

Prior to the discovery of the QHE, it was well established that in a two-dimensional system of charged particles, a voltage difference is produced transverse to the current in the conductor and to the applied magnetic field—this is the classical Hall effect. What von Klitzing found was that, when cooled to low temperatures, the conductivity of a two dimensional electron gas in a perpendicular applied magnetic field is *quantised* to take precisely integer values (in units of e^2/h). Specifically, they found that the Hall resistivity ρ_{xy} sits on a plateau for some range of magnetic fields before suddenly jumping to the next plateau, where the resistivity on each plateau takes the value

$$\rho_{xy} = \frac{h}{e^2}\frac{1}{\nu}, \quad \nu \in \mathbb{Z}.$$

For the range of magnetic fields for which ρ_{xy} sits on a plateau, the longitudinal resistivity ρ_{xx} vanishes, changing only when ρ_{xy} moves to the next plateau (see Fig. 1.1).

The surprising feature of this data is not that the Hall resistivity is quantised to take integer values—indeed, it is easy to show that Hall resistivity for ν filled Landau levels is exactly $h/(e^2\nu)$. Instead, the surprise is the existence of the plateaus, over which the quantisation persists for a range of applied magnetic fields. Typically, experimental systems are dirty and full of impurities, with large amounts of disorder obscuring the key physics of the system. The underlying physics of the IQHE however is not only robust to, but relies on, having disorder in the system—for vanishing disorder, the plateaus are expected to vanish entirely! It is worth pausing to marvel at this result, as it encodes an emergent macroscopic phenomenon which, in the presence of disorder, is described by exactly an integer[5] .

The quantisation of the Hall conductivity and the robustness against disorder provide strong clues regarding the novel physics governing the QHE. It turns out that this phenomenon can be understood without accounting for the interactions between electrons, by considering the single-particle physics of electrons spatially confined to two-dimensions and moving in an applied magnetic field. Recall however that due to the Pauli exclusion principle, electrons are not allowed to occupy the same quantum states and are thus aware of each other's presence. Despite this simple non-interacting picture, the physics of the QHE is an emergent macroscopic phenomenon, since it requires the presence of a macroscopic number of electrons occupying the macroscopic number of degenerate states in a Landau level. The precise quantisation in the QH regime is a consequence of gauge invariance, as shown by Laughlin, who related the quantised conductivity to the adiabatic charge transport in the Thouless pump [14, 15]. In a landmark paper, Thouless and collaborators then explicitly demonstrated that the quantised conductance of an IQH fluid, which is a gapped incompressible state of matter, is related to the first Chern number of filled Landau levels [16]. The Chern number is a topological invariant which only takes integer values and is defined in terms of

---

[5] The value of this integer has been measured to a precision of a part in 10^9; before comparing this to precision atomic physics experiments, remember that unlike those, quantum Hall samples are teeming with impurities.

the *global* topological properties of the band structure of non-interacting electrons; specifically, the Chern number of a filled band is given by the integral of its Berry curvature over the entire Brilloun zone. By relating the quantised Hall conductivity to a topological invariant, the TKNN formula lays bare the physics governing the macroscopic behaviour of a QH system; unlike quantum phases of matter with spontaneously broken symmetries, the essential physics of the QHE is captured not by some local order parameter, but rather by a global (non-local) quantity, sensitive only to the topology of the band structure. The robustness of the QHE to disorder is a direct consequence of this; unless the disorder is too strong, it only affects local properties of the system, leaving global quantities unchanged.

The IQH state is an example of a gapped quantum phase of matter beyond Landau's symmetry breaking paradigm, which evades description as a symmetry broken state and is instead described in terms of global topology. It is important to note that the topology here refers not to the topology of any physical sample, but rather to the abstract space of quantum ground states of the local, gapped Hamiltonian. As such, it is an example of a class of quantum phases of matter which are distinguished by the quantum mechanical properties of their wave functions—in this case the Berry curvature—instead of by the breaking of global symmetries. An even more striking example of such a quantum phase of matter was discovered in the Fractional Quantum Hall effect, where plateaux in the Hall resistivity were seen to occur at fractional filling fractions [13]. Unlike the IQHE, which can be described in terms of non-interacting electrons, a FQH liquid is a strongly correlated system, where interactions between electrons are responsible for the emergent behaviour displayed by this phase. Most striking of these is the phenomenon of *fractionalization*, wherein quasi-particle excitations above the ground state carry a fraction of an electron's charge. This is rather astonishing—after all, isn't the charge of an electron a fundamentally indivisible quantity? And yet experiments provide clear evidence for excitations carrying, for instance, charge $e/3$ [17, 18].

There is no paradox here, as fractionalization is (yet another) example of hitherto unexpected phenomena emerging in systems of interacting quantum many-body systems. In the FQHE, the

fractional charge and statistics of quasi-particles are a result of a drastic reconfiguration of the microscopic electrons, reflecting a pattern of long-range entanglement in the quantum ground state. In other words, the Hilbert space can no longer be described in terms of a direct product of local Hilbert spaces and instead obeys certain local constraints, forcing the ground state wave function into a complicated superposition of basis states. Once again, we see that there exist phases which are not characterised in terms of symmetry breaking or a local order parameter but are instead described by global, non-local properties of their ground states. Such gapped quantum phases with a pattern of long-range entanglement in their ground states, examples of which include the experimentally observed FQH states and the theoretically predicted quantum spin liquids [19–21], are said to be *topologically ordered*[6] phases.

Various remarks are in order regarding the nature of topological order[7] :

- Besides inextricably linking the concepts of emergence, long-range entanglement, and fractionalization, the FQHE also brings to the fore the remarkable concept of *universality* in many-body systems. Displaying profound physical insight, in a result whose importance cannot be overstated even decades later, Laughlin proposed an ansatz for the many-body ground state of the $\nu = 1/3$ FQH liquid [24]. Despite not being the exact ground state for a system of interacting electrons in a strong magnetic field, the Laughlin ansatz accurately captures the universal low energy physics displayed by the FQH state. In other words, the Hamiltonian for which Laughlin's wave function is the true ground state and the real, physical Hamiltonian belong to the same universality class and hence display the same emergent macroscopic behaviour.

- The universal long-distance physics of topologically ordered states is effectively captured by a *topological* quantum field theory. This description encapsulates the intrinsically non-local character of states with topological order, which endows them with a robustness against

---

[6] In contrast, IQH states possess invertible topological order [22], since they do not host any fractionalized excitations but still cannot be smoothly connected to a product state on account of the presence of edge states with non-vanishing chiral central charge.

[7] The reader is referred to the excellent set of lecture notes by David Tong [23] for a detailed review of the Quantum Hall effect.

arbitrary local perturbations, and correctly predicts the fractionalization patterns of quasi-particles.

- Unlike symmetry breaking, which can occur in classical statistical systems, the phenomenon of long-range entanglement (and thus also topological order) is intrinsically quantum. The presence of long-range entanglement implies that the Hilbert space of the system is locally constrained, with the fundamental degrees of freedom restructured in a particular way, giving rise to complex macroscopic behaviour. The appropriate theoretical framework for describing such locally constrained Hilbert spaces is that of *gauge theory*, with Wegner's Ising gauge theory being an early example of a long-range entangled phase with $\mathbb{Z}_2$ topological order [25].

Ok, enough commenting on the nature of topological order. Let's parrot Billy Pilgrim and come unstuck in time to the early aughts[8] .

The New Cartographers

The years ensuing the discoveries of the integer and fractional quantum Hall effects saw many theoretical developments in the field of gapped topological phases of matter, especially in two-spatial dimensions. Haldane, for instance, realised that the key ingredient for IQH behaviour in a lattice model of fermions was not an external magnetic field but rather the breaking of time-reversal symmetry [26]. In the meantime, Wen, amongst others, realised that the low energy behaviour of two-dimensional topological order is neatly encapsulated in the Chern-Simons topological field theories [27–29] studied by Witten [30]. An unanticipated breakthrough was made by Kitaev, who realised that non-Abelian anyons—excitations with non-Abelian braiding statistics which appear in certain quantum Hall states, such as the Moore-Read Pfaffian at filling fraction $\nu = 5/2$ [31]—could provide a viable platform for fault-tolerant quantum computation [32]. Earlier, in a remarkable result of their own, Moore and Read discovered a profound connection between the bulk wave

---

[8] An unfortunate term referring to the first decade of the 21st century, a perversion of the almost-synonym for "anything" familiar to that Danish prince who never gave Ophelia aught.

function of a QH state and the conformal field theory (CFT) living on the boundary of that state [31]. A comprehensive discussion of these developments and other important advances may be found in [33].

An open question remained whether explicitly breaking time-reversal and parity symmetry was required in all topological states of matter. This was answered in the negative by the theoretical prediction of the quantum Spin Hall effect (QHSE) [34–38]. This novel phenomenon occurs in time-reversal symmetric phases built out of non-interacting fermions in two- and three-spatial dimensions, which exhibit a quantised bulk response encapsulated by a topological invariant not entirely dissimilar to the Chern number in IQH states. A key feature of these states is the presence of gapless edge excitations which are robust against arbitrary local perturbations, including disorder, but crucially, this protection lasts only as long as the perturbations are themselves invariant under time-reversal symmetry.

These predictions were followed by rapid developments in the classification and characterisation of quantum phases of matter—both in and out of equilibrium, both topological and not—with large swaths of previously hidden phenomena uncovered by those charting the endlessly fascinating landscape defined by systems of many interacting particles. Instead of following these developments gradually, let's confront this landscape suddenly and all at once[9] . A panorama of quantum phases of matter in equilibrium is depicted in Fig. 1.2, with a (decidedly less scientific) depiction which includes phases arising in a non-equilibrium setting shown in Fig. 1.5.

The bulk of this thesis is concerned with the study of gapped quantum phases of matter, mostly in equilibrium, so let us focus first on the right-half of Fig. 1.2. A central notion in the classification of local gapped Hamiltonians in terms of topology is that of *adiabatic continuity*. Locality here implies that the Hamiltonian is a sum of terms which act on spatially localized regions and we assume here that the system has a unique ground state (on an infinite geometry) with a finite gap to all excitations. Two quantum states of matter are considered to be in the same phase

---

[9] Both so as to mimic the rapid onslaught of new advances which has occurred over the past decade and also to avoid testing the patience of even the most indulgent of readers.
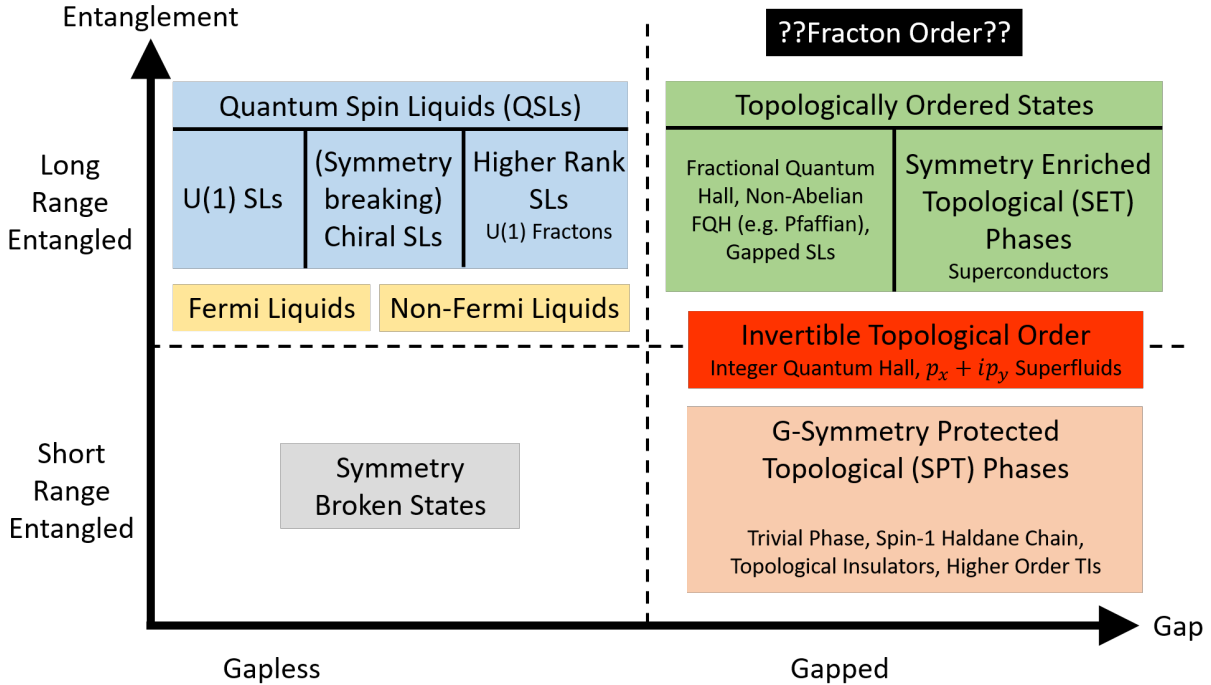
Figure 1.2: A broad view of the current landscape of equilibrium quantum phases of matter.

if their Hamiltonians can be continuously deformed into each other without ever closing the gap i.e. if they are adiabatically connected. This allows for a natural partition of the space of all gapped Hamiltonians into equivalence classes, with all states within the same class being adiabatically connected. To avoid accidentally distinguishing systems which differ only by some frozen degrees of freedom, we allow the addition of a trivial atomic insulator, such that the Hamiltonian acting on this new part of the Hilbert space is simply a sum of strictly local non-overlapping terms.

Intrinsic Topological Order

In the absence of any global symmetries, and given both the spatial dimensions and the statistics of the microscopic constituents (bosons or fermions), we can partition the space of all gapped local Hamiltonians into equivalence classes as shown in Fig. 1.3. This landscape consists of connected regions throughout which the gap remains open, separated from each other by intervening gapless states. The simplest of these regions is the trivial topological phase, which is adiabatically
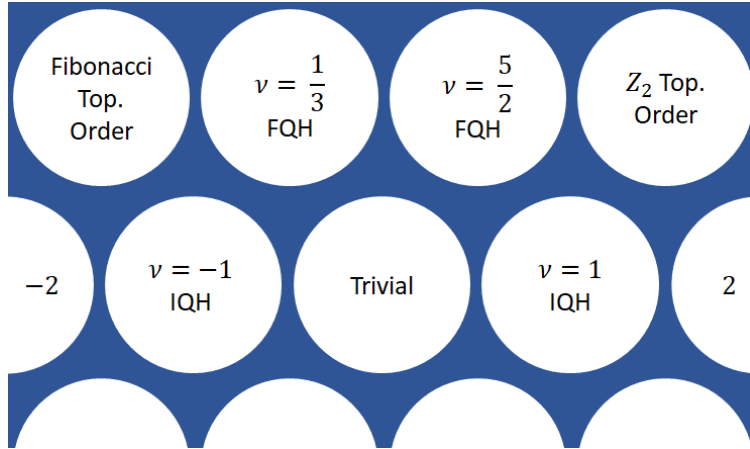
Figure 1.3: Distinct topologically ordered phases of fermions in two-spatial dimensions. White circles represent gapped topological phases with the gap closing at the blue borders. Examples include the trivial phase, which includes the atomic insulator, distinct IQH states labelled by integer filling fractions, FQH states at distinct filling fractions, and $\mathbb{Z}_2$ topological order.

connected to the trivial atomic insulator. All other disconnected regions are said to possess *intrinsic* topological order and cannot be smoothly deformed into the trivial phase without closing the gap. Here, the term intrinsic refers to the fact that the topological nature of these states does not rely on any global symmetries.

A modern viewpoint for distinguishing states with intrinsic topological order from the topologically trivial phase involves the notion of entanglement. Specifically, all gapped quantum phases of matter within the trivial phase are short-range entangled (SRE)[10] i.e. their ground state wave function can be smoothly deformed into a direct product state (the ground state for the atomic insulator) by a series of local unitary operations, without encountering a phase transition. In contrast, topologically ordered states show a pattern of long-range entanglement (LRE) in their ground state wave functions [39–41], with no series of local unitary operations able to smoothly interpolate between two distinct topologically ordered phases without the gap closing or encountering a phase transition.

Topologically ordered phases, examples of which include the fractional quantum Hall states

---

[10] There are duelling definitions of what constitutes a SRE gapped phase. One states that a SRE phase is one with a unique ground state on any closed spatial manifold. The point of view taken in this thesis defines an SRE state as any state which is smoothly deformable into a direct product state without undergoing a phase transition.

and $\mathbb{Z}_2$ spin liquids, exhibit striking features including excitations with fractionalized statistics and quantum numbers, and locally indistinguishable degenerate ground states[11] on topologically non-trivial closed spatial manifolds [24, 31, 42–47]. In general, it has now been understood that the correct mathematical framework for understanding topological order in $d = 2$ spatial dimensions is that of tensor category theory, given that the universal long wavelength physics of the phase is captured by a topological quantum field theory (TQFT). Specifically, quasi-particles—anyons—in such phases are described by objects in a modular tensor category [48, 49]. This can be seen explicitly in Kitaev's quantum double models, wherein anyons are labelled by the irreducible group representations of the quantum double of a finite gauge group G, $\mathcal{Z}(G)$ [50]. In addition, the universal low-energy physics of a large class of topological states is simply described in terms of the string-net Hamiltonians introduced by Levin and Wen [51], which are exactly soluble models for non-chiral topological orders i.e. those with a vanishing thermal Hall conductivity. Compared to topologically ordered phases in $d = 2$, the characterization and classification of topological order in $d = 3$ is less understood, but has been studied through exactly solvable models such as the Kitaev model [52], color codes [53], and models which exhibit string-net condensation in $d = 3$ but are not exactly solvable [51].

Symmetry Protected Topological Phases

So much for topologically ordered states in the absence of any symmetries. Prior to delving into the classification of gapped topological phases, we had briefly encountered the quantum Spin Hall effect. Does this phase fit into the framework developed so far and if so, where? It turns out that the topological classification of quantum phases becomes more refined when certain symmetries are imposed on gapped local Hamiltonians, with the QHSE being just one example of what we now understand as the class of *symmetry protected topological* (SPT) phases. Most symmetries under consideration are expected to be generically present in materials, such as time-reversal symmetry

---

[11] States which are LRE but host no fractionalized excitations and have a unique ground state on arbitrary closed manifolds, such as the IQH states, are said to possess invertible topological order.
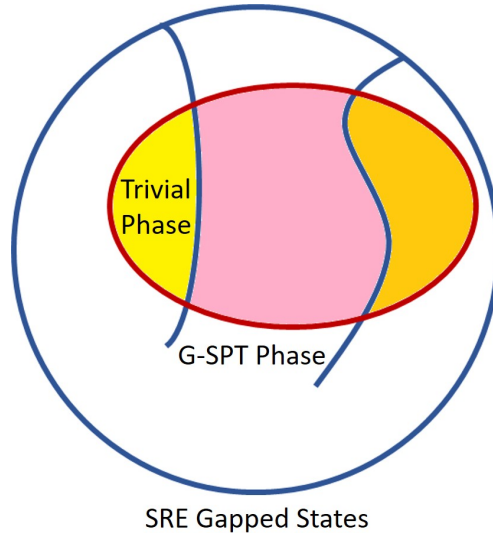
Figure 1.4: In the presence of a symmetry group G, the space of SRE gapped local Hamiltonian obeying that symmetry (contained within the red ellipse) gets partitioned into distinct SPT phases which cannot be continuously deformed into each other without closing the gap or breaking the symmetry G.

or U(1) charge conservation. While the former is broken in the presence of a magnetic field and the latter in superconductors, these are non-generic examples and it is typically reasonable to study systems with some unbroken symmetry at low energies (which could, in principle, be the residual symmetry of some larger symmetry group which gets restored at higher energies).

Suppose we impose a symmetry group G on the class of local gapped Hamiltonians which, in the absence of that symmetry, belonged to the topologically trivial phase. In other words, suppose we start from the set of all SRE states, which lack any intrinsic topological order and are adiabatically connected to the atomic insulator, and restrict ourselves to Hamiltonians respecting the symmetry G. Let us further demand that these states admit only a unique ground state since we are not interested in symmetry-broken states here. In the presence of this symmetry G, states which were continuously deformable into each in the absence of the symmetry may now become separated, as shown in Fig. 1.4. Thus, distinct SPT phases protected by the same symmetry cannot be smoothly deformed into each other without undergoing a phase transition as long as the deformation preserves the symmetry. On the other hand, all such distinct SPT states can be

adiabatically connected to the same direct product state without encountering a phase transition when the deformation breaks the symmetry.

Thus, SPT phases are gapped quantum phases of matter which, despite being short-range entangled, cannot be adiabatically transformed into trivial product states in the presence of an unbroken global symmetry [54–56]. Unlike states with intrinsic topological order, SPT phases have non-degenerate ground states and do not possess fractionalized excitations, but are described by topological invariants which are robust against local, symmetry-preserving perturbations. A distinctive feature of these topologically non-trivial phases, of which the 1d Haldane phase for spin-1 chains [54, 57–59] and topological insulators [34–38] are paradigmatic examples, is the presence of non-trivial boundary excitations[12] . The mathematical framework for the classification of SPT phases has been recognised as that of group cohomology theory [56], and while early studies focused mainly on on-site symmetries such as time-reversal or charge conservation, this has recently been extended to crystalline symmetries, leading to the prediction and observation of topological crystalline phases (see e.g. [61] for a review of recent progress in this direction).

Symmetry Enriched Topological Phases

Instead of starting with the class of SRE states (without intrinsic topological order) and studying the finer classification which appears with the addition of global symmetries, one could consider starting from any of the classes with topological order and restrict attention to the subclass of Hamiltonians with global symmetry G. This leads to the concept of *symmetry enriched topological* phases: states which in the absence of any symmetry possess the same intrinsic topological order and are adiabatically connected, but in the presence of a global symmetry display distinct patterns of symmetry fractionalization and cannot be continuously deformed into each other without breaking the symmetry or going through a phase transition. SET phases provide a platform on which to study the interplay between symmetry and topology in quantum phases of matter, and much recent

---

[12] For instance, an interacting $d = 3$ SPT state can host either a protected gapless surface state, a symmetry breaking state, or a symmetry preserving but topologically ordered state on its surface [60].

progress has been made in understanding these phases, at least in two-dimensional systems.

It is worth noting that there also exists a remarkable and intimate relationship between (LRE) topologically ordered phases and (SRE) SPT phases [62–64]: given an SPT phase protected by a discrete symmetry G, there exists a duality between that SPT phase with gauged symmetry G and a topologically ordered phase whose fusion rules are derived from the group multiplication rule of G. This provides an alternate route for studying SET phases, which occur in complicated interacting systems and are typically more challenging to study than their SPT counterparts.

All Things Besides

All this to say that gapped quantum phases of matter comprise a substantial chunk of the condensed matter landscape and much has been understood about the topological nature of these systems in a fairly short amount of time. There is still the matter of gapless phases of matter (left-half of Fig. 1.2). Some of these we've already encountered in the form of symmetry breaking states, such as superfluids, which are guaranteed a gapless mode thanks to Goldstone's theorem. Novel topological gapless states have also received much theoretical and experimental attention lately. Most prominent amongst these are *Weyl semi-metals*, realised in systems of non-interacting $d = 3$ fermions, which host topologically protected point-like crossings of two bands and host exotic Fermi arc surface states [65, 66]. Also of much interest are long-range entangled gapless phases which, despite the absence of a bulk gap, host excitations with fractionalized quantum numbers and, in certain exactly solvable models, have been conjectured to exhibit topologically protected gapless edge modes [67]. Gapless quantum spin liquids are a familiar example of gapless long-range entangled states which can display a plethora of interesting symmetry fractionalization patterns, but such states have so far evaded the clean mathematical classification which applies to gapped topological phases; this is primarily due to the breakdown of notions of "adiabaticity" in the absence of a well-defined bulk gap. Much more could be said about quantum phases in equilibrium: an entirely different thesis by an author with entirely different biases and motivations could easily have devoted the preceding pages to a discussion of phase transitions and critical phenomena, including

the remarkable concept of deconfined quantum criticality [68]. The reader is left to their own (electronic) devices to track down the appropriate references for these matters.

Recent advances in the cooling, trapping, and manipulation of atoms in atomic, molecular, and optical systems, in concurrence with the development of novel methods in condensed matter systems, have allowed one to study, in a controlled manner, systems of strongly interacting quantum many-body systems. This has led to a resurgence of interest in understanding the dynamical behaviour of closed quantum systems. Unlike traditional formulations of quantum statistical mechanics, which implicitly assume that the system of interest is in contact with an external reservoir, recent studies have focused on isolated quantum systems not coupled to any such reservoir. The central question of interest regarding such an interacting, closed many-body quantum system is whether, after an arbitrary long time, it thermalizes or remains localized. Thermalization in a closed quantum system occurs when the system is able to act as a reservoir for its subsystems; in such cases, even though the system undergoes unitary evolution, all information regarding the initial state of the system is rendered inaccessible since all local quantities appear thermal. Localized states, however, fail to act as reservoirs for themselves and can thus retain a memory of initial conditions accessible through certain local quantities. In this sense, localized states fail to reach thermal equilibrium at even infinitely long times and evade descriptions in terms of conventional statistical mechanics.

The recent discovery of localization in interacting many-body quantum systems in isolation, dubbed "many-body localization," has elicited tremendous interest from both theoretical and experimental communities, challenging and extending our existing notions of quantum statistical mechanics. An excellent introductory exposition of this endlessly fascinating subject can be found in [69]. The development of MBL states, which are distinct from thermalized states only in a dynamical sense, has coincided with a general interest in the discovery and characterisation of novel phases of matter out of equilibrium with no equilibrium counter-parts. Examples include the so-called "discrete time-crystals" and other phases of matter which occur in systems driven periodically out of equilibrium ("Floquet" phases) (see e.g. [70, 71] and references contained therein). A

distinct but equally fascinating area of research concerns the spreading of entanglement in chaotic quantum many-body systems which reach thermal equilibrium but display intriguing behaviour in their approach to equilibrium [72], inviting connections between black-holes, holography, quantum information, and condensed matter systems.

Suffice it to say that the landscape of open and interesting problems outside the realm of gapped quantum phases of matter is decidedly Brobdingnagian and anything beyond the preceding perfunctory discussion lies outside the scope of this dissertation.

The Jabberwock Cometh

Perhaps you have already noticed a glaring omission from the preceding discussion of topological states of matter, denoted "fracton order" in the panorama of quantum phases (Fig. 1.2). This separation of fracton phases is intentional, since the theoretical development of the field is fairly recent and our understanding of it limited, especially when contrasted with the vast array of tools for studying conventional topological phases at our disposal[13] . Despite the intense ongoing research in the field, there exist certain well-established notions regarding the nature of topological quantum phases; for instance, the ground state degeneracy of a topologically ordered phase should depend only on the global topology of the spatial manifold on which it is defined and not on geometric properties such as the system size. Thus, the discovery by Haah[14] of an exactly soluble lattice model in three-dimensions [75] which openly flouts some of these notions has generated a frisson of excitement and added a layer of intrigue to the study of topological order.

Following Haah's pioneering work, similarly strange phases were discovered in certain exactly solvable lattice spin models [74, 76]. The unifying feature of these exotic phases is the existence of point-like excitations with *restricted mobility*, which are fundamentally immobile or which are confined to move only along sub-dimensional manifolds. The immobility of certain excitations,

---

[13] "Thus the facts, did we possess them, are too imprecisely few to warrant our certitude."—James Joyce, *Finnegans Wake*, paraphrased.

[14] Historically, the first model displaying fracton order was introduced by Chamon circa 2005 [73]; however, the interpretation of Chamon's model as one with fracton order did not appear until later work by Vijay and collaborators [74].

dubbed "fractons," stems from the lack of any one-dimensional string-like operator at the ends of which they may be created. Instead, depending on the specific model, fractons are created either at the corners of two-dimensional membrane [73, 74, 76] or fractal [75, 77] operators, with the corresponding models referred to as "type-I" or "type-II" fracton models respectively in the taxonomy of Vijay, Haah, and Fu [76]. While type-I models host additional topologically charged excitations which can move only along $c < d$ sub-manifolds and are hence termed "dim-c" excitations, type-II models, such as Haah's code, have *no* mobile excitations which carry topological charge. Despite the striking appearance of these exotic quasiparticles, these fracton models display many features familiar from topological order: they have a gap to all excitations, display long-range entanglement in their ground state, and support topologically charged excitations which cannot be created locally. In stark contrast with topologically ordered phases however, which have a finite ground state degeneracy on non-trivial manifolds, fracton phases instead have a sub-extensive number of locally indistinguishable ground states on the 3-torus. Since their ground state degeneracy explicitly depends on the geometry of the manifold, fracton order is, strictly speaking, incompatible with our usual understanding of topological order.

Much recent progress has been made regarding the nature of type-I fracton order, specifically in the context of the paradigmatic X-Cube model [74]. For instance, it has been understood that this model can be constructed by appropriately coupling together inter-penetrating layers of $d = 2$ $\mathbb{Z}_2$ topological orders, providing a route for approaching fracton order via the more established framework of topological order [78, 79]. Concurrently, a series of stimulating works by Pretko [80, 81] has established the existence of *gapless* U(1) fracton models in the context of symmetric higher-rank tensor gauge theories. The key idea here is that symmetric tensor gauge theories allow for a wider variety of constraints on the low-energy Hilbert space than their vectorial counterparts, with an immediate consequence being the emergence of stricter conservation laws on the charges of the theory. In the "scalar charge theory," for example, the dipole moment of charges is conserved in addition to their charge, naturally enforcing the creation of charges at the corners of a membrane operator. These tensor gauge theories thus provide an alternate platform for realising

fracton phenomenology, while also harbouring intimate connections with gravity, elasticity, and generalised Chern-Simons theories [82–85].

Although the discovery of Haah's code pre-dates that of type-I models such as the X-Cube, it has proved much harder to gain physical insight into the nature of a model which possesses no mobile topological excitations and where the elementary geometric object at the ends of which excitations appear is a Sierpinski tetrahedron. It remains an open question whether Haah's code admits a description in terms of coupled $d = 2$ or $d = 3$ topological orders or if there exists any analogue of a tensor gauge theoretic description for type-II fracton order. Given the truly puzzling and seemingly indecipherable nature of Haah's code[15] , it is only natural to equate it to that mythical creature from Wonderland, the Jabberwock, with the simpler fracton phases being mere bandersnatches. We will encounter all manners of gapped and gapless fracton phases in more detail in §§ 4 and 5; nonetheless, the reader is referred to [86] for an excellent overview of the current consensus regarding fracton phases of matter.

Outline of Dissertation

The landscape of interacting many-body quantum phases of matter is vast and varied, with many strange and exotic phenomena lurking in the shadows, waiting to be discovered. In this dissertation, we will predominantly concern ourselves with the study of gapped topological phases and their characterisations. Broadly, this thesis can be divided into two parts: the first part studies familiar topological phases, specifically superfluids and superconductors, while the second tackles novel phenomena arising in systems with finite densities of fractons and their bound states, with a brief foray into the physics of gapless U(1) fractons in § 5. The unifying theme through all of these studies is the identification of striking behaviour which arises in quantum many-body systems governed primarily by their underlying topology.

This thesis comprises four previously published papers [47, 85, 87, 88].

---

[15] It is often colloquially remarked within fracton circles that the only person who truly understand Haah's code is Haah himself.

- § 1 contains introductory material, of which you are approaching the end.

- § 2 is based on [87], in which we compute the orbital angular momentum L_z of an s-wave paired superfluid in the presence of an axisymmetric multiply quantized vortex. For vortices with winding number $|k| > 1$, we find that in the weak-pairing BCS regime L_z is significantly reduced from its value $\hbar N k/2$ in the Bose-Einstein condensation (BEC) regime, where N is the total number of fermions. This deviation results from the presence of unpaired fermions in the BCS ground state, which arise as a consequence of spectral flow along the vortex sub-gap states. We support our results analytically and numerically by solving the Bogoliubov-de-Gennes equations within the weak-pairing BCS regime.

- § 3 is based on [47], where we develop a unified low-energy description for spin-singlet paired states by deriving topological Chern-Simons field theories for s-wave, $d + id$, and chiral higher even-wave superconductors. These theories capture the quantum statistics and fusion rules of Bogoliubov quasiparticles and vortices and incorporate global continuous symmetries - specifically, spin rotation and conservation of magnetic flux - present in all singlet superconductors. For all such systems, we compute the Hall response for these symmetries and investigate the physics at the edge. In particular, the weakly-coupled phase of a chiral $d + id$ chiral state has a spin Hall coefficient $\nu_s = 2$ and a vanishing Hall response for the magnetic flux symmetry. We argue that the latter is a generic result for two-dimensional superconductors with gapped photons, thereby demonstrating the absence of a spontaneous magnetic field in the ground state of chiral superconductors. We also show that the Chern-Simons theories of chiral spin-singlet superconductors derived here fall into Kitaev's 16-fold classification of topological superconductors.

- § 4 is based on [88], where we investigate relaxation in fracton models and discover that these models naturally host glassy quantum dynamics in the absence of quenched disorder. We begin with a discussion of "type I" fracton models, in the taxonomy of Vijay, Haah, and Fu, and demonstrate that in these systems, the mobility of charges is suppressed *exponen-*

tially in the inverse temperature. We further demonstrate that when a zero temperature type I fracton model is placed in contact with a finite temperature heat bath, the approach to equilibrium is a *logarithmic* function of time over an exponentially wide window of time scales. Generalizing to the more complex "type II" fracton models, we find that the charges exhibit *subdiffusion* upto a relaxation time that diverges at low temperatures as a *super-exponential* function of inverse temperature. This behaviour is reminiscent of "nearly localized" disordered systems, but occurs with a translation invariant three-dimensional Hamiltonian. We also conjecture that fracton models with conserved charge may support a phase which is a *thermal* metal but a *charge* insulator.

- § 5 is based on [85], in which we consider systems with a finite density of either fractons or their dipolar bound states, with a focus on the $U(1)$ fracton models. We study some of the phases in which emergent fractonic matter can exist, thereby initiating the study of the "condensed matter" of fractons. We begin by considering a system with a finite density of fractons, which we show can exhibit microemulsion physics, in which fractons form small-scale clusters emulsed in a phase dominated by long-range repulsion. We then move on to study systems with a finite density of mobile dipoles, which have phases analogous to many conventional condensed matter phases. We focus on two major examples: Fermi liquids and quantum Hall phases. A finite density of fermionic dipoles will form a Fermi surface and enter a Fermi liquid phase. Interestingly, this dipolar Fermi liquid exhibits a finite-temperature phase transition, corresponding to an unbinding transition of fractons. Finally, we study chiral two-dimensional phases corresponding to dipoles in "quantum Hall" states of their emergent magnetic field and establish numerous aspects of these generalized quantum Hall systems.

- § 6 closes this thesis with a discussion of open questions and future directions.

Various appendices include the details of various technical calculations.

Figure 1.5: An (incompetent) artist's depiction of the current landscape of quantum phases of matter.

Chapter 2

Vortices in Fermionic Superfluids: Stay in Bed, Float Upstream

In which Benny,

turning and turning in the widening gyre,

despairs.

For several decades, the orbital angular momentum (OAM) of the A-phase of liquid ^{3}He remained a topic of intense theoretical debate in the condensed matter community. ^{3}He-A represents an example of a fermionic chiral superfluid (SF), which breaks parity and time-reversal symmetry in addition to charge conservation. Specifically, it is a $p_x + ip_y$ paired state of spin-polarized fermions, a state with invertible topological order which hosts a gapless chiral Majorana mode on its boundary [89]. More generally, one can consider a system of fermions with pairing symmetry $(p_x + ip_y)^\nu$, which for odd ν corresponds to a spin-triplet paired state with ν Majorana modes on the boundary and for even ν corresponds to spin-singlet paired state with 2ν Majorana modes on the boundary (the factor of two arises due to spin). Each Cooper pair in such a state carries angular momentum ν and the broken chiral symmetry in these systems is directly manifested in the OAM.

The debate surrounded the precise value of the OAM in various chiral SFs, with warring points of view leading to substantially different predictions. One simple argument is as follows: in a system comprised of N fermions, each of the $N/2$ Cooper pairs possesses an OAM ν, with the total OAM $L_z = \nu N/2$. On the other hand, if we consider starting from a non-superconducting state, with $L_z = 0$, then the formation of Cooper pairs would lead to a non-trivial OAM. However, since

only fermions in the vicinity of the original Fermi surface should contribute to physical quantities at low energies, we expect that the OAM would be suppressed by some positive power of $\sim \Delta_0/E_F$, where E_F is the Fermi energy and Δ_0 the pairing amplitude.

This apparent paradox was recently resolved by Tada et al [90] who considered the OAM of a fermionic chiral SF in both the strongly paired Bose-Einstein condensation (BEC) regime, where pairs of fermions are tightly bound into bosonic molecules which undergo Bose-Einstein condensation, and the weakly paired Bardeen-Cooper-Schrieffer (BCS) regime, where weakly bound Cooper pairs condense. In the non-topological BEC regime, the SF is found to have an OAM $L_z = \nu N/2$ consistent with naïve expectations. The BCS regime however, in which the SF is a topological superfluid with gapless chiral edge states, shows strikingly different behaviour for $\nu = 1$ and $\nu \geq 2$. In particular, when $\nu = 1$, the chiral Majorana edge mode carries no OAM and so the bulk OAM $L_z = N/2$ agrees with the OAM in the BEC regime. On the other hand, when $\nu \geq 2$, the gapless boundary modes carry OAM counter to that carried by the Cooper pairs due to the presence of unpaired fermions localized around the boundary, leading to a significant reduction of the OAM, $L_z \approx 0$. Thus, the presence of the topological edge modes significantly influences the behaviour of physical observables such as the OAM.

The initial impetus of our work was to study analogous behaviour in a non-chiral s-wave superfluid, but in the presence of non-trivial topological defects—vortices. Given the current experimental challenges in realising chiral SFs even in ultra-cold atomic experiments, a key motivation was to find an experimentally feasible model which exhibits much of the same physics expected in chiral SFs. In this chapter, this is accomplished by studying multiply quantized vortices i.e. vortices with a winding number ≥ 1, in the BCS regime of an s-wave paired SF, which are found to host unpaired fermions localized around the vortex core, thereby reducing the OAM of the SF significantly. While much of the physics is found to resemble that of chiral SFs, an advantage of the system in consideration here is the insensitivity of the OAM to the microscopic details of the boundary, leading to a more robust signature than that expected in chiral SFs.

A version of this chapter was first presented as [87] under the title "Multiply Quantized Vor-

tices in Fermionic Superfluids: Angular Momentum, Unpaired Fermions, and Spectral Asymmetry,"
and is a collaboration with Sergej Moroz, Victor Gurarie, and Leo Radzihovsky,

Phys. Rev. Lett. 119, 067003 (2017)[1]
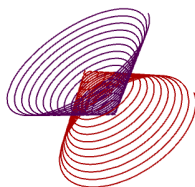
2.1   Introduction

Quantized vortices are a hallmark of superfluids (SFs) and superconductors. These topological defects form in response to external rotation or magnetic field and play a key role in understanding a broad spectrum of phenomena, such as the Berezinskii-Kosterlitz-Thouless transition in two-dimensional (2D) SFs [8, 9], superconductor/insulator transitions [91–93], turbulence [94], and dissipation [95, 96]. In fermionic s-wave paired states, the structure of the ground state and low lying excitations of an axisymmetric singly quantized vortex has been established through analytical and numerical studies in both the strong-pairing regime (where the SF phase is understood as a Bose-Einstein condensate (BEC) of bosonic molecules) and in the weak-pairing Bardeen Cooper Schrieffer (BCS) regime. In the BEC regime, the microscopic Gross-Pitaevskii equation provides a reliable framework [97, 98], while in the BCS regime the (self-consistent) Bogoliubov-deGennes (BdG) theory is key in identifying the structure of the ground state [99, 100] and the spectrum of sub-gap fermionic excitations [101].

Multiply quantized vortices (MQVs) have however not received much attention. Generically in a homogeneous bulk system, the logarithmic repulsion between vortices, which scales as the square of the vortex winding number k, energetically favors an instability of a multiply quantized vortex into separated elementary unit vortices [102]. However, MQVs are of interest since

---
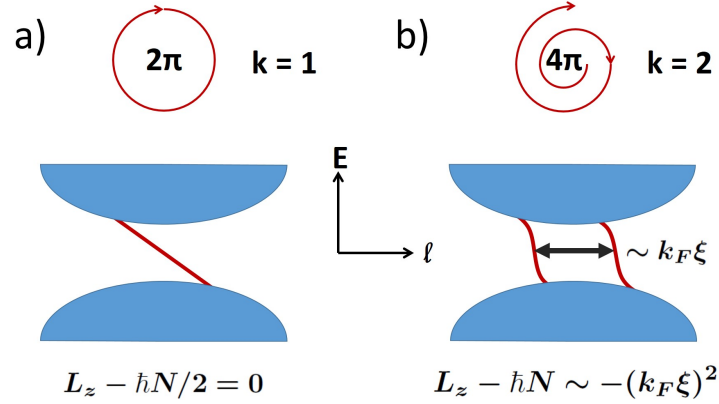
Figure 2.1: Summary of main result: a) For an elementary vortex ($k = 1$), the fermionic spectrum has a vanishing spectral asymmetry and thus all fermions are paired in the ground state, resulting in $L_z = \hbar N/2$ in the BCS regime. b) In stark contrast, for an MQV ($k = 2$ pictured here as an example) mid-gap states confined to the vortex core induce a non-trivial spectral asymmetry, which leads to unpaired fermions in the ground state. These reduce L_z from its naïve value $\hbar N$ by an amount that scales quadratically with the splitting between the red branches.

under certain circumstances, the interaction between vortices is not purely repulsive and can support multi-vortex bound states, at least as metastable defects. This can happen, for instance, in type-II mesoscopic superconductors, where MQVs have been predicted [103] and experimentally observed [104–107]. In addition, it has been argued that MQVs are expected to be energetically stable in multicomponent superconductors [108, 109] and in chiral p-wave superconductors [110, 111]. In fermionic SFs, a doubly quantized vortex was predicted [112] and observed in ^{3}He-A [113]. It has further been argued that fast rotating Fermi gases trapped in an anharmonic potential will support an MQV state [114–116]. Similar vortex states have been created in rotating BEC experiments [117–120].

Surprisingly, as we demonstrate in this chapter, there is a fundamental difference between a singly quantized vortex ($|k| = 1$) and an MQV ($|k| > 1$) in a weakly-paired fermionic s-wave SF. This difference is manifested most clearly in the orbital angular momentum (OAM) L_z, as illustrated in Fig. 2.1. At zero temperature in the BEC regime, a microscopic Gross-Pitaevskii calculation predicts $L_z = \hbar Nk/2$, where N is the total number of fermions. Intuitively, this corresponds to a simple picture where an MQV induces a quantized OAM k per molecule. For an

elementary vortex, this result also holds in the BCS regime, as confirmed within the self-consistent BdG framework [99, 100]. As we show in this chapter, for vortices with $|k| > 1$ however, the BCS ground state contains unpaired fermions which carry OAM opposite to that carried by the Cooper pairs, thereby significantly reducing the total L_z from its BEC value by an amount $\sim (k_F\xi)^2$, where k_F is the Fermi momentum and ξ the coherence length. While the proportionality constant is non-universal and depends on the vortex core structure, the scaling with k_F and ξ is robust, being independent of any boundary effects.

2.2 BdG Hamiltonian and Generalized Angular Momentum

To derive our main result, we consider a 2D^2 s-wave paired SF in the weak-pairing BCS regime at zero temperature within the BdG framework. The mean-field Hamiltonian describing a spin-singlet two-dimensional superfluid (SF) with pairing symmetry $(p_x + ip_y)^\nu$ and in the presence of an axisymmetric MQV with winding number k is

$$\hat{H}_\nu = \int d^2r \sum_{\sigma=\uparrow,\downarrow} \psi_\sigma^\dagger \left(-\frac{\nabla^2}{2} + V(r) - \mu\right)\psi_\sigma + \left[\int d^2r\, \psi_\uparrow^\dagger \Delta(r)e^{ik\varphi/2}(p_x + ip_y)^\nu e^{ik\varphi/2}\psi_\downarrow^\dagger + \text{h.c.}\right]. \tag{2.1}$$

The case $\nu = 0$ corresponds to the s-wave spin-singlet paring, which will be the focus of this chapter, while spin-singlet chiral SFs are obtained by taking non-zero even values of ν.

The fermionic operators satisfy canonical anti-commutation relations,

$$\{\psi_\sigma(\mathbf{r}), \psi_{\sigma'}^\dagger(\mathbf{r}')\} = \delta_{\sigma\sigma'}\delta(\mathbf{r} - \mathbf{r}'). \tag{2.2}$$

In terms of the Nambu spinors

$$\Psi = \begin{pmatrix} \psi_\uparrow \\ \psi_\downarrow^\dagger \end{pmatrix}, \quad \Psi^\dagger = \left(\psi_\uparrow^\dagger, \psi_\downarrow\right), \tag{2.3}$$

which satisfy

$$\{\Psi_i(\mathbf{r}), \Psi_j^\dagger(\mathbf{r}')\} = \delta_{ij}\delta(\mathbf{r} - \mathbf{r}'), \tag{2.4}$$

---

[2] Due to the axial symmetry of the vortex line, it is sufficient to consider a two-dimensional BdG problem with a point vortex.

the Hamiltonian becomes

$$
\begin{aligned}
\hat{H}_\nu = & \int d^2 r \, \Psi^\dagger \left(-\frac{\nabla^2}{2} + V(r) - \mu \right) \tau_3 \Psi \\
& + \int d^2 r \, \Psi^\dagger \Delta(r) \left(e^{ik\varphi/2}(p_x + ip_y)^\nu e^{ik\varphi/2} \tau_+ + e^{-ik\varphi/2}(p_x - ip_y)^\nu e^{-ik\varphi/2} \tau_- \right) \Psi.
\end{aligned}
\tag{2.5}
$$

For the remainder of this chapter, we will focus on *non-chiral* s-wave superfluids with an MQV, in which case the Hamiltonian (2.5) simplifies to

$$
\hat{H} \equiv \hat{H}_{\nu=0} = \int d^2 r \, \Psi^\dagger \left(-\nabla^2/2 + V(r) - \mu \right) \tau_3 \Psi + \int d^2 r \, \Psi^\dagger \Delta(r) \left(e^{ik\varphi} \tau_+ + e^{-ik\varphi} \tau_- \right) \Psi, \tag{2.6}
$$

where τ_i are Pauli matrices, $\tau_\pm = (\tau_1 \pm i\tau_2)/2$, $\hbar$ and the elementary fermion mass are set to unity, and μ is the chemical potential. In principle, $\Delta(r)$ should be determined self-consistently but since our results depend only weakly on its form, we use a fixed pairing term that for our numerical analysis is taken to be $\Delta(r) = \Delta_0 \tanh(r/\xi)$, where $\xi = k_F/\Delta_0$ and Δ_0 is the BCS gap.

Due to the pairing term, neither the total particle number

$$
\hat{N} = \int d^2 r \, \Psi^\dagger \tau_3 \Psi \tag{2.7}
$$

nor the OAM

$$
\hat{L}_z = \int d^2 r \, \Psi^\dagger \left(-i \frac{\partial}{\partial \varphi} \right) \Psi \tag{2.8}
$$

commutes with $\hat{H}$, and so neither are separately conserved. Instead, as pointed out in [121, 122], the generalized OAM operator $\hat{\mathscr{L}} = \hat{L}_z - k\hat{N}/2$ generates a symmetry and thus, the BdG ground state and all quasi-particle excitations carry a sharp $\hat{\mathscr{L}}$ quantum number. More generally, in a chiral SF with pairing symmetry $\sim (p_x + ip_y)^\nu$ and with an MQV, the conserved operator is $\hat{L}_z - (k+\nu)\hat{N}/2$. In order to see this, it is convenient to work in polar coordinates, where

$$
(p_x \pm ip_y) = -ie^{\pm i\varphi} \left(\frac{\partial}{\partial r} \pm \frac{i}{r} \frac{\partial}{\partial \varphi} \right). \tag{2.9}
$$

In addition, the anti-commutation relations Eq. (2.4) lead to the following identity

$$
[\Psi^\dagger \hat{A} \Psi, \Psi^\dagger \hat{B} \Psi] = \Psi^\dagger [\hat{A}, \hat{B}] \Psi. \tag{2.10}
$$

Putting everything together, it is now straightforward to show that

$$[\hat{L}_z, \hat{H}_\nu] = \Delta(r) \left[e^{ik\varphi/2}(p_x + ip_y)^\nu e^{ik\varphi/2}\tau_+ - e^{-ik\varphi/2}(p_x - ip_y)^\nu e^{-ik\varphi/2}\tau_- \right] \times (k + \nu),$$

$$[\hat{N}, \hat{H}_\nu] = \Delta(r) \left[e^{ik\varphi/2}(p_x + ip_y)^\nu e^{ik\varphi/2}\tau_+ - e^{-ik\varphi/2}(p_x - ip_y)^\nu e^{-ik\varphi/2}\tau_- \right] \times 2. \qquad (2.11)$$

From this it follows that

$$\hat{\mathscr{L}} = \hat{L}_z - \frac{k + \nu}{2}\hat{N} \qquad (2.12)$$

commutes with $\hat{H}_\nu$. The above calculation easily generalizes to the case of spin-triplet chiral SFs (where ν is odd) with MQVs, where the same operator Eq. (2.12) is conserved. While the OAM of vortex-free chiral paired SFs ($k = 0$) was analysed in [90, 123, 124], here we focus on s-wave SFs ($\nu = 0$) with MQVs, noting that our results readily generalize to chiral states with MQVs.

Physically, $\hat{\mathscr{L}}$ measures the deviation of OAM in the BCS ground state from its expectation value

$$L_z^{\mathrm{BEC}} = kN/2 \qquad (2.13)$$

in the BEC regime (with $N = \langle \hat{N} \rangle$). The suppression of L_z in the BCS regime will hence be reflected in the eigenvalue $\mathscr{L}$ of $\hat{\mathscr{L}}$, evaluated in the ground state of the BdG Hamiltonian. We consider a disc geometry with Dirichlet boundary conditions, i.e.

$$V(r) = \begin{cases} 0, & r \leq R \\ \\ \infty, & r > R \end{cases} \qquad (2.14)$$

Expanding the fermionic operators in a single particle basis as

$$\psi_\sigma(\mathbf{r}) = \sum_{n,l} a_{nl\sigma}\Phi_{nl}(\mathbf{r}) \qquad (2.15)$$

where Φ_{nl} satisfies

$$\left[-\nabla^2/2 + V(r) - \mu \right] \Phi_{nl}(\mathbf{r}) = \epsilon_{nl}\Phi_{nl}(\mathbf{r}), \qquad (2.16)$$

the Hamiltonian becomes

$$\hat{H} = \sum_l \sum_{n,n'} \begin{pmatrix} a^\dagger_{n,l+k\uparrow} \\ a_{n,-l\downarrow} \end{pmatrix}^T \begin{pmatrix} \epsilon_{n,l+k}\delta_{n,n'} & \Delta^{(l)}_{n,n'} \\ \Delta^{(l)*}_{n,n'} & -\epsilon_{n,-l}\delta_{n,n'} \end{pmatrix} \begin{pmatrix} a_{n',l+k\uparrow} \\ a^\dagger_{n',-l\downarrow} \end{pmatrix} \qquad (2.17)$$

with

$$\Delta_{n,n'}^{(l)} = \int d^2r \, \Phi_{n,l+k}^* \Delta(r) e^{ik\varphi} \Phi_{n',-l}^* \tag{2.18}$$

and where n, l are the radial and angular momentum quantum numbers respectively. Denoting the single-particle Hamiltonian matrix as $H^{(l)}$, particle-hole (PH) symmetry connects the different l-sectors through

$$H^{(l)*} = -CH^{(-l-k)}C^{-1} \tag{2.19}$$

such that the spectrum is PH symmetric about $l = -k/2$.

2.3   The BCS Ground State

In the absence of a vortex ($k = 0$), the ground state wave function in the weakly paired BCS regime can be straightforwardly found through the conventional Bogoliubov transformation. However, in the presence of an MQV, the ground state of the BdG Hamiltonian is constructed using a generalized Bogoliubov transformation [125, 126]. In this section, we explicitly construct the ground state wave function and derive the eigenvalue $\mathscr{L}$ of the generalized OAM operator $\hat{\mathscr{L}}$, evaluated in the BCS ground state. Before delving into the details of this calculation, it is useful to first sketch the key steps involved in order to understand the unusual ground state structure in the presence of an MQV.

2.3.1   Construction of the Ground State I: the simple version

In order to proceed with the derivation of the BCS ground state wave function, we must first regularize the BdG Hamiltonian $H^{(l)}$ by introducing a cutoff $M \gg 1$ on n, n'. Generically, $H^{(l)}$ will have a different number of positive and negative eigenvalues, $M_+^{(l)}$ and $M_-^{(l)}$ respectively. The (unitary) Bogoliubov transformation is then written as

$$\begin{pmatrix} b_m^{(l)} \\ d_{\bar{m}}^{(l)\dagger} \end{pmatrix} = \sum_{n=1}^{M} \begin{pmatrix} S_{1,mn}^{(l)} & S_{2,mn}^{(l)} \\ S_{3,\bar{m}n}^{(l)} & S_{4,\bar{m}n}^{(l)} \end{pmatrix} \begin{pmatrix} a_{n,l+k\uparrow} \\ a_{n,-l\downarrow}^{\dagger} \end{pmatrix}, \tag{2.20}$$

where $m = 1, \ldots M_+^{(l)}$, $\bar{m} = 1, \ldots M_-^{(l)}$, and $M_+^{(l)} + M_-^{(l)} = 2M$. The Bogoliubov operator $b_m^{(l)}$ annihilates a quasi-particle with positive energy $E_m^{(l)}$, $\mathscr{L}$-charge[3] $l + k/2$, and spin $\uparrow$. Alternatively, by PH symmetry we can interpret it as the creation operator for a spin $\downarrow$ state with negative energy $-E_m^{(l)}$ and $\mathscr{L}$-charge $-l - k/2$. In addition, we introduce the operator $d_{\bar{m}}^{(l)}$ that creates a spin $\uparrow$ state with negative energy $E_{M_+^{(l)}+\bar{m}}^{(l)}$ and $\mathscr{L}$-charge $l + k/2$.

In terms of these operators, the ground state $|BCS\rangle \sim \otimes_l |BCS\rangle_l$ is defined as the vacuum for all positive energy quasi-particles and thus satisfies $b_m^{(l)} |BCS\rangle = 0$ and $d_{\bar{m}}^{(l)} |BCS\rangle = 0$. For systems with $M_+^{(l)} = M_-^{(l)}$, the ground state $|BCS\rangle$ closely resembles a Fermi sea with all negative energy states occupied

$$|BCS\rangle \sim \otimes_l \prod_{m=1}^{M} b_m^{(l)} \prod_{\bar{m}=1}^{M} d_{\bar{m}}^{(l)} |0\rangle, \tag{2.21}$$

where $|0\rangle$ is the Fock vacuum for $a_{n,l\sigma}$. This ground state can be understood in terms of Cooper pairs, where spin $\uparrow$ quasi-particles with $\mathscr{L}$-charge $v = l + k/2$ (created by $d^{(l)}$) are paired with quasi-particles of the opposite spin $\downarrow$ and with the opposite $\mathscr{L}$-charge $-v$ (created by $b^{(l)}$). Re-expressing the quasi-particle operators in terms of elementary fermions, we find a familiar exponential form,

$$|BCS\rangle_l = \exp\left(a_{n,l+k\uparrow}^\dagger K_{n,n'}^{(l)} a_{n',-l\downarrow}^\dagger\right) |0\rangle, \tag{2.22}$$

where $K^{(l)}$ is an $M \times M$ matrix (derived in Sec. 2.3.2), and the sum over n, n' is implicit. Since $b^{(l)}$ and $d^{(l)}$ carry opposite $\mathscr{L}$-charge, the ground state Eq. (2.21) has a vanishing $\mathscr{L}$ eigenvalue.

When $M_+^{(l)} \neq M_-^{(l)}$ however, the ground state is no longer given by Eq. (2.21) since there will exist an imbalance between the number of quasi-particles with $\mathscr{L}$-charge $l + k/2$ and with $\mathscr{L}$-charge $-l - k/2$. This mismatch is quantified by the spectral asymmetry of the energy spectrum

$$\eta_l = \sum_m \text{sgn}(E_m^{(l)}) = M_+^{(l)} - M_-^{(l)}, \tag{2.23}$$

where $\{E_m^{(l)}\}_{m \in \mathbb{N}}$ are the eigenvalues of $H^{(l)}$. In order to demonstrate that the presence of a non-trivial η_l leads to unpaired fermions in the ground state, we perform a judiciously chosen unitary rotation on $a_{n,l\sigma}$ to a new basis of fermions $\tilde{a}_{j,l\sigma}$ via a conventional (non-Bogoliubov) rotation

---

[3] The quasi-particle operators carry a sharp $\mathscr{L}$-charge $l - k/2$, rather than an l quantum number. Nevertheless, since the former differs from l by a constant shift, it is convenient to continue labelling the states by l.

which does not mix creation and annihilation operators (see Sec 2.3.2). Through a separate unitary rotation, we simultaneously transform the Bogoliubov operators $b^{(l)}, d^{(l)}$ into a new basis $\tilde{b}^{(l)}, \tilde{d}^{(l)}$.

The new fermions $\tilde{a}$ and Bogoliubov quasi-particles $\tilde{b}, \tilde{d}$ are related through a Bogoliubov transformation which, as always, takes the schematic form $\tilde{b} = U\tilde{a} + V\tilde{a}^\dagger$, where the matrix-valued coefficients U, V satisfy $|U|^2 + |V|^2 = 1$. Following [126], we find that the preceding transformations naturally distinguish between operators for which either U vanishes exactly: $U = 0, V = 1$ (*occupied* levels), or V vanishes exactly: $V = 0, U \neq 0$ (*empty* levels), with the remaining operators, for which both $U, V \neq 0$, describing *paired* levels. In the new basis, the ground state is superficially similar to Eq. (2.21) since it can be expressed as

$$|BCS\rangle \sim \otimes_l \prod_m{}' \tilde{b}_m^{(l)} \prod_{\bar{m}}{}' \tilde{d}_{\bar{m}}^{(l)} |0\rangle . \tag{2.24}$$

Importantly however, the restricted products here run only over paired and occupied levels. Bogoliubov operators $\tilde{b}, \tilde{d}$ for empty states, which are linear super-positions of $\tilde{a}$'s, annihilate the bare vacuum $|0\rangle$ and are thus disallowed in Eq. (2.24). Conversely, occupied states contribute to Eq. (2.24) but since these states create unitarily rotated fermions with certainty, $\tilde{b}, \tilde{d} \sim \tilde{a}^\dagger$, they do not participate in pairing.

The eigenvalue of $\hat{\mathscr{L}}$ can now be obtained directly from Eq. (2.24) by summing the individual contributions of the filled quasi-particle states and noting that $\tilde{b}^{(l)}, \tilde{d}^{(l)}$ carry the same $\mathscr{L}$-charges as $b^{(l)}, d^{(l)}$. While contributions from the paired levels cancel out, the occupied levels lead to

$$\mathscr{L} = -\frac{1}{2} \sum_l \left(l + \frac{k}{2} \right) \eta_l, \tag{2.25}$$

since the number of occupied (and also empty) $\tilde{b}_m^{(l)}$ and $\tilde{d}_{\bar{m}}^{(l)}$ levels are $M_\downarrow^{(l)}$ and $M_\uparrow^{(l)}$ respectively, with $M_{\uparrow,\downarrow}^{(l)} = \max(0, M - M_{+,-}^{(l)})$ such that the spectral asymmetry is given by $\eta_l = 2(M_\downarrow^{(l)} - M_\uparrow^{(l)})$. In order to establish these relations between the number of unpaired levels and the spectral asymmetry, we have borrowed our results from the detailed calculation of the ground state wave function, which we now proceed to discuss.

2.3.2 Construction of the Ground State II: the detailed version

While the preceding qualitative discussion allowed us to understand the presence of both paired and unpaired levels in the BCS ground state with an MQV, in order to quantify the number of unpaired levels and their relation to the spectral asymmetry, it is necessary to explicitly construct the ground state. A generalized framework for deriving the ground state of a paired Hamiltonian through a Bogoliubov transformation was constructed in [125]. Here, we present a self-contained discussion and obtain the ground state wave functions for SFs with MQVs. While we focus on s-wave SFs here, this construction can be readily generalized to chiral SFs with vortices as well.

The eigenstates $(u, v)^T$ of the BdG Hamiltonian satisfy

$$\sum_{n'=1}^{M} H_{n,n'}^{(l)} \begin{pmatrix} u_{n'm}^{(l)} \\ v_{n'm}^{(l)} \end{pmatrix} = E_m^{(l)} \begin{pmatrix} u_{nm}^{(l)} \\ v_{nm}^{(l)} \end{pmatrix}, \tag{2.26}$$

where we have introduced a cut-off $M \gg 1$ on the radial quantum numbers n, n'. As before, suppose the number of positive and negative eigenvalues of $H^{(l)}$ are $M_+^{(l)}$ and $M_-^{(l)}$ respectively, with $M_+^{(l)} + M_-^{(l)} = 2M$. In the absence of spectral asymmetry, $M_+^{(l)} = M_-^{(l)}$, but in general, $M_+^{(l)} \neq M_-^{(l)}$. Let us now order the energies such that $E_1^{(l)} \geq \cdots \geq E_{2M}^{(l)}$, with

$$E_m^{(l)} > 0, \ m = 1, \ldots, M_+^{(l)}, \qquad E_{m+M_+^{(l)}}^{(l)} < 0, \ m = 1, \ldots, M_-^{(l)}. \tag{2.27}$$

Next, we introduce the (inverse) Bogoliubov transformation

$$a_{n,l+k\uparrow} = \sum_{m=1}^{M_+^{(l)}} u_{nm}^{(l)} b_m^{(l)} + \sum_{\bar{m}}^{M_-^{(l)}} u_{n,\bar{m}+M_+^{(l)}}^{(l)} d_{\bar{m}}^{(l)\dagger},$$

$$a_{n,-l\downarrow}^{\dagger} = \sum_{m=1}^{M_+^{(l)}} v_{nm}^{(l)} b_m^{(l)} + \sum_{\bar{m}}^{M_-^{(l)}} v_{n,\bar{m}+M_+^{(l)}}^{(l)} d_{\bar{m}}^{(l)\dagger}. \tag{2.28}$$

Here, $b_m^{(l)}$ are Bogoliubov operators that annihilate a spin $\uparrow$ state with energy $E_m^{(l)}$ and $\mathscr{L}$-charge $l + k/2$. We can exploit the PH symmetry of the system to alternatively interpret $b_m^{(l)}$ as the creation operator for a spin $\downarrow$ state with energy $-E_m^{(l)}$ and $\mathscr{L}$-charge $-l - k/2$. In addition, we have introduced another set of Bogoliubov operators

$$d_{\bar{m}}^{(l)} \equiv b_{\bar{m}+M_+^{(l)}}^{(l)\dagger}, \ \bar{m} = 1, \ldots, M_-^{(l)}, \tag{2.29}$$

such that the operator $d_{\bar{m}}^{(l)}$ creates a spin $\uparrow$ state with energy $E_{\bar{m}+M_+^{(l)}}^{(l)} < 0$ and $\mathscr{L}$-charge $l + k/2$. As a matter of principle, we note that since the pairing Hamiltonian does not commute with the angular momentum operator $\hat{L}_z$, the Bogoliubov quasi-particles b and d carry $\mathscr{L}$-charge rather than an l quantum number and thus the energy eigenvalues $E_k^{(l)}$ should be labelled instead by their $\mathscr{L}$ quantum number, $v = l - k/2$. However, since v is simply l shifted by a constant, it is more convenient to continue labelling the eigenvalues and quasi-particles by l.

The BCS ground state is defined as the vacuum with respect to all positive energy quasi-particles, $|BCS\rangle \sim \otimes_l |BCS\rangle_l$, and must thus satisfy

$$b_m^{(l)} |BCS\rangle = 0 \ (m = 1, \ldots, M_+^{(l)}),$$

$$d_{\bar{m}}^{(l)} |BCS\rangle = 0 \ (\bar{m} = 1, \ldots, M_-^{(l)}). \tag{2.30}$$

When $M_+^{(l)} = M_-^{(l)}$, the ground state may be expressed as the state with all negative energy excitations occupied, with

$$|BCS\rangle_l = \prod_{m=1}^{M} b_m^{(l)} \prod_{\bar{m}=1}^{M} d_{\bar{m}}^{(l)} |0\rangle, \tag{2.31}$$

where $|0\rangle$ is the Fock vacuum with respect to elementary fermions $a_{n,l\sigma}$. The paired nature of this state is evident in the wave function Eq. (2.31) as expressed in terms of the Bogoliubov operators, since a spin $\downarrow$ quasi-particle with $\mathscr{L}$-charge $-l - k/2$ (created by $b_m^{(l)}$) is paired with a spin $\uparrow$ quasi-particle with $\mathscr{L}$-charge $l + k/2$ (created by $d_{\bar{m}}^{(l)}$).

However, when $M_+^{(l)} \neq M_-^{(l)}$, there will be some states left unpaired as a consequence of the asymmetry in the spectrum. In order to elucidate the nature of the ground state in the presence of unpaired fermions, it is instructive to transform to a particular bases of elementary fermions and of Bogoliubov quasi-particles in which the structure of the ground state becomes especially transparent. Before presenting technical details of this procedure, we briefly describe the steps involved.

Fig. 2.2 illustrates the series of transformations that we perform in order to express $|BCS\rangle$ in a transparent form. First, we unitarily rotate the elementary fermions operators $a_{n,l\sigma}$ into a new basis of fermionic operators $\tilde{a}_{n,l\sigma}$ (where the $\tilde{a}$'s are linear combinations of only a's but not
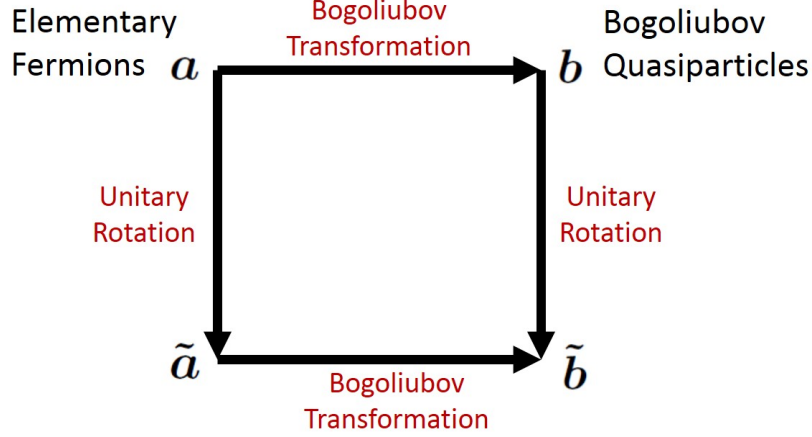
Figure 2.2: Relations between different fermionic operators used in this section.

$a^\dagger$'s). While the states destroyed by operators $\tilde{a}_{n,l\sigma}$ carry well defined spin and angular momentum quantum numbers, σ and l respectively, they are not energy eigenstates of the non-interacting Hamiltonian. In a similar spirit, we will unitarily rotate the quasi-particle operators b, d into a new basis of quasi-particle operators $\tilde{b}, \tilde{d}$. Importantly, since this operation does not mix quasi-particle creation and annihilation operators, the ground state is still defined as the vacuum with respect to positive energy excitations and hence satisfies $\tilde{b}_m^{(l)} |BCS\rangle = 0$ and $\tilde{d}_{\bar{m}}^{(l)} |BCS\rangle = 0$.

Having established these new bases, we will then relate the rotated fermions $\tilde{a}$ to the rotated quasi-particles $\tilde{b}, \tilde{d}$ through a Bogoliubov transformation akin to Eq. (2.28). This relation then allows us to express $|BCS\rangle$ in terms of the rotated fermions $\tilde{a}$ in a manner that makes explicit the nature of pairing in the ground state since it naturally distinguishes between paired and unpaired states. We note that the purpose of these transformations is not to diagonalize the BdG Hamiltonian $H^{(l)}$ (which is diagonalized by the original Bogoliubov transformation Eq. (2.28)) but rather to explicitly construct the ground state wave function for an s-wave SF with an MQV.

We now discuss the above procedure in detail. To begin, we first invert Eq. (2.28) and write the unitary Bogoliubov transformation as

$$
\begin{pmatrix} b_m^{(l)} \\ d_{\bar{m}}^{(l)\dagger} \end{pmatrix} = \sum_{n=1}^{M} \begin{pmatrix} S_{1,mn}^{(l)} & S_{2,mn}^{(l)} \\ S_{3,\bar{m}n}^{(l)} & S_{4,\bar{m}n}^{(l)} \end{pmatrix} \begin{pmatrix} a_{n,l+k\uparrow} \\ a_{n,-l\downarrow}^{\dagger} \end{pmatrix},
\tag{2.32}
$$

where $S_1^{(l)}, S_2^{(l)}$ are $M_+^{(l)} \times M$ and $S_3^{(l)}, S_4^{(l)}$ are $M_-^{(l)} \times M$ dimensional matrices, respectively. Next, we perform a singular value decomposition on the matrices S_2 and S_3, $S_i^{(l)} = U_i^{(l)} \Sigma_i^{(l)} V_i^{(l)\dagger}$ where $U_i^{(l)}, V_i^{(l)}$ are unitary matrices and $\Sigma_i^{(l)}$ is a rectangular diagonal matrix with non-negative real entries. We then perform unitary rotations on the elementary fermions a and the Bogoliubov quasi-particles, b and d,

$$\tilde{a}_{j,l+k\uparrow} = \sum_{n=1}^{M} V_{3,jn}^{(l)\dagger} a_{n,l+k\uparrow} \quad j = 1, \ldots, M,$$

$$\tilde{a}_{j,-l\downarrow}^{\dagger} = \sum_{n=1}^{M} V_{2,jn}^{(l)\dagger} a_{n,-l\downarrow}^{\dagger} \quad j = 1, \ldots, M,$$

$$\tilde{b}_j^{(l)} = \sum_{n=1}^{M_+^{(l)}} U_{2,jn}^{(l)\dagger} b_n^{(l)} \quad j = 1, \ldots, M_+^{(l)},$$

$$\tilde{d}_j^{(l)\dagger} = \sum_{n=1}^{M_-^{(l)}} U_{3,jn}^{(l)\dagger} d_n^{(l)\dagger} \quad j = 1, \ldots, M_-^{(l)}. \tag{2.33}$$

It is straightforward to check that these transformed operators satisfy the canonical anti-commutation relations. In this new basis, the Bogoliubov transformation is expressed as

$$\begin{pmatrix} \tilde{b}_m^{(l)} \\ \tilde{d}_{\bar{m}}^{(l)\dagger} \end{pmatrix} = \sum_{m=1}^{M} \begin{pmatrix} \Lambda_{1,mn}^{(l)} & \Sigma_{2,mn}^{(l)} \\ \Sigma_{3,\bar{m}n}^{(l)} & \Lambda_{4,\bar{m}n}^{(l)} \end{pmatrix} \begin{pmatrix} \tilde{a}_{n,l+k\uparrow} \\ \tilde{a}_{n,-l\downarrow}^{\dagger} \end{pmatrix}, \tag{2.34}$$

where $\Lambda_1^{(l)} = U_2^{(l)\dagger} S_1^{(l)} V_3^{(l)}$ and $\Lambda_4^{(l)} = U_3^{(l)\dagger} S_4^{(l)} V_2^{(l)}$. Before proceeding with the construction of the ground state, it is necessary to establish some properties of $\Sigma_2^{(l)}$ and $\Sigma_3^{(l)}$. In particular, we will show now that in the presence of a non-trivial spectral asymmetry $\eta_l = M_+^{(l)} - M_-^{(l)}$, either one of $\Sigma_2^{(l)}$ or $\Sigma_3^{(l)}$ have $|\eta_l|/2$ entries on the diagonal which are equal to one. To prove this, let us assume without loss of generality that $M_+^{(l)} < M < M_-^{(l)}$. Since the Bogoliubov transformation is unitary, the transformation matrix

$$S^{(l)} \equiv \begin{pmatrix} S_1^{(l)} & S_2^{(l)} \\ S_3^{(l)} & S_4^{(l)} \end{pmatrix} \tag{2.35}$$

satisfies $S^{(l)\dagger} S^{(l)} = S^{(l)} S^{(l)\dagger} = \mathbb{I}_{2M \times 2M}$. This leads to the conditions

$$S_1^{(l)} S_1^{(l)\dagger} + S_2^{(l)} S_2^{(l)\dagger} = \mathbb{I}_{M_+^{(l)} \times M_+^{(l)}},$$

$$S_1^{(l)\dagger} S_1^{(l)} + S_3^{(l)\dagger} S_3^{(l)} = \mathbb{I}_{M \times M}. \tag{2.36}$$

Since $S_3^{(l)\dagger}S_3^{(l)}$ and $S_2^{(l)}S_2^{(l)\dagger}$ are Hermitian matrices, they have real eigenvalues and eigenvectors,

$$\left(S_2^{(l)}S_2^{(l)\dagger}\right) y_{2j}^{(l)} = \lambda_{2j}^{(l)} y_{2j}^{(l)} \quad j = 1, \ldots, M_+^{(l)},$$
$$\left(S_3^{(l)\dagger}S_3^{(l)}\right) y_{3j}^{(l)} = \lambda_{3j}^{(l)} y_{3j}^{(l)} \quad j = 1, \ldots, M. \tag{2.37}$$

Eq. (2.36) then implies

$$\left(S_1^{(l)}S_1^{(l)\dagger}\right) y_{2j}^{(l)} = \left(1 - \lambda_{2j}^{(l)}\right) y_{2j}^{(l)} \quad j = 1, \ldots, M_+^{(l)},$$
$$\left(S_1^{(l)\dagger}S_1^{(l)}\right) y_{3j}^{(l)} = \left(1 - \lambda_{3j}^{(l)}\right) y_{3j}^{(l)} \quad j = 1, \ldots, M. \tag{2.38}$$

The singular values of $S_1^{(l)}$, however, are the square roots of the non-zero eigenvalues of both $S_1^{(l)\dagger}S_1^{(l)}$ and $S_1^{(l)}S_1^{(l)\dagger}$. Since $S_1^{(l)\dagger}S_1^{(l)}$ has exactly $M - M_+^{(l)}$ more eigenvalues than $S_1^{(l)}S_1^{(l)\dagger}$, those extra eigenvalues must necessarily be zero. This in turn implies that $S_3^{(l)\dagger}S_3^{(l)}$ has $M_\uparrow^{(l)} = M - M_+^{(l)}$ unity eigenvalues, or equivalently, that $\Sigma_3^{(l)}$ has precisely $M_\uparrow^{(l)}$ unity entries on the diagonal. In addition, since $\Sigma_3^{(l)}$ is a rectangular diagonal $M_-^{(l)} \times M$ matrix, its last $M_-^{(l)} - M = M - M_+^{(l)} = M_\uparrow^{(l)}$ rows contain only zeros.

Following this discussion, in general for any $M_+^{(l)}$ and $M_-^{(l)}$ we can define the quantities $M_\uparrow^{(l)} = \max\left(M - M_+^{(l)}, 0\right)$ and $M_\downarrow^{(l)} = \max\left(M - M_-^{(l)}, 0\right)$. Using the fact that $M_+^{(l)} + M_-^{(l)} = 2M$, we can also show that $M_+^{(l)} = M + M_\downarrow^{(l)} - M_\uparrow^{(l)}$ and $M_-^{(l)} = M - M_\downarrow^{(l)} + M_\uparrow^{(l)}$. From this, it follows that

$$\eta_l = M_+^{(l)} - M_-^{(l)} = 2(M_\downarrow^{(l)} - M_\uparrow^{(l)}) = \begin{cases} 2(M - M_-^{(l)}) > 0, & M_+^{(l)} > M > M_-^{(l)} \\ 0, & M_-^{(l)} = M = M_+^{(l)} \\ 2(M_+^{(l)} - M) < 0, & M_+^{(l)} < M < M_-^{(l)} \end{cases} \tag{2.39}$$

Combining the above results with the unitarity of the Bogoliubov transformation Eq. (2.34), we conclude that in the presence of spectral asymmetry we will have cases where $\tilde{b}^{(l)} = \tilde{a}_{-l\downarrow}^{\dagger}$ or $\tilde{d}^{(l)} = \tilde{a}_{l+k\uparrow}^{\dagger}$, which will give rise to unpaired fermions in the ground state.

Specifically, we find that the Bogoliubov transformation Eq. (2.34) splits into three classes

$$\tilde{b}_m = \tilde{a}^\dagger_{m,-l\downarrow} \quad m = 1, \ldots, M_\downarrow,$$

$$\tilde{d}^\dagger_{\bar{m}} = \tilde{a}_{\bar{m},l+k\uparrow} \quad \bar{m} = 1, \ldots, M_\uparrow, \tag{2.40}$$

$$\tilde{b}_{M_\downarrow+m} = \sum_{n=1}^{M-M_\uparrow} (\Lambda_1)_{M_\downarrow+m,M_\uparrow+n} \, \tilde{a}_{M_\uparrow+n,l+k\uparrow} + \sum_{n=1}^{M-M_\downarrow} (\Sigma_2)_{M_\downarrow+m,M_\downarrow+n} \, \tilde{a}^\dagger_{M_\downarrow+n,-l\downarrow}, \tag{2.41}$$

$$m = 1, \ldots, M - M_\downarrow - M_\uparrow,$$

$$\tilde{d}^\dagger_{M_\uparrow+m} = \sum_{n=1}^{M-M_\uparrow} (\Sigma_3)_{M_\uparrow+m,M_\uparrow+n} \, \tilde{a}_{M_\uparrow+n,l+k\uparrow} + \sum_{n=1}^{M-M_\downarrow} (\Lambda_4)_{M_\uparrow+m,M_\downarrow+n} \, \tilde{a}^\dagger_{M_\downarrow+n,-l\downarrow}, \tag{2.42}$$

$$m = 1, \ldots, M - M_\downarrow - M_\uparrow, \tag{2.43}$$

and

$$\tilde{b}_{M-M_\uparrow+m} = \sum_{n=1}^{M-M_\uparrow} (\Lambda_1)_{M-M_\uparrow+m,M_\uparrow+n} \, \tilde{a}_{M_\uparrow+n,l+k\uparrow}, \quad m = 1, \ldots, M_\downarrow,$$

$$\tilde{d}^\dagger_{M-M_\downarrow+m} = \sum_{n=1}^{M-M_\downarrow} (\Lambda_4)_{M-M_\downarrow+m,M_\downarrow+n} \, \tilde{a}^\dagger_{M_\downarrow+n,-l\downarrow}, \quad m = 1, \ldots, M_\uparrow, \tag{2.44}$$

where we have omitted the (l) superscript to simplify notation. Physically, these three classes correspond to three different kinds of quasi-particle operators [126]:

- Occupied levels Eq. (2.40) are those where $\tilde{b} = \tilde{a}^\dagger_\downarrow$ or $\tilde{d} = \tilde{a}^\dagger_\uparrow$. These operators create a unitarily rotated fermion with unit probability.

- Paired levels Eq. (2.41) are those for which $\tilde{b}$ and $\tilde{d}$ are non-trivial superpositions of $\tilde{a}_\uparrow$ and $\tilde{a}^\dagger_\downarrow$.

- Empty levels Eq. (2.44) $\tilde{b}$ and $\tilde{d}$ are linear superpositions of $\tilde{a}_\uparrow$'s and $\tilde{a}_\downarrow$'s, respectively. These operators annihilate the Fock vacuum $|0\rangle$.

The ground state is still the vacuum with respect to all positive energy quasi-particles and, in terms of the unitarily rotated Bogoliubov quasi-particles, it is given by $|BCS\rangle \sim \otimes_l |BCS\rangle_l$ with

$$|BCS\rangle_l = \prod_m{}' \tilde{b}_m^{(l)} \prod_{\bar{m}}{}' \tilde{d}_{\bar{m}}^{(l)} |0\rangle \tag{2.45}$$

where the restricted product runs over all paired and occupied levels. Since empty levels annihilate

the Fock vacuum, they are not included in Eq. (2.45). By construction this state satisfies

$$\tilde{b}_m^{(l)} |BCS\rangle_l = 0, \quad \tilde{d}_{\bar{m}}^{(l)} |BCS\rangle_l = 0, \tag{2.46}$$

for all $m = 1, \ldots, M_+^{(l)}$ and $\bar{m} = 1, \ldots, M_-^{(l)}$. We can further simplify the ground state since it

factorizes into unpaired and paired terms,

$$|BCS\rangle_l = \underbrace{\left(\prod_{j=1}^{M_\downarrow^{(l)}} \tilde{a}_{j,-l\downarrow}^\dagger \right) \left(\prod_{j=1}^{M_\uparrow^{(l)}} \tilde{a}_{j,l+k\uparrow}^\dagger \right)}_{\text{unpaired}} \underbrace{\left(\prod_{m>M_\uparrow^{(l)}}^{M}{}' \prod_{\bar{m}>M_\downarrow^{(l)}}^{M}{}' \tilde{b}_m^{(l)} \tilde{d}_{\bar{m}}^{(l)} \right)}_{\text{paired}} |0\rangle . \tag{2.47}$$

The first two terms in the product clearly indicate that for $M_\sigma^{(l)} \neq 0$, there are unpaired fermions

in the ground state. Following [125], we can now write the paired part of the ground state in terms

of creation operators $\tilde{a}^\dagger$ of elementary (unitarily rotated) fermions

$$|BCS\rangle_l = \left(\prod_{j=1}^{M_\downarrow^{(l)}} \tilde{a}_{j,-l\downarrow}^\dagger \right) \left(\prod_{j=1}^{M_\uparrow^{(l)}} \tilde{a}_{j,l+k\uparrow}^\dagger \right) \exp\left(\sum_{j>M_\uparrow^{(l)}}^{M} \sum_{j'>M_\downarrow^{(l)}}^{M} \tilde{a}_{j,l+k\uparrow}^\dagger \mathcal{K}_{j,j'}^{(l)} \tilde{a}_{j',-l\downarrow}^\dagger \right) |0\rangle , \tag{2.48}$$

where the kernel $\mathcal{K}$ satisfies

$$\sum_{j'>M_\uparrow^{(l)}}^{M} \Lambda_{1,jj'}^{(l)} \mathcal{K}_{j',j''}^{(l)} = -\Sigma_{2,jj''}^{(l)} , \tag{2.49}$$

with $j, j'' > M_\downarrow^{(l)}$.

With the BCS ground state wave function in hand, we can now reproduce Eq. (2.25), which

encodes the relationship between the spectral asymmetry and the expectation value $\mathscr{L}$ of the

generalized OAM operator in the ground state. Note that we can express the conserved operator

$\hat{\mathscr{L}} = \hat{L} - k\hat{N}/2$ in terms of the elementary fermions as

$$\hat{\mathscr{L}} = \sum_{nl\sigma} \left(l - \frac{k}{2} \right) a_{n,l\sigma}^\dagger a_{n,l\sigma} = \sum_{nl\sigma} \left(l - \frac{k}{2} \right) \tilde{a}_{n,l\sigma}^\dagger \tilde{a}_{n,l\sigma}, \tag{2.50}$$

where the last equality follows since the $\tilde{a}$'s are unitarily related to the a's. Since the set of operators that appear in the exponential part of $|BCS\rangle_l$ anti-commute with those that appear in the products (unpaired fermions), we can consider the action of $\hat{\mathscr{L}}$ on these separately. First, we evaluate the commutator

$$\left[\hat{\mathscr{L}}, \prod_{j=1}^{M_\downarrow^{(l)}} \tilde{a}_{j,-l\downarrow}^\dagger \right] = -M_\downarrow^{(l)} \left(l + \frac{k}{2} \right) \left(\prod_{j=1}^{M_\downarrow^{(l)}} \tilde{a}_{j,-l\downarrow}^\dagger \right), \tag{2.51}$$

and similarly,

$$\left[\hat{\mathscr{L}}, \prod_{j=1}^{M_\uparrow^{(l)}} \tilde{a}_{j,l+k\uparrow}^\dagger \right] = M_\uparrow^{(l)} \left(l + \frac{k}{2} \right) \left(\prod_{j=1}^{M_\uparrow^{(l)}} \tilde{a}_{j,l+k\uparrow}^\dagger \right), \tag{2.52}$$

which follows from the usual anti-commutation relations satisfied by the rotated fermions $\tilde{a}$. Next, we consider the action of $\hat{\mathscr{L}}$ on the exponential (paired) sector of the wave function. This is done by first calculating the contribution from the spin $\uparrow$ sector,

$$\left[\sum_{nl'} \left(l' - \frac{k}{2} \right) \tilde{a}_{n,l'\uparrow}^\dagger \tilde{a}_{n,l'\uparrow}, \left(\sum_{j>M_\uparrow^{(l)}}^{M} \sum_{j'>M_\downarrow^{(l)}}^{M} \tilde{a}_{j,l+k\uparrow}^\dagger \mathcal{K}_{j,j'}^{(l)} \tilde{a}_{j',-l\downarrow}^\dagger \right) \right]$$
$$= \left(l + \frac{k}{2} \right) \sum_{j>M_\uparrow^{(l)}}^{M} \sum_{j'>M_\downarrow^{(l)}}^{M} \tilde{a}_{j,l+k\uparrow}^\dagger \mathcal{K}_{j,j'}^{(l)} \tilde{a}_{j',-l\downarrow}^\dagger, \tag{2.53}$$

and then observing that the contribution from the spin $\downarrow$ sector

$$\left[\sum_{nl'} \left(l' - \frac{k}{2} \right) \tilde{a}_{n,l'\downarrow}^\dagger \tilde{a}_{n,l'\downarrow}, \left(\sum_{j>M_\uparrow^{(l)}}^{M} \sum_{j'>M_\downarrow^{(l)}}^{M} \tilde{a}_{j,l+k\uparrow}^\dagger \mathcal{K}_{j,j'}^{(l)} \tilde{a}_{j',-l\downarrow}^\dagger \right) \right]$$
$$= -\left(l + \frac{k}{2} \right) \sum_{j>M_\uparrow^{(l)}}^{M} \sum_{j'>M_\downarrow^{(l)}}^{M} \tilde{a}_{j,l+k\uparrow}^\dagger \mathcal{K}_{j,j'}^{(l)} \tilde{a}_{j',-l\downarrow}^\dagger, \tag{2.54}$$

exactly compensates for that coming from the spin $\uparrow$ sector. Hence, we see that $\hat{\mathscr{L}}$ commutes with the exponential part of the wave function and so the paired levels do not contribute to $\mathscr{L}$,

$$\left[\hat{\mathscr{L}}, \exp\left(\sum_{j>M_\uparrow^{(l)}}^{M} \sum_{j'>M_\downarrow^{(l)}}^{M} \tilde{a}_{j,l+k\uparrow}^\dagger \mathcal{K}_{j,j'}^{(l)} \tilde{a}_{j',-l\downarrow}^\dagger \right) \right] = 0. \tag{2.55}$$

Since the $\tilde{a}$'s are unitarily related to the a's, $|0\rangle$ is also the Fock vacuum with respect to $\tilde{a}_{j,l\sigma}$.

Putting the above together, we hence find that the eigenvalue $\mathscr{L}$ of the operator $\hat{\mathscr{L}}$ when evaluated in the ground state $|BCS\rangle \sim \otimes_l |BCS\rangle_l$, with $|BCS\rangle_l$ given by Eq. (2.48), is

$$\mathscr{L} = \sum_l \left(l + \frac{k}{2}\right)\left(M_\uparrow^{(l)} - M_\downarrow^{(l)}\right) = -\frac{1}{2}\sum_l \left(l + \frac{k}{2}\right)\eta_l,$$

where $\eta_l = 2(M_\downarrow^{(l)} - M_\uparrow^{(l)})$. The above relation between the spectral asymettry and $\mathscr{L}$ Eq. (2.25) has previously appeared in the literature in the context of chiral SFs [90, 123], where k is replaced by the chirality ν. Physically, Eq. (2.25) quantifies the contribution of unpaired fermions to the OAM.

2.4   Vortex Core States

The physics originating from unpaired fermions in the ground state of a paired state was previously identified and studied in nuclear physics [126], FFLO superfluids [127], and chiral superfluids paired in higher partial waves [90, 123, 124, 128, 129]. We now demonstrate that for a weakly-paired s-wave SF with an MQV, a nontrivial η_l and the associated unpaired fermions arise as a consequence of vortex core states.

2.4.1   Analytic Solution for Vortex Core States

In the BCS regime, the spectrum of the vortex core (vc) states for a singly quantized vortex $|k| = 1$ was calculated analytically by Caroli-deGennes-Matricon (CdGM) [101] who found a single branch $E_{\text{vc}}^{(l)}$ (per spin projection) that crosses the Fermi level. This branch is PH symmetric with respect to itself, $E_{\text{vc}}^{(l)} = -E_{\text{vc}}^{(-l-1)}$ and at low energies ($E_{\text{vc}} \ll \Delta_0$) behaves linearly $E_{\text{vc}}^{(l)} = -\omega_0(l + 1/2)$, where the mini-gap $\omega_0 \sim \Delta_0/(k_F\xi)$. By numerically diagonalizing $H^{(l)}$ for $k = 1$, we find that $\eta_l = 0$ for all l and hence there are no unpaired fermions in the BCS ground state of an s-wave paired SF with an elementary vortex. Eq. (2.25) then predicts $\mathscr{L} = 0$ and thus the ground state expectation value $L_z = N/2$, which agrees with self-consistent BdG calculations [99]. The physics here is analogous to that of weakly paired $p + ip$ SFs, where there is a single PH symmetric edge mode that carries no OAM [90, 130, 131].

For an MQV with winding number k, the CdGM method can be generalized and the vortex core spectrum analytically calculated within the BdG framework. For a step-like pair-potential, an explicit solution was obtained previously in [132, 133]. The procedure presented here applies more generally to any pairing term $\Delta(r)$ and agrees with that calculation where the regimes of validity overlap.

We start with an s-wave state with a vortex of vorticity k. The (symmetric) gap function is thus $\Delta(r)e^{ik\varphi}$ where $\lim_{r\to 0} \Delta(r) = 0$ and $\lim_{r\to\infty} \Delta(r) = \Delta_0$. The BdG equations are hence

$$\begin{pmatrix} -\frac{1}{2}\nabla^2 - \mu & \Delta(r)e^{ik\varphi} \\ \Delta(r)e^{-ik\varphi} & \frac{1}{2}\nabla^2 + \mu \end{pmatrix} \begin{pmatrix} u \\ v \end{pmatrix} = E \begin{pmatrix} u \\ v \end{pmatrix}. \tag{2.56}$$

Separating the angular and radial dependence of the BdG solutions, we let

$$u = u(r)e^{i\left(l+\frac{k}{2}\right)\varphi},$$

$$v = v(r)e^{i\left(l-\frac{k}{2}\right)\varphi}, \tag{2.57}$$

where $l \in \mathbb{Z} \left(\mathbb{Z} + \frac{1}{2}\right)$ if $k \in \text{Even(Odd)}$, such that Eq. (2.56) becomes

$$-\frac{1}{2}\left(\frac{\partial^2}{\partial r^2} + \frac{1}{r}\frac{\partial}{\partial r} - \frac{\left(l+\frac{k}{2}\right)^2}{r^2} + 2\mu\right)u(r) + \Delta(r)v(r) = Eu(r),$$

$$\frac{1}{2}\left(\frac{\partial^2}{\partial r^2} + \frac{1}{r}\frac{\partial}{\partial r} - \frac{\left(l-\frac{k}{2}\right)^2}{r^2} + 2\mu\right)v(r) + \Delta(r)u(r) = Ev(r). \tag{2.58}$$

We now rewrite these equations in the form

$$-\frac{1}{2}\left(\frac{\partial^2}{\partial r^2} + \frac{1}{r}\frac{\partial}{\partial r} - \frac{\alpha^2}{r^2} + 2\mu\right)u(r) + \Delta(r)v(r) = \left(E - \frac{\beta}{2r^2}\right)u(r),$$

$$\frac{1}{2}\left(\frac{\partial^2}{\partial r^2} + \frac{1}{r}\frac{\partial}{\partial r} - \frac{\alpha^2}{r^2} + 2\mu\right)v(r) + \Delta(r)u(r) = \left(E - \frac{\beta}{2r^2}\right)v(r), \tag{2.59}$$

where we have defined $\alpha = \sqrt{l^2 + \frac{k^2}{4}}$ and $\beta = lk$.

In order to derive an analytic solution for these coupled equations, we introduce a radius $r = r^*$ such that $\frac{1}{k_F} \ll r^* \ll \xi$, where $k_F = \sqrt{2\mu}$ is the Fermi momentum and $\xi = k_F/\Delta_0$ is the coherence length. We then consider the BdG equations (2.56) separately in the limits where $r \ll r^*$ and where $r \gg r^*$. Demanding that the wave function be continuous, we then match the solutions from these two regimes at $r = r^*$ to arrive at a solution that holds over the entire range.

We first consider the limit where $r \ll r^*$. For physically relevant pairing terms, $\Delta(r) \to 0$ in this limit and we are hence justified in ignoring the pairing term. The BdG equations (2.56) thus decouple in this limit,

$$\left(\frac{\partial^2}{\partial r^2} + \frac{1}{r} \frac{\partial}{\partial r} - \frac{\left(l + \frac{k}{2}\right)^2}{r^2} + 2(\mu + E) \right) u = 0 \,,$$

$$\left(\frac{\partial^2}{\partial r^2} + \frac{1}{r} \frac{\partial}{\partial r} - \frac{\left(l - \frac{k}{2}\right)^2}{r^2} + 2(\mu - E) \right) v = 0 \,. \tag{2.60}$$

The solutions to these equations are Bessel functions parametrized by $\sqrt{2(\mu \pm E)}$. Since we are interested in understanding the nature of the vortex core states close to zero energy, we make an additional approximation and consider energies such that $E \ll \mu$. Reinstating all the proper units, this corresponds to

$$(\mu \pm E)^{1/2} = \sqrt{\frac{\hbar^2}{2m_e}} \left(k_F^2 \pm \frac{2m_e E}{\hbar^2} \right)^{\frac{1}{2}} \approx \sqrt{\frac{\hbar^2}{2m_e}} \left(k_F \pm p \right) \,, \tag{2.61}$$

where we have defined $p = \frac{E m_e}{\hbar^2 k_F}$. Thus, the solutions for $r \ll r^*$ are

$$u(r) = C_1 J_{l + \frac{k}{2}} \left((k_F + p) r \right) \,,$$

$$v(r) = C_2 J_{l - \frac{k}{2}} \left((k_F - p) r \right) \,, \tag{2.62}$$

where C_1 and C_2 are arbitrary constants and where the Bessel functions of the second kind Y are chosen to have vanishing amplitudes since we require a well behaved solution in the limit $r \to 0$.

Next, we consider the case where $r \gg r^*$. In this limit, we expect that the pairing term is approximately constant $\Delta(r) \to \Delta_0$. Hence, we write the BdG solutions as rapidly oscillating Hankel functions enveloped by functions that vary slowly i.e.,

$$\begin{pmatrix} u(r) \\ v(r) \end{pmatrix} = \begin{pmatrix} f(r) H_\alpha^{(1)}(k_F r) \\ g(r) H_\alpha^{(1)}(k_F r) \end{pmatrix} + \begin{pmatrix} \tilde{f}(r) H_\alpha^{(2)}(k_F r) \\ \tilde{g}(r) H_\alpha^{(2)}(k_F r) \end{pmatrix} \,, \tag{2.63}$$

where $H^{(1,2)}(r)$ are Hankel functions of the first and second kind. Substituting this ansatz into the BdG equations (2.56) and considering only the $H^{(1)}$ component of the solution (since the other

follows from this immediately), we find

$$-\frac{1}{2}\left(f''H_\alpha + 2f'H'_\alpha + \frac{1}{r}H_\alpha f'\right) + \Delta H_\alpha g = \left(E - \frac{\beta}{2r^2}\right)fH_\alpha\,,$$

$$\frac{1}{2}\left(g''H_\alpha + 2g'H'_\alpha + \frac{1}{r}H_\alpha g'\right) + \Delta H_\alpha f = \left(E - \frac{\beta}{2r^2}\right)gH_\alpha\,. \tag{2.64}$$

Here, $H_\alpha \equiv H_\alpha^{(1)}$. Since we are in the regime $k_F r \gg 1$, we use the asymptotic expansion for the Hankel functions

$$\frac{\partial}{\partial r}H_\alpha^{(1)}(k_F r) \approx ik_F H_\alpha^{(1)}(k_F r)\,, \tag{2.65}$$

and drop the terms $f'', g'', \frac{f'}{r}, \frac{g'}{r}$, which is justified since we are considering the limit $r \gg \frac{1}{k_F}$. With these further approximations, we find that the slowly varying envelope functions f, g satisfy

$$-ik_F f' + \Delta g = \left(E - \frac{\beta}{2r^2}\right)f\,,$$

$$ik_F g' + \Delta f = \left(E - \frac{\beta}{2r^2}\right)g\,. \tag{2.66}$$

To solve these coupled equations, we treat the right hand side as a perturbation. To zeroth order,

$$-ik_F f' + \Delta g = 0\,,$$

$$ik_F g' + \Delta f = 0\,. \tag{2.67}$$

Imposing the condition that the solutions remain well behaved as $r \to \infty$, we find that the solutions are

$$\begin{pmatrix} f \\ g \end{pmatrix} = B\exp\left(-\frac{1}{k_F}\int_0^r dr'\,\Delta(r')\right)\begin{pmatrix} 1 \\ -i \end{pmatrix}\,. \tag{2.68}$$

In order to find the solution to first order in E, we make the ansatz

$$\begin{pmatrix} f \\ g \end{pmatrix} = B\exp\left(-\frac{1}{k_F}\int_0^r dr'\,\Delta(r')\right)\begin{pmatrix} e^{i\psi(r)} \\ -ie^{-i\psi(r)} \end{pmatrix}\,, \tag{2.69}$$

which when substituted into Eq. (2.66) leads to

$$k_F\psi' - 2\Delta\sin(\psi) = \left(E - \frac{\beta}{2r^2}\right)\,. \tag{2.70}$$

Approximating $\sin(\psi) \approx \psi$, this is equivalent to

$$k_F \psi' - 2\Delta\psi = \left(E - \frac{\beta}{2r^2} \right) , \tag{2.71}$$

the solution to which is

$$\psi(r) = -\frac{e^{\frac{2}{k_F} \int_0^r dr' \, \Delta(r')}}{k_F} \int_r^\infty dr' \left(E - \frac{\beta}{2r'^2} \right) e^{-\frac{2}{k_F} \int_0^{r'} dr'' \, \Delta(r'')} . \tag{2.72}$$

With this, we find that the leading order solution of Eq. (2.56) in the limit $r \gg r^*$ is

$$\begin{pmatrix} u(r) \\ v(r) \end{pmatrix} = \begin{pmatrix} B_1 e^{i\psi(r)} H_\alpha^{(1)}(k_F r) + B_2 e^{-i\psi(r)} H_\alpha^{(2)}(k_F r) \\ -iB_1 e^{-i\psi(r)} H_\alpha^{(1)}(k_F r) + iB_2 e^{i\psi(r)} H_\alpha^{(2)}(k_F r) \end{pmatrix} \times \exp\left(-\frac{1}{k_F} \int_0^r dr' \, \Delta(r') \right), \tag{2.73}$$

with $\psi(r)$ given by Eq. (2.72).

We have thus constructed the general solution of the BdG equations (2.56), with the solution in the limits $r \ll r^*$ and $r \gg r^*$ given by Eq. (2.62) and Eq. (2.73) respectively. In order to completely fix the undetermined coefficients and to get the quantization condition on the energy, we demand that the solution be continuous and match the solution in the regime $r < r^*$ with that in the regime $r > r^*$.

Since we wish to extend the solution for $r \ll r^*$ Eq. (2.62) to the vicinity of r^*, we use the asymptotic expansion

$$J_\nu(k_F r) \approx \sqrt{\frac{2}{\pi k_F r}} \cos\left(k_F r + \frac{\nu^2 - \frac{1}{4}}{2k_F r} - \frac{2\nu + 1}{4}\pi \right) , \tag{2.74}$$

such that Eq. (2.62) becomes

$$u(r) \approx C_1 \sqrt{\frac{2}{\pi k_F r}} \cos\left((k_F + p)r + \frac{\left(l + \frac{k}{2}\right)^2 - \frac{1}{4}}{2k_F r} - \frac{2\left(l + \frac{k}{2}\right) + 1}{4}\pi \right) ,$$

$$v(r) \approx C_2 \sqrt{\frac{2}{\pi k_F r}} \cos\left((k_F - p)r + \frac{\left(l - \frac{k}{2}\right)^2 - \frac{1}{4}}{2k_F r} - \frac{2\left(l - \frac{k}{2}\right) + 1}{4}\pi \right) . \tag{2.75}$$

Similarly, we want to extend the solution from the opposite regime $(r \gg r^*)$ towards the vicinity of r^* and we use the asymptotic expansion

$$H_\nu^{(1),(2)}(k_F r) \approx \sqrt{\frac{2}{\pi k_F r}} \exp\left[i\left(k_F r \pm \frac{\nu^2 - \frac{1}{4}}{2k_F r} \mp \frac{2\nu + 1}{4}\pi \right) \right] , \tag{2.76}$$

such that Eq. (2.73) becomes

$$
\begin{pmatrix} u(r) \\ v(r) \end{pmatrix} \approx \sqrt{\frac{2}{\pi k_F r}} e^{-\frac{1}{k_F} \int_0^r dr' \Delta(r')} \begin{pmatrix} B_1 e^{i\psi(r)+i\gamma(r)} + B_2 e^{-i\psi(r)-i\gamma(r)} \\ -iB_1 e^{-i\psi(r)+i\gamma(r)} + iB_2 e^{i\psi(r)-i\gamma(r)} \end{pmatrix} ,
$$

(2.77)

where $\gamma(r) = k_F r + \frac{\alpha^2 - \frac{1}{4}}{2k_F r} - \frac{2\alpha+1}{4}\pi$. We must now match the solutions from Eqs. (2.75) and (2.77) at $r \sim r^*$ in order to find a continuous solution.

We first match $u(r)$. Making the ansatz $B_1 = \frac{C_1}{2} e^{i\kappa}$ and $B_2 = \frac{C_1}{2} e^{-i\kappa}$ and matching the solutions at $r \sim r^*$ leads to a condition on $\psi(r)$

$$
\psi(r^*) + \kappa - \frac{E r^*}{k_F} + \left(l - \alpha + \frac{k}{2} \right) \frac{\pi}{2} - \frac{\beta}{2k_F r^*} = 0 .
$$

(2.78)

Next, we match $v(r)$, which leads to

$$
\psi(r^*) - \kappa - \frac{E r^*}{k_F} - \left(l - \alpha - \frac{k}{2} \right) \frac{\pi}{2} - \frac{\beta}{2k_F r^*} + \left(n + \frac{1}{2} \right) \pi = 0 .
$$

(2.79)

Here, $n \in \mathbb{Z}$. Comparing Eqs. (2.78) and (2.79), we find that the parameter κ is

$$
\kappa = (\alpha - l)\frac{\pi}{2} + \left(n + \frac{1}{2} \right) \frac{\pi}{2} .
$$

(2.80)

Thus, we find that at $r \sim r^*$ the function $\psi(r)$ is approximately

$$
\psi(r^*) \sim \frac{E r^*}{k_F} + \frac{\beta}{2k_F r^*} - \frac{k+1}{4}\pi - \frac{n}{2}\pi .
$$

(2.81)

However, recall that we earlier found that $\psi(r)$ is given by Eq. (2.72) while constructing the BdG solution in the regime $r \gg r^*$. Hence, in order to have a consistent solution, we must compare the approximate solution Eq. (2.81) with Eq. (2.72). Since we want to understand the behavior of $\psi(r)$ in the regime where $r \sim r^* \gg \frac{1}{k_F}$, as a first approximation we can drop the term $e^{\frac{2}{k_F} \int_0^r dr' \Delta(r')}$. This is justified since the pairing term $\Delta(r)$ approaches 0 at least linearly and, as we are working in the regime where $r \ll \xi$, we can approximate this term as $e^{\frac{\Delta_0 r}{k_F}} = e^{\frac{r}{\xi}} \sim 1$. Thus, in order to understand the behavior of $\psi(r)$ in the vicinity of r^* we need only consider the integral

$$
I = \int_r^\infty dr' \, e^{-\frac{2}{k_F} \int_0^{r'} dr'' \Delta(r'')} \left(E - \frac{\beta}{2r'^2} \right) .
$$

(2.82)

We write $I = I_1 + I_2$ where

$$I_1 = E \int_r^\infty dr' \, e^{-\frac{2}{k_F} \int_0^{r'} dr'' \Delta(r'')},$$

$$I_2 = -\frac{\beta}{2} \int_r^\infty \frac{dr'}{r'^2} \, e^{-\frac{2}{k_F} \int_0^{r'} dr'' \Delta(r'')}. \tag{2.83}$$

We can now approximate I_1 as

$$I_1 \sim -Er + E \int_0^\infty dr' \, e^{-\frac{2}{k_F} \int_0^{r'} dr'' \Delta(r'')}, \tag{2.84}$$

and can further write

$$I_2 = \frac{\beta}{2} \int_r^\infty dr' \, \frac{\partial}{\partial r'} \left(\frac{1}{r'} \right) e^{-\frac{2}{k_F} \int_0^{r'} dr'' \Delta(r'')}. \tag{2.85}$$

Integrating I_2 by parts, we find

$$I_2 = \frac{\beta}{2} \left[\frac{e^{-\frac{2}{k_F} \int_0^{r'} dr'' \Delta(r'')}}{r'} \right]_r^\infty + \frac{\beta}{k_F} \int_r^\infty \frac{dr'}{r'} \Delta(r') e^{-\frac{2}{k_F} \int_0^{r'} dr'' \Delta(r'')}. \tag{2.86}$$

We can then approximate I_2 as

$$I_2 = -\frac{\beta}{2r} + \frac{\beta}{k_F} \int_0^\infty \frac{dr'}{r'} \Delta(r') \, e^{-\frac{2}{k_F} \int_0^{r'} dr'' \Delta(r'')}, \tag{2.87}$$

since we only make an exponentially small error in extending the integral (which is further suppressed by a factor of k_F) over the entire range. Thus, we approximate Eq. (2.82) as

$$I = -Er - \frac{\beta}{2r} + \int_0^\infty dr' \left(E + \frac{\beta}{k_F} \frac{\Delta(r')}{r'} \right) e^{-\frac{2}{k_F} \int_0^{r'} dr'' \Delta(r'')}. \tag{2.88}$$

In the vicinity of r^*, we hence find that the function $\psi(r)$ (Eq. (2.72)) is approximately

$$\psi(r^*) \sim \frac{Er^*}{k_F} + \frac{\beta}{2k_F r^*} - \frac{1}{k_F} \int_0^\infty dr' \left(E + \frac{\beta}{k_F} \frac{\Delta(r')}{r'} \right) e^{-\frac{2}{k_F} \int_0^{r'} dr'' \Delta(r'')}. \tag{2.89}$$

Comparing this asymptotic behavior with Eq. (2.81), we find the vortex core energies

$$E = -\omega_0 \, k \, l + \left(n + \frac{k-1}{2} \right) \tilde{\omega}, \tag{2.90}$$

where

$$\omega_0 = \frac{1}{k_F} \frac{\int_0^\infty dr' \, \frac{\Delta(r')}{r'} e^{-\frac{2}{k_F} \int_0^{r'} dr'' \Delta(r'')}}{\int_0^\infty dr' \, e^{-\frac{2}{k_F} \int_0^{r'} dr'' \Delta(r'')}} \quad \text{and} \quad \tilde{\omega} = \frac{\pi}{2} \frac{k_F}{\int_0^\infty dr' \, e^{-\frac{2}{k_F} \int_0^{r'} dr'' \Delta(r'')}}. \tag{2.91}$$

For an elementary vortex $k = 1$, l is a half integer, and thus with $n = 0$, we reproduce the CdGM solution [101]. For an MQV with $k = 2$, we see that we cannot get a zero-energy solution since $n \in \mathbb{Z}$. Moreover, for any k, we find $|k|$ branches of vortex core states (per spin projection) by taking the appropriate values of n such that $E \ll \Delta_0$ since our calculation is only valid in this regime. This result is in agreement with an argument relating the number of vortex core branches to a topological invariant [134]. While our method does not reproduce the detailed structure of the sub-gap states away from zero energy, it allows us to analytically estimate the spectral asymmetry, since we can extract the separation between the branches from the spectrum found above.

In order to better understand the nature of the vortex core states, we now consider the specific pairing profile used in our numerical analysis,

$$\Delta(r) = \Delta_0 \tanh\left(\frac{r}{\xi}\right) . \tag{2.92}$$

Since the coherence length $\xi = \frac{k_F}{\Delta_0}$, we find that

$$E = -\left(a\frac{\Delta_0}{k_F\xi}\right) k\,l + \left(n + \frac{k-1}{2}\right)\frac{b\,k_F}{\xi} , \tag{2.93}$$

where $a = 7\zeta(3)/\pi^2$ and $b = \pi/2$. From this, we then see that the mini-gap $\omega_0 \sim \frac{\Delta_0}{k_F\xi}$ and furthermore, we find (pseudo) zero-energy states when

$$l_n = \frac{k_F\xi}{k}\left(n + \frac{k-1}{2}\right)\gamma , \tag{2.94}$$

where $\gamma = b/a \approx 1.8$. Imposing the condition $|l| \lesssim k_F\xi$, we see that we should restrict to $n = 0, -1, -2, \ldots, 1-k$ which gives us exactly k branches of vortex core states. Our calculation thus demonstrates that the angular momenta where the branches cross zero energy, called crossing points, are separated by an amount $\sim k_F\xi$, in agreement with our numerical results. Furthermore, we observe that taking a different form of the pair profile simply changes the constant γ (e.g., for $\Delta(r) = \Delta_0\theta(r - \xi)$, we find $\gamma = 4.5$) but does not affect the scaling of the crossing points l_n with k_F and ξ.

Thus, we have analytically shown that, at low energies, vortex core states disperse linearly, $E_j(l) = -\omega_0(l - l_j)$, where $j = 1, \ldots, k$ indexes the branches and the l_j's are the angular momenta

at which the branches cross the Fermi level. This is consistent with results obtained by numerically diagonalizing the BdG Hamiltonian $H^{(l)}$ (for $k = 2$, see Fig. 2.3i) and with previous results on MQVs in superconductors, obtained through quasi-classical approximations [134–136] and numerical simulations [137–140]. We note that while the spectrum for chiral states with singly quantized vortices has previously been calculated [141], the method presented here easily generalizes to chiral states with MQVs.

2.5   Non-trivial η_l and Suppression of OAM in the BCS Ground State

Since in the BEC regime the spectrum is completely gapped for any k, we find $\eta_l = 0$ for all l and thus the ground state OAM is exactly $L_z = kN/2$. On the other hand, in the weakly-paired regime the energy spectrum of an MQV exhibits a nontrivial spectral asymmetry. We consider the case $k = 2$ first (Fig. 2.3i), where there exist two vortex core branches with linear dispersions at low energies, $E_{vc,\pm}^{(l)} \sim -\omega_0(l - l_\pm)$ with $l_+ > l_-$. Under PH symmetry, these branches are exchanged as $E_{vc,+}^{(l)} = -E_{vc,-}^{(-l-2)}$ which fixes $l_- = -(l_+ + 2)$. As shown in Fig. 2.3ii, we find that at these crossing points η_l acquires a non-zero value: $\eta_l = -2$ for $l_- < l < -1$ and $\eta = +2$ for $-1 < l < l_+$, with $\eta_l = 0$ at $l = -1$. Intuitively, this can be understood as follows—at large negative l, the branches are merged into the bulk and since there are no sub-gap states, $\eta_l = 0$. On increasing l, the branches begin separating from the bulk but since both have positive energy, η_l still vanishes. At l_- however, one of the branches crosses the Fermi energy, creating a difference of precisely two between the number of negative and positive energy eigenvalues of $H^{(l)}$. At $l = -1$, η_l necessarily vanishes due to PH symmetry, which also fixes η_l for $l > -1$. In contrast with $|k| = 1$, the branches are not PH symmetric with respect to themselves, allowing the spectral asymmetry to acquire a non-zero value in the BCS regime. The fact that η_l changes from the BEC to the BCS regime can also be understood as a consequence of spectral flow along the vortex core states, since η_l (and hence $\mathscr{L}$) cannot change its value in any other way.

A non-zero spectral asymmetry η_l appears generally for any $|k| \geq 2$ within the BCS regime: for even k (see Fig. 2.3iv), there are $|k|/2$ pairs of branches such that the branches within each pair
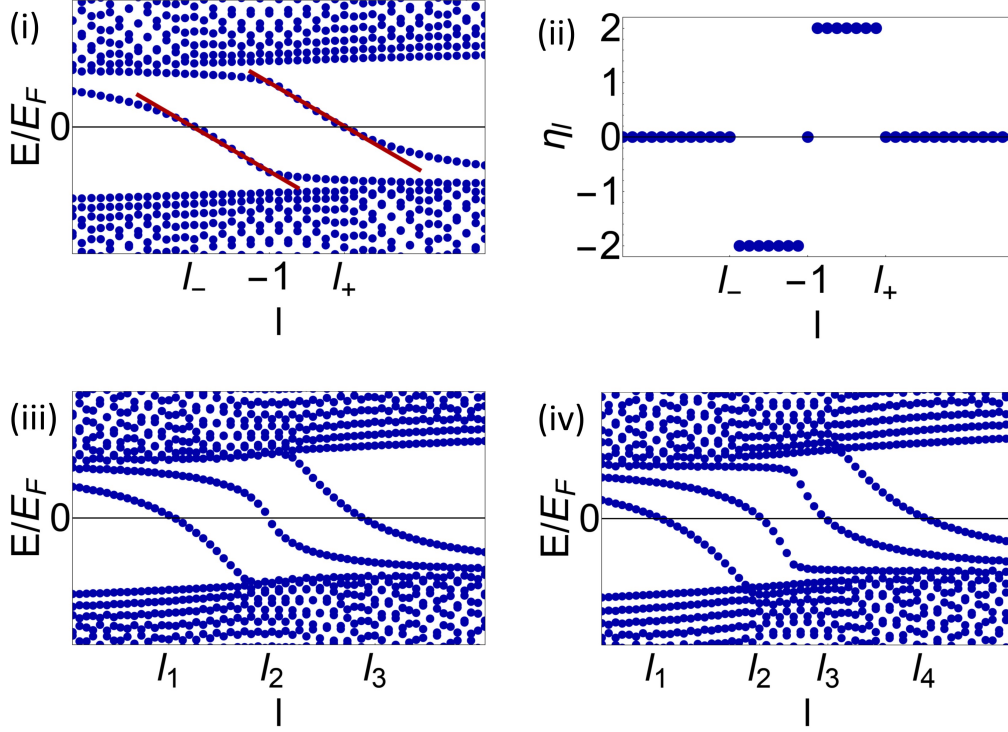
Figure 2.3: BdG solution for MQVs with $\Delta_0 = 0.15 E_F$, $\mu = E_F$, and $k_F R = 80$: (a) Comparison of energy spectrum for $k = 2$ with analytic approximation (in red); (b) spectral asymmetry for $k = 2$; (c) energy spectrum for $k = 3$ and (d) for $k = 4$.

are PH symmetric with each other. η_l then changes by ± 2 whenever one of these branches crosses the Fermi level; for odd k (see Fig. 2.3iii) there are $(|k| - 1)/2$ pairs that contribute to a non-trivial η_l, since the branches within each pair go into each other under a PH transformation, while the remaining branch is PH symmetric with respect to itself and therefore does not contribute to η_l.

Having established the existence of a non-vanishing η_l, we see that there must exist unpaired fermions in the BCS ground state for $|k| \geq 2$, and as a consequence of Eq. (2.25), $\mathscr{L}$ acquires a non-trivial ground state eigenvalue. For $k = 2$, this is $\mathscr{L} = -l_+^2 - l_+$, where we used PH symmetry to relate l_- to l_+. Importantly, the analytic calculation of the vortex core states (see Sec. 2.4.1) demonstrates that the positions of the crossing points are located at $l_\pm \sim k_F \xi$ with the pre-factor fixed by the form of $\Delta(r)$. This scaling persists in self-consistent numerical calculations [138–140]. Eq. (2.25) along with this scaling thus establishes the reduction of the OAM of the $k = 2$ MQV in
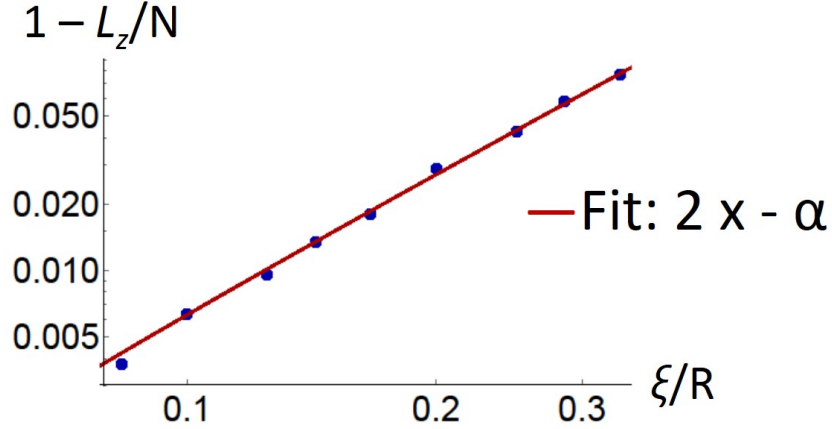
Figure 2.4: The analytic prediction $L_z/N = 1 - \alpha(\xi/R)^2$ (red line) fits the numerical data (blue dots) well over a wide window within the BCS regime, $0.05 \lesssim \Delta_0/E_F \lesssim 0.25$, for an MQV with $k = 2$. The slope of the fit equals two as shown on a log-log plot.

the weakly paired regime. To leading order in $k_F\xi$,

$$\mathscr{L} = L_z - N \sim - \left(k_F\xi\right)^2. \tag{2.95}$$

As a result, the OAM is significantly suppressed from $L_z^{BEC} = N$ since $k_F\xi \gg 1$ in the BCS regime $(\Delta_0 \ll E_F)$. This analysis confirms that the unpaired fermions carry angular momentum opposite to that carried by the Cooper pairs. On a disc, $N \approx (k_F R)^2/2$, leading to $L_z/N \approx 1 - \alpha\left(\xi/R\right)^2$, where α is an $O(1)$ constant fixed by $\Delta(r)$. As an independent check, we have verified this behavior by numerically calculating L_z/N using the full BdG solution (see Appendix A for details). In Fig. 2.4, the quadratic scaling is shown to be in good agreement with the numerical data. We thus expect a substantial reduction of the OAM in the BCS regime, where ξ can be comparable to R [104]. We also expect that when two elementary vortices merge into a $k = 2$ MQV [135, 136], the ground state OAM decreases from $L_z = N$ by an amount $\sim (k_F\xi)^2$.

2.6   Conclusions

In this chapter, we have shown that the presence of a topological defect in a BCS superfluid can significantly alter the nature of pairing in the ground state. Specifically, we have established that an MQV in the weak-pairing regime of a fermionic superfluid hosts unpaired fermions localized

around the vortex core, which lead to a significant suppression of the OAM in the BCS ground state.

A central feature of our result is that the suppression of L_z for $|k| \geq 2$ is independent of any boundary effects and is solely determined by the splitting between the vortex core branches. Given this insensitivity to boundary details, we expect our results to hold for more general sample geometries, which may lack axial symmetry. Unlike the ground state energy, which might depend strongly on the gap profile, the OAM thus exhibits universal scaling behavior in the weak pairing BCS regime. The lack of dependence of the OAM on the system boundary is in stark contrast with weakly-paired chiral (e.g., $d+id$) SFs, where it was shown [90, 124] that the OAM is suppressed due to the topological edge modes, but that this effect is strongly dependent on the edge details [123, 128, 129, 142]. Our analysis hence suggests that s-wave SFs with MQVs may prove to be a more robust platform for investigating the intriguing suppression of the OAM in paired SFs. While the OAM has been measured in SFs [143–145], we also expect signatures of unpaired fermions—which create a current localized around the vortex core that flows counter to the superflow—in local supercurrent density measurements in MQV states [105].

Chapter 3

Interplay of Symmetry and Topology in Superconductors: Here, There, and Everywhere

In which Benny superbly orchestrates

an escape from quotidian order,

only to run into himself.

Last chapter, we encountered fermionic superfluids: systems of electrically neutral fermions which, for chiral states paired in higher angular momentum channels, possess chiral gapless edge excitations and are topologically non-trivial. In contrast, a *superconductor* is a system of interacting electrically charged particles which couple to the physical U(1) electromagnetic gauge field. Unlike superfluids, which spontaneously break U(1) charge conservation, the appropriate theoretical framework for understanding the physics of superconductors is that of the Higgs mechanism, which leads to the characteristic signature of superconducting states—the Meissner effect. The conventional textbook explanation of superconductivity as a broken symmetry state is strictly true only for a neutral system and relies on qualitative arguments relating the response functions of the neutral system to the screened response of the charged system. Crucially, a charged system coupled to dynamical electromagnetism is a U(1) gauge theory and, as a consequence of Elitzur's theorem, *does not* admit a non-trivial local order parameter since the expectation values of all gauge non-invariant quantities, such as the pairing amplitude, are strictly vanishing [146]. Such a system, which is fully gapped at zero temperature due to the Higgs mechanism, is instead described by a *non-local* order parameter, a clear indication of intrinsic topological order.

The idea that superconductors coupled to dynamically fluctuating electromagnetism are correctly thought of as topologically ordered states was expounded upon in a beautiful paper by Hansson et al [46]. Of particular interest is their development of a low-energy topological quantum field theory description for s-wave superconductors in $d = 2$ spatial dimensions, which turns out to be the Chern-Simons theory for $\mathbb{Z}_2$ topological order. The restriction to $2 + 1\mathrm{D}$ requires that the electrodynamics is that of the $2 + 1\mathrm{D}$ Maxwell term, which no longer describes physical electromagnetism even if the electrons are spatially confined to 2d (such situations arise in thin film superconductors, where the electrons live in $d = 2$ but the electromagnetic field remains three-dimensional). Nevertheless, such a simplification is justified from a theoretical standpoint as it provides an analytically tractable framework for studying of topological order, complementary to studies of the FQHE and quantum spin liquids.

The presence of topological order in $d = 2$ s-wave superconductors was firmly established in [46] by demonstrating the presence of fractionalized quasi-particles (vortices and Bogoliubov fermions) and the existence of a finite ground state degeneracy on a torus, hallmarks of gapped LRE states with topological order. However, that work left open various important questions, the resolutions of which form the basis of this chapter. First, can this analysis be extended to superconductors paired in higher partial waves, such as the chiral $d + id$ state which hosts gapless edge excitations and excitations with semionic mutual statistics [89]? Second, all spin-singlet superconductors possess a pair of internal unbroken global symmetries: spin-rotation and "magnetic flux," the latter of which follows from the electromagnetic Bianchi identity, valid in the absence of magnetic monopoles. Can these global symmetries be systematically included in the low-energy TQFT description of $2 + 1\mathrm{D}$ superconductors and the response properties of all spin-singlet superconductors identified? In this chapter, we answer both of these questions in the affirmative by deriving low-energy descriptions of all spin-singlet (Abelian) superconductors, thereby placing them in the class of symmetry enriched topological (SET) phases.

A version of this chapter was first presented as [47] under the title "Topological Order, Symmetry, and Hall Response of Two-Dimensional Spin-singlet Superconductors," and is a collaboration

with Sergej Moroz, Victor Gurarie, and Leo Radzihovsky,

When I get to the bottom, I go back to the top.

3.1   Introduction

Topological order is a cornerstone of contemporary quantum condensed matter physics [147, 148]. Rooted in the discovery of the fractional quantum Hall effect, it arises in numerous phases of matter such as spin liquids and fractional quantum Hall liquids. Topological order manifests itself in the fractionalization of low-energy excitations, ground state degeneracy on closed manifolds, and long-range entanglement [149].

The idea that *two-dimensional superconductors*, i.e., electrically charged paired fermions that couple to a *dynamical* two-dimensional electromagnetic field, are topologically ordered has been appreciated for some time [46, 89, 150–152]. Due to the Higgs mechanism, there are no Goldstone modes in the energy spectrum and, at zero temperature, the superconductor is *fully gapped*. There are two types of *point* excitations in a two-dimensional superconductor: *Bogoliubov quasiparticles* and *vortices*. At energies much lower than the gap, only the topological properties of these low-energy excitations (their braiding and fusion rules) and their symmetry quantum numbers matter.

This information can be effectively encoded in a *topological* field theory. For an s-wave superconductor, a topological Chern-Simons theory was elucidated and described in detail in a beautiful paper by Hansson, Oganesyan, and Sondhi [46].

More recently, attempts have been made to construct topological theories for non-abelian $p + ip$ superconductors [153, 154]. These states are an important example in the field of two-dimensional fermionic *chiral* superfluidity and superconductivity, which has been the focus of experimental and theoretical condensed matter physics for decades. Today, chiral $p + ip$ pairing plays a central role in research fields as diverse as the physics of ^3He [155, 156], quantum Hall physics [89], unconventional superconductivity [157], cold atoms [158, 159], and topological quantum computation [160].

Our focus in this chapter is on *chiral spin-singlet* paired states which have also received some attention in the past. For example, in the weakly-coupled *abelian* topological phase, which falls into class C of the ten-fold way classification [161], a chiral $d + id$ superconductor is predicted to exhibit a spin Hall effect [89, 162], support four protected chiral edge modes [163], and have a non-universal edge mass current carried by unpaired fermions [90, 124]. Over the past few years, new physical motivations necessitating further study of chiral $d + id$ pairing have emerged. Specifically, two-dimensional materials with a *hexagonal* lattice symmetry necessarily have degenerate $d_{x^2-y^2}$ and d_{xy} gaps [157], which makes them good candidates for chiral $d + id$ superconductors. Two well-known examples where $d + id$ pairing is currently believed to be relevant are the pnictide SrPtAs [164, 165] and graphene doped to the van Hove filling [166–168]. Chiral spin-singlet superconductors paired in higher partial even-waves are also theoretically interesting and are likely to become experimentally relevant in the future.

In a two-dimensional chiral superconductor, the spontaneous breaking of parity and time-reversal symmetries might lead one to expect a *spontaneous* generation of a finite magnetic field in the ground state, which originates from the internal motion of fermions orbiting around each other in Cooper pairs. For a type II superconductor, this would result in a finite density of quantum vortices in the ground state. One might thus anticipate a relation between the density of elementary fermions, n_f, and the density of vortices, n_v, of the form $n_v = \nu_v n_f$. An important question that

motivated this work is whether ν_v is a universal quantized number for chiral paired states such as a $d + id$ superconductor.

To answer this question and to extend the understanding of superconductors as topologically ordered states, we present a general framework for studying the low-energy physics of spin-singlet superconductors. We start from the *microscopic* theory of these states that are spin-rotationally invariant and conserve magnetic flux. From there, we *derive* topological field theories for different *gapped* abelian states, i.e., *s*-wave, $d + id$, and chiral superconductors paired in higher partial even-waves. The virtue of this approach is that it naturally encodes the braiding and fusion rules of low-energy excitations, incorporates symmetries, and captures the physics at the edge. In the case of chiral states, we reproduce the known spin Hall effect [89, 162]. Moreover, we investigate the vortex Hall response associated with the magnetic flux symmetry. The coefficient ν_v, introduced above, equals the Hall coefficient for this response. Importantly, we demonstrate explicitly that for all superconductors considered here, ν_v is *zero*. As a result, we predict that there is no *spontaneous magnetic field*, and thus no dense array of vortices in the ground state of a chiral two-dimensional superconductor. By merging the ideas discussed above, our work unifies topological order and symmetries in superconductors and firmly establishes them as *symmetry enriched topological* (SET) phases [56].

It is worth remembering that in this work the electromagnetic field is assumed to be strictly confined to *two* spatial dimensions. Is such flatland electromagnetism actually realizable in an experiment? It is clear that without special arrangements electromagnetism will penetrate into the third dimension, and as a result, one has to deal with a *mixed dimension* problem where paired fermions are confined to two spatial dimensions but electromagnetism is three-dimensional. By embedding two dimensional electrons inside a specific dielectric medium, however, electromagnetism can also be made *effectively* two-dimensional. To this end, one can engineer a two-dimensional logarithmic potential between electric charges by surrounding the sample by a low-permittivity medium with a dielectric constant $\epsilon_{medium} \ll \epsilon_{sample}$ [169]. Secondly, the magnetic field lines can be arranged to be transverse to the boundary of the quasi-two dimensional sample by sandwiching it

between a high-permeability ($\mu_{\text{medium}} \gg \mu_{\text{sample}}$) material. Thus, at least static electromagnetism can be effectively confined to two dimensions.

The outline of this chapter is as follows: In Sec. 3.2, we first introduce our framework – an abelian Chern-Simons field theory that captures the topological properties, symmetries, and edge physics of abelian gapped states. Next, in Sec. 3.3, we introduce topologically ordered spin-singlet superconductors and identify their internal global symmetries. Then, in Sec. 3.4, we derive the topological theories of s-wave and $d + id$ superconductors by starting from the low-energy model of a non-relativistic $d_{x^2-y^2}$ paired state. In that section, we also extend this derivation to chiral superconductors paired in higher partial even-waves. In Sec. 3.5, we analyze the resulting Chern-Simons theories. Here, we first devote Sec. 3.5.1 to a conventional (s-wave) superconductor. In Sec. 3.5.2, we then investigate the effective theory of a $d + id$ superconductor and calculate its spin and vortex Hall responses. Next, in Sec. 3.5.3, we describe the extension of our construction to chiral spin-singlet superconductors paired in higher partial even-waves and demonstrate that these fall into the sixteen-fold way classification of chiral superconducting states developed by Kitaev [50]. Sec. 3.6 presents a general argument that elucidates why chiral superconductors have a zero vortex Hall coefficient. Finally, in Sec. 3.7, we close with some open questions that go beyond the scope of this thesis.

3.2   Abelian topological field theories

The low-energy physics of a completely gapped two-dimensional state of matter is encoded in a topological field theory. Moreover, since the spin-singlet superconductors studied here are known to form only abelian phases,[2] we propose that topological aspects of such phases can be captured by an abelian Chern-Simons field theory [27–29]

$$\mathcal{L}_{\text{bulk}} = \frac{1}{4\pi} \epsilon^{\mu\nu\rho} a_\mu^I K_{IJ} \partial_\nu a_\rho^J - a_\mu^I j_I^\mu - \frac{1}{2\pi} t_{AI} \epsilon^{\mu\nu\rho} \mathcal{A}_\mu^A \partial_\nu a_\rho^I. \tag{3.1}$$

---

[2] An *abelian phase* is characterized by a unique anyon resulting from the fusion of any two excitations. On the other hand, *non-abelian* anyons can fuse into different outcomes.

Here a^I is a multiplet ($I = 1, 2, \ldots, N$) of auxiliary statistical gauge fields,[3] K_{IJ} is a symmetric *integer-valued* $N \times N$ matrix that determines the self and mutual statistics of excitations, and j_I are quasiparticle currents. Note that a_μ are coupled to *quantized* charges carried by the currents j_I. As a result, the first-quantized current densities are $j_I^0(\mathbf{r}) = \sum_n l_I^{(n)} \delta(\mathbf{r} - \mathbf{r}^{(n)})$, characterized by an integer-valued gauge charge vector $l^{(n)}$ and the position $\mathbf{r}^{(n)}$ of the nth quasiparticle excitation. The third term in Eq. (5.34) represents the coupling to external sources $\mathcal{A}^A$ of $A = 1, 2, \ldots, M$ *global* $\text{U}(1)_A$ symmetries. The theory (5.34) has proven to be successful in describing the low-energy properties of abelian quantum Hall fluids [170].

Importantly, *topological order* is simply encoded in the effective theory (5.34). Indeed, the ground state degeneracy on a torus, a direct manifestation of topological order, is fixed by the determinant of the K-matrix [170]

$$\#\text{GS} = |\det K|. \tag{3.2}$$

Moreover, this determinant also fixes the number of independent anyon types (see, for example, [171]).

While the effective field theory (5.34) is quite an inefficient formalism for encoding the fusion and braiding rules of the bulk excitations,[4] it is in fact very well suited for understanding the physics of the edge. Following Wen [172], in the absence of external sources $\mathcal{A}^A$, one finds a chiral Luttinger theory of N chiral bosons ϕ^I propagating along the edge

$$\mathcal{L}_{\text{edge}} = \frac{1}{4\pi} \left[K_{IJ} \partial_t \phi^I \partial_x \phi^J - V_{IJ} \partial_x \phi^I \partial_x \phi^J \right]. \tag{3.3}$$

Here V_{IJ} is a non-universal positive-definite real matrix that depends on the microscopic properties of the edge.

Systems with a finite chiral central charge c at the edge have a non-zero thermal Hall conductance and host c *co-propagating* bosonic edge modes that cannot be gapped by backscattering.

---

[3] A remark regarding *compactness*: The statistical fields dual to global conserved currents are non-compact which ensures absence of instanton magnetic monopoles and strict conservation of these currents. On the other hand, compact statistical gauge fields are also present sometimes, but these do not encode any strict conservation laws.

[4] Indeed, the number of entries of the K-matrix might be much larger than the number of independent braiding phases.

In particular, for chiral spin-singlet superconductors, with the chirality parameter k to be defined in Eq. (3.10), one finds $c = k$.

A natural next question to ask is whether *counter-propagating* edge modes can be gapped without breaking any symmetries or if they are symmetry-protected , i.e., are stable against arbitrary symmetry preserving local perturbations. In the rest of this section, we present a brief analysis of this question.

To understand the structure of a straight edge along the x direction in the presence of external sources $\mathcal{A}^A$, we start from Eq. (5.34) in the absence of quasiparticle currents j_I^μ. Following [172], we first impose a gauge fixing condition in the bulk

$$a_t^I + v^I a_x^I = 0. \tag{3.4}$$

The Gauss law constraint (or incompressibility condition)

$$2\pi \frac{\delta S}{\delta a_t^I} = K_{IJ} b^J - t_{AI} \mathcal{B}^A = 0, \tag{3.5}$$

where $b^I = \epsilon^{ij} \partial_i a_j^I$ and $\mathcal{B}^A = \epsilon^{ij} \partial_i \mathcal{A}_j^A$, is automatically satisfied by

$$a_i^I = \partial_i \phi^I + K_{IJ}^{-1} t_{AJ} \mathcal{A}_i^A. \tag{3.6}$$

Substituting Eqs. (3.4) and (3.6) into the bulk action (5.34), with some manipulations, will result in the generalization of the effective edge action (5.5.2.4) in the presence of sources $\mathcal{A}^A$. For the purposes of understanding the fate of counter-propagating edge modes in the presence of symmetries, however, it suffices to work out the transformation properties of the edge fields ϕ_I. Under a local U(1)$_A$ transformation parametrized by α_A, the background gauge fields and the edge multiplet transform as

$$\delta \mathcal{A}_\mu^A = -\partial_\mu \alpha_A,$$
$$\delta \phi_I = \alpha_A K_{IJ}^{-1} t_{AJ}. \tag{3.7}$$

The last equation follows from Eq. (3.6) and the U(1)$_A$ neutrality of all statistical gauge fields a^I. We consider now an edge perturbation of the form

$$\int dx\, dt\, \cos(l_I \phi_I). \tag{3.8}$$

First, the requirement of locality of this term enforces that $\vec{l} \in \mathbb{Z}^N$ must be bosonic (have trivial self and mutual statistics) [171]. Moreover, it follows from Eq. (3.7) that these terms (sometimes called "Higgs" terms) are invariant under all global symmetries if $l^T \cdot K^{-1} \cdot t_A = 0$ for all $A = 1, \ldots, M$. In addition, according to the null vector condition of [173], such symmetry allowed Higgs terms can now gap a pair of counter-propagating edge modes if and only if $l^T \cdot K^{-1} \cdot l = 0$ since the two fields can then be rotated such that they form a single non-chiral Luttinger liquid that is gapped by backscattering [174]. More generally, for gapping n pairs of counter-propagating edge modes, we will require n-independent (commuting) Higgs terms that can simultaneously provide energy gaps to all of these edge modes.

In summary, in the presence of U(1) global symmetries, n pairs of counter-propagating edge modes can be gapped if and only if one can find $\vec{l}_i \in \mathbb{Z}^N (i = 1, \cdots, n)$ such that

- The Higgs terms are constructed from elementary bosonic excitations:

$$2\pi l_i^T \cdot K^{-1} \cdot l' = 0 \quad (\text{mod } 2\pi) \quad \forall i, \forall \vec{l'} \in \mathbb{Z}^{\mathbb{N}} \tag{3.9a}$$

- The Higgs terms are charge neutral under all global symmetries:

$$l_i^T \cdot K^{-1} \cdot t_A = 0 \quad \forall i, \forall A \tag{3.9b}$$

- The null vector conditions are satisfied:

$$l_i^T \cdot K^{-1} \cdot l_j = 0 \quad \forall i, j \tag{3.9c}$$

As shown later, all systems considered in this chapter host at least one pair of counter-propagating modes which are gapped out by the Higgs terms satisfying the above conditions.

3.3 Spin-singlet superconductors: topological order and symmetries

In this chapter, we consider *two-dimensional* electrically charged spinful fermions which couple to a *dynamical* electromagnetic gauge field that is also confined strictly to two spatial dimensions. We will *assume* that, due to electromagnetism and some spin-independent short-range

attractive interaction, the fermions pair in a *spin-singlet* chiral channel with the gap

$$\Delta_{\mathbf{p}} = (p_x \pm ip_y)^k \Delta_0 \qquad (3.10)$$

where the sign defines the chirality and k is an even integer due to antisymmetry of the fermionic singlet pair wave-function. In fact, k is just the orbital angular momentum carried by a Cooper pair.

We will discuss separately a conventional s-wave superconductor ($k = 0$), $d + id$ superconductor ($k = 2$), and higher partial even-wave chiral superconductors ($k = 4, 6, \ldots$). The explicit construction and analysis of the topological Chern-Simons theories of these superconductors depends on the chirality parameter, k, and will appear in separate sections below. Here, we first highlight the generic properties that all of these systems have in common:

- **Topological order:** Two-dimensional spin-singlet superconductors with a *dynamical* gauge field exhibit *topological order*. For an s-wave superconductor this has been emphasized in [46], where the ground state degeneracy on a torus was found to be equal to four. In fact, this result also holds for the $d + id$ superconductor [89] and can be easily extended to higher partial wave spin-singlet chiral pairing. As a result, all superconductors considered here have $|\det K| = 4$ and contain four independent anyons, which we call 1, e, m, and ϵ, following a common convention. As we will see in the following, topological order in superconductors leads to fractionalization of the quantum numbers and statistics of low-energy excitations.

- **Internal continuous global symmetries:** In a superconductor, electromagnetism, being a *gauge redundancy*, is *not* a global symmetry. There are, however, two internal global symmetries of spin-singlet superconductors to be considered in this thesis: First, the spin-singlet structure of the pairing implies that a non-abelian $\mathrm{SU}(2)_s$ spin rotation is a global symmetry. Since by construction, the effective theory (5.34) can couple only to *abelian* sources, here we consider the Cartan subalgebra of $\mathrm{SU}(2)_s$ with the charge $Q_s \sim S_z$ and introduce in Eq. (5.34) an external abelian spin source $\mathcal{A}^s$ that couples to the z-component of the

spin current. We will see that in superconductors, this charge is carried only by Bogoliubov quasiparticles while vortices are spinless. Second, *any* two-dimensional superconductor has a global abelian $\mathrm{U}(1)_v$ *magnetic flux* symmetry with a charge $Q_v = \int d^2 x B$ [175]. The conservation of this charge follows from the electromagnetic Bianchi identity (Faraday's law) $\epsilon^{\mu\nu\rho} \partial_\mu F_{\nu\rho} = 0$, which is valid provided there are no magnetic monopoles. This appears naturally in a model where the electromagnetic $\mathrm{U}(1)$ gauge group is *non-compact*, which we consider here. In a type-II superconductor, a vortex carries one-half of a magnetic flux quantum, i.e., a π-flux, while a Bogoliubov quasiparticle is *neutral* with respect to this symmetry. As a result, in a superconductor the flux charge defined above is carried only by vortices. Correspondingly, in the effective theory (5.34) we introduce an external abelian source, $\mathcal{A}^v$, which couples to the charge Q_v. It is worth emphasizing that due to the presence of a gap, neither of the two global symmetries introduced above are broken spontaneously in a superconducting ground state.

3.4 Derivation of Chern-Simons topological field theories of spin-singlet superconductors

We start from the low energy model of a weakly-coupled non-relativistic $d_{x^2-y^2}$ superconductor and, by deforming it, will derive the topological Chern-Simons theories for s-wave and $d + id$ superconductors. At the end of this section, we will also extend this derivation to spin-singlet chiral superconductors that are paired in higher partial even-waves.

Before presenting the derivation, it is worth noting that for a relativistic s-wave superconductor a topological Chern-Simons theory was derived in [46]. In contrast to that construction, our derivation applies to all gapped spin-singlet non-relativistic superconductors and includes coupling to external magnetic flux and spin symmetry sources.

Our starting point is the Lagrangian of a gapless two-dimensional $d_{x^2-y^2}$ superconductor[5]

$$
\mathcal{L}^0 = -\frac{1}{4}F_{\mu\nu}F^{\mu\nu} - n_s\mathcal{D}_t\varphi + \frac{n_s}{2}\frac{1}{c_s^2}(\mathcal{D}_t\varphi)^2 - \frac{n_s}{2}(\mathcal{D}_i\varphi)^2
$$
$$
- A_\mu j_{\text{ions}}^\mu + \mathcal{L}_{\text{qp}}^0(\psi_i, A; \mathcal{A}^s) - \frac{1}{2\pi}\epsilon^{\mu\nu\rho}\tilde{\mathcal{A}}_\mu^v\partial_\nu A_\rho,
$$

(3.11)

where the covariant derivative $\mathcal{D}_\mu\varphi = \partial_\mu\varphi - A_\mu$, n_s is the superfluid density, and c_s is the speed of sound. The first term[6] in Eq. (3.11) encodes the Maxwell dynamics of the electromagnetic field A and the next three terms incorporate the dynamics of the fluctuating part, φ, of the superconductor phase. In addition, we have included the neutralizing ion static background that carries the electromagnetic current $j_{\text{ions}}^\mu = n_f\delta^{\mu 0}$, where n_f is the density of elementary fermions that undergo pairing. $\mathcal{L}_{\text{qp}}^0$, specified later in this section, incorporates the low-energy physics of gapless spinful fermionic quasiparticles that couple to electromagnetism, A, and to the spin source, $\mathcal{A}^s$. Finally, the last term in Eq. (3.11) describes the coupling of the magnetic flux symmetry current to its external source, $\tilde{\mathcal{A}}^v$. Its prefactor fixes the magnetic flux charge of an elementary counterclockwise vortex to $Q_v = +1/2$ (see footnote[5]).

3.4.1 Vortices

In the presence of vortices the superconductor phase φ can be split into the regular part φ_{reg} and the vortex part φ_{v}, which has singularities at the positions of vortices. By a suitable regular gauge transformation, the regular part φ_{reg} can be absorbed into the electromagnetic potential, A_μ (Higgs mechanism). On the other hand, the singular part φ_{v} determines the *conserved* vortex current

$$
j_{\text{v}}^\mu = \frac{1}{\pi}\epsilon^{\mu\nu\rho}\partial_\nu\partial_\rho\varphi_{\text{v}}.
$$

(3.12)

---

[5] For simplicity we set the mass of an elementary fermion to unity. Its electric charge e is set to *minus* unity, which fixes the magnetic flux carried by an elementary (counterclockwise) vortex $\varphi(\mathbf{x}) = \arg(\mathbf{x})/2$ to $+\pi$, i.e., a half of a magnetic flux quantum.

[6] Here the indices are raised and lowered with the Minkowski metric.

After introducing the statistical gauge field $a_\mu \equiv \partial_\mu \varphi_{\rm v}$, that is dual to the vortex current, the Lagrangian (3.11) becomes

$$\mathcal{L}^0 = -\frac{1}{4}F_{\mu\nu}F^{\mu\nu} - b_\mu\Big(j_{\rm v}^\mu - \frac{1}{\pi}\epsilon^{\mu\nu\rho}\partial_\nu a_\rho\Big) - n_s(a_t - A_t) + \frac{n_s}{2}\frac{1}{c_s^2}(a_t - A_t)^2$$
$$- \frac{n_s}{2}(a_i - A_i)^2 - A_\mu j_{\rm ions}^\mu + \mathcal{L}_{\rm qp}^0(\psi_i, A; \mathcal{A}^s) - \frac{1}{2\pi}\epsilon^{\mu\nu\rho}\tilde{\mathcal{A}}_\mu^v \partial_\nu A_\rho,$$

(3.13)

where following [46] we introduced the (Lagrange multiplier) statistical gauge field b_μ, whose equation of motion enforces the condition (3.12).

3.4.2 Bogoliubov quasiparticles

We now specify the quasiparticle Lagrangian, $\mathcal{L}_{\rm qp}^0$. The $d_{x^2-y^2}$ superconductor has four nodes on the Fermi surface (see Fig. 3.1), where Bogoliubov quasiparticles become gapless. After linearizing near these nodes one finds *four* massless two-component Dirac modes $\psi_{i\alpha}$, where we introduced the nodal index $i = 1, 2$ and the spin index $\alpha =\uparrow, \downarrow$. The low-energy Dirac Lagrangian of these quasiparticles was derived in [152, 176] and also discussed in [177]. In the absence of electromagnetism it is given by

$$\mathcal{L}_{\rm qp}^0 = \psi_1^\dagger i\partial_t \psi_1 + \psi_1^\dagger\Big(iv_F \partial_X \tau_z + iv_\Delta \sum_{s=+,-} e^{is\varphi}\partial_Y e^{is\varphi}\tau_s\Big)\psi_1 + (1 \leftrightarrow 2, X \leftrightarrow Y),$$

(3.14)

where $\tau_\pm = (\tau_x \pm i\tau_y)/2$. Here we have introduced the node-aligned spatial coordinates $X = (x + y)/\sqrt{2}$ and $Y = (-x + y)/\sqrt{2}$ and suppressed both the spin index α and Dirac index in particle-hole space, where the Pauli matrices τ_i operate. The gap terms proportional to τ_+ and τ_- contain the coupling to the superconductor phase φ. Note that our normalization of this phase differs from the normalization used in [152, 176] by a factor of two.

Since $\psi_{i\alpha}$ transforms as a doublet under the spin $SU(2)_s$ symmetry, the quasiparticles couple to the spin source $\mathcal{A}^s$ via the minimal coupling $\partial_\mu \to \partial_\mu + i\sigma_z \mathcal{A}_\mu^s/2$, where the Pauli matrix σ_z acts in spin space. On the other hand, the Bogoliubov quasiparticle spinor $\psi_{i\alpha}$ is a combination of a particle and hole, and thus it is more subtle to introduce the electromagnetic potential A into Eq. (3.14). In fact, A appears only in the kinetic terms (but not in the gap term) in Eq. (3.14) via the minimal coupling $\partial_\mu \to \partial_\mu + ie\tau_z A_\mu$, where we set $e = -1$ (see footnote[5]). In
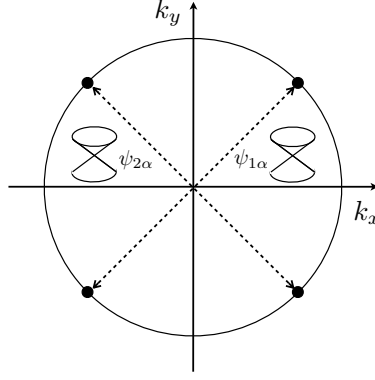
Figure 3.1: Four Dirac fermions $\psi_{i\alpha}$ arising from the two pairs of nodes (connected by dashed lines) at the Fermi surface of a $d_{x^2-y^2}$ superconductor.

the absence of vortices it is customary at this point to transform to electrically neutral fermions, $\tilde{\psi}_i = \exp(-i\varphi\tau_z)\psi_i$, which eliminates the phase φ from the gap term [152]. Importantly, in the presence of vortices this transformation is not single-valued,[7] and instead one should perform a single-valued transformation [178] (see also [179] for a general discussion)

$$\tilde{\psi}_i = \exp(-i\varphi\tau_z \pm i\varphi_{\rm v})\psi_i. \tag{3.15}$$

The presence of these neutral fermions, that braid trivially with all other quasiparticles, will be reflected in the fermionic nature of the K-matrices discussed in Sec. 3.5. After performing the transformation with the minus sign in Eq. (3.15), we find

$$\mathcal{L}_{\rm qp}^0(\tilde{\psi}_i, A; \mathcal{A}^s) = \tilde{\psi}_1^\dagger\big[i\mathcal{D}_t + \tau_z(A_t - a_t)\big]\tilde{\psi}_1 + \tilde{\psi}_1^\dagger v_F\big[i\mathcal{D}_X\tau_z + (A_X - a_X)\big]\tilde{\psi}_1$$
$$+ \tilde{\psi}_1^\dagger v_\Delta i\mathcal{D}_Y\tau_x\tilde{\psi}_1 + (1 \leftrightarrow 2, X \leftrightarrow Y), \tag{3.16}$$

where

$$\mathcal{D}_\mu = \partial_\mu + ia_\mu - i\sigma_z\mathcal{A}_\mu^s/2. \tag{3.17}$$

---

[7] Indeed, across the vortex branch cut, the phase of every Dirac component of the spinor $\tilde{\psi}_i = \exp(-i\varphi\tau_z)\psi_i$ changes by $\pm\pi$.
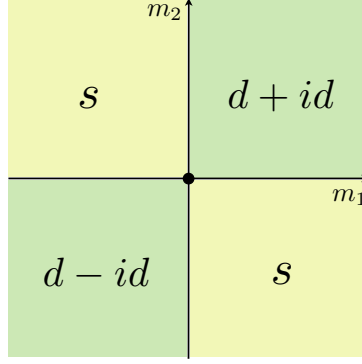
Figure 3.2: Topological phase diagram of a deformed $d_{x^2-y^2}$ superconductor as a function of masses m_i of the Dirac modes ψ_i. The origin represents the $d_{x^2-y^2}$ superconductor.

3.4.3 s-wave and $d+id$ deformations of $d_{x^2-y^2}$ superconductor

Crucially for us, one can enter into the s-wave or $d+id$ gapped phase by adding appropriate masses to nodal Dirac quasiparticles that were introduced above. In particular, the terms [162]

$$\mathcal{L}_{\mathrm{qp}}^{\delta} = -\delta(\tilde{\psi}_1^{\dagger}\tau_y\tilde{\psi}_1 \pm \tilde{\psi}_2^{\dagger}\tau_y\tilde{\psi}_2) \tag{3.18}$$

add to the $d_{x^2-y^2}$ superconductor some amount of is and id_{xy} pairing, respectively. Topologically, the resulting phases are equivalent to the s-wave and $d+id$ superconductors. We see thus that that Eq. (3.18) is nothing but the mass term for the nodal Dirac particles,[8] with masses $m_1 = \delta$ and $m_2 = -\delta$. More generally, allowing arbitrary masses m_i for the spinors ψ_i, one can show that their signs are the same $(m_1 m_2 > 0)$ for the $d+id$ phase, while they are opposite $(m_1 m_2 < 0)$ for the s-wave phase. The resulting phase diagram is summarized in Fig. 3.2. Since the s-wave and the $d+id$ superconductors differ only in the sign of the mass of the Dirac mode $\tilde{\psi}_2$, in the following we consider them in parallel.

3.4.4 Integrating out electromagnetism

Henceforth, we will assume that the Bogoliubov quasiparticles ψ_i have a sufficiently large gap and thus carry an electric density and current that are negligible compared to the superfluid

---

[8] To this end, perform the following transformation of the last term in Eq. (3.16): first rotate by a $\pi/2$ angle, i.e., $X \to -Y$, $Y \to +X$ and second apply a unitary rotation $U = \exp(i\pi\tau_z)$ to $\tilde{\psi}_2$.

density and the supercurrent. As a result, the superfluid density n_s is equal to the density n_f of the elementary fermions. Given this, we first impose the charge neutrality condition $n_s + j^0_{\text{ions}} = 0$ in Eq. (3.13). Combining now Eqs. (3.13), (3.16) and (3.18), we integrate out the massive electromagnetic field A_μ, which to lowest order in derivatives is equivalent to the substitutions $A_\mu \to a_\mu$. Keeping now only the leading terms in derivatives, we find

$$\mathcal{L} \to -b_\mu \left(j^\mu_{\text{v}} - \frac{1}{\pi} \epsilon^{\mu\nu\rho} \partial_\nu a_\rho \right) - n_s a_t + \mathcal{L}^{\mathcal{D}}_{\text{qp}}(\tilde{\psi}_i) - \frac{1}{2\pi} \epsilon^{\mu\nu\rho} \tilde{\mathcal{A}}^v_\mu \partial_\nu a_\rho \tag{3.19}$$

with

$$\begin{aligned}
\mathcal{L}^{\mathcal{D}}_{\text{qp}}(\tilde{\psi}_i) = \tilde{\psi}^\dagger_1 \left(i\mathcal{D}_t + iv_F \tau_z \mathcal{D}_X + iv_\Delta \tau_x \mathcal{D}_Y - \delta\tau_y \right) \tilde{\psi}_1 \\
+ \tilde{\psi}^\dagger_2 \left(i\mathcal{D}_t + iv_F \tau_z \mathcal{D}_X + iv_\Delta \tau_x \mathcal{D}_Y \mp \delta\tau_y \right) \tilde{\psi}_2,
\end{aligned} \tag{3.20}$$

where the covariant derivative $\mathcal{D}_\mu$ was defined in Eq. (3.17).

Since in a superconductor an elementary fermion carries a 2π flux of the vortex magnetic field (see Appendix B), a finite density of these fermions gives rise to a finite background value of $\mathcal{B}^v$. It thus seems natural at this point to absorb the term $-n_s a_t$ in Eq. (3.19) into the source term. This indeed can be done by writing $n_s a_t \to \epsilon^{\mu\nu\rho} \bar{\mathcal{A}}^v_\mu \partial_\nu a_\rho / (2\pi)$ with $\bar{\mathcal{A}}^v_t = 0$ and $\bar{\mathcal{B}}^v = 2\pi n_s$. As the result, Eq. (3.19) simplifies to

$$\mathcal{L} = \frac{1}{\pi} \epsilon^{\mu\nu\rho} a_\mu \partial_\nu b_\rho - b_\mu j^\mu_{\text{v}} - \frac{1}{2\pi} \epsilon^{\mu\nu\rho} \mathcal{A}^v_\mu \partial_\nu a_\rho + \mathcal{L}^{\mathcal{D}}_{\text{qp}}(\tilde{\psi}_i), \tag{3.21}$$

where $\mathcal{A}^v = \bar{\mathcal{A}}^v + \tilde{\mathcal{A}}^v$.

3.4.5   Topological field theory

Finally, we integrate out massive Dirac fermions in Eq. (3.20), which are minimally coupled to the statistical gauge field a and the spin source $\mathcal{A}^s$. The resulting statistical and spin Hall response is

$$\mathcal{L}^{\mathcal{D}}_{res} = \frac{1}{8\pi} \sum_{i=1,2} \sum_{\alpha=\uparrow,\downarrow} \frac{m_i}{|m_i|} \epsilon^{\mu\nu\rho} \left(a_\mu \partial_\nu a_\rho + q_s^2 \mathcal{A}^s_\mu \partial_\nu \mathcal{A}^s_\rho \right), \tag{3.22}$$

where the unit of spin charge $q_s = 1/2$. This can be encoded within the Chern-Simons theories of two statistical gauge fields $c^\uparrow$ and $c^\downarrow$.

Specifically, for the s-wave case, where $\sum_{i,\alpha} m_i/|m_i| = 0$, we use the zero-chirality theory

$$
\begin{aligned}
\mathcal{L}_{\text{qp}}^{\mathcal{D}} \to &\frac{1}{4\pi}\epsilon^{\mu\nu\rho}\big(c_\mu^\uparrow\partial_\nu c_\rho^\uparrow - c_\mu^\downarrow\partial_\nu c_\rho^\downarrow\big) + \frac{1}{2\pi}\epsilon^{\mu\nu\rho}a_\mu\partial_\nu(c_\rho^\uparrow + c_\rho^\downarrow) \\
&- \frac{1}{2\pi}\epsilon^{\mu\nu\rho}\mathcal{A}_\mu^s\partial_\nu(c_\rho^\uparrow - c_\rho^\downarrow) - c_\mu^\uparrow j_\uparrow^\mu + c_\mu^\downarrow j_\downarrow^\mu - \frac{1}{\pi}\epsilon^{\mu\nu\rho}\mathcal{A}_\mu^s\partial_\nu a_\rho
\end{aligned}
\tag{3.23}
$$

which by construction has a vanishing Hall response. In particular, integrating out $c^\uparrow$ and $c^\downarrow$ results in a term $\sim \mathcal{A}^s\partial a$ which is exactly cancelled by the last term in Eq. (3.23).

On the other hand, for the $d+id$ case with $\sum_{i,\alpha} m_i/|m_i| = 4$ we employ the chiral theory

$$
\begin{aligned}
\mathcal{L}_{\text{qp}}^{\mathcal{D}} \to &\frac{1}{4\pi}\epsilon^{\mu\nu\rho}\big(c_\mu^\uparrow\partial_\nu c_\rho^\uparrow + c_\mu^\downarrow\partial_\nu c_\rho^\downarrow\big) + \frac{1}{2\pi}\epsilon^{\mu\nu\rho}a_\mu\partial_\nu(c_\rho^\uparrow + c_\rho^\downarrow) \\
&- \frac{1}{2\pi}\epsilon^{\mu\nu\rho}\mathcal{A}_\mu^s\partial_\nu(c_\rho^\uparrow - c_\rho^\downarrow) - c_\mu^\uparrow j_\uparrow^\mu - c_\mu^\downarrow j_\downarrow^\mu.
\end{aligned}
\tag{3.24}
$$

In Eqs. (3.23) and (3.24), we also included the coupling to gapped spin-up and spin-down Bogoliubov quasiparticles that are represented in the Chern-Simons field theory by external bosonic currents $j_\uparrow$ and $j_\downarrow$, respectively.[9] By putting Eqs. (3.23), (3.24) that capture the quasiparticle sector of the full Lagrangian into Eq. (3.21) results in the completely topological *four-component* $(a, b, c^\uparrow, c^\downarrow)$ Chern-Simons theories for s-wave and $d+id$ superconductors which will be discussed in detail in Secs. 3.5.1 and 3.5.2, respectively.

3.4.6   Extension to higher partial waves

The above construction can be straightforwardly generalised to chiral superconductors paired in the kth partial wave, for $k \in 2\mathbb{Z}/\{0\}$. We start from a time-reversal invariant superconductor with a gap proportional to the real part of $(p_x \pm ip_y)^k$ which has k pairs of nodes at the Fermi surface. This leads to k massless Dirac spin doublets. We can deform into the chiral $(p_x + ip_y)^k$ state by adding masses of the same sign to all Dirac modes. This procedure gives rise to the Chern-Simons theory that will be investigated in Sec. 3.5.3, following our presentation and analysis for the s-wave and $d+id$ cases.

---

[9] It would be instructive to derive Eqs. (3.23), (3.24) rigorously by using the functional bosonization approach developed in [180].

3.5 Topological field theories of spin-singlet superconductors

In this section we analyze the topological theories that were derived in the previous section. In addition to summarizing the braiding properties of quasiparticles, we investigate the role of global symmetries in the bulk and at the edge of spin-singlet superconductors.

3.5.1 s-wave superconductor

Having encoded the topological properties of vortices in Eq. (3.21) and of the nodal Dirac quasiparticles in Eq. (3.23), we combine these to arrive at the four-component Chern-Simons theory of the form (5.34) with $a^I = (a, b, c^\uparrow, c^\downarrow)$. The resulting K-matrix characterizing the s-wave state is

$$
K = \begin{pmatrix}
0 & 2 & 1 & 1 \\
2 & 0 & 0 & 0 \\
1 & 0 & 1 & 0 \\
1 & 0 & 0 & -1
\end{pmatrix}.
\tag{3.25}
$$

This K-matrix is *fermionic* (with two odd integers on the diagonal) encoding the presence of an *elementary*[10] fermionic excitation in the spectrum of the superconductor. Notably, the K-matrix (3.25) does contain the (toric code) bosonic block $\begin{pmatrix} 0 & 2 \\ 2 & 0 \end{pmatrix}$, which, for the s-wave superconductor, was derived previously in [46]. The l-vectors, defining integer-valued charges of independent excitations with respect to statistical gauge fields $a, b, c^\uparrow, c^\downarrow$, are shown[11] in Fig. 3.3. The self and mutual statistical angles can be extracted from the topological theory (5.34) as

$$
\theta_l = \pi l^{\mathrm{T}} \cdot K^{-1} \cdot l, \qquad \theta_{l,l'} = 2\pi l^{\mathrm{T}} \cdot K^{-1} \cdot l'.
\tag{3.26}
$$

Thus, we find that e and m are bosons and ϵ is a fermion for the s-wave superconductor. In addition, any mutual braiding gives the statistical angle π.

---

[10] By definition, an elementary excitation has trivial mutual statistics with all anyons.

[11] Specifically, in Fig. 3.3 we chose to identify ϵ with the spin-up Bogoliubov quasiparticle that carries the current $j_\uparrow$ in Eq. (3.23). Alternatively, in the s-wave case one can choose $l_{\epsilon\downarrow} = (0, 0, 0, -1)$ which corresponds to the spin-down Bogoliubov quasiparticle. The latter identification gives the same braiding and fusion rules as the former, but obviously differs by the sign of the spin charge. Note that for the $d + id$ state, Eq. (3.24) leads to $l_{\epsilon\downarrow} = (0, 0, 0, 1)$.
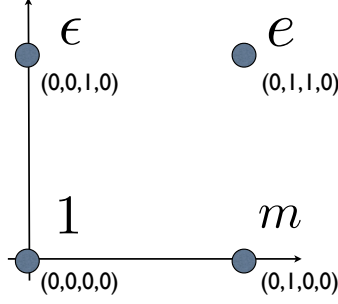
Figure 3.3: Integer-valued l-vectors of 1, e, m, ϵ excitations for the s-wave and $d + id$ superconductor.

Now we consider the symmetries: In a generic effective theory (5.34) the charge Q_A of an excitation characterized by the l-vector is given by

$$Q_l^A = t_A^T \cdot K^{-1} \cdot l. \tag{3.27}$$

For the s-wave state, it follows from the derivation in Sec. 3.4 that the t-vectors for the spin and magnetic flux symmetry are $t_s^T = (2, 0, 1, -1)$, $t_v^T = (1, 0, 0, 0)$. This fixes the spin and vortex charges of m, ϵ and e to be

$$Q_s^m = 0, \qquad Q_s^\epsilon = 1, \qquad Q_s^e = 1,$$
$$Q_v^m = 1/2, \qquad Q_v^\epsilon = 0, \qquad Q_v^e = 1/2. \tag{3.28}$$

Since we previously defined that in a superconductor, Bogoliubov particles carry *only spin* and vortices carry *only magnetic flux*, we now must identify ϵ and m with the Bogoliubov quasiparticle and vortex respectively. As expected, the Bogoliubov quasiparticle ϵ is a fermion, while the vortex m is a boson. Their composite e is a *boson*, which carries the spin and vortex charge. The mutual π-phase under the braiding of ϵ around m is consistent with the well-known fact that in a superconductor the Bogoliubov quasiparticle (despite being electrically neutral [150]) accumulates a minus sign upon encircling a vortex [181, 182].

The s-wave pairing does not violate two-dimensional parity P ($x \leftrightarrow y$) and time-reversal T ($t \rightarrow -t$). As a result, the effective theory (5.34) should be invariant under these discrete symmetries. We specify the transformation properties of all fields: First, under P and T the Bogoliubov

quasiparticle currents $j_\uparrow$, $j_\downarrow$ and the vortex current j_v transform differently. The definitions of the currents lead to the following nontrivial transformations

$$P : j_\uparrow^0 \leftrightarrow j_\downarrow^0, \quad j_\uparrow^x \leftrightarrow j_\downarrow^y, \quad j_v^0 \rightarrow -j_v^0, \quad j_v^x \leftrightarrow -j_v^y,$$
$$T : j_\uparrow^0 \leftrightarrow j_\downarrow^0, \quad j_\uparrow^i \leftrightarrow -j_\downarrow^i, \quad j_v^0 \rightarrow -j_v^0. \tag{3.29}$$

Given these, the statistical gauge fields $c^\uparrow$ and $c^\downarrow$ in Eq. (3.23) transform as

$$P : c_0^\uparrow \leftrightarrow -c_0^\downarrow, \quad c_x^\uparrow \leftrightarrow -c_y^\downarrow,$$
$$T : c_0^\uparrow \leftrightarrow -c_0^\downarrow, \quad c_i^\uparrow \leftrightarrow c_i^\downarrow, \tag{3.30}$$

while the statistical gauge field b, the vortex source $\mathcal{A}^v$ and the spin source $\mathcal{A}^s$ transform like the vortex current j_v in Eq. (3.29). Finally, under P and T the statistical gauge field a transforms like the electromagnetic gauge potential A,

$$P : a^x \leftrightarrow a^y$$
$$T : a^i \rightarrow -a^i. \tag{3.31}$$

Using these transformation properties, it is straightforward to check that the effective theory (5.34) is indeed invariant under P and T.

In the absence of external quasiparticle currents in Eq. (5.34), all statistical gauge fields can be integrated out resulting in the Hall response

$$\mathcal{L}_{res} = -\frac{1}{4\pi} \underbrace{t_A^T \cdot K^{-1} \cdot t_B}_{\nu_{AB}} \epsilon^{\mu\nu\rho} \mathcal{A}_\mu^A \partial_\nu \mathcal{A}_\rho^B. \tag{3.32}$$

A simple calculation leads to $\nu_{AB} = 0$. Thus the s-wave superconductor reassuringly exhibits no Hall effects, which is consistent with P and T invariance of this state.

Finally, we look at the edge, where there are *two pairs of counter-propagating* chiral modes because the K-matrix has two pairs of eigenvalues of the opposite sign. Note, however, that one is allowed to add to the edge Lagrangian (5.5.2.4) two independent Higgs terms $\cos(2t_s \cdot \phi)$ and $\cos(2t_v \cdot \phi)$ which satisfy the conditions Eq. (3.9). As a result, the two Higgs terms completely gap out all four edge modes of the s-wave superconductor, consistent with the expectation that

this state neither has gapless edge modes nor a Hall response. The above arguments explicitly demonstrate that the low energy physics of the s-wave state cannot be completely characterized by the toric code model since the edge of the toric code can be gapped out in two physically distinct ways [183] whereas the edge of an s-wave superconductor with $\mathrm{U}(1)_s \times \mathrm{U}(1)_v$ symmetry is gapped by the unique mechanism presented above.

3.5.2 $d + id$ superconductor

In a chiral $d + id$ superconductor, parity and time-reversal are broken spontaneously, which gives rise to *anyon* self-statistics of excitations. In parallel with the s-wave case, in Sec. 3.4 we derived the fermionic K-matrix for this state

$$
K = \begin{pmatrix} 0 & 2 & 1 & 1 \\ 2 & 0 & 0 & 0 \\ 1 & 0 & 1 & 0 \\ 1 & 0 & 0 & 1 \end{pmatrix}.
\tag{3.33}
$$

It describes a chiral state with a chiral central charge $c = k = 2$. The l-vectors are identical to the s-wave case and are illustrated in Fig. 3.3 (also see footnote[12]). As a result, in the weakly-coupled topological phase of a $d + id$ superconductor, e and m excitations are semions [50], i.e., they have the statistical angle $\theta_e = \theta_m = \pi/2$. On the other hand, ϵ is a fermion and has nontrivial mutual π statistics with e and with m.

The derivation undertaken in Sec. 3.4 fixed the symmetry t-vectors for this state to be

$$
t_s^T = (0, 0, 1, -1), \quad t_v^T = (1, 0, 0, 0).
\tag{3.34}
$$

Using Eq. (3.27), we find that the spin and vortex charges of the excitations equal

$$
\begin{aligned}
Q_s^m = 0, \qquad Q_s^\epsilon = 1, \qquad Q_s^e = 1 \\
Q_v^m = 1/2 \qquad Q_v^\epsilon = 0, \qquad Q_v^e = 1/2.
\end{aligned}
\tag{3.35}
$$

which are, in fact, identical to those for the s-wave case given in Eq. (3.28). As a result, in this case ϵ and m will be still identified with the Bogoliubov quasiparticle and vortex, respectively. In

contrast to the s-wave superconductor, the vortex here is a semion. In fact, the semion statistics of the vortex can be extracted from the Berry phase accumulated under exchange of two identical vortices in a $d + id$ superconductor, which can be computed by a simple generalization of the computation done for a $p + ip$ superconductor in [179]. Alternatively, the semion phase follows from a qualitative argument presented in [184] that views a $d \pm id$ superconductor as a stack of four spinless $p \pm ip$ layers.

The effective theory (5.34) with the K-matrix (3.33) is PT invariant, but breaks separately P and T symmetries. Consequently, we find a nontrivial Hall response

$$\nu = \begin{pmatrix} 2 & 0 \\ 0 & 0 \end{pmatrix}. \tag{3.36}$$

with ν defined in Eq. (3.32). We thus showed here that in the topological (weakly-coupled) phase a chiral d-wave superconductor exhibits the spin Hall effects with $\nu_s = 2$, but no vortex ($\nu_v = 0$) and mixed spin-vortex Hall ($\nu_{vs} = 0$) responses. For the spin part, this reproduces in appropriate units the findings from [89, 162]. In particular, in a $d + id$ paired state a position-dependent external magnetic Zeeman field $B(x, y)$ will give rise to the Hall current of the z-component of spin $j_s^i = -\sigma_s \epsilon^{ij} \partial_j B$ with the spin Hall conductivity $\sigma_s = 1/(4\pi)$.[12] But what is the physical implication of the absence of the vortex Hall effect? Since the density and current of the elementary fermions fix the background values of $\mathcal{B}^v$ and $\mathcal{E}_i^v$ (see Appendix B), a nontrivial vortex Hall effect *would* imply

$$n_v = \frac{\nu_v}{2\pi} \mathcal{B}^v = \nu_v n_f,$$
$$j_v^i = -\frac{\nu_v}{2\pi} \epsilon^{ij} \mathcal{E}_j^v = \nu_v j_f^i, \tag{3.37}$$

i.e., a linear relation between the densities of the elementary fermions and vortices in the ground state of the $d + id$ superconductor. The fact that we found $\nu_v = 0$ demonstrates explicitly that *zero* magnetic field B (an thus zero density of vortices) is generated in the ground state of the chiral d-wave superconductor. At first sight it might seem surprising that the unbroken magnetic flux

---

[12] Restoring $\hbar$, in our convention the unit of the spin charge is equal to $\hbar/2$ and thus $\sigma_s = \nu_s (\hbar/2)^2/h = \hbar/(4\pi)$.

symmetry has a vanishing Hall response in the $d + id$ paired state that breaks spontaneously parity and time-reversal. In Sec. 3.6 we present a general argument which independently supports this finding.

Consider now the edge of a chiral d-wave superconductor (3.33), where *two co-propagating chiral bosons* appear together with a *pair of counter-propagating* chiral modes. For the purpose of the upcoming discussion, it is convenient to transform the Chern-Simons theory into a $\mathrm{GL}(4, \mathbb{Z})$ equivalent form $(K, l, t) \to (\tilde{K}, \tilde{l}, \tilde{t})$, discussed in detail in Appendix C. In this formulation, the K-matrix is *block-diagonal*

$$\tilde{K}_B = \begin{pmatrix} -2 & 2 & 0 & 0 \\ 2 & 0 & 0 & 0 \\ 0 & 0 & 1 & 0 \\ 0 & 0 & 0 & 1 \end{pmatrix}, \tag{3.38}$$

the l-vectors are

$$\tilde{l}_m^T = (0, 1, 0, 0) = l_m^T,$$
$$\tilde{l}_{\epsilon\uparrow}^T = (-1, 0, 1, 0), \quad \tilde{l}_{\epsilon\downarrow}^T = (-1, 0, 0, 1), \tag{3.39}$$

and the t-vectors are unchanged from Eq. (3.34): $\tilde{t}_s = t_s$, $\tilde{t}_v = t_v$. In this basis, the counter-propagating modes $\tilde{\phi}^1$ and $\tilde{\phi}^2$ are gapped out by the Higgs term $\cos(2\tilde{t}_v \cdot \tilde{\phi})$ that fulfils the conditions (3.9) introduced at the end of Sec. 3.2. On the other hand, due to quantization of the thermal Hall conductance [50, 185], the remaining two co-propagating chiral states $\tilde{\phi}^3$ and $\tilde{\phi}^4$ cannot be gapped by edge interactions or disorder. These chiral states are neutral under the magnetic flux $\mathrm{U}(1)_v$ symmetry. This implies that there is no $\mathrm{U}(1)_v$ gauge anomaly at the edge, consistent with the vanishing vortex Hall effect found above (see also Sec. 3.6). In contrast, the spin Hall effect with $\nu_s = 2$ implies that the edge theory must have a spin gauge anomaly. In fact, the current associated with the spin chiral boson $\tilde{l}_s \cdot \tilde{\phi}$ with

$$l_s^T = \tilde{l}_{\epsilon\uparrow}^T - \tilde{l}_{\epsilon\downarrow}^T = (0, 0, 1, -1) \tag{3.40}$$

realizes the $\mathrm{U}(1)_2$ Kac-Moody affine algebra, where the subscript denotes the level. From a standard argument [186], the current affine algebra $\mathrm{U}(1)_2$ can be actually extended to a larger affine algebra

$SU(2)_1$. The spin sector is thus described by the chiral $SU(2)_1$ Wess-Zumino-Witten edge theory [89] that has the spin gauge anomaly. The complete bulk plus edge theory is of course consistent because the edge anomaly is canceled by the inflow of the bulk spin Hall current.

Curiously, the current associated with the orthogonal combination $l_{tot}^T = \tilde{l}_{\epsilon\uparrow}^T + \tilde{l}_{\epsilon\downarrow}^T = (-2, 0, 1, 1)$ realizes another copy of the $U(1)_2 \rightarrow SU(2)_1$ Kac-Moody affine algebra. The above arguments thus suggest that the edge theory of the chiral d-wave superconductor has an extra $SU(2)_{tot}$ symmetry. As discussed in [89], the $SU(2)_{tot}$ is emergent and does not have a microscopic origin. In a $d \pm id$ superconductor, with the spin and particle-hole symmetries, the velocities of the two co-propagating chiral modes are necessarily *equal*. Therefore the edge supports an anomalous $SO(4) \cong SU(2)_s \otimes SU(2)_{tot}$ symmetry which rotates four edge Majorana modes; for more details, see [89]. In the following subsection, we show how this discussion generalizes to superconductors paired in higher partial even-waves.

3.5.3   Higher partial waves and the 16-fold way

So far, we have analyzed Chern-Simons theories for the specific cases of conventional s-wave and chiral d-wave superconductors, the latter being the simplest example of a spin-singlet chiral state. At this point we extend the discussion to include all chiral spin-singlet superconductors paired in partial even-waves.

In [50], Kitaev demonstrated that chiral superconductors have a $\mathbb{Z}_{16}$ *bulk* classification. Using either the language of axiomatic topological field theory or by considering stacked $p+ip$ layers [184], it can be shown that the statistical angle acquired upon exchanging two e-particles (or two m-particles) has a 16-fold periodicity. That is, given a chiral superconductor with Chern number ν that hosts ν Majorana chiral modes at the edge, the exchange angle of excitations [50]

$$\theta_e = \theta_m = 2\pi\nu/16, \qquad \theta_\epsilon = \pi. \tag{3.41}$$

Since every Majorana mode contributes a half unit of the central charge, the total chiral central charge $c = \nu/2$. Thus, systems with $c = 0$ and $c = 8$ have identical bulk anyonic excitations but
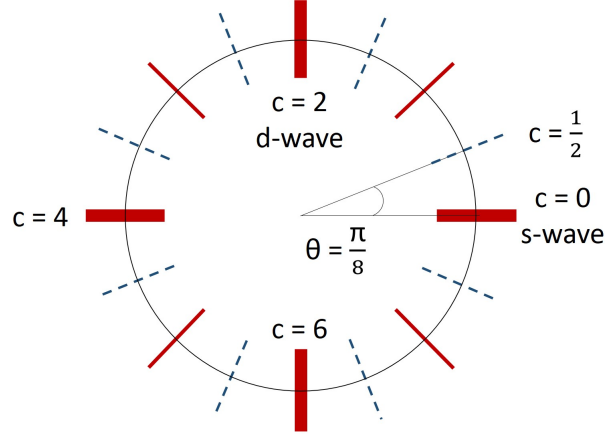
Figure 3.4: Diagrammatic representation of the 16-fold way. The abelian states considered in our work are represented by thick lines and the other abelian states by thin lines. Dashed lines indicate the non-abelian states. For each state, the angle θ equals the exchange angle $\theta_e = \theta_m$.

have different edge theories manifested in different thermal Hall conductivities. The 16-fold way is diagrammatically depicted in Fig. 3.4, where the angle θ represents θ_e for the different states. The states with half-integer central charge (represented by dashed lines) are *non-abelian* whereas those with integer central charge (represented by solid lines) are *abelian*. Among the latter, the thick lines indicate states with $c \in 2\mathbb{Z}$, which are realized by the spin-singlet superconductors studied in this thesis. For these superconductors, the chiral central charge c equals the chirality parameter k.

From Sec. 3.4, it follows that the weakly-paired chiral superconductor paired in even k^{th} partial wave has the $(k+2) \times (k+2)$ K-matrix

$$
K = \left(\begin{array}{cc|c}
0 & 2 & 1_k \\
2 & 0 & 0_k \\
\hline
1_k^T & 0_k^T & \mathbb{1}_{k \times k}
\end{array} \right),
\tag{3.42}
$$

where we introduced the notation $x_k = (\underbrace{x, x, \ldots, x}_{k \text{ times}})$. In fact, this K-matrix has previously appeared in a somewhat different context in [187]. The l-vectors of the excitations are

$$
\begin{aligned}
l_m^T &= (0, 1, 0_k), \\
l_\epsilon^T &= (0, 0, 1, 0_{k-1}).
\end{aligned}
\tag{3.43}
$$

It is straightforward to demonstrate that these spin-singlet states $k \in 2\mathbb{Z}/\{0\}$ fall into the 16-fold way since they have the chiral central charge $c = k$ and lead to the statistics (3.41). Interestingly, the states where c is an odd integer form a different class of *abelian* states which perhaps describe certain phases of spin-triplet superconductors.

The charges of excitations are given by Eq. (3.35), i.e., they are identical to the s-wave and $d + id$ cases. These states are fixed by the symmetry t-vectors, which in this case are given by

$$
\begin{aligned}
t_s^T &= (0, 0, \pm 1_k), \\
t_v^T &= (1, 0, 0_k),
\end{aligned}
\tag{3.44}
$$

where $\pm 1_k = (\underbrace{1, -1, \ldots, 1, -1}_{k/2 \text{ times}})$. We thus again find the Bogoliubov quasiparticle to be the fermion ϵ, while the vortex is the anyon m that has the statistical angle $\theta_m = \pi k / 8$. An explicit calculation gives the spin Hall coefficient $\nu_s = k$ and the vanishing vortex ($\nu_v = 0$) and mixed vortex-spin ($\nu_{vs} = 0$) coefficients. This result is a natural generalization of Eq. (3.36) found for the $d + id$ state.

One can better understand the edge theory of chiral paired states by casting the K-matrices (3.42) into two different GL$(k + 2, \mathbb{Z})$-equivalent block-diagonal forms $\tilde{K}_B$ and $\tilde{K}_C$ (see Appendix C for details). Generalizing the discussion in Sec. 3.5.2, from the form

$$
\tilde{K}_B = \begin{pmatrix} -k & 2 \\ 2 & 0 \end{pmatrix} \oplus \mathbb{1}_{k \times k},
\tag{3.45}
$$

one finds that *a pair* of counter-propagating edge modes is gapped out by the allowed Higgs term $\cos(2\tilde{t}_v \cdot \phi)$. Similar to the $d + id$ case, the remaining gapless chiral theory is neutral under the magnetic flux U$(1)_v$ symmetry. On the other hand, symmetries of the edge appear naturally from the Cartan block-diagonal form

$$
\tilde{K}_C = A_{k \times k}^{\text{SO}(2k)} \oplus \begin{pmatrix} 1 & 0 \\ 0 & -1 \end{pmatrix},
\tag{3.46}
$$

where $A_{k \times k}^{\text{SO}(2k)}$ is the *Cartan matrix* of the Lie algebra SO$(2k)$ and is defined in Eq. (C.8). For

example, for the $d + id$ superconductor ($k = 2$), one finds

$$\tilde{K}_C = \begin{pmatrix} 2 & 0 \\ 0 & 2 \end{pmatrix} \oplus \begin{pmatrix} 1 & 0 \\ 0 & -1 \end{pmatrix}, \tag{3.47}$$

with the SO(4) $\cong$ SU(2)$_s \otimes$SU(2)$_{tot}$ symmetry, discussed in Sec. 3.5.2, manifest. In a similar fashion, following [186], we can show that the current operators arising from the Cartan block satisfy $SO(2k)_1$ Kac-Moody algebra. This seems to suggest that the chiral edge theory might have an internal SO($2k$) symmetry associated with rotations of the $2k$ multiplet of Majorana modes. Generically, however, we expect this symmetry to be *broken* by the velocity matrix. As illustrated in Fig. 3.5, in a chiral superconductor of chirality k, $2k$ Majorana edge modes split into $n = k/2$ quartets. The modes within each quartet are related by the spin and particle-hole symmetry, and thus have the same velocity. However, nothing prevents different quartets from having different velocities. As a result the nature of the residual symmetry at the edge of a chiral superconductor depends on the velocity matrix and hence on the microscopic details.
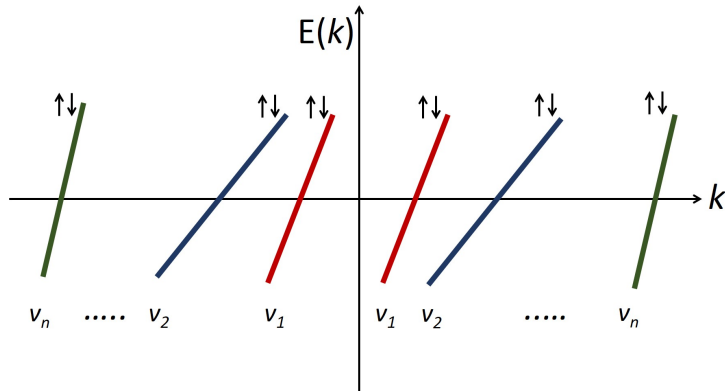
Figure 3.5: A chiral superconductor with chirality $k \in 2\mathbb{Z}$ hosts $2k$ Majorana modes at the edge. As indicated by the ($\uparrow\downarrow$) arrows, each mode is doubly degenerate due to spin symmetry and modes with the same color are related by particle-hole symmetry. Thus, the modes within a quartet have the same velocity v_i, while generically different quartets will have different velocities.

From the Cartan form (3.46) of the K-matrices, it is clear that the fermionic block, σ^z, is topologically trivial, i.e., it does not effect the ground state degeneracy, chirality, and statistics of the system. In other words, in the absence of symmetries these K-matrices are stably equivalent [188]

to the Cartan matrices $A^{\text{SO}(2k)}$.[13] However, in the presence of coupling to the vortex source $\mathcal{A}^v$, the fermionic block is essential because the vortex symmetry vector t_v (in this basis) has non-zero elements in this sector.

3.6   Absence of vortex Hall effect in superconductors

In the previous section we found for all superconductors that the vortex Hall effect for the magnetic flux symmetry is zero. While for the s-wave state this is a completely expected result, for chiral spin-singlet states it might seem surprising since parity and time-reversal are spontaneously broken and one might expect that these unbroken symmetries should exhibit nontrivial Hall responses. Here we will argue that the vortex Hall effect should vanish in *any* superconductor due to the finite mass of the photon field acquired via the Higgs mechanism.

Consider a general two-dimensional superconductor coupled to the magnetic flux source $\mathcal{A}^v$

$$\mathcal{L} = \mathcal{L}_{\text{SC}}(f, A) - \frac{1}{2\pi}\epsilon^{\mu\nu\rho}\mathcal{A}^v_\mu \partial_\nu A_\rho, \tag{3.48}$$

where the elementary fermions f undergo Cooper pairing and thus generate a mass to the electromagnetic gauge potential A via the Higgs mechanism. After integrating out f and A, the vortex Hall effect can in principle appear from the quadratic contribution to the effective action $\Gamma[\mathcal{A}^v]$. In a translation-invariant system

$$\begin{aligned}\Gamma^{(2)}[\mathcal{A}^v] &= \frac{1}{2}\int d^3x d^3y \mathcal{A}^v_\mu(x)\Gamma^{\mu\nu}(x-y)\mathcal{A}^v_\mu(y) \\ &= \frac{1}{2}\int d^3p \mathcal{A}^v_\mu(-p)\Gamma^{\mu\nu}(p)\mathcal{A}^v_\mu(p),\end{aligned} \tag{3.49}$$

where in momentum space the kernel $\Gamma^{\mu\nu}(p)$ is given by

$$\Gamma^{\mu\nu}(p) \sim \epsilon^{\mu\alpha\gamma}p_\alpha D_{\gamma\delta}(p)\epsilon^{\nu\beta\delta}p_\beta \tag{3.50}$$

with $iD_{\gamma\delta}(p)$ a fully renormalized photon propagator. The kernel is illustrated in Fig. 3.6 as a Feynman diagram.

---

[13] Incidentally, these purely bosonic Cartan K-matrices have also been proposed for describing s-wave superconductors strongly proximity-coupled to topological Chern insulators in [189].

Figure 3.6: Feynman diagram for the kernel $\Gamma^{\mu\nu}(p)$: the bold wavy line denotes the renormalized photon propagator $iD_{\gamma\delta}(p)$, the red cross represents the vertex originating from the last term in Eq. (3.48).

Let us start in the s-wave phase which obviously has a vanishing vortex Hall coefficient $\nu_v = 0$. As in Sec. 3.4, by tuning the Dirac masses of the Bogoliubov quasiparticles we can enter into the chiral $d + id$ phase (see Fig. 3.2). Importantly, during this process the photon propagator *always* remains gapped due to the Higgs mechanism. Since ν_v can only change at a point where the photon gap closes, this shows that as we enter the $d + id$ phase ν_v remains zero. This result should be contrasted to the spin Hall effect which arises from the *fermionic* one-loop diagram [89, 162]. It is clear from Fig. 3.2 that after starting in the s-wave state the fermionic gap must close as one enters the $d + id$ phase, allowing the spin Hall coefficient to jump from $\nu_s = 0$ (s-wave) to $\nu_s = 2$ ($d + id$).

Clearly the argument above can be generalized to other chiral superconductors that can be obtained by deformations of a time-reversal invariant superconducting state. In summary, as long as the Higgs mechanism produces a finite gap for the photon field (along the deformation trajectory), the Hall coefficient for the magnetic flux symmetry should *vanish*. This is in a stark contrast to the standard probes of time-reversal breaking, such as the polar Kerr, spin Hall and Nernst/Ettingshausen effects that should give non-vanishing signals in chiral superconducting states.

3.7   Open questions and outlook

In this work we have developed a topological framework for the low-energy physics of two-dimensional spin-singlet superconductors. Here we discuss some open questions that go beyond the scope of this thesis and are left for future studies.

As emphasized throughout this chapter, in this work the electromagnetic field is strictly

confined to *two* spatial dimensions. On the other hand, in thin film superconductors the *mixed-dimensional* problem of two-dimensional paired fermions interacting with a three-dimensional electromagnetic field is realized most naturally. For this reason, this system deserves to be studied in detail. It also might fall into the class of quasi-topological phases introduced by Bonderson and Nayak in [190].

Additionally, here we have considered a theory that allows topological defects (vortices) of the matter field, but not topological defects (magnetic monopoles) in the electromagnetic (non-compact) sector. It might be interesting to investigate a two-dimensional superconductor with a *compact* electromagnetism; in this version of the theory, magnetic monopoles are allowed and appear in the form of spacetime instantons [191]. As a result, the magnetic flux symmetry is lost because a pair of vortices can instantly disappear into a monopole. This rich problem naturally arises in the physics of spin liquids and was investigated in the seminal paper of Fradkin and Shenker [192]. In the future, it would be interesting to extend our work to this model and to investigate the interplay of the unbroken $SU(2)_s$ spin symmetry and topological order in it.

We have demonstrated in this chapter that all superconductors have a vanishing vortex Hall response due to the finite gap of the photon field that arises from the Higgs mechanism. As long as this gap can be closed, however, it seems possible that one can enter a distinct phase of matter with $\nu_v \neq 0$. In contrast to a superconductor, this phase is characterized by a finite flux of magnetic field in the ground state, corresponding to a dense collection of vortices. It will hence be of interest to find ways of closing the photon gap in our problem.

Moreover, the realization of the magnetic flux symmetry might be subtle in the problem studied here. For a bosonic toric code model, for instance, it is known that it is *impossible* to realize an internal global $U(1)$ symmetry with the charges $Q_e = Q_m = 1/2$ in a purely two-dimensional world. In fact, this realization of a symmetry can only appear on the surface of a three-dimensional system. This is known as the statistical anomaly and, for bosonic systems, is discussed in detail in [193, 194]. We believe that the fate of this anomaly in two-dimensional fermionic superconductors deserves future investigation.

Recently, it has also become clear that in a weakly paired $d + id$ superfluid (and also in chiral superfuids paired in higher partial waves) not all fermions in the ground state are paired in the presence of an edge [90]. These unpaired fermions are localized close to the edge and carry a mass current that partially compensates the angular momentum $L = lN/2$ carried by the chiral Cooper pairs. This current is *non-universal* since it depends on the structure of the edge. It would be interesting to investigate the nature of this current in the presence of a dynamical electromagnetism.

A limitation of the K-matrix formalism is that it allows us to incorporate only the coupling to the abelian subgroup of the spin symmetry. Currently, the Chern-Simons field theory does not allow coupling to the full nonabelian spin symmetry because we do not know how to fractionalize representations of nonabelian groups. Using an alternative formalism that allows coupling to all non-abelian $\mathrm{SU}(2)_s$ sources could thus generalize our work. In addition, since any physical system breaks the spin symmetry due to *spin-orbit coupling*, it would be useful to study the effects of (weakly) breaking this symmetry.

Finally, it is known that two-dimensional chiral superconductors and superfluids exhibit a non-vanishing "shift" and Hall viscosity [195–197]. Following the seminal work of Wen and Zee [198], it should be possible to account for these phenomena by coupling the spin connection to the topological Chern-Simons theories developed here.

Chapter 4

Dynamics in Fracton Models: Life in the Slow Lane

In which Benny extricates himself

from all manners of tangled knots and

comes vertically unstuck.

The first half of this dissertation dealt with familiar quantum phases of matter—superfluids and superconductors—albeit in novel settings. We now come to phases less familiar: fractons. As discussed briefly in § 1, fracton phases of matter first appeared in certain exactly solvable models in $d = 3$ spatial dimensions and host strange new excitations with restricted mobilities. These gapped phases seem to evade our current frameworks for understanding topological order since their ground state degeneracy on non-trivial manifolds is *not* entirely determined by the topology of the underlying manifold but instead also depends on the geometry through e.g. the system size.

In this chapter we consider the closed quantum dynamics of gapped fracton phases, in particular those described by stabilizer Hamiltonians, including the X-Cube model [76] or Haah's code [75]. At the exactly solvable point, the dynamics of these models is trivial: since any configuration of local excitations is locally created by terms in the Hamiltonian and is hence labelled by stabilizer eigenvalues, it is an eigenstate. Thus, we must consider arbitrary local perturbations in order to find any non-trivial dynamical behaviour. Owing to the finite gap of the fracton phases under consideration, we are guaranteed to remain in the fracton phase as long as the typical energy scale of the perturbations is smaller than that set by the gap i.e. these phases are robust against local perturbations [199, 200].

Under such a setting, one can begin to study the quantum dynamics of isolated fracton models. In particular, we can consider initializing the system in some eigenstate of the unperturbed Hamiltonian, with a definite real-space configuration of excitations, and then study its evolution under the dynamics of the full Hamiltonian. For states initialized with a vanishing density of topological excitations, such a program was carried out in [201], where it was argued that the superselection rules of gapped fracton phases allow them to retain a memory of their initial conditions in local observables. At least in the subspace with a vanishing density of topological excitations, fracton phases thus display a form of "localization" physics. The question addressed in this chapter is whether this behaviour persists in the presence of a finite energy density of excitations (equivalently, at finite temperature). We show that gapped fracton phases display a form of asymptotic many-body localization, with a glassy approach to equilibration, and argue that these phases constitute an intriguing platform for studying the interplay between topological protection and constrained Hamiltonian dynamics within the same translation invariant models.

A version of this chapter was first presented as [88] under the title "Glassy Quantum Dynamics in Translation Invariant Fracton Models," and is a collaboration with Jeongwan Haah and Rahul Nandkishore,

Phys. Rev. B 95, 155133 (2017) (2017)[1]
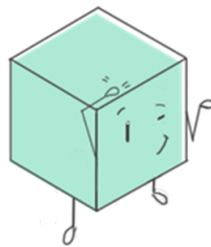
Oh that magic feeling, nowhere to go.

4.1   Introduction and Motivation

Recent years have witnessed an explosion of interest in many body localization (MBL) [69, 202–207], whereby isolated quantum systems with quenched disorder can exhibit ergodicity breaking and fail to thermalize even at infinite times. Interest in the phenomenon is in part intrinsic (e.g. many body localized systems can support entirely new types of quantum order [208–211]), in part practical (e.g. MBL systems can serve as ideal quantum memories [69]), and in part due to the tantalizing connections to other fields. For example, MBL can be viewed as a type of "ideal quantum glass" which does not reach equilibrium at infinite times—can insights from MBL inform the study of classical structural glass? (This particular question has been the focus of intensive work [212–219] without any definitive conclusions). Recent experimental progress [220–226] has further intensified interest in the field. However, theoretical insights have been hard won, due to the fundamental challenges of describing a non-ergodic, non-equilibrium, strongly correlated, highly disordered phase. Indeed most theoretical progress has required either a new idea (such as the notion of emergent integrability [207, 227–230]), a new technique (such as dynamical versions of real space renormalization [231])—or a new class of models which provide access to a new and formerly unforeseen phenomenology (e.g. [232]).

The study of topological phases in three spatial dimensions has brought to light a new class of models [73–77, 233] which have remarkable properties. These exactly solvable three-dimensional (3D) lattice models have ground states that exhibit a sub-extensive topological degeneracy on the 3D torus and possess point-like excitations, dubbed "fractons" [74] that cannot move without creating additional excitations. Such systems are related by duality to spin models with symmetries along lower-dimensional subsystems [76, 234] and were recently classified into Type I and Type II fracton phases. In the Type I phases, fractons are created by the application of a membrane operator and pairs of fractons form composite topological excitations that can move along lower-dimensional subsystems. In the Type II phases, fractons are created by the application of a fractal operator and all topological excitations are strictly immobile. The fracton models that have been introduced to

date have all involved discrete symmetries, although there does not in principle appear to be any obstruction to constructing continuous fracton models—indeed a stimulating series of works from Pretko [80, 81] appears to reproduce much of the fracton phenomenology within a continuum field theory with $U(1)$ symmetry. Layer constructions of these phases have also recently been advanced [78, 79].

In this chapter, we combine emerging ideas from research into (fracton) topological phases and MBL by studying the *dynamical* behaviour of fracton models, revealing an intimate and provocative connection between the two fields. We begin by discussing type I fracton models at finite energy density and demonstrate that in these models, the mobility of charges is suppressed *exponentially* in the inverse temperature. When a type I fracton model prepared in its ground space (i.e. at zero energy density) is placed in contact with a finite temperature heat bath, we show that the equilibration exhibits $\log t$ behaviour over an exponentially wide window of time scales—a classic signature of glassy dynamics (see e.g. [235] and references contained therein). We emphasize that this glassy quantum dynamics occurs in a *three-dimensional, translation invariant* Hamiltonian. We then turn to type II fracton models, and demonstrate that charges exhibit subdiffusion upto a relaxation time that diverges at low temperatures as a *super-exponential* function of temperature, reminiscent of "near MBL" disordered systems [236, 237] and the 'fragile liquid' regime of classical glaasses. Finally, we conjecture that fracton models with conserved $U(1)$ charge could realize exotic three-dimensional phases that are thermal metals but charge insulators.

Our work has striking implications for MBL, for the study of fracton phases, and for possible technological applications of both. For MBL, our work illuminates new connections to glasses, introducing a new class of models that exhibit glassy quantum dynamics with translation invariant Hamiltonians. It may also inform investigations of localization and glassy dynamics in higher dimensions [237–239]. For the field of fracton phases, our work reveals that not only do these models have an unusual ground state structure, they also support rich quantum dynamics, thus opening a new line of investigation for three-dimensional topological phases. Practically speaking, our work also uncovers a new route to information storage, as well as identifying a potential

class of three-dimensional phases that are thermal metals but charge insulators. These last could have applications e.g. in high density electronics, where the problem of heat dissipation currently constrains possibilities for miniaturization.

4.2   Fracton Models

Fracton topological phases are a new class of three-dimensional phases of matter that display features that go beyond those familiar from gauge theory. These phases can be obtained as the quantum duals of three-dimensional systems with symmetries along lower dimensional sub-systems, specifically along planes and fractals. A unified framework, based on a generalized lattice gauge theory, for fracton topological order was recently proposed in [76]. Given the novelty of these phases, in this section we provide a self-contained exposition of fracton systems, focusing primarily on specific examples to elucidate the features most relevant to the dynamics.

Fracton phases arise in exactly solvable lattice models in three spatial dimensions and exhibit a sub-extensive topological ground state degeneracy on the 3D torus. The distinguishing feature of these systems is the presence of point-like fractional excitations—fractons—that are fundamentally immobile i.e., they cannot move without creating additional topological excitations. In contrast with anyons in two-dimensional topologically ordered systems, where anyons are created at the ends of a Wilson line and are thus allowed to move by application of a local line-like operator, there exists no local line-like operator that creates a pair of fractons. Instead, fractons are created at the ends of membrane or fractal operators, leaving a single fracton immobile. A classification scheme for fracton topological order was recently proposed in [76], where these systems were divided into type I and type II phases.

Type I fracton phases, such as the X-Cube model discussed below, host fracton excitations at the ends of membrane operators. While single fractons are immobile, bound-states of fractons form composite topological excitations that are free to move along lower-dimensional subsystems such as a line or a plane. There may also exist additional quasi-particles that are confined to move only along lower-dimensional subsystems. In type II phases, such as Haah's code [75], fractons are

created by the application of fractal operators and **all** topological excitations are strictly immobile. The latter feature leads to a fundamental difference between the dynamics of type I and II fracton phases, which we now consider separately in the following sections.

4.3   Type I Fracton Models

The physics of type I fracton topological order is best illustrated through the example of the X-Cube model [76] that displays the essential features of these phases. The X-Cube model is an exactly solvable lattice model defined on a cubic lattice with Ising spins living on each link. The Hamiltonian is

$$H_{XC} = -\sum_c A_c - \sum_{v,k} B_c^{(k)}, \tag{4.1}$$

where the first term is the sum over all cubes of a twelve-spin σ_x interaction and the second term is the sum over all vertices of planar four-spin σ_z interactions as depicted in Fig. 4.1. In contrast with two-dimensional topologically ordered states, such as the Toric Code, that have a finite and constant topological ground state degeneracy on the two-torus, the ground state of the pure X-Cube model on the three-torus of linear dimension L has a sub-extensive topological ground state degeneracy D, where $\log_2 D = 6L - 3$.

A fracton is created by flipping the eigenvalue of the cubic interaction term. However, there exists no local operator that can create a single pair of fractons. Indeed, applying a σ_z operator to a link flips the eigenvalues of the four cubes sharing that link. Acting on the ground state by σ_z along a membrane operator $\hat{\mathcal{M}}$ creates four fractons at the corners of the membrane, as shown in Fig. 4.2i. A single fracton, denoted $e^{(0)}$ (where the superscript denotes that it is a dimension-0 excitation), is thus fundamentally immobile, as moving it would create additional fractons. This is the fundamental "superselection" rule [201] that will lead to glassy dynamics. Pairs of fractons are however free to move by repeated application of local membrane operators. A straight Wilson line of σ_z operators creates a pair of fractons at each end—each pair is a composite excitation that can move in two dimensions, and which we refer to as a dimension-2 (dim-2) excitation $e^{(2)}$, as shown

$$A_c = \prod_{j \in \partial c} \sigma_x^j$$

$$B_v^{(xy)} = \sigma_z^i \sigma_z^j \sigma_z^k \sigma_z^l$$
$$B_v^{(yz)} = \sigma_z^j \sigma_z^n \sigma_z^l \sigma_z^m$$
$$B_v^{(xz)} = \sigma_z^i \sigma_z^n \sigma_z^k \sigma_z^m$$
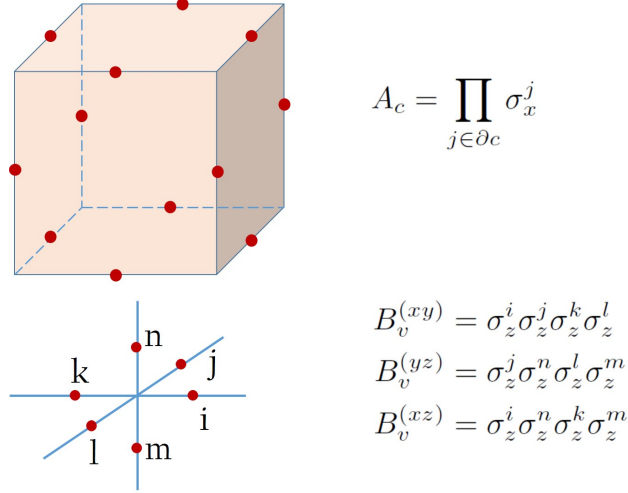
Figure 4.1: The X-Cube model is represented by spins σ placed on the links of a cubic lattice and is given by the sum of a twelve-spin σ_x operator at each cube c and planar four-spin σ_z operators at each vertex v.

in Fig. 4.2ii. In the X-Cube model, there exist additional dimension-1 excitations $(m^{(1)})$ created at the ends of a Wilson line of σ_x operators, that are mobile along one-dimensional sub-manifolds. Henceforth we will refer to the fully mobile four-fracton composites, created by single σ_z operators, as the topologically neutral sector, and the lower dimensional excitations (fractons and $e^{(2)}$'s) as the topologically charged sector.

In the following sections, we will focus specifically on the X-Cube model in the presence of transverse fields,

$$H = -J \sum_c A_c - \sum_{v,k} B_c^{(k)} + \Lambda \sum_i \sigma_z + \lambda \sum_i \sigma_x, \tag{4.2}$$

where i goes over all links in the cubic lattice. Since the pure X-Cube model Eq. (4.1) is a sum of commuting projectors, the relative coefficient J simply sets the energy scale between the e and m excitations when $\Lambda, \lambda = 0$. In the presence of the transverse fields, we expect that the fracton phase will survive up to some finite Λ/J and λ/J since this is a gapped phase of matter that is stable to local perturbations [199, 200]. In the limit of large transverse fields however, the fracton topological order will be destroyed, but the precise nature of the transition between the fracton phase and the trivial paramagnetic phase has yet to be understood [76]. Since we are interested in the dynamics
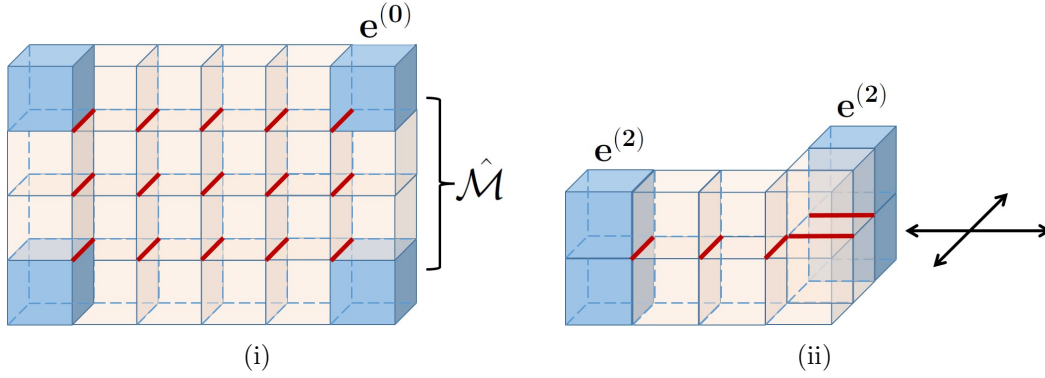
Figure 4.2: Topological excitations of the X-Cube model are depicted in (i) and (ii). Fractons $e^{(0)}$ are created at corners by acting on the ground state by a membrane operator $\mathcal{M}$ that is the product of σ_z operators along red links. Wilson line operators create a composite topological excitation $e^{(2)}$.

within the fracton phase, allowing only for weak local perturbations, we set $J = 1$, noting that our analysis holds as long J is $O(1)$. In addition, we will first set $\lambda = 0$ and consider only the dynamics of the fractons and their composites. After analysing this sector, we will comment on the consequences of a non-zero λ, which would allow the $m^{(1)}$ particles to hop as well. The Hamiltonian pertinent for the following discussions is thus

$$H = -\sum_c A_c - \sum_{v,k} B_c^{(k)} + \Lambda \sum_i \sigma_z, \tag{4.3}$$

with the perturbation strength $\Lambda \ll 1$. We note that while we are focusing on the specific example of the X-Cube model, the results presented here hold broadly for all type I fracton phases.[2]

4.3.1 Type I Fractons at Finite Energy Density

We begin our discussion of dynamics in fracton models by considering the X-Cube model Eq. (4.3) at finite energy density. Since we have switched off the term that would allow m's to hop, we have three kinds of excitations with dynamics in our system: neutral composites, which, being fully mobile and created by local terms, are three-dimensional bosons; dim-2 excitations $e^{(2)}$, which

---

[2] The X-Cube model lacks an exact electromagnetic duality, present in other type I models e.g., the Majorana cube or Checkerboard models, which have two distinct fracton excitations, $e^{(0)}$ and $m^{(0)}$. However, we can always choose to initialize the system with only one topological excitation or perturb the system only by terms that allow one of the excitations to hop.

are two-dimensional bosons [76]; and the topologically charged fractons. These excitations and their properties are summarized in Table. 4.1. A word on notations—since both the neutral composites and $e^{(2)}$'s are bosonic, we will henceforth refer to the former as the composite (c) sector and the latter as the bosonic (b) sector, with fractons (f) sometimes also referred to as the (topologically) charged sector.

From the preceding general discussion of the model, it is clear that each fracton hop is accompanied by the creation of two additional fractons, and so energetically costs an amount $W = 4$. We will henceforth refer to this charge gap simply as W, since the analysis applies also to generalizations of Eq. (4.3) that are in the same phase, but perhaps with a different charge gap. A single fracton hop is depicted in Fig. 4.3: starting with an isolated fracton, we can move this over by one site by acting by a single σ_z operator on the link adjacent to the fracton. This creates two additional topological excitations; however, this pair is a dim-2 $e^{(2)}$ excitation and can be moved off to infinity at no additional energy cost. Thus, each hop takes the system off energy shell. To fully understand the relaxation in the fracton sector, we must thus take into account the fully mobile neutral composites and the dim-2 excitations. These sectors act as a thermalizing bath for the
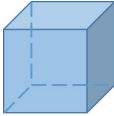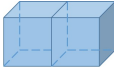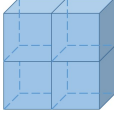
Excitation	Type	Energy Gap	Properties
	Fracton, $e^{(0)}$	$W/2$	Immobile, topologically charged, fracton(f) sector
	Dim-2 Boson, $e^{(2)}$	W	Mobile along planes, topologically charged, bosonic(b) sector
	Boson	$2W$	Fully mobile, topologically neutral, composite(c) sector

Table 4.1: Excitations in the X-Cube model. A single cube excitation is an immobile fracton while a bound state of two fractons is mobile along two-dimensional manifolds. There exist additional "magnetic" excitations, but these are not considered in detail here.
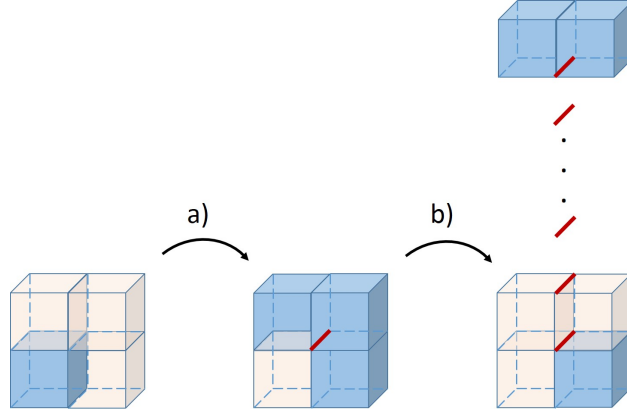
Figure 4.3: A single fracton hop. Starting from a single isolated fracton, we can move it over by one site by the action of a σ_z operator, shown in red, in step a). However, this creates two additional fractons which together form a dimension-1 excitation that can move along a line without creating any further excitations. As shown in b), this pair can then be moved off to infinity by the action of a Wilson line of σ_z operators.

fractons as rearrangements within these sectors allow the system to come back on energy shell after each hop.

Before studying the non-equilibrium dynamics, we consider the system—comprised of fractons, $e^{(2)}$'s, and neutral composites—in equilibrium, at some temperature $T \ll W$. The local energy scale in the topologically charged sector is W, where W is the charge gap, i.e., the cost of creating two fractons. Further, the fracton sector is coupled to a dense, high temperature bath of neutral composites which hop at a rate $\Lambda \ll W$. Here each species is gapped, with a gap of $W/2$, W, and $2W$ for creating a single fracton, $e^{(2)}$, and composite respectively. Additionally, since the composites and $e^{(2)}$'s are neutral, with the fractons carrying only a $\mathbb{Z}_2$ charge, the density and temperature of these excitations cannot be controlled independently; rather, the equilibrium temperature uniquely determines the density of each species,

$$n_f \sim e^{-\frac{W}{2T}}, \quad n_b \sim e^{-\frac{W}{T}}, \quad n_c \sim e^{-\frac{2W}{T}}, \tag{4.4}$$

where n_f is the density of fractons, n_b is the density of dim-2 bosonic excitations, and n_c is the density of the composites.

Due to the form of the perturbation, σ_z, the only processes that lead to an exchange of energy
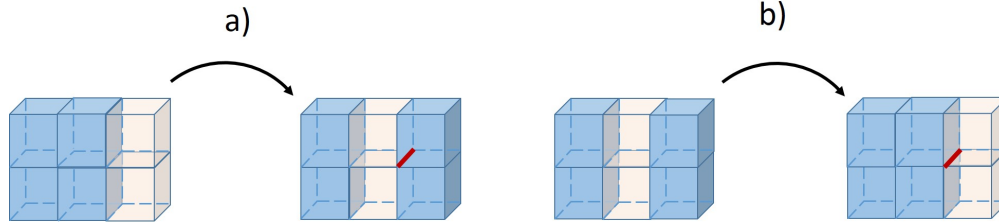
Figure 4.4: a) Acting by a single σ_z operator decomposes a neutral composite (bosons) into two dim-2 excitations (bosons). b) The reverse process, where two $e^{(2)}$'s combine into a single composite.

between the three sectors are those where the total $\mathbb{Z}_2$ charge along each row and each column of the cubic lattice is conserved. For instance, in Fig. 4.3, the initial and final topological charges along each column and each row are preserved (modulo 2). From all possible on-shell processes by which the three sectors can exchange energy, we will consider only two body processes that are up to second order in Λ (shown in Figs. 4.4 and 4.6) since all others will be further suppressed either by density factors or by the perturbation strength. As an illustration, Fig. 4.4 depicts the processes where a composite breaks into two $e^{(2)}$'s and where two $e^{(2)}$'s combine into a composite.

Within the thermalizing bath, the composites and $e^{(2)}$'s can either hop at a rate Λ or scatter off each other while remaining locally on-shell, at a rate Λ^2/W. Since we are interested in the regime where $\Lambda \ll W$, the heat bath has a narrow local bandwidth $\sim \Lambda$, determined primarily by the hopping. As discussed earlier, a single fracton hop takes the system off energy shell by an amount W, and hence a single rearrangement within the bath cannot place the system on shell. The traditional analysis of localized systems coupled to narrow bandwidth baths [236, 240, 241] makes use of many body rearrangements in the charge sector to obtain a relaxation rate that is power law slow in the bandwidth of the bath. However, in that setting the charge sector admits local re-arrangements that are "uphill" or "downhill," which may be combined into a many body re-arragement that is off shell by much less than W. The present situation differs in that *every* local re-arrangement in the charge sector is "uphill" in energy, so the dominant relaxation mechanism from Ref. [236, 240, 241] does not apply. Since the maximum energy the bath can provide is $\tilde{\Lambda} = \min(\Lambda, T)$, the bath must be probed $n \sim W/\tilde{\Lambda}$ times for the fractons to borrow enough energy
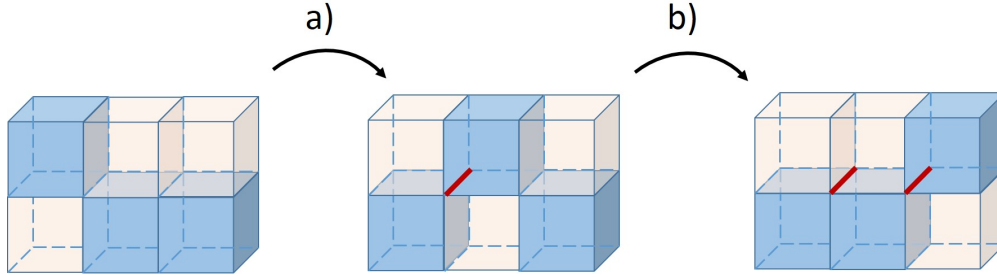
Figure 4.5: A fracton hop mediated by an $e^{(2)}$ excitation. a) Starting from a single isolated fracton and an $e^{(2)}$, we first act by a σ_z operator (in red) resulting in three fractons. b) Acting with another σ_z takes us to a configuration with an $e^{(2)}$ and a fracton that has moved over by two sites. In this manner, fractons can hop while remaining on-shell.

to perform a single hop. This leads to a relaxation rate in the charge sector that is *exponentially slow* in $W/\tilde{\Lambda}$, scaling as

$$\Gamma \sim n_f e^{-n} \sim n_f e^{-W/\tilde{\Lambda}}. \tag{4.5}$$

Alternatively, we could make use of the extensive nature of the many body bandwidth in the bath and could use an $n \sim W/\tilde{\Lambda}$ particle rearrangement in the bath to place fracton rearrangements on shell. However, this yields [242] an exponentially slow relaxation of the same form as Eq. (4.5), up to subleading prefactors.

The fractons, however, have an additional channel through which they can hop in an on-shell manner. This process, depicted in Fig. 4.5, requires the presence of an $e^{(2)}$ excitation in the vicinity of the fracton. During this process, the fracton hops once, destroying the neighbouring $e^{(2)}$, and hops again, thereby returning the system on-shell by creating an $e^{(2)}$ particle. Since this process is mediated by the $e^{(2)}$'s, the rate at which it proceeds is additionally suppressed by the density of the bosons n_b

$$\Gamma \sim n_f n_b \sim n_f\, e^{-W/T}, \tag{4.6}$$

Thus, the fractons have two possible hopping channels—either by borrowing energy from the bath or by using the bosons as intermediaries. The faster rate will dominate and so

$$\Gamma \sim n_f \max\left(e^{-W/T}, e^{-W/\tilde{\Lambda}}\right) \sim n_f\, e^{-W/T}. \tag{4.7}$$

This behaviour is in marked contrast with the usual case of activated transport. In typical gapped phases, the relaxation displays an Arrhenius law $\Gamma_A \sim n \sim e^{-\Delta/T}$, where n is the density of charge carries and Δ is the charge gap. This exponential slowness of the relaxation is governed primarily by the exponential rarity of charge carriers, since the mobility of these excitations is generically $\sim O(1)$. In type I fracton models, while the relaxation is suppressed by the density of fractons n_f, which is exponentially small in the inverse temperature, it displays an additional suppression due to mobility, which is also exponentially small in the inverse temperature. This is conceptually different from Arrhenius behaviour. Additionally, we observe that insofar as T is the potentially ergodicity restoring parameter here and the relaxation rate is exponentially small therein, Eq. (4.7) corresponds to "asymptotic many body localization" in the taxonomy of Ref. [217, 218].

We note that hole burning, a scenario where, after a certain number of fracton hops, there is a depletion in the density of composites causing the remaining fractons to essentially be frozen until the composite sector thermalizes, does not arise here. This is due to the exponentially long time scales, $t \sim e^{W/T}$, over which the composite bath is probed, allowing it to effectively thermalize between probing attempts. Hole burning would only occur if the energy "consumption" $W\Gamma$ is larger than the energy "supply" T

$$We^{-W/T} > T, \tag{4.8}$$

which does not hold true for a low temperature bath.

We note that we have thus far neglected the "back action" of the fractons on the composite sector. Insofar as $W/T \gg 1$, the back action is strong, and it thus may be tempting to postulate that the composite sector itself could be localized by the coupling to the charge sector, in a form of MBL proximity effect [241, 243, 244]. If the bath gets localized, then the relaxation rate will be zero. However, there will inevitably be regions where the density of fractons is low enough for the composite sector to be locally ergodic, and this argument will thus inevitably run into the rare region obstruction to perturbative constructions that have derailed previous attempts to establish translation invariant MBL [214]. We therefore do not pursue this particular line of reasoning

further, noting only that Eq. (4.5) should properly be understood only as an upper bound on the relaxation rate, which could be slower because of back action on the bath.

The situation considered above is one where the three sectors are in equilibrium. We could, in principle, prepare the system out of equilibrium with the bath comprised only of the composites and not the dim-2 $e^{(2)}$'s. In this case, the hopping would proceed at a rate

$$\Gamma \sim n_f \, e^{-W/\tilde{\Lambda}}, \tag{4.9}$$

since the channel where hopping proceeds through an intermediate boson will be unavailable. Hole burning will again be avoided here as we have a narrow bandwidth bath at high temperature. However, as we show in Appendix D.1, there will be a rapid equilibration between the composite and bosonic sectors, and upon equilibration, the relaxation will revert to the rate $n_f \, e^{-W/T}$.

4.3.2   Glassy dynamics in the approach to equilibrium

We now consider the non-equilibrium dynamics of type I fracton models prepared in their ground state (i.e., at vanishing energy density) in contact with a low but finite temperature bath comprised of neutral composites (the fully mobile bosons) and dim-2 excitations (the two-dimensional bosons). Let us begin our discussion more generally, by initializing the fractons at a temperature $T_f^{(0)}$ such that the density of fractons $n_f \sim e^{-W/2T_f^{(0)}}$, where W is again the local energy scale in the fracton sector. The neutral composites are prepared at a temperature $T_c^{(0)}$ and the $e^{(2)}$'s are prepared at $T_b^{(0)}$, with corresponding densities $n_c \sim e^{-2W/T_c^{(0)}}$ and $n_b \sim e^{-W/T_b^{(0)}}$. Furthermore, since all three species are gapped here, every species has an exponentially small heat capacity, $C_i \sim n_i$, for each species $i = b, c, f$. We note that the usual low-temperature T^3 heat capacity that we expect for three-dimensional bosons holds only when the bosons are gapless and thus does not apply to the neutral composites. Similarly, for the dim-2 bosons the usual T^2 be-haviour which follows from the Stefan-Boltzmann law does not hold here since that applies only to

gapless bosons. Hence, here we expect that

$$E_c \sim 2W n_c \implies C_c \sim \frac{4W^2}{T_c^2} e^{-\frac{2W}{T_c}},$$

$$E_b \sim W n_b \implies C_b \sim \frac{W^2}{T_b^2} e^{-\frac{W}{T_b}},$$

$$E_f \sim \frac{W}{2} n_f \implies C_f \sim \frac{W^2}{4T_f^2} e^{-\frac{W}{2T_f}}. \tag{4.10}$$

The regime of interest is $T_i^{(0)} \ll \Lambda$ where $i = c, b, f$, and we henceforth work in this regime. We further show in the Appendix D that even if we start with $T_c \neq T_b$ the boson and composite sectors rapidly equilibrate, so we henceforth assume that $T_c = T_b$. That is, we assume that the bath is itself in equilibrium, and examine the equilibration of the fracton sector with the bath.

We note that here we are interested in understanding equilibration within a closed quantum system, in order for which we must initialize the different sectors at different temperatures. In principle, this can be achieved by first allowing all sectors to equilibrate with a heat bath at some initial low temperature $T_f^{(0)}$. Next, couple the system briefly to another heat bath at a temperature $T_b^{(0)} \gg T_f^{(0)}$. The mobile bosonic and composite sectors will rapidly equilibrate with the heat bath while the fracton sector will remain close to $T_f^{(0)}$, since it heats very slowly. This protocol will hence naturally produce a fracton sector at a temperature $\sim T_f^{(0)}$ and bosonic and composite sectors at $\sim T_b^{(0)}$, allowing us to then study equilibration between these sectors.

4.3.2.1   Equilibration between Fractons and bath

We now consider the dynamics of the fractons when placed in contact with the thermal sector which contains composites and $e^{(2)}$'s at some initial temperature $T_b^{(0)}$. The fractons are prepared at a low temperature, $T_f^{(0)} \ll T_b^{(0)}$, as we are interested in the dynamics of fractons prepared in their ground state. Further, we will consider only two-body (processes involving more excitations will be further suppressed by density factors) on-shell processes (upto second order in perturbation theory) that lead to an exchange of energy between the bath and the $\mathbb{Z}_2$-charged fracton sector. Since we are assuming that the composites and bosons have already equilibrated, the dominant processes through which the bath and the $\mathbb{Z}_2$-charged fracton sector exchange energy will involve only the
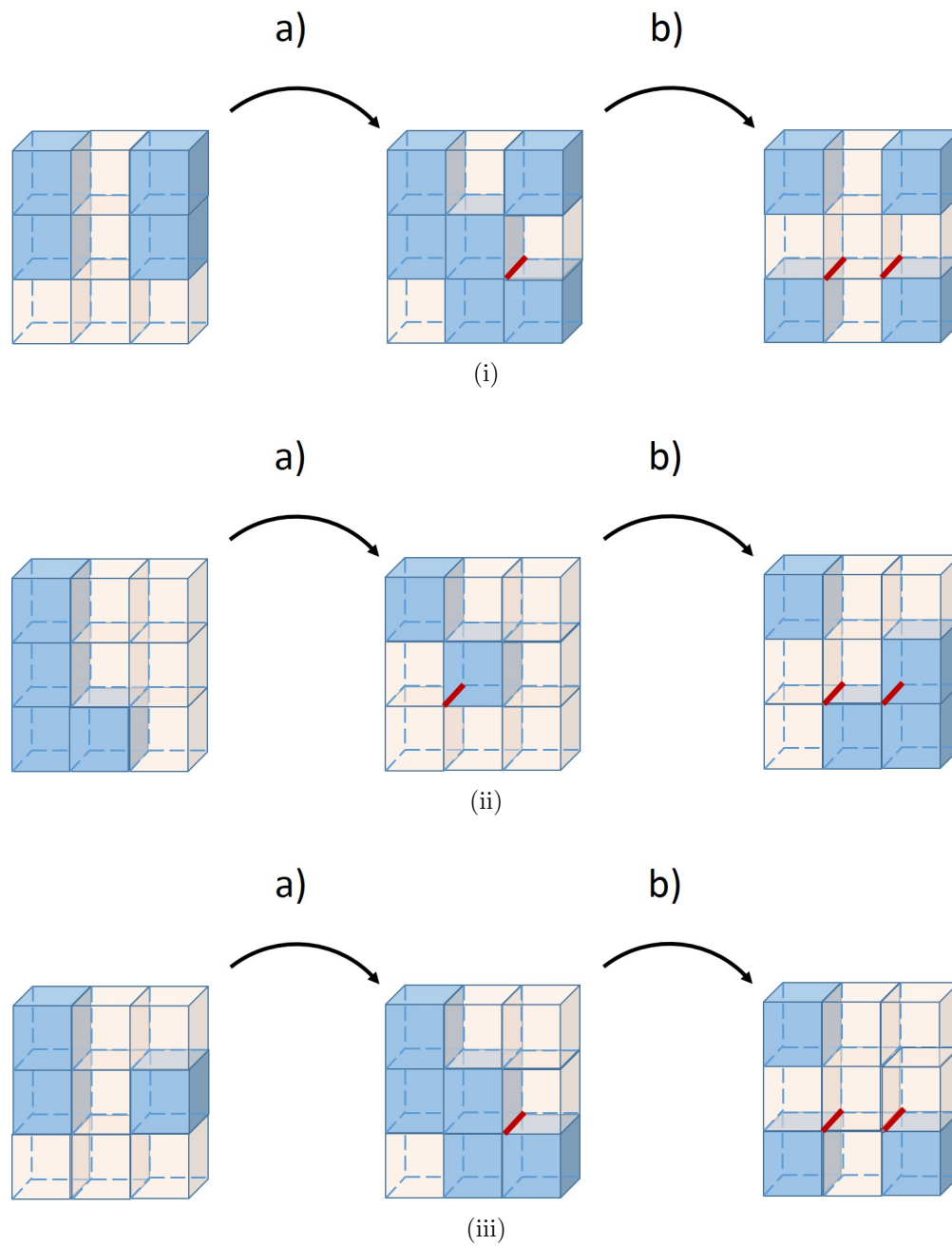
Figure 4.6: Dominant second order on-shell processes between charged fracton sector and thermal bath. (i) Two bosons convert into four fractons. (ii) Two bosons convert into a boson and two fractons. (iii) A boson and a fracton convert into three fractons.

bosons and the fractons. This is because the density of neutral composites $\sim e^{-2W/T_b}$ while that of the bosons $\sim e^{-W/T_b}$, which dominates in the regime of interest $T_b \ll W$. The dominant processes, shown in Fig. 4.6, are then

(1) Boson + Boson $\leftrightarrow$ 4 Fractons,

(2) Boson + Boson $\leftrightarrow$ Boson + 2 Fractons,

(3) Boson + Fracton $\leftrightarrow$ 3 Fractons.

Two fractons cannot convert into a single boson due to the form of the perturbation, and all other two body processes will involve at least one composite and are hence suppressed compared to the others. Processes where a single composite converts into a pair of bosons which then convert into four fractons or a boson and two fractons occur at third order in perturbation theory and can hence safely be ignored. The above three channels all occur at second order and their rates are controlled by the densities of the excitations involved. For instance, channel 1 (boson + boson) occurs at a rate $\Gamma \sim \frac{\Lambda^2}{W} n_b^2$. Since the bath lends energy $2W$ during this process, $dE_b/dt \sim -2W\Gamma = -2\Lambda^2 n_b$. Following this example, we can establish a detailed balance between the thermal and the charged sector,

$$\frac{dE_b}{dt} = -\Lambda^2 \left(3n_b^2 + n_b n_f - n_b n_f^2 - n_f^3 - 2n_f^4\right) = -\frac{dE_f}{dt}. \tag{4.11}$$

Here, the integer coefficients' magnitude should not be taken seriously, since they are strongly model dependent. However, the conclusions we draw below will not depend on these coefficients, lending our results broader applicability across type I fracton phases.

Since the heat capacities are given by Eq. (4.10), the detailed balance leads to the rate equations

$$\frac{dT_b}{dt} = -\frac{\Lambda^2 T_b^2}{W^2} \left(3n_b + n_f - n_f^2 - \frac{n_f^3}{n_b} - 2\frac{n_f^4}{n_b}\right),$$
$$\frac{dT_f}{dt} = \frac{4\Lambda^2 T_f^2}{W^2} \left(3\frac{n_b^2}{n_f} + n_b - n_b n_f - n_f^2 - 2n_f^3\right). \tag{4.12}$$
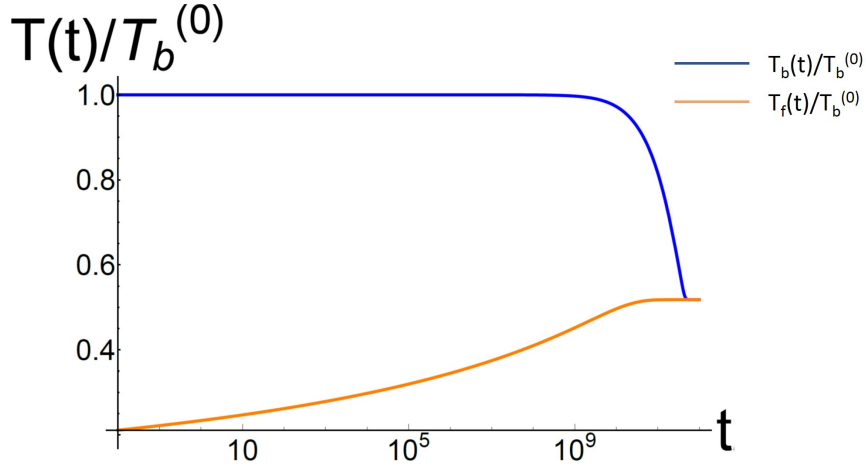
Figure 4.7: Time dependence of the charged fracton $T_f(t)$ and thermal $T_b(t)$ sectors found by numerically solving the detailed balance equation, Eq. (4.12). We have initialized the system at $W = 1$, $\Lambda = 10^{-1}$, $T_b^{(0)} = 5 \times 10^{-2}$, and $T_f^{(0)} = 5 \times 10^{-4}$.

We can analytically study the equilibration process in two regimes—when the fractons are prepared in their ground space ($T_f \sim 0$) and when the system nears equilibration ($T_b \sim T_f$).

In the case where the fractons are initially prepared at a vanishing energy density, we are in the regime where $T_f^{(0)} \ll T_b^{(0)}$. Here, we find that (see Appendix D for details)

$$T_f(t) = -\frac{W/2}{\log\left(\frac{6\Lambda^2}{W}t + b\right) - \frac{2W}{T_b^{(0)}}}, \tag{4.13}$$

where $b = \exp\left(\frac{2W}{T_b^{(0)}} - \frac{W}{2T_f^{(0)}}\right)$, and

$$T_b(t) = \frac{W}{\log\left(\frac{3\Lambda^2}{W}t + e^{W/T_b^{(0)}}\right)}, \tag{4.14}$$

such that the fractons display logarithmically slow heating and the bath correspondingly cools logarithmically slowly. This behaviour persists until the fractons are close to equilibration, i.e., over an exponentially long time scale

$$0 \leq t \lesssim t^* = \frac{W}{6\Lambda^2}\exp\left(\frac{W}{T_b^{(0)}}\right). \tag{4.15}$$

Until this time scale, the dominant processes are those of channels 1 and 2, where two bosons combine to pump energy into the fracton sector. Beyond this, however, channel 3 is activated
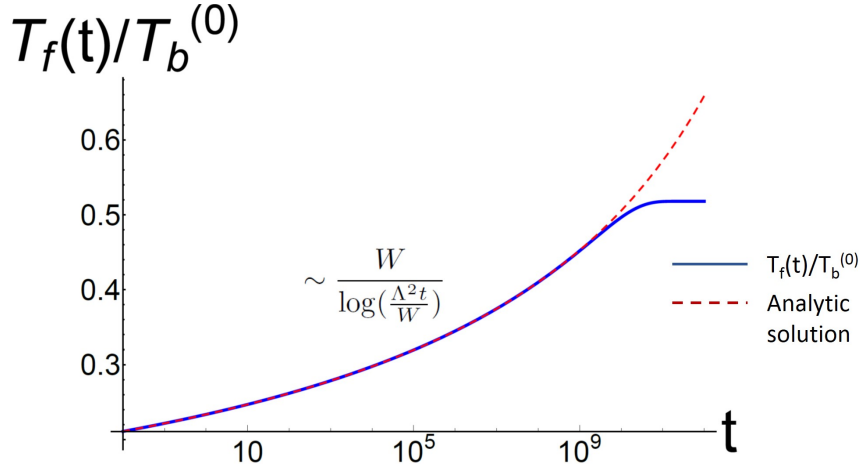
Figure 4.8: The time dependence of the fracton sector $T_f(t)$ displays a $\log(t)$ behaviour over an exponentially long time scale. The red dashed line is the analytic approximation, Eq. (4.13) to the solution of Eq. (4.12), with the numerical solution shown in blue. The same parameters are used as those in Fig. 4.7.

since the fractons are close to equilibration $(T_f(t^*) \sim T_b^{(0)}/2)$ while the bath's temperature has only changed slightly $(T_b(t^*) \sim T_b^{(0)})$, such that $n_f(t^*) \sim n_b(t^*)$. Hence, we can no longer ignore processes where a boson and a fracton convert into three fractons and the behaviour of the bath is modified at this time scale,

$$T_b(t) \sim \frac{W^2}{\Lambda^2 t} e^{W/T_b^{(0)}}, \quad t > t^*. \tag{4.16}$$

Thus, the bath first cools logarithmically over an exponentially long time scale, and then rapidly equilibrates with power-law behaviour, since the logarithmic heating of the charged fracton sector establishes a finite density of fractons at $t \sim t^*$. This behaviour can be explicitly seen by numerically solving Eq. (4.12) (see Fig. 4.7) and matching the analytic solutions with the numerical curves. As can be seen in Fig. 4.8, the fractons display logarithmic heating essentially until equilibration while the bath displays logarithmic cooling followed by rapid, power-law cooling, as shown in Fig. 4.9.

Thus, placing a type I fracton model prepared in its ground space[3] in contact with a finite temperature heat bath leads to equilibration that exhibits glassy behaviour (i.e. a $\log t$ approach

---

[3] We note that while we are primarily interested in the limit $T_f^{(0)} \ll T_b^{(0)}$, due to the form of Eq. (4.12), our discussion holds more generally as long as $T_f^{(0)} < T_b^{(0)}/2$.
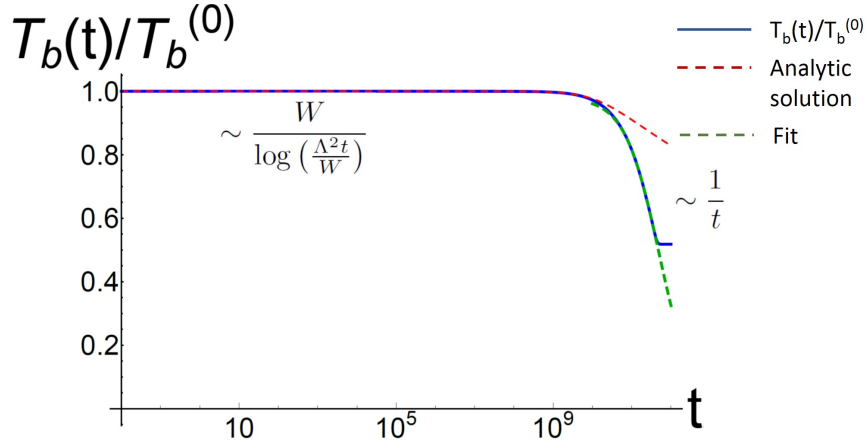
Figure 4.9: The time dependence of the bath $T_b(t)$ displays a $\log(t)$ behaviour over an exponentially long time scale, followed by power law cooling until equilibration. The red dashed line is the analytic approximation, Eq. (4.14) to the solution of Eq. (4.12), with the numerical solution shown in blue. The green dashed line is a fit to the $1/t$ behaviour. The same parameters are used as those in Fig. 4.7.

to equilibrium) over an exponentially wide window of intermediate time scales,

$$0 \leq t \lesssim \frac{cW}{\Lambda^2} \exp\left(\frac{W}{T_b^{(0)}}\right), \tag{4.17}$$

for some positive constant c.

At long times, the system eventually equilibrates, $T_b = T_f$ and close to equilibration, we recover the standard exponential relaxation expected from Newton's law of cooling,

$$\delta T(t) \sim \exp\left(-\frac{\Lambda^2}{W} e^{-\frac{W}{T_b^{(0)}}} t\right), \tag{4.18}$$

where $\delta T = T_b - T_c$. Thus, over exponentially long time scales, governed by $W/T_b^{(0)}$, the relaxation displays logarithmic (glassy) dynamics but close to equilibrium we recover an exponential relaxation with a relaxation rate that is exponentially small in $W/T_b^{(0)}$.

4.3.2.2 Fracton dynamics in an open quantum system

In principle, we can also consider an open quantum system such that the temperature of the composites (and so also the dim-2 bosons) is pinned to that of an external heat bath. In this situation, we are interested in the dynamics of the charged fracton sector which, following the

discussion in the previous system, we expect will again demonstrate logarithmically slow heating over exponentially long time scales.

We consider initializing the charged fracton sector at a temperature $T_f^{(0)}$, with the neutral composites and dim-2 bosons coupled to an external bath at a temperature $T \gg T_f^{(0)}$. Since the fracton sector only exchanges energy with the composites and bosons, most of the discussion from the previous section holds i.e., the dominant processes by which the fracton sector exchanges energy are unchanged. Hence, the rate equation for the fractons is

$$\frac{dT_f}{dt} = \frac{4\Lambda^2 T_f^2}{W^2} \left(3\frac{n_b^2}{n_f} + n_b - n_b n_f - n_f^2 - 2n_f^3\right),\tag{4.19}$$

where $n_b = e^{-W/T}$ is set by the external heat bath and $n_f = e^{-W/2T_f}$. In the regime of interest, $T_f^{(0)} \ll T$, the dynamics are initially governed by channels 1 and 2, such that the fractons display logarithmically slow heating (see Appendix D for details)

$$T_f(t) = -\frac{W/2}{\log\left(\frac{6\Lambda^2}{W}t + b\right) - \frac{2W}{T}},\tag{4.20}$$

where $b = \exp\left(\frac{2W}{T} - \frac{W}{2T_f^{(0)}}\right)$. This behaviour persists over an exponentially long time scale,

$$0 \leq t \lesssim t^* = \frac{W}{6\Lambda^2} \exp\left(\frac{W}{T}\right),\tag{4.21}$$

controlled by the temperature of the heat bath, $T \ll W$. Around $t = t^*$, however, channel 3 is activated since a finite density of fractons has been established, and the behaviour of the fractons is modified,

$$T_f(t) \approx -\frac{W/2}{\frac{2\Lambda^2}{W}e^{-W/T}t + \log\left(3e^{-W/T}\right)}, \quad t > t^*.\tag{4.22}$$

Hence, the fractons display logarithmically slow heating over an exponentially long time scale, followed by rapid power-law behaviour until they are close to equilibration (see Fig. 4.10). Near equilibration, $T_f \sim T$, and the fractons follow the usual exponential behaviour expected from Newton's law

$$\delta T \sim \exp\left(-\frac{4\Lambda^2 t}{W}e^{-W/T}\right),\tag{4.23}$$
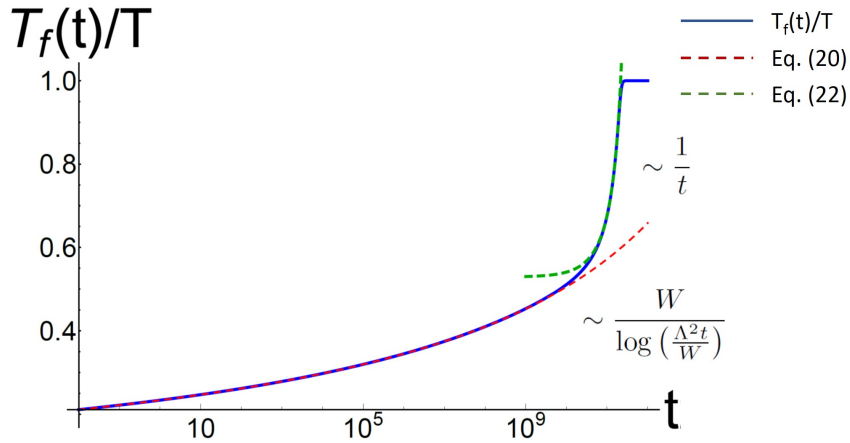
Figure 4.10: In an open quantum system the fractons $T_f(t)$ display a $\log(t)$ behaviour over an exponentially long time scale, followed by power law heating until equilibration. The red dashed line is the analytic approximation, Eq. (4.20) to the solution of Eq. (4.19), with the numerical solution shown in blue. The green dashed line depicts the $1/t$ behaviour, Eq. (4.22). The parameters are $W = 1$, $\Lambda = 0.1$, $T = 0.05$, and $T_f^{(0)} = 10^{-3}$.

where $\delta T = T - T_f$. Thus, even in an open quantum system, fractons display glassy behaviour over exponentially long time scales when prepared in their ground state, where the time scales are controlled by W/T i.e., by the initial temperature of the heat bath. In principle, our discussion applies as long as $T_f^{(0)} < T/2$, in which case the width of the $\log(t)$ behaviour will depend on the initial temperature of the fractons, but the situation considered here $T_f^{(0)} \ll T$ is of more interest.

While we have focused on the example of the X-Cube model Eq. (4.1) here, we expect that our results should hold in general for Type I fracton models. In particular, our results here are consistent with the glassy behaviour demonstrated for the related CBLT model [73], where a Type I fracton system initialized with an isolated set of fractons and coupled to an external bath was shown to display logarithmic relaxation. While that work considered fractons which were coupled directly to the bath, in contrast we prepare our system with a finite density of fractons which are coupled to neutral composites and dim-2 excitations held at a fixed temperature T.

4.3.3   Role of $m^{(1)}$ excitations

Type I models, such as the X-Cube model Eq. (4.1), may host additional excitations created in pairs at the ends of Wilson lines of σ_x operators. These excitations are free to move in one-dimension and hence referred to as $m^{(1)}$ excitations. In order to study the X-Cube model in full generality, we must thus consider the model in the presence of transverse fields, Eq. (4.2)

$$H = -J \sum_c A_c - \sum_{v,k} B_c^{(k)} + \Lambda \sum_i \sigma_z + \lambda \sum_i \sigma_x \tag{4.24}$$

where the term $\lambda \sigma_x$ introduces dynamics for the $m^{(1)}$ excitations. Importantly, since the $m^{(1)}$ excitations are created by σ_x operators, they do not inter-convert with the e excitations (composites, dim-2 bosons, and fractons). Thus, the only coupling between the e's and m's will be through the exchange of energy between the two sectors.

Let us first consider the case where $J = 1$ with $\lambda, \Lambda \ll W$. Acting with a single σ_x operator violates four vertex terms, $B^{(k)}$, such that the gap for creating a single $m^{(1)}$ is equal to W, which is the same as that of creating a dim-2 boson. For a system in equilibrium at some temperature T, the density of $m^{(1)}$'s will thus be $n_m \sim e^{-W/T}$. In addition to the relaxation channels considered in Sec. 4.3.1, the finite density of $m^{(1)}$'s will then provide an additional relaxation channel for the fractons, since they can now borrow energy from the one-dimensional bath of $m^{(1)}$'s with a bandwidth controlled by the hopping rate λ.

Since the "magnetic" bath can supply a maximum energy $\tilde{\lambda} = \min(\lambda, T)$, the relaxation rate of the fractons due to coupling to this channel will proceed at a rate $\Gamma \sim n_f e^{-W/\tilde{\lambda}}$. If $T < \lambda$, then the relaxation will proceed at a rate controlled by the temperature T and λ will be rendered irrelevant. On the other hand, if $T > \lambda$, then it is more efficient for the fractons to couple to the "electric" bath, since boson mediated hopping (see Fig. 4.5) proceeds at a faster rate $\sim n_f e^{-W/T}$. Hence, including the dim-1 excitations does not effect the relaxation of fractons, at least in equilibrium, and can safely be ignored insofar as λ is weak enough to not destroy the fracton topological order.

As long as $J = 1$, the gap for creating an $m^{(1)}$ and an $e^{(2)}$ is the same. Thus, even if we were to consider a system in non-equilibrium, there will be an efficient equilibration between the dim-2

bosons and the dim-1 magnetic excitations, since processes where two $m^{(1)}$'s are destroyed and two $e^{(2)}$'s are simultaneously created will proceed in an on-shell manner, with the rate of equilibration controlled by the relative strength of the transverse fields λ, Λ. Once these sectors have rapidly equilibrated, we can again ignore the $m^{(1)}$'s since the most dominant processes through which the fractons equilibrate will be those considered in Sec. 4.3.2.

If $J \neq 1$, however, then there will exist an imbalance between the electric and magnetic gaps and the equilibration between the $e^{(2)}$'s and $m^{(1)}$'s will no longer proceed in an on-shell manner. Since the case where $J \neq 1$ may also de-stabilise the fracton topological order, depending on the perturbation strengths, we leave the dynamics of the X-Cube model in this case as an open question, to be studied once the phase diagram of this model is better understood [78, 79].

4.4   Type II Fracton Models

We now turn to type II fracton models, such as Haah's code [75]. The fundamental difference between type I and II models is the lack of any local string-like operator that allows topological excitations to move in the latter. As we saw in the type I case, pairs of fractons form dimension-1 topological excitations, and as pairs are created at the ends of Wilson-lines, they can move along the Wilson lines without creating any further excitations. However, in type II models, there are no mobile subdimensional excitations.

$$G_c^Z = \sigma_z^i \mu_z^j \sigma_z^k \mu_z^l \sigma_z^m \mu_z^n \sigma_z^r \mu_z^r$$

$$G_c^X = \sigma_x^i \mu_x^j \sigma_x^k \mu_x^l \sigma_x^m \mu_x^n \sigma_x^p \sigma_x^p$$
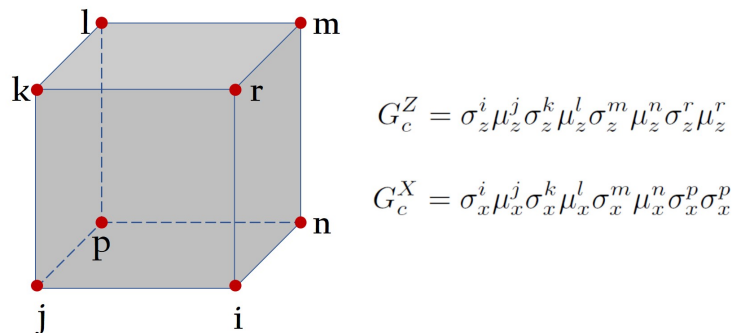
Figure 4.11: The Cubic Code model is defined on a cubic lattice with two spins (qubits) living on each vertex. The Hamiltonian is a sum of two eight-spin operators on each cube c.

As a specific example of a type II fracton phase, let us consider Haah's cubic code model. This is an exactly solvable lattice model defined on a three-dimensional cubic lattice where each site has two spins (or qubits) placed on it. The Hamiltonian is given by the sum over all cubes of two eight-spin interaction terms

$$H = -J \sum_c G_c^X - \sum_c G_c^Z \qquad (4.25)$$

with G_c^X and G_c^Z defined in Fig. 4.11. In analogy with the X-Cube model, Eq. (4.1), we set $J = 1$ here, noting that once we perturb the system, our analysis will hold for J being order unity. The pure Cubic Code model has a topological ground state degeneracy since the ground states cannot be distinguished by any local operator. On a three-torus of length L, the ground state degeneracy is $2^{k(L)}$ for some integer $2 \le k(L) \le 4L$; see [245, Corollary 9.3] for an explicit formula. There exist two kinds of excitations in this model: e type (violation of the G_c^X term) and m type (violation of the G_c^Z term). This model has an exact duality between the two types as they are lattice inversions of each other, so it suffices to consider only one sector. We can see that these topological excitations are immobile since a single σ_z operator on a link creates four cube excitations (see Fig. 4.12i) and there exists no local string-like operator that can create just a single pair of fractons. Here, single fractons are created at the ends of fractal operators, as shown in Fig. 4.12ii. Importantly, the "no-strings" rule [75] implies that **any** cluster of defects with a non-trivial topological charge must be immobile.

Unlike type I fracton phases, where there is a finite and constant energy barrier for topological charges to move, in type II fracton phases there exists an extensive logarithmic energy barrier preventing topologically charged excitations from diffusing. In particular, as proved in [246], there exists an energy barrier $\sim c \log(R)$ for creating an isolated fracton with no defects within a distance R, for some constant c.

The logarithmic energy barrier can be understood as follows. The transition from Fig. 4.12i to 4.12ii is realized by overlaying four copies of 4.12i in the designated geometry. The resulting configuration F_1 of fractons in 4.12ii is similar to the configuration F_0 in 4.12i with similarity ratio
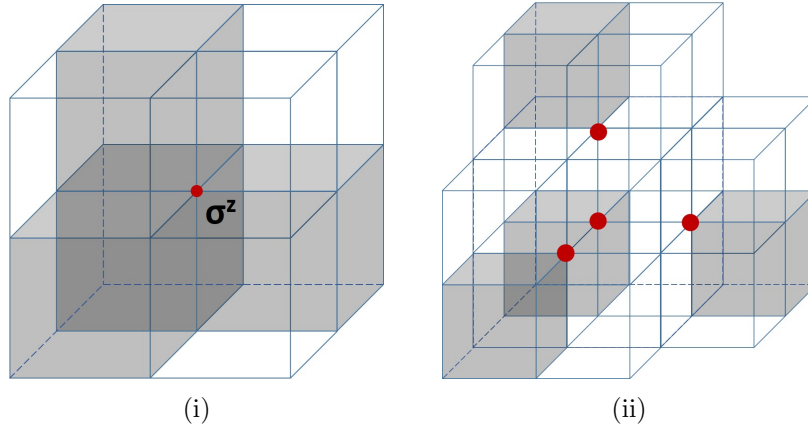
Figure 4.12: Excitations of the Cubic Code Model. Two spins (qubits) live on each vertex of the cubic lattice. Acting by a σ_z operator on the ground state, as shown in (i), creates four fracton excitations. Four fracton excitations are also created by acting by a μ^z operator or by violating the G_c^X term. Acting by a fractal operator of σ_z's, as in (ii), separates the fractons.

2. One can build a similar configuration F_2 of four fractons with similarity ratio $2^2 = 4$ relative to F_0 by overlaying four copies of F_1. Continuing, one builds a configuration F_n of four fractons that is similar to F_0 by similarity ratio $2^n = R$. In order to separate the fractons by a distance R, one needs to iterate the process $n = \log_2 R$ times. Now, consider a local process where one applies a single σ_z at a time. Let Δ_k denote the maximum energy reached by intermediate states while building a standalone F_k under the local process. To go from F_k to F_{k+1}, one has to build three other copies F_k', F_k'', F_k''' of F_k. The given configuration F_k already has four fractons of total energy $2W$, among which three fractons are far from the region F_k' is being built on. Hence, while building F_k' (or any other copy of F_k), the system's energy will reach $\Delta_k + O(W)$. This implies that $\Delta_{k+1} = \Delta_k + O(W)$, and therefore $\Delta_n = O(nW) = O(W \log R)$.

The argument above only proves an upper bound on the energy barrier. The claim that there is no process that uses less energy requires a separate proof, which relies on a quantitative form of the no-strings rule and uses a renormalization-group-inspired argument [246].

Let us consider a type II fracton system in contact with a narrow bandwidth heat bath of composites, with bandwidth $\Lambda \ll W$ and temperature T. Let us consider a (non-equilibrium) initial state containing a single fracton. Following our logic in the type I case and replacing the

energy scale W in the charged sector by the new energy scale $Wc \log R$, we conclude that to move a distance R will take a time

$$t = (R)^{\frac{cW}{\tilde{\Lambda}}} \; ; \quad \tilde{\Lambda} = \min(T, \Lambda). \tag{4.26}$$

Inverting this relation we obtain $R \sim t^{\tilde{\Lambda}/cW}$, which for $\tilde{\Lambda} \ll W$ implies strongly *subdiffusive* behaviour in a translation invariant three-dimensional model. This subdiffusive behaviour will persist up to the relaxation time, which (as we will shortly show) is super-exponentially long at low temperatures, scaling as $t_{relax} \sim \exp(+c' \frac{W^2}{T^2})$.

Of course, a type II system left in contact with a heat bath will eventually equilibrate to have a non-zero density of fractons—fractons will be created in groups of four (borrowing the energy to do this from the heat bath), and will then be redistributed over the system. However, to achieve an equilibrium distribution with a thermal density of fractons $n_f \sim \exp(-W/2T)$, it will be necessary to move fractons over a lengthscale $a \sim \exp(2W/3T)$ (given that fractons can only be created in groups of four). Substitution into the above equation then leads us to conclude that the equilibration time will follow the "super-Arrhenius" scaling

$$t_{equilibrate} \sim \exp\left(+c' \frac{W^2}{T^2}\right), \tag{4.27}$$

when $T < \Lambda$, where c' is an $O(1)$ numerical constant. This is consistent with a lower bound on relaxation rates derived in [247]. This "super-Arrhenius" scaling is reminiscent of various "near MBL" models e.g. [236, 237] and provides another example of the provocative connections between fracton dynamics and MBL.

We note that classical spin systems, such as the Newman-Moore model [248], have been known to display similar phenomenology, in that there exists a logarithmic energy barrier for transporting defects, leading to glassy behaviour. However, unlike type II fracton models, these classical spin models do not have a topologically ordered ground-state subspace and hence lack the robustness against generic local perturbation inherent in quantum fracton models, such as Haah's code [199, 200].

We now compare our results to [249], who argued that the memory of the initial conditions

in the cubic code relaxes for long enough times at finite temperature, with a relaxation time that scaled similarly to Eq. (4.27). Our broad conclusions are in agreement with [249]. However, our analysis differs in that [249] examined dynamics towards Gibbs states making use of the Lindblad formalism, which assumes decoherence, whereas we are discussing closed system quantum dynamics, with equilibration implicitly defined in terms of eigenstate thermalization [69] and are making no assumptions about decoherence. We note also that equilibration in closed quantum systems and equilibration coupled to an external heat bath are conceptually different problems - closed quantum systems can fail to equilibrate when isolated from the environment (see [69] for a review) but even such 'non-equilibrating' quantum systems will equilibrate if connected to an external heat bath. (see e.g. [241] and references contained therein).

To conclude, our analysis reveals that type II models exhibit *subdiffusion* of fractons on time scales short compared to the relaxation time, and additionally the relaxation time diverges at low temperatures as a *super-exponential* function of inverse temperature. This is reminiscent of MBL, in that the closed system quantum dynamics of a zero temperature fracton sector coupled to a finite temperature neutral sector could preserve a memory of the initial conditions in local observables over extremely long times that, while finite, are *super-exponentially* long at low temperature.

4.5   Discussion and Conclusions

We have shown that fracton models naturally demonstrate glassy dynamics. Type I fracton models at finite energy density exhibit a mobility that is exponentially small in the "temperature," corresponding to a type of "asymptotic many body localization." Meanwhile, the equilibration of type I fracton models at low temperatures involves a *logarithmic* approach to equilibrium over an exponentially wide range of time scales—another signature of glassy dynamics. In Type II models, individual fractons exhibit *subdiffusive* dynamics up to a relaxation time that is super-exponentially long at low temperature, reminiscent of various near-MBL systems, but involving a *translation invariant* three-dimensional Hamiltonian.

This work has intimate connections to earlier literature on glassy dynamics. For example,

the dynamical rules governing the relaxation of fracton models are reminiscent of 'kinetically con-strained' theories of classical glasses, in particular those in the 'East model' class (for a review see e.g. [250, 251] and references contained therein). These classical models exhibit 'dynamical facili-tation,' whereby excitations can move only in the vicinity of other excitations - a property that also arises in the fracton models that we study. Such 'dynamical facilitation' provides a robust route to glassy behavior (see e.g. [252, 253] and references contained therein). However, in kinetically constrained models these dynamical constraints are imposed 'by hand,' whereas for fracton models they emerge naturally from Hamiltonian dynamics.

It is worth noting, however, that classical 'plaquette models' also exhibit naturally emerging dynamical constraints (see e.g. [248, 254]), and indeed the earliest fracton models were specifically designed to be quantum generalizations of these, exhibiting naturally emerging kinetic constraints, dynamic facilitation, and glassy dynamics [73, 255]. These earlier works (particularly [73, 255]) provide the intellectual inheritance on which we build. However, we emphasize also that this earlier literature focuses on systems in contact with an external heat bath, whereas we have focused on the conceptually different problem of many body quantum dynamics in an *isolated* quantum system. In doing so our work makes contact between this earlier literature and the recent developments in closed system quantum dynamics, localization and thermalization (see Ref.[69] for a review), and highlights the connections between classical theories of glass and the rapidly developing theory of slow dynamics in closed quantum systems.

This work has provocative implications for numerous fields. Firstly, it opens up a new direction for the investigation of three-dimensional topological order, suggesting that certain three-dimensional topologically ordered phases (the fracton models) naturally exhibit a rich glassy dy-namics more conventionally associated with disordered systems. Can ideas from localization and disordered systems be fruitfully employed to understand three-dimensional topological order? Are there more surprises in store regarding the dynamical behaviour of such models? Given the novelty of these systems, it seems likely that there is more to be discovered.

Additionally, this work may have implications for quantum foundations, in that it identifies

a class of quantum systems as being unusually robust to thermalization (in which coupling to a heat bath "observes" the system and "collapses" the wavefunction). This robustness is particularly strong for type II models, for which the time scale for thermalization diverges super-exponentially fast at low temperatures. These models could also have important technological implications, insofar as they display a long lived memory of the initial conditions.

There may also be a connection to the "quantum disentangled liquids" (QDL) introduced in [213]. The hallmark of the QDL is that it contains two species of particles, and the many body eigenstates have volume law entanglement entropy, but after performing a projective measurement on the more mobile species of particles, the resulting wavefunction has only area law entanglement entropy. In the fracton models at non-zero temperature, there are indeed two species of particles (fractons and neutral composites), and the neutral composites are in a thermal state, so the eigenstates will indeed have volume law entanglement entropy. However, the fractons themselves can *only* hop by coupling to the neutral sector, and after performing a projective measurement on the neutral sector, the "fracton only" portion of the wavefunction may well have sub-volume law entanglement entropy. If so, then finite temperature fracton models would provide a three-dimensional realization of a quantum disentangled liquid. Unfortunately, a direct numerical test of this scenario seems difficult, since these models are intrinsically three-dimensional, and numerical tools capable of dealing with three-dimensional glassy many body systems are severely limited.

Thus far we have worked with models with only a Z_2 charge. However, fracton models should admit of generalizations with $U(1)$ conserved charge [80, 81] allowing us to define a charge *conductivity*. It should then follow, through reasoning analogous to our previous discussion of type II fracton models, that at zero temperature (but with the neutral composites prepared at finite density), that these models should realize a phase that is a *thermal* conductor but a *charge* insulator.

Finally, there are the implications for the study of MBL and glass physics. We have introduced a new class of translation invariant models which naturally exhibit glassy dynamics in three dimensions. This new class of models may well provide a new line of attack on important unsolved problems such as MBL in translation invariant systems [212–219] and in higher dimen-

sions [239, 256]. Finally, while the fracton models are defined on lattices, analogous phenomenology can also be obtained in the continuum by making use of higher rank gauge theories. Given the interest in MBL in the continuum [237, 238], these too may be worthy of investigation. We leave exploration of these various issues to future work.

Chapter 5

Fractons at Finite Density: Behold the Constant Crowd

In which Benny returns to street level.

In the penultimate chapter of this thesis, we commence the study of new emergent phenomena which may arise in the presence of a finite *charge* density of fractons and their bound states, in a sense initiating investigations into the "condensed matter physics" of fractons. The gapped spin models considered in the previous chapter, such as the X-Cube model and Haah's code, admit only a $\mathbb{Z}_2$ fracton charge i.e fracton charge is only conserved modulo two. Owing to the lack of a conserved U(1) charge in these models, we cannot independently tune the charge density and energy density, since the temperature alone determines both.

To overcome the lack of a chemical potential with which to independently control the density of fractons, we switch over to the framework of symmetric tensor gauge theories, briefly alluded to in § 1, allowing us to more fully explore the space of possible "fractonic" phenomena. These theories encode fracton phenomenology through the presence of higher moment conservation laws, e.g. dipole moment conservation, which restricts the set of local operators at the ends of which isolated fractons may be created. Within this gauge theoretic framework, we can independently tune the densities of both fractons and their dipolar bound states by introducing separate chemical potentials for the two sectors. We can thus study the ground state properties of either fractons or their bound states, since finite charge densities of either can now be attained at vanishing energy density.

Besides providing a platform in which to study the thermodynamics of fractons or their

bound states at finite charge densities, symmetric tensor gauge theories naturally capture *gapless* fracton theories. In these gapless states, fractons are strictly immobile only in isolation since at finite densities, fractons endow each other with inertia. This becomes clear when considering two fractons: while each fracton is immobile in isolation, it can now move by "pushing off" the other by exchanging a virtual dipole. Since such processes conserve the overall dipole moment of the system, they permit fractons to gain a mobility which is set by the background density of fractons. This establishes a short-range attraction between fractons, which when balanced against the generic power-law repulsion between them, creates a range of possible phases in which a finite density of fractons can exist, delineated in this chapter. Also considered here are systems with a finite density of bound states of fractons.

Similarly to compact vector U(1) gauge theories in $2+1$D, compact tensor gauge theories are unstable to a trivial gapped confined phase. However, much like their vectorial counterparts, we show that the addition of a (generalized) Chern-Simons term completely gaps out the gauge mode of the tensor gauge theory and leads to a stable chiral phase with deconfined fractonic excitations in $d = 2$ spatial dimensions. This allows us both to bring fractons down a dimension and to establish a connection between these states and quantum Hall physics.

A version of this chapter was first presented as [87] under the title "Emergent Phases of Fractonic Matter," and is a collaboration with Michael Pretko and Rahul Nandkishore,

<div align="center">

Phys. Rev. B 97, 085116 (2018)[1]

</div>

<div align="center">
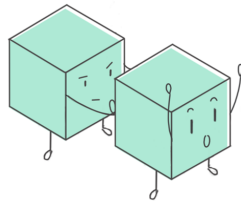
With a little help from my friends...

</div>

5.1 Introduction

Quantum phases of matter with long-range entanglement, such as spin liquids and fractional quantum Hall systems, are strikingly characterised by the presence of fractionalized quasiparticles. As a familiar example, two-dimensional systems can host anyon excitations, characterized by their non-trivial braiding statistics. In the presence of symmetries, these excitations can carry fractional quantum numbers, exhibiting the phenomenon of symmetry fractionalization. Perhaps the most famous manifestation of this behavior occurs in the celebrated $\nu = 1/3$ Laughlin fractional quantum Hall state [24], where the charge $e/3$ quasi-particles have been directly observed in experiment [17, 18, 257]. The phenomenon of fractionalization has been studied in great detail, specifically in the context of symmetry enriched topological (SET) phases [43, 258–264]. It is now well-established that the appropriate theoretical framework for understanding fractionalization is that of gauge theories, which also describe the fundamental forces of our universe. The resulting theoretical developments on fractionalization have led to a fruitful exchange of ideas between the condensed matter and high energy communities.

The most familiar types of gauge theories can be formulated in terms of a vector gauge field $\vec{A}$, just as in ordinary electromagnetism. Such vector gauge fields account not only for all gauge-mediated interactions in the Standard Model, but also for the theory of the fractional quantum Hall effect [147], superconductors with dynamical electromagnetism [46, 47], and most known examples of spin liquid states [43]. As such, treatments of fractionalization have historically focused almost exclusively on vector gauge fields. However, there is no reason in principle why the gauge field must transform as a vector object under rotations. Motivated by this, recent work has set out to study fractionalization patterns described by more general tensor gauge fields [80, 81, 265]. For instance, a quantum phase of matter could be described by a two-index tensor A_{ij}, or a tensor of even higher rank.

Gauge theories with such a tensor gauge field can describe a radically different form of fractionalization from that occurring in conventional vector gauge theories. Whereas vector gauge

theories only feature fractionalization of internal quantum numbers, like charge or spin, particles coupled to a tensor gauge field can exhibit fractionalization of the ability to move through space. The most notable example of this phenomenon is the existence of "fracton" excitations in certain tensor gauge theories. These new particles, first seen in the context of exactly solvable spin models [73–77, 233, 247, 255], have no ability to move by themselves, i.e. an isolated fracton is strictly immobile. Nevertheless, when a fracton combines with an appropriate number of other fractons, it can form a mobile bound state which is free to move around the system [2] . In this sense, a fracton is only a fraction of a conventional mobile excitation. The condensed matter literature has seen a flurry of recent activity fleshing out the properties of these strange new particles [78, 79, 82, 84, 88, 234, 266–278].

More generally, the restriction on mobility of charges in tensor gauge theories need not occur in all directions. There are other types of "subdimensional particles" which are immobile in only certain directions [80]. For example, some tensor gauge theories host one-dimensional particles, which are free to move only along a particular line. The physics of tensor gauge theories is therefore much richer than simply the theory of fractons. Nevertheless, fracton excitations have been studied in more detail than the other members of the subdimensional family, and we will focus in this work on fractons and their bound states.

Essentially all research in this area to date has focused on the properties of fractons in isolation, or in the presence of a small number of other fractons. Such treatments are, in a sense, determining the fundamental particle physics governing the behavior of fractons. For example, previous work has formulated the generalized electromagnetic interactions between fractons and $U(1)$ tensor gauge fields [81]. We can regard all of these previous studies as mapping out the "Standard Model" of fractons.

While the fundamental behavior of fractons has been studied in detail, there has been comparatively little work studying the behavior of a system with a finite density of fractons. This

---

[2] The smallest mobile bound state of fractons is usually also a non-trivial excitation of the system, which cannot decay directly into the vacuum, and therefore exists as a stable particle. The exception to this is in certain "fractal" fracton models, such as Haah's code, where all mobile bound states are trivial [75].

is an important problem to study, since a system with emergent tensor gauge structure will not necessarily be at zero chemical potential of fractons. In fact, there are multiple different chemical potentials to consider. As we will review, these tensor gauge theories have higher moment charge conservation laws, beyond the conventional monopolar charge conservation law. As a simple example, some systems exhibit conservation of both charge and dipole moment of fractons, which leads directly to their immobility. This extra conservation law allows us to consider a second type of chemical potential in the system. Even when there is zero net charge density of fractons, we can still tune a dipolar chemical potential to obtain a finite density of dipoles. To fully understand the behavior of fracton systems, we must therefore study not only finite densities of fractons, but also finite densities of the non-trivial bound states. In doing so, we will be formulating the "condensed matter theory" of fractons, mapping out the phases in which emergent fractonic matter can exist. In this thesis, we will content ourselves with studying fracton systems which have two non-trivial types of particles: immobile fractons and fully mobile dipoles. Many of these principles can be carried over to future studies of more complicated systems.

We will begin by studying the case of a finite density of fractons. This may seem trivial at first, since fractons tend to be locked in place. However, while a fracton in isolation is strictly immobile, multiple fractons are capable of limited motion via "pushing off" of each other, leading to a mutual sense of inertia, in a manifestation of Mach's principle [82]. In particular, for a system of fractons at density ρ, the fractons will possess a finite effective mass, $m \sim \rho^{-1}$. While the fractons have now lost their characteristic immobility, there is still one crucial difference between fractons and conventional mobile particles. Like-charged fractons in a $U(1)$ tensor gauge theory experience two types of forces: a long-range repulsion mediated by the gauge field [81], and an effective "gravitational" attraction which is generically short-ranged [82]. This type of situation, with short-range attraction and long-range repulsion, provides the natural conditions for microemulsion physics. The fractons will bind into small-scale clusters dominated by the short-range attraction, which in turn act as droplets "emulsed" in a phase dominated by the long-range repulsion. At low densities, the system will form a Wigner crystal of such fracton clusters. As the strength of the repulsion is increased, the

size of clusters will decrease until the system becomes a Wigner crystal of individual fractons. We will determine the necessary conditions on the repulsive potential for microemulsion physics to hold and will estimate the typical size of fracton clusters.

We will then move on to the study of systems with zero fracton density, but with a finite density of dipoles. We will assume throughout that dipole moment is quantized (such that there is a minimal dipole moment) as is always the case when the theory arises from an underlying lattice model.[80] Dipoles are intrinsically mobile particles, which allows their phases of matter to be studied through more conventional means. Furthermore, these dipoles can have either bosonic or fermionic statistics. We can therefore imagine putting these mobile dipoles into almost any phase encountered in conventional condensed matter. In this thesis, we will focus on the dipolar analogues of two familiar phases of matter: Fermi liquids in three-dimensions (3D) and quantum Hall phases in two-dimensions (2D).

We study a system with a finite density of fermionic dipoles, primarily focusing on the case of a single species of dipole (*i.e.* all polarized in one direction) in 3D. In this case, we expect the dipoles to form a Fermi surface. In the fracton model we focus on, the dipoles interact with a $1/r$ repulsive interaction, which will be screened at finite density, just like the conventional Coulomb interaction between electrons. All of the usual arguments for Fermi liquid theory can be carried over esssentially unchanged. One notable feature of this dipolar Fermi liquid is the behavior of fractons. We show that fractons in such a system have a logarithmic interaction energy. This leads to a finite-temperature phase transition, corresponding to the unbinding of fractons, in similar spirit to a BKT transition. In the low-temperature phase, the presence of a sharp Fermi surface will result in Friedel oscillations in the spin density, which is a useful experimental diagnostic. When this phase is realized in a weak Mott insulator (*i.e.* close to the metal-insulator transition), one should also be able to observe Friedel oscillations in the charge density.

Finally, we will consider systems in two spatial dimensions which have both a finite density of dipoles and a non-zero expectation value of the emergent magnetic field associated with the tensor gauge field. In this case, the mobile dipoles will respond to this field much like an electron would

respond to an external magnetic field, forming the dipolar analogue of a quantum Hall state [3] . We will show that these dipolar quantum Hall states fit naturally into the framework of the recently discovered chiral fracton phases, described by tensor Chern-Simons theories [272]. We will study many of the natural questions associated with these generalized quantum Hall states, such as their level quantization and ground state degeneracy. We will also demonstrate the existence of gapless chiral edge modes, which will result in a robust thermal Hall effect.

5.2 Review of $U(1)$ Fractons

Recently, in a series of papers [80–82, 269, 272], one of the authors (M.P.) has worked out the properties of 3D U(1) tensor gauge theories, which host fractons and other subdimensional excitations. These theories provide the natural analogue of the discrete fracton theories formulated by Vijay, Haah, and Fu [74, 76]. We will here review the simplest example of a $U(1)$ tensor gauge theory—the "scalar charge theory"—in order to illustrate the main principles underlying these phases.

Instead of a conventional vector gauge field A^i, this theory is formulated in terms of a rank 2 symmetric tensor gauge field A^{ij} and its canonical conjugate, E^{ij}. The properties of the theory are almost entirely determined by the form of the Gauss's law for the theory, which takes the form [4]

$$\partial_i \partial_j E^{ij} = \rho. \tag{5.1}$$

Whereas the conventional Gauss's law only leads to the conservation of charge, this new Gauss's law has two associated conservation laws,

$$\int \rho = \text{const.}, \quad \int \vec{x}\rho = \text{const.}, \tag{5.2}$$

corresponding to conservation of charge and dipole moment respectively. This extra conservation law has a severe consequence for the charges of the theory. A single charge cannot move while

---

[3] Importantly, there is no quantum Hall effect of normal electrical conductivity. Physically, these states will be most likely to occur in Mott insulating spin liquids.

[4] In this thesis, we use a notation where Greek indices vary over space-time components ($\mu = 0, 1, 2, 3$) and Latin indices are used for spatial components only ($i = 1, 2, 3$). Repeated indices will be implicitly summed over and we will work in units where $e = \hbar = c = 1$, with c being the velocity of the gauge mode.

conserving the dipole moment of the system. Therefore, isolated charges in this system are locked in place and are fracton excitations. A charge can only move if it combines with an opposite charge to form a dipolar bound state, which is free to move around the system. Such dipoles are themselves non-trivial objects, since dipole conservation prevents them from decaying directly into the vacuum.

Within the low-energy sector, where $\partial_i \partial_j E^{ij} = 0$, the system is invariant under the following gauge transformation

$$A_{ij} \rightarrow A_{ij} + \partial_i \partial_j \alpha, \tag{5.3}$$

for gauge parameter $\alpha(\vec{x})$ with arbitrary spatial dependence. The most relevant "magnetic field" object consistent with this gauge transformation takes the form of a non-symmetric traceless rank 2 tensor

$$B_{ij} = \epsilon_{iab} \partial^a A^b{}_j. \tag{5.4}$$

In terms of the electric and magnetic fields, the Hamiltonian for this theory is given by

$$\mathcal{H} = \int \left(\frac{1}{2} E^{ij} E_{ij} + \frac{1}{2} B^{ij} B_{ij} + A^{ij} J_{ij} \right), \tag{5.5}$$

where J_{ij} is a symmetric current tensor describing the motion of fractons. Note that, whereas normal particles have a vector current describing their motion, fractons can only move through multi-body hopping processes, which are conveniently captured by a symmetric tensor satisfying

$$\partial_t \rho + \partial_i \partial_j J^{ij} = 0. \tag{5.6}$$

which serves as the generalized continuity equation of the theory [81].

This theory can also be formulated in Lagrangian language as

$$\mathcal{L} = \frac{1}{2} \left(\dot{A}_{ij} - \partial_i \partial_j \phi \right)^2 - \frac{1}{2} B^{ij} B_{ij} - A^{ij} J_{ij} - \phi \rho, \tag{5.7}$$

where dots denote temporal derivatives and where ϕ is a field analogous to the temporal component, A_0, of the more familiar rank 1 gauge theory, serving as a Lagrange multiplier enforcing Gauss's law [272]. (Note that this theory does not have Lorentz invariance, so ϕ does not transform as a

"0 component" of the gauge field.) In this language, we can write a more general time-dependent gauge transformation within the low-energy sector

$$A_{ij} \to A_{ij} + \partial_i \partial_j \alpha, \quad \phi \to \phi + \dot{\alpha} \tag{5.8}$$

for scalar field $\alpha(\vec{x}, t)$ with arbitrary dependence on space and time.

One curious feature of this particular model is the fact that the interfracton potential grows linearly, $V(r) \sim r$. (This is not generic to $U(1)$ fractons, which in other models have a standard decaying potential.) In conventional vector gauge theories, a linear interparticle potential is indicative of an instability to a gapped confined phase. In this theory, however, there is a stable gapless phase, regardless of the large energy cost necessary to separate particles [80, 265]. Furthermore, once this energy cost has been paid, the immobility of fractons stabilizes them from collapsing directly back into the vacuum. Nevertheless, the linear energy cost indicates that these fractons cannot be thermally excited in large numbers. We will see later, however, that the presence of a dipolar Fermi surface can screen the linear potential down to a logarithmic interaction, which will allow for the proliferation of fractons above a certain temperature.

5.3   Microemulsions of Fractons

We begin by considering a three-dimensional system which has a finite density of $U(1)$ fractons. At finite density, fractons endow each other with inertia through the virtual exchange of dipole moment, and their characteristic immobility disappears [82]. Even though the fractons can now freely move around the system, there is still one crucial feature which sets fractons apart from conventional mobile particles. A fracton will lower its effective inertia, and thereby move more quickly, when it is in the immediate vicinity of another fracton. The result is an always-attractive geometric force between fractons, which plays the role of an effective gravitational interaction. As shown in previous work [82], the gravitational attraction between fractons is generically short ranged in the models studied in the condensed matter literature. The effective short-ranged attractive potential

takes the form

$$V_s(r) = -V_0 e^{-Mr}, \tag{5.9}$$

where M is the mass scale of the mobile dipoles and V_0 is a constant.

While the emergent gravitational force provides a short-range attraction, this is not the only interaction between fractons. Like-charged fractons in $U(1)$ models also exhibit a conventional gauge-mediated long-range repulsion. The precise power law of this repulsive interaction depends on the model, but we can readily identify an interesting universal feature which holds for a range of different potentials. A model with short-range attraction and long-range repulsion provides precisely the sort of conditions necessary for microemulsion physics (for discussions of microemulsion physics in a more traditional context, see [279–281]). At short distances, fractons attract each other and will have a tendency to bind together into clusters. At longer distances, however, we expect the power-law repulsion to take over, preventing the fractons from coalescing into a single large cluster. Instead, fracton clusters will have some typical intermediate size and will behave as mesoscopic "particles" with an effective repulsive interaction. This repulsion will keep the fracton clusters emulsed in the surrounding medium, instead of phase separating into a single large cluster. The situation is reminiscent of protons in a nucleus, held together by short-range attraction, which interact with other nuclei through a long-range Coulomb repulsion. At low densities, the system will form a Wigner crystal of fracton clusters.

This physical picture, while appealing, will turn out to hold only for a certain range of potentials. If the repulsion is too weak, all fractons will collapse into a single cluster. If the repulsion is too strong, all clusters will break apart into a Wigner crystal of individual fractons. In order to make more concrete statements, we must consider the precise form of the repulsive interaction. We will break up the analysis into two classes of repulsive power-law potentials, both of which are relevant in fracton phases.
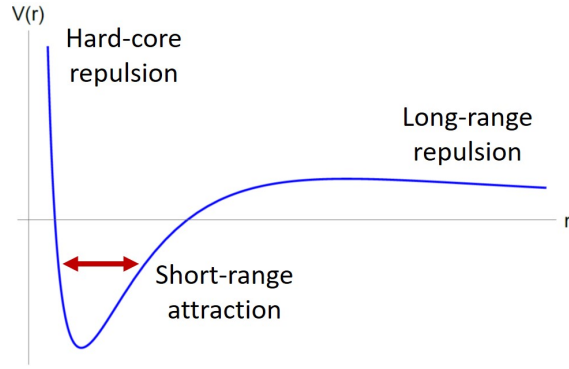
Figure 5.1: $V(r)$ vs r. The decaying potential has both long-range and "hard-core" repulsions, with a region of attraction just outside the core.

5.3.1   Decaying Potentials

We first assume that, in addition to the short range attraction, the fractons have a conventional decaying repulsive potential

$$V_l(r) = \frac{\alpha}{r^n},\tag{5.10}$$

for some power n. This is the situation which holds in some fracton models, such as the Gu-Wen emergent gravity model, for which $n = 1$ (*i.e.* a Coulomb potential) [282, 283]. Such a potential provides both a long-range repulsion and also a "hard-core" repulsion at the shortest distances, with the short-range interaction providing an attraction immediately outside the core (see Figure 5.1).

On short scales, we expect to see fractons clustering together into bound states. Taking the fractons to have a hard core of radius a, the lowest energy configuration will be approximately close-packed out to some radius R, as in Figure 5.2. The total number N of particles in the cluster scales as $N \sim (R/a)^3$. In order to determine the most energetically favorable value for N (and thereby R), we need to estimate the contributions to the energy of the cluster from both the short-range and long-range potentials.

For the short-range potential, it is sufficient to consider interaction energy between nearest neighbors. We therefore approximate the potential by $V_s = -V_0$ for nearest neighbor pairs, $V_s = 0$ otherwise. The total contribution to the energy of the cluster from the short-range interaction is
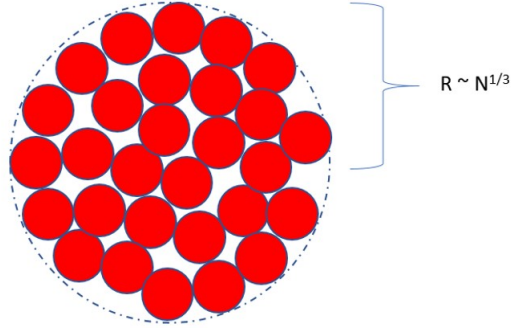
Figure 5.2: We consider a cluster of fractons that is approximately close-packed, assuming a hard-core radius a for the fractons. The radius of the cluster scales as $R \sim N^{1/3}$.

then given by

$$E_s = -c_1 V_0 N + c_2 V_0 N^{2/3}, \tag{5.11}$$

where c_1 and c_2 are positive numbers of order unity. The first term represents the interaction energy of particles in the bulk, with c_1 quantifying the number of nearest neighbors. The positive $N^{2/3}$ term represents the number of particles on the surface, which do not get all the energetic benefits of particles in the bulk, due to having fewer nearest neighbors. Keeping this surface term will turn out to be crucial.

In addition to the short-range interaction energy, we also need the contribution to the energy from the long-range repulsive potential. This interaction energy behaves as $E_l \sim \alpha N^2 / R^n \sim \alpha N^{2-\frac{n}{3}} / a^n$, so we write

$$E_l = c_3 \frac{\alpha}{a^n} N^{2-\frac{n}{3}}, \tag{5.12}$$

for c_3 of order unity. The total energy of the cluster is then given by

$$E = -c_1 V_0 N + c_2 V_0 N^{2/3} + c_3 \frac{\alpha}{a^n} N^{2-\frac{n}{3}}, \tag{5.13}$$

and the energy per fracton is

$$\frac{E}{N} = -c_1 V_0 + c_2 V_0 N^{-1/3} + c_3 \frac{\alpha}{a^n} N^{1-\frac{n}{3}}. \tag{5.14}$$

We can find the most energetically favorable configuration of the whole system by minimizing the
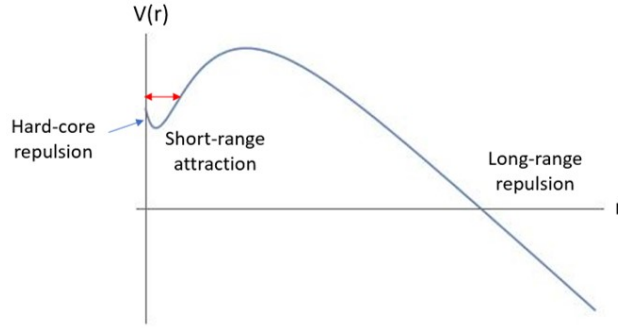
Figure 5.3: $V(r)$ vs r. The growing potential has a similar profile to the decaying case, except that the long-range repulsive potential now grows unbounded in magnitude, destabilizing the microemulsion.

energy per fracton

$$\frac{d(E/N)}{dN} = -\frac{1}{3}c_2 V_0 N^{-4/3} + c_3(1 - \frac{n}{3})\frac{\alpha}{a^n}N^{-n/3} \tag{5.15}$$

$$\Rightarrow N_c \sim \left(\frac{V_0 a^n}{\alpha(1 - \frac{n}{3})}\right)^{\frac{3}{4-n}} \sim \left(\frac{V_s(a)}{V_l(a)(1 - \frac{n}{3})}\right)^{\frac{3}{4-n}}. \tag{5.16}$$

In other words, the optimal particle number of the cluster is determined by the ratio of the short-range and long-range interaction energies of neighboring fractons. When the total number of fractons in the system is less than N_c, all of the fractons will clump together into a single cluster. At larger particle numbers, the system will have multiple clusters, interacting with each other through the long-range repulsion. The typical size of these clusters is given by

$$R \sim a N_c^{1/3} \sim a \left(\frac{V_s(a)}{V_l(a)(1 - \frac{n}{3})}\right)^{\frac{1}{4-n}}. \tag{5.17}$$

It is worth noting that, for $n \geq 3$, the cluster size blows up. This indicates that a long-range repulsion weaker than $1/r^3$ is no longer enough to keep the fractons from phase-separating into a single cluster, in a form of "gravitational collapse" of the system [5] . We therefore see that only repulsive interactions with $n < 3$ will exhibit microemulsion physics.

---

[5] Note that the hard core prevents the fractons from further collapsing into a black hole. Whether or not black hole physics is accessible within the fracton framework remains an important open question.

5.3.2   Growing Potentials

While some $U(1)$ fracton models feature a conventional decaying potential, other models have a repulsive potential which increases in magnitude as the fractons are separated. For example, we have already discussed that the scalar charge theory exhibits a linear repulsive potential between fractons, $V = -\alpha r$. More generally, we can consider a growing repulsive potential of the form

$$V_l(r) = -\alpha r^n. \tag{5.18}$$

When combined with short-range effects, this produces the potential energy profile seen in Figure 5.3. For a potential of this form, the system can always lower its energy by breaking apart a cluster into a configuration with well-separated fractons. This becomes readily apparent if we attempt to determine the typical cluster size using the strategy of the previous section. All previous statements about the short-range interaction carry over directly. The long-range interaction is slightly trickier. This contribution to the energy behaves as

$$E_l \sim -\alpha N^2 (R^n - L^n), \tag{5.19}$$

where L is the system size. We are here writing the energy of the cluster relative to a state in which the fractons are well-separated, which has energy of order $-\alpha N^2 L^n$. With respect to this reference point, the total energy of a cluster is given by

$$E = -c_1 V_0 N + c_2 V_0 N^{2/3} + c_3 \alpha L^n N^2 - c_4 \alpha a^n N^{2+\frac{n}{3}}. \tag{5.20}$$

The energy per particle is given by

$$\frac{E}{N} = -c_1 V_0 + c_2 V_0 N^{-1/3} + c_3 \alpha L^n N - c_4 \alpha a^n N^{1+\frac{n}{3}}. \tag{5.21}$$

Since $L \gg a$, the fourth term is negligible compared to the third, so we can drop it. (The fourth term only becomes relevant when $N \sim (L/a)^3$, at which point the notion of separate clusters breaks down anyway.) Within this approximation, we can find the optimal cluster size by minimizing the remaining terms with respect to N,

$$\frac{d(E/N)}{dN} = -\frac{1}{3}c_2 V_0 N^{-4/3} + c_3 \alpha L^n \tag{5.22}$$

$$\Rightarrow N_c \sim \left(\frac{V_0}{\alpha L^n} \right)^{3/4}. \tag{5.23}$$

If we take the thermodynamic limit, $L \to \infty$, we see that the typical cluster size vanishes, $N_c \to 0$, indicating that the repulsion has caused all clusters to break apart. The resulting state will feature fractons which are spaced apart as much as possible, in a Wigner crystal configuration.

We have now seen that a repulsive potential $V \sim r^n$ for $n > 0$ leads to no clusters at all in the system, whereas a potential $V \sim r^{-n}$ for $n \geq 3$ leads to the formation of a single phase-separated cluster. We can therefore conclude that microemulsion physics, with finite size clusters emulsed in a Wigner crystal of clusters, only holds for repulsive potentials $V \sim r^{-n}$ with $0 < n < 3$. Stronger repulsions will result in a single-particle Wigner crystal, while weaker repulsions will result in the "gravitational collapse" of the fractons.

5.4 Dipolar Fermi Liquids

We now move on to study a system which does not have a finite density of fractons, but rather a finite density of mobile dipoles. We will focus our attention specifically on the dipoles of the scalar charge theory, discussed in Section 5.2. We will assume throughout that there is a certain minimal size for dipole moments (*i.e.* dipole moment is quantized), as is always the case when the scalar charge theory arises from an underlying lattice model [80]. These dipoles can be either bosons or fermions, as discussed in Appendix F. In this work, we will focus on fermionic dipoles, which have phases of matter directly analogous to conventional electronic phases. For a system with a finite density of fermionic dipoles, the simplest fate for the system would seem to be that the dipoles form a Fermi surface, which is the first possibility that we will explore. We will study a three-dimensional system, where there are no instanton effects which could destabilize the system. It is possible that a two-dimensional dipolar Fermi surface is stable as well, similar to the conventional 2D spinon Fermi surface [284], but this would require a more detailed analysis which we leave to future studies.

We first study the case where there is only a finite density of one species of dipole p^i, with a specific orientation of dipole moment. Recall that dipole moment is a conserved quantity, so an isolated dipole cannot change its orientation. Furthermore, dipole moment is quantized in the system, so scattering between dipoles cannot change the orientation without paying a large finite energy cost. We assume that all interaction energies in the problem are small compared to this scale. It is then valid to consider a system of only p^i-oriented dipoles. Of course, such a polarized state breaks any rotational or inversion symmetries of the system. In terms of the microscopic degrees of freedom from which these dipoles emerge (*e.g.* spins in a spin liquid), a single-species dipolar Fermi liquid will be a state in which symmetry breaking and long-range entanglement coexist.

5.4.1   Justification of Fermi Liquid Theory

A finite density of noninteracting fermions will always form a Fermi surface. But in order to justify the existence of a stable interacting Fermi liquid, we must examine precisely how these dipoles interact with each other. We will confine our attention to the scalar charge theory discussed earlier. From the generalized electromagnetism of this model [81], we know that the interparticle potential between two dipoles, p and p', takes the form

$$V(r) = \frac{(p \cdot p')}{8\pi r} - \frac{(p \cdot r)(p' \cdot r)}{8\pi r^3}. \tag{5.24}$$

For identical dipoles, $p = p'$, this reduces to

$$V(r) = \frac{p^2 \sin^2 \theta}{8\pi r}, \tag{5.25}$$

where θ is the angle between p and r. The corresponding force between identical dipoles is generically repulsive, except for a line of zero force at $\theta = 0$. Importantly, the force is never attractive. Also, we note that the $1/r$ potential (and corresponding $1/r^2$ force) scales exactly like the normal Coulomb interaction between electrons. We can hence essentially regard the interaction between dipoles as simply an anisotropic Coulomb force. Then, just as in normal Fermi liquid theory, the dipoles will be able to screen each other. (The details of dipolar screening are worked out explicitly

in Appendix E.) After accounting for screening, the resulting screened quasiparticles will only have weak short-range interactions.

At this point, the dipole moment of the fermions becomes mostly irrelevant to the problem. We have a system of fermions with short-range interactions, with the dipole moment simply serving as an extra internal quantum number which has no effect on the traditional Fermi liquid analysis. All of the usual interesting aspects of Fermi liquid theory will carry over unchanged. There will be a discontinuity in dipole occupation number at a sharp Fermi surface in momentum space (with a quasi-particle residue $Z < 1$). Also, for appropriate values of Landau parameters, the system will host a zero sound mode, representing oscillations of the Fermi surface, which provides a way to distinguish the system from a free Fermi gas of dipoles.

While the dipole quantum number does not significantly affect the Fermi liquid analysis, there is one important way in which it makes its presence known in the low-energy physics. While the bare interaction of Eq. (5.25) is screened, it remains highly anisotropic, with a strong repulsion between side-by-side dipoles and zero interaction between end-to-end dipoles. As such, the dipoles will tend to be arranged more densely in the direction of their dipole moment. This corresponds to a larger Fermi momentum k_F, in this direction than in the two perpendicular directions. Thus, the anisotropic interaction between dipoles will lead to a Fermi surface which is elongated along the direction of the dipole orientation. Starting from a nearly isotropic system, the interactions will cause the Fermi surface to roughly take the shape of a prolate spheroid, as illustrated in Figure 5.4.

This elongation should manifest itself in the Friedel oscillations of the system, which will have a shorter wavelength in the direction of the dipole moment. When this dipolar phase of matter is realized in a Mott insulating spin liquid, these Friedel oscillations will be most prominently seen in the spin density, since the dipoles will carry spin but not charge. However, for a weak Mott insulator (close to the metal-insulator transition), the coupling between the charge and spin sectors is strong enough to observe Friedel oscillations in the charge density as well, as seen in certain Mott transitions with a "ghost" Fermi surface [285].

It is worth noting that, as in more familiar $U(1)$ spin liquids with spinon Fermi surfaces, the
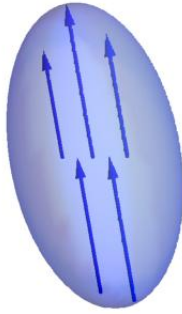
Figure 5.4: The anisotropic nature of the interaction between dipoles will cause the Fermi surface to elongate in the direction of the dipole moment, forming roughly a prolate spheroid.

Fermi velocity of the dipoles will generically be of the same order as the speed of the gapless gauge mode. As such, the dynamical screening of this system will be more complicated than that of a normal metal, which should manifest itself in the response functions of the system. We leave the detailed study of dynamical screening as a problem for future study.

5.4.2   Finite-Temperature Phase Transition

Another important aspect of the dipolar Fermi liquid to investigate is the behavior of fractons, which still occur as excitations of the system (even though they are no longer at finite density). The bare fractons of the scalar charge theory have a linear interfracton potential, $V \sim r$. This is the phenomenon of "electrostatic confinement" [80], which usually makes these fractons irrelevant to the low-energy physics. In the presence of a finite density of dipoles, however, previous work [269] has indicated that the interfracton potential is partially screened. The present case is slightly different from previous work due to the presence of a Fermi surface and also due to having only one orientation of dipole. We leave the details of the calculation to Appendix E. Here, we simply quote the result that the screened potential grows only logarithmically,

$$V_{scr}(r) \sim \frac{1}{\sqrt{g}} \log r, \tag{5.26}$$

where g is the density of states of dipoles at the Fermi surface. The fractons now interact through a logarithmically increasing potential, which is a much milder sort of growth than the bare linear potential.

The logarithmic potential still results in a significant energy cost for an isolated fracton, scaling as $\log L$, where L is the system size, much like a vortex in a two-dimensional superfluid. Just as in a superfluid, we expect that the fractons will only proliferate above a certain temperature. The free energy associated with an isolated fracton in a system of size L will take the schematic form

$$F \sim \left(\frac{1}{\sqrt{g}} - k_B T \right) \log L. \tag{5.27}$$

Fractons will therefore only proliferate at temperatures above a certain critical temperature, where the free energy per particle becomes negative

$$T_c \sim \frac{1}{k_B \sqrt{g}}. \tag{5.28}$$

Below this temperature, fractons will mostly exist in small bound states, such as dipoles. Above the transition temperature, fractons will be able to unbind and behave independently, just like in the BKT transition of vortices in a superfluid. When this happens, the dipoles will lose their integrity and break apart into separate fractons, destroying the Fermi surface. Furthermore, in such a finite temperature system, fractons lose their characteristic immobility and can move around the system (albeit very slowly) [269]. At this point, all interesting properties of both fractons and dipoles have been lost, and the system is in a trivial phase.

We note that, for a three-dimensional system, the density of states g increases with the size of the Fermi surface, indicating a decrease in T_c as the Fermi surface gets bigger. In contrast, the Fermi temperature $T_F \sim E_F$ increases with the size of the Fermi surface. For a sufficiently large dipolar Fermi surface, the transition will happen at temperatures well below the Fermi temperature, $T_c \ll T_F$, so we do not need to worry about thermal smearing of the Fermi surface. The Fermi surface should remain fairly sharp up until the critical temperature, where the dipoles are destroyed.
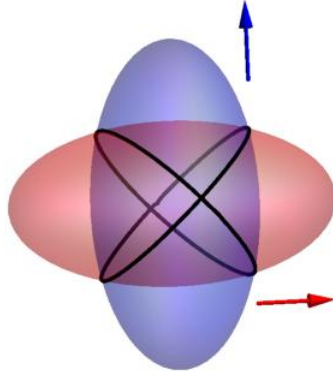
Figure 5.5: Fermi surfaces of different species of dipoles will be elongated along different directions, which drastically reduces their overlap, shown here by the solid black curves.

5.4.3   Multi-Species Fermi Liquids

One might also consider the case where there are finite densities of two or more different orientations of dipoles in the system. We would like to imagine each species as entering its own Fermi liquid phase, with perhaps some weak coupling between them. However, the form of the interaction between dipoles (Eq. (5.24)) brings a complication into this picture. For simplicity, consider the case of two species, p and p', with dipole moments of equal magnitude but in perpendicular directions. The resulting interparticle potential is

$$V(r) = -\frac{(p \cdot r)(p' \cdot r)}{8\pi r^3} = -\frac{p^2 \sin 2\theta}{16\pi r}, \tag{5.29}$$

where θ is the angle between p and the component of r in the $p - p'$ plane. Note that, whereas the interaction between identical dipoles was strictly repulsive, the interaction between perpendicular dipoles can be either attractive or repulsive depending on the relative positions of the dipoles. We now have a channel with an attractive interaction, so the system may have pairing instabilities. A further complication is the fact that the Fermi surfaces of the different dipole orientations will not overlap, as shown in Figure 5.5, which will make the interspecies pairing problem more intricate. Ultimately, the study of multi-species dipolar Fermi liquids will be a much more difficult problem than the single-species case, and we leave this to future work.

5.5   Dipolar "Quantum Hall" Phases

The preceding sections of this chapter have focused on fracton models in three spatial dimensions, which until recently had been the sole focus of the fracton community, due to folklore that fractons could not occur in less than three dimensions. The discrete spin models [74, 76] seem to have some fundamental obstruction to being realized in two dimensions (though this issue is not yet fully settled). Meanwhile, the lattice rotor fracton models [80, 265] are described by compact $U(1)$ tensor gauge theories, which are unstable in two dimensions due to instanton effects, just like a conventional compact $U(1)$ gauge field in 2D.

Despite these earlier difficulties, recent work has shown that fractons can exist in two spatial dimensions, and in fact are realized in a simple two-dimensional quantum crystal as disclination defects [84]. The elastic theory of such a crystal can be mapped directly onto a **non**compact $U(1)$ tensor gauge theory, which avoids instanton effects, thereby providing an example of a stable fracton model in two dimensions. This realization opens the door to a whole new class of fractonic phases of matter. For example, we can place the mobile dipoles into any of the conventional two-dimensional phases of matter. In this work, we will focus on dipolar analogues of one of the most well-studied types of two-dimensional phases: quantum Hall systems.

Conventional quantum Hall phases can be productively studied through the use of Chern-Simons theories, which capture the flux attachment physics of the composite fermion picture. Similarly, we should be able to study dipole "quantum Hall" states by attaching to each dipole some amount of its effective magnetic flux. Luckily, the appropriate tool for studying such dipolar flux attachment has already been developed, in the form of tensor Chern-Simons theories, first seen in the context of boundary theories to certain three-dimensional fracton models [272]. We will here apply these generalized Chern-Simons theories to the study of purely two-dimensional dipolar "quantum Hall" phases. (We will drop the quotes from here on, with the understanding that these phases do **not** exhibit a quantum Hall response to the physical electromagnetic field.) By coupling a Maxwell-type tensor gauge theory (arising from elasticity theory, for example) to a tensor Chern-

Simons gauge field, we obtain a gapped chiral phase of matter hosting fracton excitations. We work out some of the basic properties of these new two-dimensional gapped phases, such as their response properties, ground state degeneracies, and edge modes.

We note that these tensor Chern-Simons theories also provide a way to stabilize **compact** $U(1)$ tensor gauge theories in two dimensions. Such theories can arise, for example, by coupling a two-dimensional quantum crystal to a substrate [84]. They can also arise directly in lattice rotor models. A compact Maxwell tensor gauge theory of this sort has an instability to a trivial gapped confined phase, driven by instanton effects. However, by adding a tensor Chern-Simons term to the critical point, we can drive the system towards a different nontrivial gapped fixed point, described by dipolar quantum Hall physics.

We emphasize that the $U(1)$ fracton models we consider evade the usual arguments for non-existence of fracton theories in two dimensions. Such arguments apply to stabilizer code models where the fracton charge is only conserved modulo an integer. In contrast, we consider only systems of $U(1)$ fractons with an absolutely conserved charge, such as the topological defects in two-dimensional quantum crystals [84]. In the following, we will always take the tensor Chern-Simons theories to be coupled to such fractons with conserved charge.

5.5.1 Review of Chern-Simons Theory

We begin by reviewing the basics of Chern-Simons field theories described by vector gauge fields, highlighting the elements most relevant for our higher rank generalizations (for a more comprehensive review, we refer the reader to Refs. [23, 147].). The structure of these topological quantum field theories (TQFTs) was elucidated in a remarkable paper by Witten [30], and it has since been realized that they describe the low energy physics of a large class of two-dimensional gapped topological phases of matter, including quantum Hall fluids [27–29], superconductors [46, 47], and spin liquids [43]. In particular, they correctly capture the non-trivial ground state degeneracy (GSD) of topological phases on a torus (a direct manifestation of topological order), in addition to the braiding and statistics of fractionalized excitations. While a general discussion should include

non-Abelian Chern-Simons theories (which appear e.g., in the context of the $\nu = 5/2$ quantum Hall state [286] and chiral spin liquids [287]), for simplicity we will restrict our discussion to the Abelian case.

The Chern-Simons action at level k for a vector gauge field A_μ is

$$\mathcal{S}_{CS} = \frac{k}{4\pi} \int d^3x \, \epsilon^{\mu\nu\lambda} A_\mu \partial_\nu A_\lambda, \tag{5.30}$$

where $\mu, \nu, \lambda = 0, 1, 2$. This term is rotationally invariant but breaks parity and time-reversal. Moreover, it is gauge-invariant under $A_\mu \to A_\mu + \partial_\mu \alpha$

$$\mathcal{S}_{CS} \to \mathcal{S}_{CS} + \int d^3x \, \partial_\mu \left(\alpha \epsilon^{\mu\nu\lambda} \partial_\nu A_\lambda \right), \tag{5.31}$$

only upto a total derivative term which vanishes on closed manifolds. The Chern-Simons term (5.30) naturally captures the basic physics of the integer quantum Hall (IQH) effect, since

$$\frac{\delta \mathcal{S}_{CS}}{\delta A_0} = J_0 = \frac{k}{2\pi} B, \tag{5.32}$$

$$\frac{\delta \mathcal{S}_{CS}}{\delta A_i} = J_i = -\frac{k}{2\pi} \epsilon^{ij} E_i. \tag{5.33}$$

Identifying k with the number of filled Landau levels ν, we see that the Chern-Simons term captures the flux-attachment in the quantum Hall state and describes a Hall conductivity $\sigma_{xy} = \nu/(2\pi)$. While ν is naturally quantised since it describes the number of filled Landau levels, at first glance k need not be quantized. However, the level k is necessarily quantized as a result of gauge invariance (see Appendix G.1 for details).

While the above discussion focused only on the integer quantum Hall state, Chern-Simons theory can more generally describe the low-energy physics of phases with fractionalized excitations. The long-distance physics of (Abelian) topological phases is captured by an Abelian Chern-Simons field theory, with the Lagrangian

$$\mathcal{L} = \frac{1}{4\pi} \epsilon^{\mu\nu\lambda} a_\mu^I K_{IJ} \partial_\nu a_\lambda^J. \tag{5.34}$$

Here, a^I is a multiplet ($I = 1, 2, \ldots, N$) of compact U(1) statistical gauge fields and K_{IJ} is a symmetric integer-valued $N \times N$ matrix which encodes the statistics of quasi-particles. The parity of the diagonal entries of the K-matrix specify whether the state is fermionic (odd) or bosonic (even). The K-matrix describing a gapped $\mathbb{Z}_2$ spin-liquid is given by

$$K = \begin{pmatrix} 0 & 2 \\ 2 & 0 \end{pmatrix}, \tag{5.35}$$

while fractional quantum Hall (FQH) states are described by $N = 1$ and $K = m$, with m odd (even) for fermionic (bosonic) states.

As an additional simplification, let us consider this latter case, where K is simply an integer and the theory is governed by a single statistical gauge field a,

$$\mathcal{L} = \frac{m}{4\pi} \epsilon^{\mu\nu\lambda} a_\mu \partial_\nu a_\lambda. \tag{5.36}$$

In order to completely specify the phase, we would also need to specify the quantum numbers carried by quasi-particles, which in the context of FQH states refers to their charge. While this is easily accomplished within the Chern-Simons formalism by adding a mixed Chern-Simons term

$$\mathcal{L}_{\text{mixed}} = -\frac{1}{2\pi} \epsilon^{\mu\nu\lambda} A_\mu \partial_\nu a_\lambda \tag{5.37}$$

to the Lagrangian (5.36), it leads to a description of the phase as not simply topologically ordered, but rather as a symmetry enriched topological (SET) phase, which is outside the scope of this review.

A clear manifestation of topological order in the Chern-Simons description of topological phases is that the degeneracy of ground states depends on the topological properties of the manifold the system lives on. Specifically, it is possible to show that while there are no topologically degenerate ground states if the system (5.36) is defined on a sphere, on a torus the GSD is m (see Appendix G.2 for details). More generally, it can be shown that the ground state degeneracy of the K-matrix theory (5.34) on an arbitrary Riemann surface of genus g is $|\det(K)|^g$ [170].

Another characteristic feature of FQH states is the existence of chiral gapless edge excitations, which cannot be gapped by any local perturbations. Placing the system described by (5.36) on a

semi-infinite plane, it is possible to derive the effective action governing these boundary modes (see Appendix G.3 for details). The resultant theory,

$$S_{\text{edge}} = \frac{m}{4\pi} \int d^2x \ (\partial_t\varphi\partial_x\varphi - v\partial_x\varphi\partial_x\varphi) , \tag{5.38}$$

is a conformal field theory (CFT), also known as a chiral Luttinger liquid or level m Kac-Moody theory, which describes a chiral boson moving at a velocity v. Importantly, these one-dimensional boundary CFTs allow us to directly calculate the wave-function of the two-dimensional bulk, as was established in a landmark paper by Moore and Read [31]. For instance, from the conformal blocks of the chiral CFT (5.38) it is possible to derive the Laughlin wave-function for the $\nu = 1/m$ FQH state.

5.5.2 Generalized Chern-Simons Theories

We now turn our attention towards two-dimensional higher rank generalizations of Chern-Simons theories, which host excitations with restricted mobility, including fractons. Here, we will focus on a specific chiral phase described by a rank 2 symmetric tensor gauge field—the "scalar charge theory" in the taxonomy of Ref. [272]—to demonstrate the general phenomenology of such phases, with generalizations to different higher rank theories left for future work.

We first consider a phase described by a rank 2 spatial symmetric tensor A_{ij}, with its canonically conjugate variable E_{ij} playing the role of an electric field tensor. This theory, similar to the 3D rank 2 theory reviewed in Section 5.2, is uniquely specified by a generalized Gauss' law which takes the form

$$\partial_i\partial_j E^{ij} = \rho, \tag{5.39}$$

for a scalar charge density ρ. The excitations carrying this charge obey two constraints,

$$\int \rho = \text{const.}, \quad \int \vec{x}\rho = \text{const.}, \tag{5.40}$$

corresponding to the conservation of charge and of dipole moment respectively. The fundamental charges of this theory are hence fractons, unable to move in any direction due to the dipole moment

conservation law. Importantly, however, the dipolar bound states of this theory are completely mobile, possessing both longitudinal and transverse motion [81]. The constraint in the low energy sector, $\partial_i \partial_j E^{ij} = 0$, leads to invariance under the gauge transformation

$$A_{ij} \to A_{ij} + \partial_i \partial_j \alpha, \tag{5.41}$$

for gauge parameter $\alpha(\vec{x}, t)$ with arbitrary space-time dependence. The long-distance Hamiltonian consistent with this gauge structure is

$$\mathcal{H} = \frac{1}{2} E^{ij} E_{ij} + \frac{1}{2} B^i B_i, \tag{5.42}$$

where the magnetic field is a vector quantity,

$$B^j = \epsilon^{ib} \partial_i A_b{}^j, \tag{5.43}$$

and the constraint $\partial_i \partial_j E^{ij} = 0$ is implicitly assumed. The Hamiltonian (5.42) leads to a linearly dispersing gapless gauge mode with two polarizations. We also note that the magnetic flux vector B^i in this case satisfies the constraint

$$\int x_i B^i = \text{const.}, \tag{5.44}$$

which implies that the magnetic fluxes are one-dimensional, with only transverse mobility.

Following the discussion presented in Ref. [272], we can also formulate this theory in terms of a Lagrangian by introducing a Lagrange multiplier field ϕ which imposes the Gauss' law constraint. The Lagrangian of this two-dimensional theory is

$$\mathcal{L}_0(A_{ij}, \phi) = \frac{1}{2} \left(\dot{A}_{ij} - \partial_i \partial_j \phi \right)^2 - \frac{1}{2} B^i B_i, \tag{5.45}$$

which is gauge-invariant under the transformations

$$\begin{aligned} A_{ij} &\to A_{ij} + \partial_i \partial_j \alpha, \\ \phi &\to \phi + \dot{\alpha}, \end{aligned} \tag{5.46}$$

where $\alpha(\vec{x}, t)$ has arbitrary space-time dependence.

5.5.2.1   Feeding the Gauge Field

Having established the properties of the tensor gauge field with a Maxwell action, we now consider the effects of a Chern-Simons term, which we expect will gap the theory and perform some type of flux attachment. As we discuss in the next section, a tensor Chern-Simons term attaches magnetic flux to dipoles. First however, we verify that the Chern-Simons term fully gaps the gauge field, giving a gapped chiral phase of matter with fracton excitations.

We introduce a Chern-Simons term for the tensor gauge field A_{ij} as:

$$\mathcal{S}[A_{ij}, \phi] = \mathcal{S}_0[A_{ij}, \phi] + \mathcal{S}_{gCS}[A_{ij}, \phi], \tag{5.47}$$

where we have added to the Lagrangian (5.45) a generalized Chern-Simons action

$$\mathcal{S}_{gCS}[A_{ij}, \phi] = -\frac{\theta}{4\pi^2} \int d^3x \, \phi \epsilon^{bi} \partial_i \partial_j A_b{}^j + \frac{\theta}{8\pi^2} \int d^3x \, \epsilon^{bi} \dot{A}_{ij} A_b{}^j, \tag{5.48}$$

parametrized by θ. We note that this Chern-Simons action can be derived as the boundary theory of a 3D higher rank tensor gauge field with a generalized "E·B" term parametrized by a coefficient θ [272]. Here, we study the action (5.48) in strictly two-spatial dimensions, observing that, unlike the vector Chern-Simons theory (5.30), the generalized action (5.48) does not describe a topological quantum field theory, as there does not appear to be any metric-independent formulation of this theory [272].

In order to understand the consequences of the Chern-Simons action for the gapless gauge modes, we decouple the symmetric gauge field A_{ij} into its trace γ and a symmetric traceless tensor $\tilde{A}_{ij}$

$$A_{ij} = \tilde{A}_{ij} + \gamma \delta_{ij}. \tag{5.49}$$

Substituting this into the action (5.47), we obtain

$$\begin{aligned}
\mathcal{S}[\tilde{A}_{ij}, \gamma, \phi] = &\frac{1}{2} \int d^3x \left(\dot{\tilde{A}}_{ij} - \left(\partial_i \partial_j - \frac{1}{2} \delta_{ij} \partial^2 \right) \phi \right)^2 - \frac{1}{2} \int d^3x \left(\partial_i \gamma + \epsilon^{ij} \epsilon^{ab} \partial_a \tilde{A}_{bj} \right)^2 \\
&+ \int d^3x \left(\dot{\gamma} - \frac{1}{2} \partial^2 \phi \right)^2 + \mathcal{S}_{gCS}[\tilde{A}_{ij}, \phi].
\end{aligned} \tag{5.50}$$

Let us unpack this expression. First, we note that in terms of the separated fields $\tilde{A}_{ij}$ and γ, the action is invariant, up to a boundary term, under the gauge-transformation

$$\tilde{A}_{ij} \to \tilde{A}_{ij} + \left(\partial_i\partial_j - \frac{1}{2}\delta_{ij}\partial^2\right)\alpha,$$

$$\gamma \to \gamma + \frac{1}{2}\partial^2\alpha, \tag{5.51}$$

$$\phi \to \phi + \dot{\alpha},$$

where $\alpha(\vec{x},t)$ has arbitrary space-time dependence. Remarkably, we see that the trace component does not appear in the Chern-Simons action, which ostensibly gives a mass only to the traceless component of the gauge mode while leaving the trace component massless.

To decipher the fate of the traceless component, we focus on the terms in the action (5.50) containing γ,

$$\mathcal{S}[\tilde{A}_{ij},\gamma,\phi] = \int d^3x \left(\dot{\gamma} - \frac{1}{2}\partial^2\phi\right)^2 - \frac{1}{2}\int d^3x \left(\partial_i\gamma + \epsilon^{ij}\epsilon^{ab}\partial_a\tilde{A}_{bj}\right)^2 + \mathcal{S}_2[\tilde{A}_{ij},\phi] \tag{5.52}$$

where $\mathcal{S}_2$ contains the remaining terms in the action. Re-parametrizing $\tilde{A}_{ij}$ in terms of an effective gauge field

$$\Gamma^i = \epsilon^{ij}\epsilon^{ab}\partial_a\tilde{A}_{bj}, \tag{5.53}$$

we can re-write Eq. (5.50) as

$$\mathcal{S}[\tilde{A}_{ij},\gamma,\phi] = \int d^3x \left[\left(\dot{\gamma} - \frac{1}{2}\partial^2\phi\right)^2 - \frac{1}{2}\left(\partial_i\gamma + \Gamma_i\right)^2\right] + \mathcal{S}_2[\tilde{A}_{ij},\phi]. \tag{5.54}$$

Once written in this form, it is clear that the trace mode γ couples to the effective gauge field Γ_i in a manner redolent of the coupling between a superfluid phase φ and an ordinary vector potential A_μ: $(\partial_\mu\varphi - A_\mu)^2$. By analogy with the case of a superfluid, where the vector potential "eats" the gapless Goldstone mode, we thus expect that the gapless trace mode will get eaten by the effective gauge field Γ. This can be seen explicitly by making a gauge transformation

$$\tilde{A}_{ij} \to \tilde{A}_{ij} + \left(\partial_i\partial_j - \frac{1}{2}\delta_{ij}\partial^2\right)\alpha, \quad \phi \to \phi + \dot{\alpha}, \tag{5.55}$$

with $\alpha(\vec{x},t)$ such that

$$\frac{1}{2}\partial^2\alpha = \gamma. \tag{5.56}$$

While $\mathcal{S}_2[\tilde{A}_{ij}, \phi]$ is invariant under such a transformation, the magnetic flux vector and effective gauge field transform as

$$B^j \to \tilde{B}^j = \epsilon^{ib} \partial_i \tilde{A}_b{}^j,$$

$$\Gamma_i \to \Gamma_i - \frac{1}{2} \partial_i \partial^2 \alpha = \Gamma_i - \partial_i \gamma,$$

(5.57)

thereby completely eliminating the trace mode γ from the theory. Surprisingly, we have found that the gauge field eats its own trace component, leading us to christen this higher rank tensor gauge field an "ouroboros" gauge field. We note that similar behavior may be displayed by non-Abelian vector gauge theories in the context of SU(2) spin liquids [147].

Since γ is a compact field, we should, in principle, account for the presence of vortices as is often done when studying ordinary superfluids. Specifically, on splitting γ into a regular part γ_r and a singular part γ_s, only the regular part would get absorbed into the effective gauge field Γ_i, with γ_s describing gapped vortices with short-range interactions. We can then also imagine integrating out the gapped gauge mode, leading to an effective action for these vortices, which would take the form of a conventional vector Chern-Simons theory. We leave a detailed discussion of these vortices for future work.

The preceding discussion establishes that the higher rank Chern-Simons term leads to a completely gapped phase, with the low energy physics of this phase described by a traceless symmetric rank 2 field $\tilde{A}_{ij}$ [6] . The effective action describing the long-distance physics of this gapped phase is hence the generalized Chern-Simons term

$$\mathcal{S}_{gCS}[\tilde{A}_{ij}, \phi] = -\frac{\theta}{4\pi^2} \int d^3x \, \phi \epsilon^{bi} \partial_i \partial_j \tilde{A}_b{}^j + \frac{\theta}{8\pi^2} \int d^3x \, \epsilon^{bi} \dot{\tilde{A}}_{ij} \tilde{A}_b{}^j,$$

(5.58)

since it has one fewer derivative than the Maxwell-like term in the action. As mentioned earlier, in principle we should also include the gapped vortices of the trace mode γ, but we will focus here on the physics captured by the higher rank Chern-Simons term (5.58), which is gauge-invariant (on a

---

[6] Since the trace mode disappears from the theory, it is natural to ask whether we could simply start from the theory of a traceless symmetric rank 2 tensor. However, the particle structure for such a theory would differ from the one studied here and must thus be considered separately.

closed manifold) under

$$\tilde{A}_{ij} \to \tilde{A}_{ij} + \left(\partial_i\partial_j - \frac{1}{2}\delta_{ij}\partial^2\right)\alpha, \quad \phi \to \phi + \dot{\alpha}, \tag{5.59}$$

for arbitrary $\alpha(\vec{x}, t)$.

Similarly to the quantization of the level k of a vector Chern-Simons theory, the coefficient θ of the action (5.58) is also quantized in units of 2π (see Appendix H.1 for a derivation),

$$\theta = 2\pi k, \quad k \in \mathbb{Z}. \tag{5.60}$$

We will henceforth refer to k as the level of the higher rank tensor Chern-Simons theory, which we will now demonstrate describes an emergent integer quantum Hall state of mobile dipoles at the filling fraction $\nu = k$. We note that, similarly to the CS theory describing the quantum Hall effect, we will see that when $k \in \mathbb{Z}$, the generalized CS term (5.58) describes an IQH state of dipoles while for fractional values, it is describing an FQH state.

5.5.2.2 Integer quantum Hall state of Dipoles

So far, we have established that the addition of the higher rank Chern-Simons term leads to a fully gapped phase, where the trace mode of the symmetric tensor A_{ij} has been eaten by the traceless mode $\tilde{A}_{ij}$. With the gauge sector of the theory fixed, we now examine the particle content of the low-energy theory (5.58).

The Lagrange multiplier field ϕ constrains the low-energy sector of this theory,

$$-\frac{k}{2\pi}\epsilon^{bi}\partial_i\partial_j\tilde{A}_b{}^j = \frac{k}{2\pi}\partial_j\tilde{B}^j = 0, \tag{5.61}$$

where $\tilde{B}^j$ is the magnetic flux vector. More generally, allowing for the appropriate gauge charges coupled to the Chern-Simons field,

$$\rho = -\frac{k}{2\pi}\epsilon^{bi}\partial_i\partial_j\tilde{A}_b{}^j. \tag{5.62}$$

It can readily be checked that the excitations carrying this charge obey the constraints

$$\int \rho = \text{const.}, \quad \int \vec{x}\rho = \text{const.}, \quad \int x^2\rho = \text{const.}, \tag{5.63}$$

corresponding to the conservation of charge, dipole moment, and a specific component of the quadrupole moment. The fundamental charges are thus fractons, while the dipolar bound states are only mobile in the direction transverse to their dipole moment.

While it seems surprising that the dipoles, which were fully mobile in the absence of the Chern-Simons term, now have restricted mobility, this restriction arises naturally as a consequence of flux-attachment (5.62),

$$\rho = \frac{k}{2\pi}\partial_j \tilde{B}^j, \tag{5.64}$$

which indicates that the Chern-Simons term binds a flux $2\pi/k$ to each dipole. Since the magnetic flux vector in this theory is one-dimensional, it follows that dipole excitations in the gapped deconfined phase inherit the restricted mobility of the fluxes.

The physics of this gapped phase can be understood through a simple semi-classical picture, where fully mobile dipoles at some finite density move in the presence of an emergent finite background magnetic field. In analogy with electrons in a perpendicular magnetic field, these dipoles move in quantized circular orbits and perform cyclotron motion, as depicted in Figure 5.6. In this context, the integer k has a natural interpretation as the number of filled Landau levels ν occupied by the mobile dipoles, and this phase hence corresponds to an emergent integer quantum Hall phase of dipoles. Since we are attaching an integer amount of flux to the dipoles, which are originally mobile, there is no fractionalization of charge or statistics of the deconfined quasi-particles. Instead, a striking new feature of the generalized Chern-Simons theory considered here is the fractionalization of mobility of the underlying dipoles forming the state, resulting in deconfined dipolar excitations with only one-dimensional motion allowed.

Pushing on the semi-classical picture further, we expect that the circular orbits will reduce to skipping orbits in the presence of a boundary, leading to a chiral dipolar current propagating along the edge. Indeed, as we will show later (see Section 5.5.2.4), the presence of these boundary modes can be established directly by placing the tensor Chern-Simons theory (5.58) on an open manifold.

Besides these boundary modes, we can also characterize this phase through its generalized "Hall" response, which follows from varying the action (5.58) with respect to $\tilde{A}_{ij}$,

$$\langle J^{ij} \rangle = \frac{k}{4\pi} \left(\epsilon^{ib} \dot{\tilde{A}}_b{}^j + \epsilon^{jb} \dot{\tilde{A}}_b{}^i \right) = \frac{k}{4\pi} \left(\epsilon^{ib} E_b{}^j + \epsilon^{jb} E_b{}^i \right). \tag{5.65}$$

We can thus define a "Hall" conductivity which is given by

$$\sigma^{ijkl} = \frac{k}{4\pi} \left(\epsilon^{ik} \delta^{jl} + \epsilon^{jk} \delta^{il} \right). \tag{5.66}$$

The only non-trivial components of this tensor are

$$\sigma^{xyyy} = \sigma^{yxyy} = -\sigma^{yxxx} = -\sigma^{xyxx} = \frac{k}{4\pi}, \tag{5.67}$$

and

$$\sigma^{xxyx} = -\sigma^{yyxy} = \frac{k}{2\pi}. \tag{5.68}$$

Unlike the Hall response in an integer quantum Hall state of electrons, which represents the response of the system to an externally varying electric field, here the conductivity tensor σ^{ijkl} encodes the response to the internal emergent tensor field E_{ij}.

5.5.2.3   Fractional quantum Hall analogues

Thus far, we have focused on the case where k is restricted to take integer values, which is reflected in the lack of fractional charges in the system and corresponds to a generalized Hall response
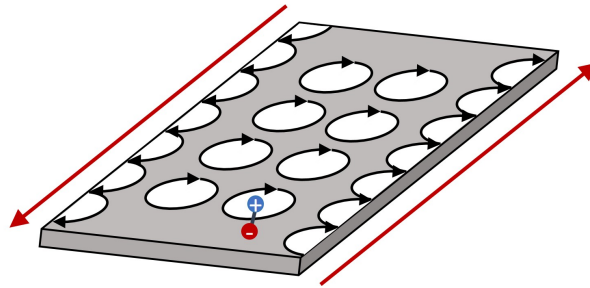
Figure 5.6: Fully mobile dipoles, indicated by the pair of connected spheres, in the presence of an emergent finite background magnetic field perform cyclotron motion. In the presence of a boundary, these skipping orbits result in chiral dipolar edge currents.

which is an integer multiple of a fundamental constant. In analogy with the fractional quantum Hall effect, we can also consider fractional values of the level k, which will lead to deconfined fractons with fractional charges and a fractional generalized Hall response.

In order to study the fractional generalizations of the tensor Chern-Simons theory, we introduce a rank 2 symmetric traceless gauge field a_{ij}. In analogy with the Chern-Simons description of FQH states (see Section 5.5.1), the higher rank Chern-Simons theory of this compact U(1) statistical gauge field will capture the long-distance physics of a fracton phase with fractionalized charges. The effective low-energy theory for an emergent fractional quantum Hall state of dipoles at filling fraction $\nu = k = 1/m$ ($m \in \mathbb{Z}$) is described by

$$\mathcal{S}[\tilde{A}_{ij}, \phi; a_{ij}, \chi] = \mathcal{S}_{gCS}[a_{ij}, \chi] + \mathcal{S}_c[\tilde{A}_{ij}, \phi; a_{ij}, \chi] + \mathcal{S}_{Max}[\tilde{A}_{ij}, \phi]. \tag{5.69}$$

The first term in the action is the generalized Chern-Simons term at level m for the statistical gauge field a_{ij} and a Lagrange multiplier field χ, which enforces a low-energy constraint on the theory, leading to fractionalized excitations with restricted mobility. The last term is the bare Maxwell action of the original tensor gauge field of the emergent fractons.

The middle term

$$\mathcal{S}_c = \frac{1}{2\pi} \int d^3x \, \phi \, \epsilon^{bi} \partial_i \partial_j a_b{}^j + \frac{1}{2\pi} \int d^3x \, \chi \, \epsilon^{bi} \partial_i \partial_j \tilde{A}_b{}^j - \frac{1}{2\pi} \int d^3x \, \epsilon^{bi} \dot{\tilde{A}}_{ij} a_b{}^j, \tag{5.70}$$

describes the coupling between the emergent electro-magnetic field $\tilde{A}_{ij}$ and a_{ij}; this is the analogue of the mixed Chern-Simons term (5.37) in the vector Chern-Simons theory, which couples the statistical gauge field to the physical gauge potential. This coupling term will be our primary focus from hereon. Though the field $\tilde{A}_{ij}$ is technically dynamical, we will now treat it as an effective static background source. This is completely analogous to the normal treatment of quantum Hall states, where the dynamical electromagnetic field is treated as an effective background.

That the action (5.69) is indeed the correct low energy description of an emergent FQH state can be verified directly by integrating the massive gauge field a_{ij} out of the theory—a few lines of algebra will lead to the action (5.58) with coefficient $\theta = -2\pi/m$, where $2\pi m$ flux is attached to each

dipole. Note that while we could have added a generalized Chern-Simons term for $\tilde{A}_{ij}$ to (5.69), this merely shifts the generalized Hall response by an integer. Thus, setting the coefficient of this term to zero corresponds to working in the lowest Landau level.

Alternatively, we could have started from the effective theory for $\tilde{A}_{ij}$ and introduced a finite density of dipoles ρ in addition to a current J_{ij}, by including source terms

$$\mathcal{L}_{\text{source}} = -\phi\rho - \tilde{A}_{ij}J^{ij}, \tag{5.71}$$

to the action (5.58). As discussed in Section 5.2, these satisfy the generalized continuity equation

$$\dot{\rho} + \partial_i\partial_j J^{ij} = 0, \tag{5.72}$$

which is solved by taking

$$\rho = \frac{1}{2\pi}\epsilon^{ib}\partial_i\partial_j a_b{}^j, \quad J^{ij} = \frac{\epsilon^{bi}}{2\pi}\left(\dot{a}_b{}^j + \partial_b\partial^j\chi\right), \tag{5.73}$$

for arbitrary χ. Inserting these into $\mathcal{L}_{\text{source}}$ and adding a generalized Chern-Simons term for the a_{ij}, χ fields leads precisely to the action (5.69) for an emergent FQH fracton phase. Note that similar arguments are used to arrive at a Chern-Simons effective description for conventional FQH states of electrons [147].

The field χ plays the role of a Lagrange multiplier and places a low-energy constraint on the gauge charges of the statistical gauge field a_{ij}. Specifically, these charges are fractons, while their dipolar bound states are one-dimensional, with mobility only in the direction transverse to their dipole moment. We can also explicitly see that the quasi-particle excitations carry fractionalized charge by introducing an excitation that carries gauge charge q under a_{ij}. This is achieved by adding a term

$$\delta\mathcal{L} = q\chi\,\delta(\vec{x} - \vec{x}_0) \tag{5.74}$$

to the action (5.69). Varying the action with respect to χ leads to the equation of motion

$$\rho = \frac{1}{2\pi m}\partial_j B^j + \frac{q}{m}\delta(\vec{x} - \vec{x}_0), \tag{5.75}$$

which explicitly demonstrates that the filling fraction of the underlying dipoles forming the state is $\nu = 1/m$ and that the one-dimensional dipolar excitations carry fractional charge q/m. Following the arguments for electronic FQH states [147], it is now easy to show that the excitations in this theory have fractional statistics [7] . In particular, we can define a "braiding" process along intersecting lines for a q_1 dipole with a q_2 dipole which has dipole moment orthogonal to that of the q_1 dipolar quasi-particle. Such a process will induce a phase

$$\theta_{12} = \frac{2\pi}{m} q_1 q_2. \tag{5.76}$$

Additionally, we can infer from the equation of motion (5.75) that a quasi-particle carrying m units of a_{ij} charge corresponds to a dipole excitation forming the FQH liquid. We can identify the excitations carrying m units of the a charge with the bosonic (fermionic) dipoles forming the underlying FQH state when m is even (odd).

As discussed above, for cases where $k = 1/m$, the excitations exhibit fractionalized charge and statistics, and our experience with FQH states of electrons would lead us expect a constant ground state degeneracy on a torus. There is, however, a crucial difference between electrons and the dipolar bound states—the dipoles have mobility only transverse to their dipole moment. Imagine placing the system on an $R_x \times R_y$ periodic lattice with lattice spacing $a = 1$. Now consider the Wilson-line operator that creates a pair of dipoles at spatial position $(x, y) = (0, 0)$, wraps one of the dipoles along a non-contractible cycle in the y-direction, and annihilates it with its partner to return the system to the vacuum state. If the dipoles were fully mobile, this operator could be locally deformed into one which initially creates the pair at $(x, y) = (1, 0)$. Due to the one-dimensional nature of the dipoles, it appears that these operators may no longer be continuously deformed into one another. While this may lead one to expect a ground state degeneracy which grows exponentially with system size, there in fact exist a sub-extensive number of relations between certain products of the Wilson string operators which reduce the degeneracy to a constant[8] . Indeed,

---

[7] While the dipolar excitations are one-dimensional, there still exists a well-defined notion of statistics for sub-dimensional particles. This is discussed in detail in the context of discrete fracton models [78].

[8] A similar situation arises in discrete fracton models such as the X-Cube model, where certain relations between products of Wilson string operators reduce the ground state degeneracy from $\sim 2^{L^2}$ down to $\sim 2^L$ [273]

a detailed derivation (see Appendix H.2) shows that the ground state degeneracy for the generalized Chern-Simons theory $\mathcal{S}_{gCS}[a_{ij}, \chi]$ for the statistical field a_{ij} at level m (where $k = 1/m$ is the filling fraction) is a constant,

$$\text{GSD} = 2m, \tag{5.77}$$

where the factor of m arises as a consequence of the fractional statistics (the factor of two stems from having two species of dipoles).

Having established this formalism, it is now tempting to generalize this construction to dipolar analogues of hierarchical quantum Hall states, described by a K-matrix and a multiplet of tensor gauge fields a_{ij}^I, or of non-Abelian quantum Hall states, such as the Moore-Read Pfaffian state [31, 286]. While such generalizations appear fairly straightforward to construct, we will leave this for future work and focus instead on the novel boundary theories of these generalized Chern-Simons theories.

5.5.2.4 Chiral Edge Modes

From the semi-classical picture for the emergent quantum Hall state of dipoles, where a finite density of dipoles responds to a finite background magnetic field, we expect that the system will host chiral modes localized at spatial boundaries. This is illustrated schematically in Figure 5.6 for the quantum Hall state of dipoles, described by the higher rank Chern-Simons theory with level $m \in \mathbb{Z}$.

Here, we will show the existence of chiral edge modes explicitly, working with the generalized Chern-Simons theories for dipolar FQH states at filling fraction $1/m$. Indeed, in analogy with vector Chern-Simons theories describing FQH states of electrons, we expect that the chiral higher rank Chern-Simons theories also exhibit a chiral anomaly, a direct manifestation of which are gapless chiral edge modes. Note that the case $m = 1$ describes dipoles in a completely filled lowest Landau level, i.e., an IQH state of dipoles.

Consider the higher rank Chern Simons term describing dipoles at filling fraction $\nu = k =$

$1/m$,

$$S[a_{ij}, \chi] = -\frac{m}{2\pi} \int d^3x \, \chi \epsilon^{bi} \partial_i \partial_j a_b{}^j + \frac{m}{4\pi} \int d^3x \, \epsilon^{bi} \dot{a}_{ij} a_b{}^j, \tag{5.78}$$

where a_{ij} is a compact U(1) symmetric traceless tensor of rank 2. Under a gauge transformation

$$a_{ij} \rightarrow a_{ij} + \left(\partial_i \partial_j - \frac{1}{2} \delta_{ij} \delta^2 \right) \alpha,$$

$$\chi \rightarrow \chi + \dot{\alpha}, \tag{5.79}$$

this action is invariant only up to a boundary term,

$$S[a_{ij}, \chi] \rightarrow S[a_{ij}, \chi] + \frac{m}{4\pi} \int d^3x \, \partial_i \left(\epsilon^{bi} \partial_j \dot{\alpha} \, \partial_b \partial^j \alpha \right). \tag{5.80}$$

To derive the action for the boundary degrees of freedom, we fix the gauge $\chi = 0$ in the bulk such that the constraint imposed by the gauge-fixing condition remains

$$\epsilon^{bi} \partial_i \partial_j a_b{}^j = 0. \tag{5.81}$$

This constraint can be solved in terms of the field φ

$$a_b{}^j = \epsilon^{ij} \partial_i \partial_b \varphi. \tag{5.82}$$

Note that unlike the edge theory of a vector CS theory (see Appendix G.3), which is described in terms of compact scalar field, here φ has dimensions of length ($[\varphi] = L^1$) and it is instead $\partial \varphi$ which is a compact dimensionless field. In addition, since a_{ij} is a symmetric tensor, φ must be a solution of the two-dimensional Laplace equation

$$\partial^2 \varphi = 0. \tag{5.83}$$

Tracelessness of a_{ij} is automatically satisfied by (5.82).

For concreteness, we consider the semi-infinite geometry depicted in Figure 5.7, which has a spatial boundary at $y = 0$ between the dipolar FQH state and vacuum. Inserting the solution (5.82) into the action (5.78), we obtain the edge action

$$S_{gCS} = \frac{m}{4\pi} \int_{y=0} dxdt \, (\partial_t \partial_x \varphi \, \partial_x \partial_x \varphi) + \frac{m}{4\pi} \int_{y=0} dxdt \, (\partial_t \partial_y \varphi \, \partial_x \partial_y \varphi). \tag{5.84}$$

Since φ and $\partial_y\varphi$ can be varied independently on the boundary, we have thus found two modes propagating along the boundary.

Physically, it is natural to expect two distinct boundary modes corresponding to the two linearly independent dipole orientations. This is depicted schematically in Figure 5.7. In particular, this figure illustrates the distinct nature of these two boundary modes. Consider first dipoles with their dipole moment oriented perpendicular to the boundary and propagating transversely to their dipole moment. Labelled by a in Figure 5.7, the motion of these dipoles along the boundary looks identical to that of a usual charged particle. The boundary action for this mode should hence be identical to that of a chiral Luttinger liquid of electrons. Indeed, when re-phrased in terms of a new compact scalar field $\xi \equiv \partial_y\varphi$, the boundary action for ξ becomes

$$\mathcal{S}_{\text{edge}}[\xi] = \frac{m}{4\pi} \int_{y=0} dxdt \, (\partial_t\xi \, \partial_x\xi) , \tag{5.85}$$

which is precisely the chiral CFT describing the boundary of a conventional FQH state (see Section 5.5.1). We can thus introduce a velocity for this field by adding a term $-v\partial_x\xi \, \partial_x\xi$ to the action. Given the extensive literature on edge theories of quantum Hall states (see e.g., [147]), we will not investigate this mode further.

In addition to the conventional mode described by ξ, the boundary of a rank 2 Chern-Simons
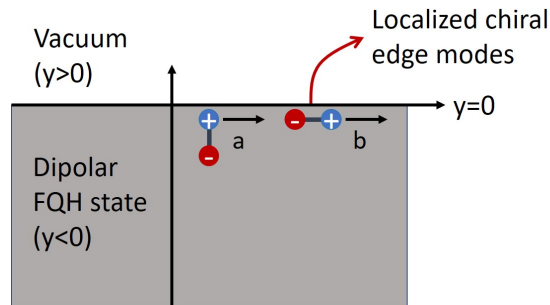
Figure 5.7: Semi-infinite geometry for studying the edge physics of the higher rank Chern-Simons theory. The boundary at $y = 0$ separates the dipolar FQH state from the vacuum. The boundary hosts two independent co-propagating gapless chiral modes, which correspond to the motion of dipolar bound states in two distinct orientations, a and b, along the edge.

theory hosts an additional chiral edge mode, with the low-energy behavior governed by

$$\mathcal{S}_{gET}[\varphi] = \frac{m}{4\pi} \int dx dt \, (\partial_t \partial_x \varphi \, \partial_x \partial_x \varphi) \,, \tag{5.86}$$

where "gET" denotes a "generalized edge theory," and it is implicit that this theory lives on the boundary $y = 0$. As depicted in Figure 5.7, this mode (b) corresponds to the motion of dipoles with their dipole moment oriented parallel to the boundary, with longitudinal motion along the boundary. Since dipole moment is conserved, these excitations are constrained to move in dipolar bound pairs even along the boundary. As a consequence of this, we expect the low energy theory describing these edge modes to obey an additional constraint besides charge conservation. We will now explicitly demonstrate this by working directly with the action (5.86).

As noted earlier, the field φ has dimensions of length and so under scale transformations of the coordinates

$$\sigma^a \to \lambda \sigma^a \tag{5.87}$$

transforms as

$$\varphi(\sigma) \to \varphi(\lambda^{-1}\sigma), \tag{5.88}$$

leaving the action (5.86) invariant under scale transformations. Indeed, due to the unconventional scaling of the field φ, the action (5.86) is a conformally invariant field theory despite initial appearances.

In addition to the term (5.86), we can also add non-universal energetic terms to the action. Following standard procedure, we identify $\partial_x \partial_x \partial_x \varphi$ as the field canonically conjugate to φ, from which we can derive the commutation relations

$$[\partial_x \varphi(x), \partial_x \varphi(x')] = -\frac{i\pi}{m}\text{sgn}(x - x'), \tag{5.89}$$

establishing both φ and $\partial_x \varphi$ as non-local fields. Thus, adding the lowest order spatial derivative term, consistent with locality, we find the low-energy theory for the field φ

$$\mathcal{S}_{gET}[\varphi] = \frac{m}{4\pi} \int dx dt \, (\partial_t \partial_x \varphi \, \partial_x \partial_x \varphi - v \partial_x \partial_x \varphi \, \partial_x \partial_x \varphi) \,, \tag{5.90}$$

which describes a chiral gapless mode with dispersion $\omega = vk$, where v is some non-universal velocity determined by the microscopic details of the edge. Note that the velocity of this mode will generically be distinct from that of the ξ edge mode, although the two modes will co-propagate, resulting in a thermal Hall coefficient which is twice that of conventional FQH states.

Given the novelty of the generalized edge theory, we leave a thorough discussion of its properties to future work. Instead, we focus on a remarkable new property of this theory, absent in boundary theories of vector Chern-Simons theories. Specifically, we observe that the density of dipoles at the boundary is defined by

$$\rho = \frac{1}{2\pi}\partial_x\partial_x\varphi, \tag{5.91}$$

as evinced by the commutation relations

$$[\rho(x), \partial_x\varphi(x')] = -\frac{i}{m}\delta(x - x'),$$
$$[\rho(x), \rho(x')] = \frac{i}{2\pi m}\partial_x\delta(x - x'). \tag{5.92}$$

Due to the additional spatial derivative present in ρ, the dipolar density at the boundary satisfies the constraints

$$\int \rho = \text{const.}, \quad \int x\rho = \text{const.}, \tag{5.93}$$

corresponding to conservation of charge and of centre of mass, the latter of which we anticipated in our earlier discussion. We have thus found that the boundary theory of the generalized Chern-Simons theory hosts gapless excitations with centre of mass conservation i.e., there exist gapless fracton excitations at the edge of a higher rank Chern Simons theory in addition to fully mobile one-dimensional dipolar bound states. Since chirality guarantees the absence of back-scattering terms, regardless of the interactions present at the boundary, we expect that both of these edge modes will be robust against arbitrary weak perturbations. However, given the unusual nature of the generalized edge theory, we leave a careful analysis of stability to future work.

Although we have focused on a semi-infinite planar geometry here, in principle we could consider other finite samples as well. Interestingly, we expect that on a square geometry (or any

sample with sharp corners) there will exist finite-energy localized modes at the corners, owing to the one-dimensional nature of the dipolar excitations. While this behavior is distinct from the zero-energy protected corner modes recently discovered in higher-order topological insulators [288–294], the existence of such corner-localized modes opens up the possibility of finding protected zero-energy corner modes or hinge states in fracton models. We leave a detailed study of the generalized edge theory and its localized modes on general finite samples for the future.

As a final remark, we note that the generalized edge theory (5.86) provides us with another window into the emergent FQH state present in the bulk. Specifically, since the edge theory is Gaussian, the correlation function for the $\partial_x \varphi$ fields can be calculated exactly and takes the suggestive form

$$\langle \partial_x \varphi(x) \partial_x \varphi(0) \rangle = -\frac{1}{m} \log(x - vt), \tag{5.94}$$

where m is the inverse filling fraction ν of the dipolar bound states. Since the boundary theory is conformal, we conjecture that the bulk-boundary correspondence for vector Chern-Simons theories holds also for the higher rank chiral theory studied here. Hence, from the correlator of the vertex operators $e^{im\partial_x \varphi}$ (which correspond to creation operators of elementary dipoles at the boundary),

$$\langle : e^{im\partial_x \varphi(x)} :: e^{im\partial_x \varphi(0)} : \rangle \sim \frac{1}{(x - vt)^m}, \tag{5.95}$$

we should be able to construct the bulk wave-function for the emergent dipolar degrees of freedom, which in this case will take the form of a Laughlin state at filling fraction $\nu = 1/m$. We stress that while this is consistent with the picture developed here, the real object of interest would be the wave-function of the underlying degrees freedom from which the higher rank tensor gauge field emerges.

Nonetheless, we have discovered an intriguing connection between "fracton" phases and quantum Hall physics, in that chiral higher rank tensor gauge fields with a finite density of mobile dipoles form an emergent fractional quantum Hall phase, albeit with novel ground state degeneracies and edge physics. We have identified chiral gapless edge theories which transport dipoles along the edge of the system. As emphasized throughout, these dipoles do not carry physical electric charge,

so there is no Hall response of the electric current. Nevertheless, the dipoles carry energy, and in the spin liquid context, will carry spin. A spin liquid supporting a dipolar quantum Hall phase will therefore be characterized by robust thermal and spin Hall responses, which will be useful for identifying these phases experimentally.

While we have focused only on a specific higher rank tensor gauge theory (the "scalar charge" theory) in this work, a larger class of chiral two-dimensional phases hosting subdimensional fractons has been recently uncovered [272]. It would certainly be of interest to generalize our analysis here to these other cases, with the aim of developing a more general framework for understanding these higher rank chiral phases. For instances, in the "traceless scalar charge" theory [81], flux is attached directly to the fractons and not their dipolar bound states, which are mobile only in the direction transverse to their dipole moment even prior to flux attachment. The physics of a finite density of fractons in a background emergent magnetic field remains to be understood, with simple analogies to quantum Hall states ruled out due to immobility of fractons. We leave such questions to future work.

5.6   Conclusion

In this chapter, we have studied systems with a finite density of fractons or their dipolar bound states, mapping out some of the interesting phases in which this emergent fractonic matter can exist. In so doing, we have initiated the study of "condensed matter" of fractons. We have uncovered a cornucopia of new phases including 'fractonic' microemulsions, Fermi liquids, and quantum Hall states, as well as new finite temperature phase transitions. Of course, there remain numerous open directions. In principle, the mobile dipoles can be placed into any phase of matter accessible to conventional bosons or fermions, and we have only studied a small sampling of possible phases. As an example, it would be interesting to investigate topologically ordered states of dipoles. There are also still many generalizations to explore within the dipolar Fermi liquid and quantum Hall frameworks, as we have discussed in the main text. Furthermore, it is far from obvious that such analogues of conventional phases provide an exhaustive account of dipolar phases of matter.

There may be intrinsically new fractonic phases of matter with no natural analogue in conventional condensed matter, which is an intriguing possibility. We leave further investigation of the condensed matter physics of fractonic matter to future work.

Chapter 6

Conclusions and Outlook

In which Benny must go on,

but can't go on,

yet will go on.

In the preceding chapters, we have discussed various emergent phenomena which may arise in many-body quantum systems with strongly correlated degrees of freedom. We saw how the presence of topological defects in fermionic superfluids unexpectedly gives rise to novel pairing mechanisms with experimentally observable consequences; how the interplay of symmetry and topology in superconductors naturally leads to a low-energy topological quantum field theory description; and finally, how finite densities of topological excitations with restricted mobilities lead to striking behaviour both in and out of equilibrium. The underlying theme unifying these seemingly disparate strands in the landscape of quantum phases of matter is that of the topology of their underlying ground states.

The phenomena encountered in this thesis clearly, however, comprise a small fraction of the cornucopia of effects associated with topological quantum phases of matter. Even amongst the topics discussed in this dissertation, there are several aspects which scream for further investigation: for instance, since the superconductors considered in § 3 were spatially confined to live in two dimensions, in order for this work to have significance outside the theoretical realm it is of interest to devise a physical situation where such flatland electromagnetism may arise. Alternatively, one should study the interplay between topological order and symmetry in a three-dimensional system

with dynamically fluctuating electromagnetism. While this generalisation appears straightforward in the s-wave case, chiral superconductors in $d = 3$ generically possess nodal points or lines and hence require more care. It might be of interest to study cases with nodal lines, since they harbour the possibility of topological phenomena not possible in $d = 2$. It is also not obvious that the procedure for gapping out nodal line follows that for gapping out the nodal Dirac points devised in § 3 and will likely require further analysis.

Beyond these specific possibilities concerning the study of topologically ordered superconductors, this work opens up several avenues for further explorations of the fractonic frontier. Given the paucity of exactly solvable gapped fracton models at our disposal, an obvious direction is the theoretical design and investigation of new models displaying excitations with restricted mobility. An intriguing possibility is opened up by the layer construction of the X-Cube model presented in [78, 79]: instead of coupling together layers of $\mathbb{Z}_2$ topological order, we can now imagine that appropriately coupling together layers of inter-penetrating non-Abelian topological orders will lead to novel fracton phases with non-Abelian excitations. Such an approach also provides an indirect route towards establishing a coherent mathematical framework for describing fracton phases which, despite sharing many features with conventional topological order, are distinctly *not* topological in the usual sense and, as such, exist beyond current categoric descriptions of gapped topologically ordered systems. With the discussion contained in § 4 in mind, it would also be worth investigating the potential applications of non-Abelian excitations with restricted mobility to topological quantum computation and quantum information storage.

So much for exactly solvable lattice models for gapped fracton phases. The language of higher-rank symmetric tensor gauge theory offers a complementary route for approaching systems with sub-dimensional excitations, with the benefit of having much in common with the usual vector gauge theories used to describe long-range entangled systems. Future studies of tensor gauge theories will certainly uncover novel new phenomena, with straightforward extensions of existing work being the study of tensor gauge theories on spatially curved manifolds and investigations of non-Abelian tensor gauge theories. The discovery of a duality between certain tensor gauge theories

and elasticity theory [83, 84] further opens the door for studying fracton physics in experimentally feasible settings, with the fracton theory naturally interpreted as a gauge theory of translations and rotations in this context. Perhaps of most immediate interest is the search for material candidates where the tensor gauge structure emerges at low-energies. A first step in this direction would be characterising the experimental signatures expected to appear in such "higher-rank spin liquids," such as their heat-capacities or pinch-point singularities.

Of course, the question of how best to demystify Haah's code casts a large yet inexorable shadow over the (currently) small but vibrant community of researchers investigating fracton order. While certain aspects, such as the closed quantum dynamics and entanglement structure, of Haah's code have been amenable to analytic study, there does not exist any description of this phase in terms of tensor gauge theory or layers of coupled topological orders. While the existence of such descriptions is not *a priori* precluded, at this juncture it does appear to be the case that Haah's code occupies its own, largely empty, page in the bestiary of ineffably strange and beautiful quantum phases of matter.

Epilogue

In which Benny attempts to tame the Jabberwock,

ETC.

T. S. Eliot, *Little Gidding*:

"We shall not cease from exploration

And the end of all our exploring

Will be to arrive where we started

And

Bibliography

[1] E. Abbott. Flatland: A Romance of Many Dimensions. Penguin Classics, New York, USA, 1998.

[2] N. P. Landsman. Spontaneous symmetry breaking in quantum systems: Emergence or reduction? Studies in History and Philosophy of Science Part B: Studies in History and Philosophy of Modern Physics, 44(4):379–394, 2013.

[3] R. B. Laughlin. A Different Universe: Reinventing Physics From the Bottom Down. Basic Books, 2008.

[4] P. W. Anderson. More is different. Science, 177(4047):393–396, 1972.

[5] K. G. Wilson. The renormalization group: Critical phenomena and the kondo problem. Rev. Mod. Phys., 47:773–840, Oct 1975.

[6] R. Shankar. Renormalization-group approach to interacting fermions. Rev. Mod. Phys., 66:129–192, Jan 1994.

[7] L. D. Landau. The theory of a fermi liquid. JETP, 3:920, 1957.

[8] V. L. Berezinskii. Destruction of long-range order in one-dimensional and two-dimensional systems having a continuous symmetry group I. Classical systems. Zh. Eksp. Teor. Fiz, 59:907, 1970. [Sov. Phys. JETP. **32**, 493 (1971)].

[9] J. M. Kosterlitz and D. J. Thouless. Ordering, metastability and phase transitions in two-dimensional systems. J. Phys. C: Solid St. Phys., 6(7):1181, 1973.

[10] N. D. Mermin and H. Wagner. Absence of ferromagnetism or antiferromagnetism in one- or two-dimensional isotropic heisenberg models. Phys. Rev. Lett., 17:1133–1136, Nov 1966.

[11] P. C. Hohenberg. Existence of long-range order in one and two dimensions. Phys. Rev., 158:383–386, Jun 1967.

[12] K. v. Klitzing, G. Dorda, and M. Pepper. New Method for High-Accuracy Determination of the Fine-Structure Constant Based on Quantized Hall Resistance. Phys. Rev. Lett., 45:494–497, Aug 1980.

[13] D. C. Tsui, H. L. Stormer, and A. C. Gossard. Two-dimensional magnetotransport in the extreme quantum limit. Phys. Rev. Lett., 48:1559–1562, May 1982.

[14] D. J. Thouless. Quantization of particle transport. Phys. Rev. B, 27:6083–6087, May 1983.

[15] R. B. Laughlin. Quantized hall conductivity in two dimensions. Phys. Rev. B, 23:5632–5633, May 1981.

[16] D. J. Thouless, M. Kohmoto, M. P. Nightingale, and M. den Nijs. Quantized hall conductance in a two-dimensional periodic potential. Phys. Rev. Lett., 49:405–408, Aug 1982.

[17] R. De-Picciotto, M. Reznikov, M. Heiblum, V. Umansky, G. Bunin, and D. Mahalu. Direct observation of a fractional charge. Nature, 389(6647):162, 1997.

[18] L. Saminadayar, D. C. Glattli, Y. Jin, and B. Etienne. Observation of the $e/3$ fractionally charged laughlin quasiparticle. Phys. Rev. Lett., 79:2526–2529, Sep 1997.

[19] V. Kalmeyer and R. B. Laughlin. Equivalence of the resonating-valence-bond and fractional quantum hall states. Phys. Rev. Lett., 59:2095–2098, Nov 1987.

[20] X.-G. Wen, Frank Wilczek, and A. Zee. Chiral spin states and superconductivity. Phys. Rev. B, 39:11413–11423, Jun 1989.

[21] L. Savary and L. Balents. Quantum spin liquids: a review. Reports on Progress in Physics, 80(1):016502, 2017.

[22] X.-G. Wen. Colloquium: Zoo of quantum-topological phases of matter. Rev. Mod. Phys., 89:041004, Dec 2017.

[23] D. Tong. Lectures on the Quantum Hall Effect. arXiv:1606.06687, June 2016.

[24] R. B. Laughlin. Anomalous quantum hall effect: An incompressible quantum fluid with fractionally charged excitations. Phys. Rev. Lett., 50:1395–1398, May 1983.

[25] F. J. Wegner. Duality in generalized ising models and phase transitions without local order parameters. Journal of Mathematical Physics, 12(10):2259–2272, 1971.

[26] F. D. M. Haldane. Model for a quantum hall effect without landau levels: Condensed-matter realization of the "parity anomaly". Phys. Rev. Lett., 61:2015–2018, Oct 1988.

[27] N. Read. Excitation structure of the hierarchy scheme in the fractional quantum hall effect. Phys. Rev. Lett., 65:1502–1505, Sep 1990.

[28] X.-G. Wen and A. Zee. Classification of abelian quantum hall states and matrix formulation of topological fluids. Phys. Rev. B, 46:2290–2301, Jul 1992.

[29] J. Fröhlich and A. Zee. Large scale physics of the quantum hall fluid. Nuclear Physics B, 364(3):517 – 540, 1991.

[30] E. Witten. Quantum field theory and the jones polynomial. Comm. Math. Phys., 121(3):351–399, 1989.

[31] G. Moore and N. Read. Nonabelions in the fractional quantum hall effect. Nuclear Physics B, 360(2):362 – 396, 1991.

[32] A. Y. Kitaev. Fault-tolerant quantum computation by anyons. Annals of Physics, 303(1):2 – 30, 2003.

[33] C. Nayak, S. H. Simon, A. Stern, M. Freedman, and S. D. Sarma. Non-abelian anyons and topological quantum computation. Rev. Mod. Phys., 80:1083–1159, Sep 2008.

[34] C. L. Kane and E. J. Mele. Z_2 topological order and the quantum spin hall effect. Phys. Rev. Lett., 95:146802, Sep 2005.

[35] B. A. Bernevig, T. L. Hughes, and S.-C. Zhang. Quantum spin hall effect and topological phase transition in hgte quantum wells. Science, 314(5806):1757–1761, 2006.

[36] L. Fu, C. L. Kane, and E. J. Mele. Topological insulators in three dimensions. Phys. Rev. Lett., 98:106803, Mar 2007.

[37] R. Roy. Topological phases and the quantum spin hall effect in three dimensions. Phys. Rev. B, 79:195322, May 2009.

[38] J. E. Moore and L. Balents. Topological invariants of time-reversal-invariant band structures. Phys. Rev. B, 75:121306, Mar 2007.

[39] M. Levin and X.-G. Wen. Detecting topological order in a ground state wave function. Phys. Rev. Lett., 96:110405, Mar 2006.

[40] A. Y. Kitaev and J. Preskill. Topological entanglement entropy. Phys. Rev. Lett., 96:110404, Mar 2006.

[41] X. Chen, Z.-C. Gu, and X.-G. Wen. Local unitary transformation, long-range quantum entanglement, wave function renormalization, and topological order. Phys. Rev. B, 82:155138, Oct 2010.

[42] X. G. Wen and Q. Niu. Ground-state degeneracy of the fractional quantum hall states in the presence of a random potential and on high-genus riemann surfaces. Phys. Rev. B, 41:9377–9396, May 1990.

[43] X.-G. Wen. Quantum orders and symmetric spin liquids. Phys. Rev. B, 65:165113, Apr 2002.

[44] R. Moessner, S. L. Sondhi, and E. Fradkin. Short-ranged resonating valence bond physics, quantum dimer models, and ising gauge theories. Phys. Rev. B, 65:024504, Dec 2001.

[45] L. Balents, M. P. A. Fisher, and S. M. Girvin. Fractionalization in an easy-axis kagome antiferromagnet. Phys. Rev. B, 65:224412, May 2002.

[46] T. H. Hansson, V. Oganesyan, and S. L. Sondhi. Superconductors are topologically ordered. Annals of Physics, 313(2):497 – 538, 2004.

[47] S. Moroz, A. Prem, V. Gurarie, and L. Radzihovsky. Topological order, symmetry, and hall response of two-dimensional spin-singlet superconductors. Phys. Rev. B, 95:014508, Jan 2017.

[48] F. A. Bais, B. J. Schroers, and J. K. Slingerland. Broken quantum symmetry and confinement phases in planar physics. Phys. Rev. Lett., 89:181601, Oct 2002.

[49] E. Rowell, Richard Stong, and Zhenghan Wang. On classification of modular tensor categories. Communications in Mathematical Physics, 292(2):343–389, Dec 2009.

[50] A. Kitaev. Anyons in an exactly solved model and beyond. Ann. Phys. (N. Y)., 321:2–111, 2006.

[51] M.A. Levin and X.-G. Wen. String-net condensation: A physical mechanism for topological phases. Phys. Rev. B, 71:045110, Jan 2005.

[52] A. Hamma, P. Zanardi, and X.-G. Wen. String and membrane condensation on three-dimensional lattices. Phys. Rev. B, 72:035307, Jul 2005.

[53] H. Bombin and M. A. Martin-Delgado. Exact topological quantum order in $d = 3$ and beyond: Branyons and brane-net condensates. Phys. Rev. B, 75:075103, Feb 2007.

[54] F. Pollmann, E. Berg, A. M. Turner, and M. Oshikawa. Symmetry protection of topological phases in one-dimensional quantum spin systems. Phys. Rev. B, 85:075125, Feb 2012.

[55] Z.-C. Gu and X.-G. Wen. Tensor-entanglement-filtering renormalization approach and symmetry-protected topological order. Phys. Rev. B, 80:155131, Oct 2009.

[56] X. Chen, Z. C. Gu, Z. X. Liu, and X.-G. Wen. Symmetry protected topological orders and the group cohomology of their symmetry group. Phys. Rev. B, 87(15):1–48, 2013.

[57] F. D. M. Haldane. Continuum dynamics of the 1-d heisenberg antiferromagnet: Identification with the o(3) nonlinear sigma model. Physics Letters A, 93(9):464 – 468, 1983.

[58] I. Affleck, T. Kennedy, E. H. Lieb, and H. Tasaki. Valence bond ground states in isotropic quantum antiferromagnets. Comm. Math. Phys., 115(3):477–528, 1988.

[59] F. Verstraete, M. A. Martín-Delgado, and J. I. Cirac. Diverging entanglement length in gapped quantum spin systems. Phys. Rev. Lett., 92:087201, Feb 2004.

[60] T. Senthil. Symmetry-protected topological phases of quantum matter. Annu. Rev. Condens. Matter Phys., 6(1):299–324, 2015.

[61] Y. Ando and L. Fu. Topological crystalline insulators and topological superconductors: From concepts to materials. Annu. Rev. Condens. Matter Phys., 6(1):361–381, 2015.

[62] Z.-C. Gu and X.-G. Wen. Symmetry-protected topological orders for interacting fermions: Fermionic topological nonlinear σ models and a special group supercohomology theory. Phys. Rev. B, 90:115141, Sep 2014.

[63] L.-Y. Hung and Y. Wan. String-net models with Z_N fusion algebra. Phys. Rev. B, 86:235132, Dec 2012.

[64] M. Levin and Z.-C. Gu. Braiding statistics approach to symmetry-protected topological phases. Phys. Rev. B, 86:115109, Sep 2012.

[65] A. C. Potter, I. Kimchi, and A. Vishwanath. Quantum oscillations from surface fermi arcs in weyl and dirac semimetals. Nat. Comm., 5:5161, 2014.

[66] N. P. Armitage, E. J. Mele, and A. Vishwanath. Weyl and dirac semimetals in three-dimensional solids. Rev. Mod. Phys., 90:015001, Jan 2018.

[67] T. Scaffidi, D. E. Parker, and R. Vasseur. Gapless symmetry-protected topological order. Phys. Rev. X, 7:041048, Nov 2017.

[68] T. Senthil, A. Vishwanath, L. Balents, S. Sachdev, and M. P. A. Fisher. Deconfined quantum critical points. Science, 303(5663):1490–1494, 2004.

[69] R. Nandkishore and D. A. Huse. Many-body localization and thermalization in quantum statistical mechanics. Annu. Rev. Condens. Matter Phys., 6(0):15 – 38, 2015.

[70] P. Richerme. How to create a time crystal. Physics, 10:5, 2017.

[71] A. Eckardt. Colloquium: Atomic quantum gases in periodically driven optical lattices. Rev. Mod. Phys., 89:011004, Mar 2017.

[72] B. Swingle and N. Y Yao. Seeing scrambled spins. Physics, 10:82, 2017.

[73] C. Chamon. Quantum glassiness in strongly correlated clean systems: An example of topological overprotection. Phys. Rev. Lett., 94:040402, Jan 2005.

[74] S. Vijay, J. Haah, and L. Fu. A new kind of topological quantum order: A dimensional hierarchy of quasiparticles built from stationary excitations. Phys. Rev. B, 92:235136, Dec 2015.

[75] J. Haah. Local stabilizer codes in three dimensions without string logical operators. Phys. Rev. A, 83:042330, Apr 2011.

[76] S. Vijay, J. Haah, and L. Fu. Fracton topological order, generalized lattice gauge theory, and duality. Phys. Rev. B, 94:235157, Dec 2016.

[77] B. Yoshida. Exotic topological order in fractal spin liquids. Phys. Rev. B, 88:125122, Sep 2013.

[78] H. Ma, E. Lake, X. Chen, and M. Hermele. Fracton topological order via coupled layers. Phys. Rev. B, 95:245126, Jun 2017.

[79] S. Vijay. Isotropic Layer Construction and Phase Diagram for Fracton Topological Phases. arXiv:1701.00762, January 2017.

[80] M. Pretko. Subdimensional particle structure of higher rank U(1) spin liquids. Phys. Rev. B, 95:115139, Mar 2017.

[81] M. Pretko. Generalized electromagnetism of subdimensional particles: A spin liquid story. Phys. Rev. B, 96:035119, Jul 2017.

[82] M. Pretko. Emergent gravity of fractons: Mach's principle revisited. Phys. Rev. D, 96:024051, Jul 2017.

[83] A. Gromov. Fractional Topological Elasticity and Fracton Order. arXiv:1712.06600, December 2017.

[84] M. Pretko and L. Radzihovsky. Fracton-Elasticity Duality. arXiv:1711.11044, November 2017.

[85] A. Prem, M. Pretko, and R. M. Nandkishore. Emergent phases of fractonic matter. Phys. Rev. B, 97:085116, Feb 2018.

[86] R. M. Nandkishore and M. Hermele. Fractons. arXiv:1803.11196, March 2018.

[87] A. Prem, S. Moroz, V. Gurarie, and L. Radzihovsky. Multiply quantized vortices in fermionic superfluids: Angular momentum, unpaired fermions, and spectral asymmetry. Phys. Rev. Lett., 119:067003, Aug 2017.

[88] A. Prem, J. Haah, and R. Nandkishore. Glassy quantum dynamics in translation invariant fracton models. Phys. Rev. B, 95:155133, Apr 2017.

[89] N. Read and D. Green. Paired states of fermions in two dimensions with breaking of parity and time-reversal symmetries and the fractional quantum Hall effect. Phys. Rev. B, 61(15):10267–10297, April 2000.

[90] Y. Tada, W. Nie, and M. Oshikawa. Orbital angular momentum and spectral flow in two-dimensional chiral superfluids. Phys. Rev. Lett., 114:195301, May 2015.

[91] M. P. A. Fisher. Quantum phase transitions in disordered two-dimensional superconductors. Phys. Rev. Lett., 65:923–926, Aug 1990.

[92] M. E. Peskin. Mandelstam- 't hooft duality in abelian lattice models. Ann. Phys., 113(1):122 – 152, 1978.

[93] C. Dasgupta and B. I. Halperin. Phase transition in a lattice model of superconductivity. Phys. Rev. Lett., 47:1556–1560, Nov 1981.

[94] R.P. Feynman. Application of quantum mechanics to liquid helium. In Progress in Low Temperature Physics, volume 1, pages 17 – 53. Elsevier, New York, 1955.

[95] P. W. Anderson. Considerations on the flow of superfluid helium. Rev. Mod. Phys., 38:298–310, Apr 1966.

[96] J. Bardeen and M. J. Stephen. Theory of the motion of vortices in superconductors. Phys. Rev., 140:A1197–A1207, Nov 1965.

[97] E. P. Gross. Structure of a quantized vortex in boson systems. Il Nuovo Cimento (1955-1965), 20(3):454–477, 1961.

[98] L. P. Pitaevskii. Vortex lines in an imperfect bose gas. Sov. Phys. JETP., 13:451, 1961.

[99] N. Nygaard, G. M. Bruun, C. W. Clark, and D. L. Feder. Microscopic structure of a vortex line in a dilute superfluid fermi gas. Phys. Rev. Lett., 90:210402, May 2003.

[100] R. Sensarma, M. Randeria, and T.-L. Ho. Vortices in Superfluid Fermi Gases through the BEC to BCS Crossover. Phys. Rev. Lett., 96:090403, Mar 2006.

[101] C. Caroli, P. G. De Gennes, and J. Matricon. Bound Fermion states on a vortex line in a type II superconductor. Phys. Lett., 9(May):307–309, 1964.

[102] C. J. Pethick and H. Smith. Bose Einstein Condensation in Dilute Gases:. Cambridge University Press, Cambridge, 2 edition, 003 2008.

[103] V. A. Schweigert, F. M. Peeters, and P. S. Deo. Vortex phase diagram for mesoscopic superconducting disks. Phys. Rev. Lett., 81:2783–2786, Sep 1998.

[104] A. K. Geim, S. V. Dubonos, J. J. Palacios, I. V. Grigorieva, M. Henini, and J. J. Schermer. Fine structure in magnetization of individual fluxoid states. Phys. Rev. Lett., 85:1528–1531, Aug 2000.

[105] A. Kanda, B. J. Baelus, F. M. Peeters, K. Kadowaki, and Y. Ootuka. Experimental evidence for giant vortex states in a mesoscopic superconducting disk. Phys. Rev. Lett., 93:257002, Dec 2004.

[106] I. V. Grigorieva, W. Escoffier, V. R. Misko, B. J. Baelus, F. M. Peeters, L. Y. Vinnikov, and S. V. Dubonos. Pinning-induced formation of vortex clusters and giant vortices in mesoscopic superconducting disks. Phys. Rev. Lett., 99:147003, Oct 2007.

[107] T. Cren, L. Serrier-Garcia, F. Debontridder, and D. Roditchev. Vortex fusion and giant vortex states in confined superconducting condensates. Phys. Rev. Lett., 107:097202, Aug 2011.

[108] V. H. Dao, L. F. Chibotaru, T. Nishio, and V. V. Moshchalkov. Giant vortices, rings of vortices, and reentrant behavior in type-1.5 superconductors. Phys. Rev. B, 83:020503, Jan 2011.

[109] E. Babaev, J. Carlström, M. Silaev, and J.M. Speight. Type-1.5 superconductivity in multicomponent systems. Physica (Amsterdam), 533C:20 – 35, 2017.

[110] J. Garaud and E. Babaev. Properties of skyrmions and multi-quanta vortices in chiral p-wave superconductors. Sci. Rep., 5:17540, Dec 2015.

[111] J. A. Sauls and M. Eschrig. Vortices in chiral, spin-triplet superconductors and superfluids. New J. Phys., 11:075008, 2009.

[112] G. E. Volovik and N. B. Kopnin. Rotating ^{3}He-A. Pis'ma Zh. Eksp. Teor. Fiz., 25:26, 1977. [JETP Lett. **25**, 22 (1977)].

[113] R. Blaauwgeers, V. B. Eltsov, M. Krusius, J. J. Ruohio, R. Schanen, and G. E. Volovik. Double-quantum vortex in superfluid ^{3}He-A. Nature, 404:471–473, 2000.

[114] E. Lundh. Construction of a giant vortex state in a trapped Fermi system. New J. Phys., 8(12):304–304, 2006.

[115] E. Lundh and A. Cetoli. Hydrodynamic theory of giant vortices in trapped unitary fermi gases. Phys. Rev. A, 80:023610, Aug 2009.

[116] K. Howe, A. R. P. Lima, and A. Pelster. Rotating Fermi gases in an anharmonic trap. Eur. Phys. Journal. D, 54(3):667–682, 2009.

[117] P. Engels, I. Coddington, P. C. Haljan, V. Schweikhard, and E. A. Cornell. Observation of Long-Lived Vortex Aggregates in Rapidly Rotating Bose-Einstein Condensates. Phys. Rev. Lett., 90(17):170405, May 2003.

[118] V. Bretin, S. Stock, Y. Seurin, and J. Dalibard. Fast rotation of a Bose-Einstein condensate. Physical review letters, 92(5):050403, 2004.

[119] A. E. Leanhardt, A. Görlitz, A. P. Chikkatur, D. Kielpinski, Y. Shin, D. E. Pritchard, and W. Ketterle. Imprinting vortices in a bose-einstein condensate using topological phases. Phys. Rev. Lett., 89:190403, Oct 2002.

[120] M. F. Andersen, C. Ryu, P. Cladé, V. Natarajan, A. Vaziri, K. Helmerson, and W. D. Phillips. Quantized rotation of atoms from photons with orbital angular momentum. Phys. Rev. Lett., 97:170406, Oct 2006.

[121] M. M. Salomaa and G. E. Volovik. Quantized vortices in superfluid ^{3}He. Rev. Mod. Phys., 59(3):533–613, 1987.

[122] G. E. Volovik. Orbital angular momentum of vortices and textures due to spectral flow through the gap nodes: example of the ^{3}He-A continuous vortex. Pis'ma Zh. Eksp. Teor. Fiz., 61:935, 1995. [JETP Lett. **61**, 958 (1995)].

[123] T. Ojanen. Ground-state angular momentum, spectral asymmetry, and topology in chiral superfluids and superconductors. Phys. Rev. B, 93:174505, May 2016.

[124] G. E. Volovik. Orbital momentum of chiral superfluids and the spectral asymmetry of edge states. JETP Letters, 100(11):742–745, 2015.

[125] G. Labonté. On the nature of "strong" bogoliubov transformations for fermions. Comm. Math. Phys., 36(1):59–72, 1974.

[126] P. Ring and P. Schuck. The Nuclear Many-Body Problem. Springer-Verlag, Berlin New York, 1980.

[127] D. E. Sheehy and L. Radzihovsky. BEC–BCS crossover, phase transitions and phase separation in polarized resonantly-paired superfluids. Ann. Phys., 322(8):1790 – 1924, 2007.

[128] W. Huang, E. Taylor, and C. Kallin. Vanishing edge currents in non-p-wave topological chiral superconductors. Phys. Rev. B, 90:224519, Dec 2014.

[129] W. Huang, S. Lederer, E. Taylor, and C. Kallin. Nontopological nature of the edge current in a chiral p-wave superconductor. Phys. Rev. B, 91:094507, Mar 2015.

[130] M. Stone and R. Roy. Edge modes, edge currents, and gauge invariance in $p_x + ip_y$ superfluids and superconductors. Phys. Rev. B, 69:184511, May 2004.

[131] M. Stone and I. Anduaga. Mass flows and angular momentum density for $p_x + ip_y$ paired fermions in a harmonic trap. Ann. Phys., 323(1):2–16, 2008.

[132] J. Bardeen, R. Kümmel, A. E. Jacobs, and L. Tewordt. Structure of vortex lines in pure superconductors. Phys. Rev., 187:556–569, Nov 1969.

[133] C. Berthod. Vorticity and vortex-core states in type-II superconductors. Phys. Rev. B, 71:134513, Apr 2005.

[134] G. E. Volovik. Vortex motion in Fermi superfluids and the Callan-Harvey effect. Pis'ma Zh. Eksp. Teor. Fiz., 57(4):233, 1993. [JETP Lett., **57**, 244 (1993)].

[135] A. S. Mel'nikov and M. A. Silaev. Intervortex quasiparticle tunneling and the electronic structure of multivortex configurations in type-II superconductors. JETP Letters, 83(12):578–583, 2006.

[136] A. S. Mel'nikov, D. A. Ryzhov, and M. A. Silaev. Electronic structure and heat transport of multivortex configurations in mesoscopic superconductors. Phys. Rev. B, 78:064513, Aug 2008.

[137] Y. Tanaka, A. Hasegawa, and H. Takayanagi. Energy spectrum of the quasiparticle in a quantum dot formed by a superconducting pair potential under a magnetic field. Solid State Commun., 85(4):321 – 326, 1993.

[138] K. Tanaka, I. Robel, and B. Jankó. Electronic structure of multiquantum giant vortex states in mesoscopic superconducting disks. PNAS, 99(8):5233–5236, 2002.

[139] D. Rainer, J. A. Sauls, and D. Waxman. Current carried by bound states of a superconducting vortex. Phys. Rev. B, 54:10094–10106, Oct 1996.

[140] S. M. M. Virtanen and M. M. Salomaa. Multiquantum vortices in superconductors: Electronic and scanning tunneling microscopy spectra. Phys. Rev. B, 60:14581–14584, Dec 1999.

[141] G. Möller, N. R. Cooper, and V. Gurarie. Structure and consequences of vortex-core states in p-wave superfluids. Phys. Rev. B, 83:014513, Jan 2011.

[142] Y. Tada. Equilibrium surface current and role of U(1) symmetry: Sum rule and surface perturbations. Phys. Rev. B, 92:104502, Sep 2015.

[143] F. Chevy, K. W. Madison, and J. Dalibard. Measurement of the angular momentum of a rotating bose-einstein condensate. Phys. Rev. Lett., 85:2223–2227, Sep 2000.

[144] E. Hodby, S. A. Hopkins, G. Hechenblaikner, N. L. Smith, and C. J. Foot. Experimental observation of a superfluid gyroscope in a dilute bose-einstein condensate. Phys. Rev. Lett., 91:090403, Aug 2003.

[145] S. Riedl, E. R. Sánchez-Guajardo, C. Kohstall, J. H. Denschlag, and R. Grimm. Superfluid quenching of the moment of inertia in a strongly interacting fermi gas. New Journal of Physics, 13(3):035003, 2011.

[146] S. Elitzur. Impossibility of spontaneously breaking local symmetries. Phys. Rev. D, 12:3978–3982, Dec 1975.

[147] X.-G. Wen. Quantum Field Theory of Many-Body Systems. Oxford Graduate Texts. Oxford University Press Oxford, 2004.

[148] E. Fradkin. Field Theories of Condensed Matter Physics. Cambridge University Press, 2013.

[149] B. Zeng, X. Chen, D.-L. Zhou, and X.-G. Wen. Quantum Information Meets Quantum Matter – From Quantum Entanglement to Topological Phase in Many-Body Systems. arXiv:1508.02595, Aug 2015.

[150] S. A. Kivelson and D. S. Rokhsar. Bogoliubov quasiparticles, spinons, and spin-charge decoupling in superconductors. Phys. Rev. B, 41(16):11693–11696, 1990.

[151] X.-G. Wen. Topological Orders and Chern-Simons Theory in Strongly Correlated Quantum Liquid. Int. J. Mod. Phys. B, 05(1991):1641–1648, 1991.

[152] L. Balents, M. P. A. Fisher, and C. Nayak. Nodal liquid theory of the pseudo-gap phase of high-T_c superconductors. Int. J. Mod. Phys. B, 12(10):1033–1068, 1998.

[153] T. H. Hansson, A. Karlhede, and M. Sato. Topological field theory for p-wave superconductors. New Journal of Physics, 14(6):063017, 2012.

[154] T. H. Hansson, T. Kvorning, V. P. Nair, and G. J. Sreejith. Effective field theory for a p-wave superconductor in the subgap regime. Phys. Rev. B, 91:075116, Feb 2015.

[155] D. Vollhardt and P. Wolfle. Superfluid phases of helium 3. Taylor and Francis Ltd, 1990.

[156] G. E. Volovik. The universe in a helium droplet, volume 117. Oxford University Press New York, 2009.

[157] C. Kallin and J. Berlinsky. Chiral superconductors. Reports on Progress in Physics, 79(5):054502, 2016.

[158] V. Gurarie, L. Radzihovsky, and A. V. Andreev. Quantum phase transitions across a p-wave feshbach resonance. Phys. Rev. Lett., 94:230403, Jun 2005.

[159] V. Gurarie and L. Radzihovsky. Resonantly paired fermionic superfluids. Ann. Phys. (N. Y)., 322(1):2 – 119, 2007.

[160] C. Nayak, S. H. Simon, A. Stern, M. Freedman, and S. D. Sarma. Non-Abelian anyons and topological quantum computation. Rev. Mod. Phys., 80(3):1083, 2008.

[161] S. Ryu, A. P. Schnyder, A. Furusaki, and A. W. W. Ludwig. Topological insulators and superconductors: tenfold way and dimensional hierarchy. New J. Phys., 12(6):065010, 2010.

[162] T. Senthil, J. Marston, and M. Fisher. Spin quantum Hall effect in unconventional superconductors. Phys. Rev. B, 60(6):4245–4254, 1999.

[163] J. C. Y. Teo and C. L. Kane. Topological defects and gapless modes in insulators and superconductors. Phys. Rev. B, 82:115120, Sep 2010.

[164] Y. Nishikubo, K. Kudo, and M. Nohara. Superconductivity in the honeycomb-lattice pnictide srptas. J. Phys. Soc. Japan, 80(5):055002, 2011.

[165] M. H. Fischer, T. Neupert, C. Platt, A. P. Schnyder, W. Hanke, J. Goryo, R. Thomale, and M. Sigrist. Chiral d-wave superconductivity in $SrPtAs$. Phys. Rev. B, 89:020509, Jan 2014.

[166] R. Nandkishore, L. S. Levitov, and A. V. Chubukov. Chiral superconductivity from repulsive interactions in doped graphene. Nature Physics, 8(2):158–163, 2012.

[167] A. M. Black-Schaffer and C. Honerkamp. Chiral d -wave superconductivity in doped graphene. J. Phys., 26(42):423201, 2014.

[168] M. L. Kiesel, C. Platt, W. Hanke, D. A. Abanin, and R. Thomale. Competing many-body instabilities and unconventional superconductivity in graphene. Phys. Rev. B, 86:020507, Jul 2012.

[169] L. V. Keldysh. Coulomb interaction in thin semiconductor and semimetal films. JETP Lett., 29:658, June 1979.

[170] X.-G. Wen. Topological orders and edge excitations in fractional quantum hall states. Adv. Phys., 44(5):405–473, 1995.

[171] Y. M. Lu and A. Vishwanath. Theory and classification of interacting integer topological phases in two dimensions: A Chern-Simons approach. Phys. Rev. B, 86(12):1–33, 2012.

[172] X.-G. Wen. Theory of the Edge States in Fractional Quantum Hall Effects. Int. J. Mod. Phys. B, 06(10):1711–1762, May 1992.

[173] F. D. M. Haldane. Stability of chiral luttinger liquids and abelian quantum hall states. Phys. Rev. Lett., 74:2090–2093, Mar 1995.

[174] M. Levin. Protected edge modes without symmetry. Phys. Rev. X, 3:021009, May 2013.

[175] A. Kovner, B. Rosenstein, and D. Eliezer. Photon as a goldstone boson in $(2 + 1)$-dimensional abelian gauge theories. Nuclear Physics B, 350(1):325 – 354, 1991.

[176] L. Balents, M. P. A. Fisher, and C. Nayak. Dual order parameter for the nodal liquid. Phys. Rev. B, 60:1654–1667, Jul 1999.

[177] M. Hermanns. Order in 2D nodal superconductors. arXiv:0804.1332, Apr 2008.

[178] P. W. Anderson. Anomalous Magnetothermal Resistance of High-Tc Superconductors: Anomalous Cyclotron Orbits at a Dirac Point. arXiv:cond-mat/9812063, Dec 1998.

[179] D. Ariad, E. Grosfeld, and B. Seradjeh. Effective theory of vortices in two-dimensional spinless chiral p-wave superfluids. Phys. Rev. B, 92:035136, Jul 2015.

[180] A. Chan, T. L. Hughes, S. Ryu, and E. Fradkin. Effective field theories for topological insulators by functional bosonization. Phys. Rev. B, 87:085132, Feb 2013.

[181] B. Reznik and Y. Aharonov. Question of the nonlocality of the Aharonov-Casher effect. Phys. Rev. D, 40(12):2112–2117, 1989.

[182] A. S. Goldhaber and S. A. Kivelson. Local charge versus aharonov-bohm charge. Phys. Lett. B, 255(3):445 – 450, 1991.

[183] S. B. Bravyi and A. Y. Kitaev. Quantum codes on a lattice with boundary. arXiv:quant-ph/9811052, Nov 1998.

[184] A. Bernevig and T. Neupert. Topological superconductors and category theory. Topological Aspects of Condensed Matter Physics: Lecture Notes of the Les Houches Summer School, 103:63, Aug 2017.

[185] C. L. Kane and M. P. A. Fisher. Quantized thermal transport in the fractional quantum Hall effect. Phys. Rev. B, 55(23):15832–15837, June 1997.

[186] P. Ginsparg. Applied conformal field theory. arXiv:hep-th/9108028, 1988.

[187] Y.-Z. You, Z. Bi, A. Rasmussen, M. Cheng, and C. Xu. Bridging fermionic and bosonic short range entangled states. New J. Phys., 17(7):075010, 2015.

[188] J. Cano, M. Cheng, M. Mulligan, C. Nayak, E. Plamadeala, and J. Yard. Bulk-edge correspondence in $(2 + 1)$-dimensional abelian topological phases. Phys. Rev. B, 89:115116, Mar 2014.

[189] J. C. Y. Teo, T. L. Hughes, and E. Fradkin. Theory of twist liquids: Gauging an anyonic symmetry. Ann. Phys., 360:349–445, 2015.

[190] P. Bonderson and C. Nayak. Quasi-topological phases of matter and topological protection. Phys. Rev. B, 87:195451, May 2013.

[191] A. M. Polyakov. Gauge Fields and Strings. Contemporary concepts in physics. Taylor & Francis, 1987.

[192] E. Fradkin and S. H. Shenker. Phase diagrams of lattice gauge theories with higgs fields. Phys. Rev. D, 19:3682–3697, Jun 1979.

[193] M. A. Metlitski and A. Vishwanath. Particle-vortex duality of two-dimensional dirac fermion from electric-magnetic duality of three-dimensional topological insulators. Phys. Rev. B, 93:245151, Jun 2016.

[194] C. Wang and T. Senthil. Boson topological insulators: A window into highly entangled quantum phases. Phys. Rev. B, 87:235122, Jun 2013.

[195] N. Read. Non-abelian adiabatic statistics and hall viscosity in quantum hall states and $p_x + ip_y$ paired superfluids. Phys. Rev. B, 79:045308, Jan 2009.

[196] N. Read and E. H. Rezayi. Hall viscosity, orbital spin, and geometry: Paired superfluids and quantum hall systems. Phys. Rev. B, 84:085316, Aug 2011.

[197] C. Hoyos, S. Moroz, and D. T. Son. Effective theory of chiral two-dimensional superfluids. Phys. Rev. B, 89:174507, May 2014.

[198] X.-G. Wen and A. Zee. Shift and spin vector: New topological quantum numbers for the Hall fluids. Phys. Rev. Lett., 69(6):953–956, 1992.

[199] S. Bravyi, M. B. Hastings, and S. Michalakis. Topological quantum order: Stability under local perturbations. J. Math. Phys., 51(9):093512, 2010.

[200] S. Bravyi and M. B. Hastings. A short proof of stability of topological order under local perturbations. Commun. Math. Phys., 307(3):609, 2011.

[201] I. H. Kim and J. Haah. Localization from superselection rules in translationally invariant systems. Phys. Rev. Lett., 116:027202, Jan 2016.

[202] P. W. Anderson. Absence of diffusion in certain random lattices. Phys. Rev., 109:1492–1505, Mar 1958.

[203] I. V. Gornyi, A. D. Mirlin, and D. G. Polyakov. Interacting electrons in disordered wires: Anderson localization and low-t transport. Phys. Rev. Lett., 95:206603, Nov 2005.

[204] D. M. Basko, I. L. Aleiner, and B. L. Altshuler. Metal–insulator transition in a weakly interacting many-electron system with localized single-particle states. Ann. Phys., 321(5):1126 – 1205, 2006.

[205] M. Žnidarič, T. Prosen, and P. Prelovšek. Many-body localization in the heisenberg xxz magnet in a random field. Phys. Rev. B, 77:064426, Feb 2008.

[206] A. Pal and D. A. Huse. Many-body localization phase transition. Phys. Rev. B, 82:174411, Nov 2010.

[207] J. Z. Imbrie. On many-body localization for quantum spin chains. J. Stat. Phys., 163(5):998–1048, 2016.

[208] D. A. Huse, R. Nandkishore, V. Oganesyan, A. Pal, and S. L. Sondhi. Localization-protected quantum order. Phys. Rev. B, 88:014206, Jul 2013.

[209] R. Vosk and E. Altman. Dynamical quantum phase transitions in random spin chains. Phys. Rev. Lett., 112:217204, May 2014.

[210] D. Pekker, G. Refael, E. Altman, E. Demler, and V. Oganesyan. Hilbert-glass transition: New universality of temperature-tuned many-body dynamical quantum criticality. Phys. Rev. X, 4:011052, Mar 2014.

[211] C. W. von Keyserlingk, V. Khemani, and S. L. Sondhi. Absolute stability and spatiotemporal long-range order in floquet systems. Phys. Rev. B, 94:085112, Aug 2016.

[212] Y. Kagan and L. A. Maksimov. Effect of interparticle interaction on localization in a non-ideal crystal with a narrow band. ZhETF, 87:348, 0 1984. JETP 60, 201 (1984).

[213] T. Grover and M. P. A. Fisher. Quantum disentangled liquids. J. Stat. Mech. Theor. Exp., 2014(10):P10010, 2014.

[214] M. Schiulaz, A. Silva, and M. Müller. Dynamics in many-body localized quantum systems without disorder. Phys. Rev. B, 91:184202, May 2015.

[215] N. Y. Yao, C. R. Laumann, J. I. Cirac, M. D. Lukin, and J. E. Moore. Quasi-many-body localization in translation-invariant systems. Phys. Rev. Lett., 117:240601, Dec 2016.

[216] Z. Papic, E. M. Stoudenmire, and D. A. Abanin. Many-body localization in disorder-free systems: The importance of finite-size constraints. Ann. Phys., 362:714 – 725, 2015.

[217] W. De Roeck and F. Huveneers. Asymptotic quantum many-body localization from thermal disorder. Commun. Math. Phys., 332(3):1017–1082, 2014.

[218] W. De Roeck and F. Huveneers. Scenario for delocalization in translation-invariant systems. Phys. Rev. B, 90:165137, Oct 2014.

[219] J. M. Hickey, S. Genway, and J. P. Garrahan. Signatures of many-body localisation in a system without disorder and the relation to a glass transition. J. Stat. Mech. Theor. Exp., 2016(5):054047, 2016.

[220] S. S. Kondov, W. R. McGehee, J. J. Zirbel, and B. DeMarco. Three-dimensional anderson localization of ultracold matter. Science, 334(6052):66–68, 2011.

[221] S. S. Kondov, W. R. McGehee, W. Xu, and B. DeMarco. Disorder-induced localization in a strongly correlated atomic hubbard gas. Phys. Rev. Lett., 114:083002, Feb 2015.

[222] M. Schreiber, S. S. Hodgman, P. Bordia, H. P. Lüschen, M. H. Fischer, R. Vosk, E. Altman, U. Schneider, and I. Bloch. Observation of many-body localization of interacting fermions in a quasirandom optical lattice. Science, 349(6250):842–845, 2015.

[223] J. Choi, S. Hild, J. Zeiher, P. Schauß, A. Rubio-Abadal, T. Yefsah, V. Khemani, D. A. Huse, I. Bloch, and C. Gross. Exploring the many-body localization transition in two dimensions. Science, 352(6293):1547–1552, 2016.

[224] P. Bordia, H. P. Lüschen, S. S. Hodgman, M. Schreiber, I. Bloch, and U. Schneider. Coupling identical one-dimensional many-body localized systems. Phys. Rev. Lett., 116:140401, Apr 2016.

[225] G. A. Álvarez, D. Suter, and R. Kaiser. Localization-delocalization transition in the dynamics of dipolar-coupled nuclear spins. Science, 349(6250):846–848, 2015.

[226] S. Choi, J. Choi, R. Landig, G. Kucsko, H. Zhou, J. Isoya, F. Jelezko, S. Onoda, H. Sumiya, V. Khemani, et al. Observation of discrete time-crystalline order in a disordered dipolar many-body system. Nature, 543(7644):221, 2017.

[227] M. Serbyn, Z. Papić, and D. A. Abanin. Local conservation laws and the structure of the many-body localized states. Phys. Rev. Lett., 111:127201, Sep 2013.

[228] D. A. Huse, R. Nandkishore, and V. Oganesyan. Phenomenology of fully many-body-localized systems. Phys. Rev. B, 90:174202, Nov 2014.

[229] V. Ros, M. Müller, and A. Scardicchio. Integrals of motion in the many-body localized phase. Nucl. Phys. B, 891(0):420 – 465, 2015.

[230] S. D. Geraedts, R. N. Bhatt, and R. Nandkishore. Emergent local integrals of motion without a complete set of localized eigenstates. Phys. Rev. B, 95:064204, Feb 2017.

[231] R. Vosk and E. Altman. Many-body localization in one dimension as a dynamical renormalization group fixed point. Phys. Rev. Lett., 110:067204, Feb 2013.

[232] R. Vasseur, A. C. Potter, and S. A. Parameswaran. Quantum criticality of hot random spin chains. Phys. Rev. Lett., 114:217201, May 2015.

[233] S. Bravyi, B. Leemhuis, and B. M. Terhal. Topological order in an exactly solvable 3D spin model. Ann. Phys., 326(4):839–866, 2011.

[234] D. J. Williamson. Fractal symmetries: Ungauging the cubic code. Phys. Rev. B, 94:155128, Oct 2016.

[235] A. Amir, Y. Oreg, and Y. Imry. Electron glass dynamics. Annu. Rev. Condens. Matter Phys., 2(1):235–262, 2011.

[236] S. Gopalakrishnan and R. Nandkishore. Mean-field theory of nearly many-body localized metals. Phys. Rev. B, 90:224203, Dec 2014.

[237] I. V. Gornyi, A. D. Mirlin, M. Müller, and D. G. Polyakov. Absence of many-body localization in a continuum. Annalen der Physik, 529(7):1600365–n/a, 2017. 1600365.

[238] R. Nandkishore. Many-body localization and delocalization in the two-dimensional continuum. Phys. Rev. B, 90:184204, Nov 2014.

[239] W. De Roeck and F. Huveneers. Stability and instability towards delocalization in many-body localization systems. Phys. Rev. B, 95:155129, Apr 2017.

[240] S. A. Parameswaran and S. Gopalakrishnan. Spin-catalyzed hopping conductivity in disordered strongly interacting quantum wires. Phys. Rev. B, 95:024201, Jan 2017.

[241] R. Nandkishore and S. Gopalakrishnan. Many body localized systems weakly coupled to baths. Annalen der Physik, 2016.

[242] D. A. Abanin, W. De Roeck, and F. Huveneers. Exponentially slow heating in periodically driven many-body systems. Phys. Rev. Lett., 115:256803, Dec 2015.

[243] R. Nandkishore. Many-body localization proximity effect. Phys. Rev. B, 92:245141, Dec 2015.

[244] K. Hyatt, J. R. Garrison, A. C. Potter, and B. Bauer. Many-body localization in the presence of a small bath. Phys. Rev. B, 95:035132, Jan 2017.

[245] J. Haah. Commuting Pauli Hamiltonians as Maps between Free Modules. Communications in Mathematical Physics, 324(2):351–399, Dec 2013.

[246] S. Bravyi and J. Haah. Energy landscape of 3d spin hamiltonians with topological order. Phys. Rev. Lett., 107:150504, Oct 2011.

[247] S. Bravyi and J. Haah. Quantum self-correction in the 3d cubic code model. Phys. Rev. Lett., 111:200501, Nov 2013.

[248] M. E. J. Newman and C. Moore. Glassy dynamics and aging in an exactly solvable spin model. Phys. Rev. E, 60:5068–5072, Nov 1999.

[249] K. Siva and B. Yoshida. Topological order and memory time in marginally-self-correcting quantum memory. Phys. Rev. A, 95:032324, Mar 2017.

[250] Chleboun, P., Faggionato, A., and Martinelli, F. The influence of dimension on the relaxation process of east-like models: Rigorous results. EPL, 107(3):36002, 2014.

[251] F. Ritort and P. Sollich. Glassy dynamics of kinetically constrained models. Advances in Physics, 52(4):219–342, 2003.

[252] Y. S. Elmatad, D. Chandler, and J. P. Garrahan. Corresponding states of structural glass formers. The Journal of Physical Chemistry B, 113(16):5563–5567, 2009.

[253] G. Biroli and J. P. Garrahan. Perspective: The glass transition. The Journal of Chemical Physics, 138(12):12A301, 2013.

[254] J. P. Garrahan and M. E. J. Newman. Glassiness and constrained dynamics of a short-range nondisordered spin model. Phys. Rev. E, 62:7670–7678, Dec 2000.

[255] C. Castelnovo and C. Chamon. Topological quantum glassiness. Philosophical Magazine, 92(1-3):304–323, 2012.

[256] A. Chandran, A. Pal, C. R. Laumann, and A. Scardicchio. Many-body localization beyond eigenstates in all dimensions. Phys. Rev. B, 94:144203, Oct 2016.

[257] C. L. Kane and Ma. P. A. Fisher. Nonequilibrium noise and fractional charge in the quantum hall effect. Phys. Rev. Lett., 72:724–727, Jan 1994.

[258] M. Levin and A. Stern. Classification and analysis of two-dimensional abelian fractional topological insulators. Phys. Rev. B, 86:115131, Sep 2012.

[259] A. M. Essin and M. Hermele. Classifying fractionalization: Symmetry classification of gapped $\mathbb{Z}_2$ spin liquids in two dimensions. Phys. Rev. B, 87:104406, Mar 2013.

[260] A. Mesaros and Y. Ran. Classification of symmetry enriched topological phases with exactly solvable models. Phys. Rev. B, 87:155115, Apr 2013.

[261] Y. M. Lu and A. Vishwanath. Classification and properties of symmetry-enriched topological phases: Chern-simons approach with applications to $\mathbb{Z}_2$ spin liquids. Phys. Rev. B, 93:155121, Apr 2016.

[262] M. Barkeshli, P. Bonderson, M. Cheng, and Z. Wang. Symmetry, Defects, and Gauging of Topological Phases. arXiv:1410.4540, October 2014.

[263] C. Xu. Three-dimensional Z_2 topological phases enriched by time-reversal symmetry. Phys. Rev. B, 88:205137, Nov 2013.

[264] L.-Y Hung and X.-G. Wen. Quantized topological terms in weak-coupling gauge theories with a global symmetry and their connection to symmetry-enriched topological phases. Phys. Rev. B, 87:165107, Apr 2013.

[265] A. Rasmussen, Y.-Z. You, and C. Xu. Stable Gapless Bose Liquid Phases without any Symmetry. arXiv:1601.08235, January 2016.

[266] T. H. Hsieh and G. B. Halász. Fractons from partons. Phys. Rev. B, 96:165105, Oct 2017.

[267] K. Slagle and Y. B. Kim. Fracton topological order from nearest-neighbor two-spin interactions and dualities. Phys. Rev. B, 96:165106, Oct 2017.

[268] B. Shi and Y. M. Lu. Decipher the nonlocal entanglement entropy of fracton topological orders. arXiv:1705.09300, May 2017.

[269] M. Pretko. Finite-temperature screening of U(1) fractons. Phys. Rev. B, 96:115102, Sep 2017.

[270] S. Vijay and L. Fu. A Generalization of Non-Abelian Anyons in Three Dimensions. arXiv:1706.07070, June 2017.

[271] G. B. Halász, T. H. Hsieh, and L. Balents. Fracton topological phases from strongly coupled spin chains. Phys. Rev. Lett., 119:257202, Dec 2017.

[272] M. Pretko. Higher-spin Witten effect and two-dimensional fracton phases. Phys. Rev. B, 96:125151, Sep 2017.

[273] K. Slagle and Y. B. Kim. Quantum field theory of X-cube fracton topological order and robust degeneracy from geometry. Phys. Rev. B, 96:195139, Nov 2017.

[274] V. V. Albert, S. Pascazio, and M. H. Devoret. General phase spaces: from discrete variables to rotor and continuum limits. Journal of Physics A: Mathematical and Theoretical, 50(50):504002, 2017.

[275] T. Devakul, S. A. Parameswaran, and S. L. Sondhi. Correlation function diagnostics for type-I fracton phases. Phys. Rev. B, 97:041110, Jan 2018.

[276] O. Petrova and N. Regnault. Simple anisotropic three-dimensional quantum spin liquid with fractonlike topological order. Phys. Rev. B, 96:224429, Dec 2017.

[277] H. He, Y. Zheng, B. A. Bernevig, and N. Regnault. Entanglement entropy from tensor network states for stabilizer codes. Phys. Rev. B, 97:125102, Mar 2018.

[278] A. T. Schmitz, H. Ma, R. M. Nandkishore, and S. A. Parameswaran. Recoverable Information and Emergent Conservation Laws in Fracton Stabilizer Codes. arXiv:1712.02375, December 2017.

[279] R. Jamei, S. Kivelson, and B. Spivak. Universal aspects of coulomb-frustrated phase separation. Phys. Rev. Lett., 94:056805, Feb 2005.

[280] B. Spivak and S. Kivelson. Transport in two dimensional electronic micro-emulsions. J. Phys. IV France, 131:255–256, 2005.

[281] S. A. Parameswaran, S. A. Kivelson, S. L. Sondhi, and B. Z. Spivak. Weakly Coupled Pfaffian as a Type I Quantum Hall Liquid. Phys. Rev. Lett., 106:236801, Jun 2011.

[282] Z.-C. Gu and X.-G. Wen. A lattice bosonic model as a quantum theory of gravity. arXiv:gr-qc/0606100, June 2006.

[283] Z. C. Gu and X.-G. Wen. Emergence of helicity ± 2 modes (gravitons) from qubit models. Nuclear Physics B, 863(1):90 – 129, 2012.

[284] S.-S. Lee. Stability of the U(1) spin liquid with a spinon Fermi surface in $2+1$ dimensions. Phys. Rev. B, 78:085129, Aug 2008.

[285] D. F. Mross and T. Senthil. Charge Friedel oscillations in a Mott insulator. Phys. Rev. B, 84:041102, Jul 2011.

[286] E. Fradkin, C. Nayak, A. Tsvelik, and F. Wilczek. A Chern-Simons effective field theory for the Pfaffian quantum Hall state. Nuclear Physics B, 516(3):704 – 718, 1998.

[287] X.-G. Wen. Gapless boundary excitations in the quantum Hall states and in the chiral spin states. Phys. Rev. B, 43:11025–11036, May 1991.

[288] W. A. Benalcazar, J. C. Y. Teo, and T. L. Hughes. Classification of two-dimensional topological crystalline superconductors and majorana bound states at disclinations. Phys. Rev. B, 89:224503, Jun 2014.

[289] Z. Song, Z. Fang, and C. Fang. $(d-2)$-dimensional edge states of rotation symmetry protected topological states. Phys. Rev. Lett., 119:246402, Dec 2017.

[290] F. Schindler, A. M. Cook, M. G. Vergniory, Z. Wang, S. S. P. Parkin, B. A. Bernevig, and T. Neupert. Higher-Order Topological Insulators. arXiv:1708.03636, August 2017.

[291] J. Langbehn, Y. Peng, L. Trifunovic, F. von Oppen, and P. W. Brouwer. Reflection-symmetric second-order topological insulators and superconductors. Phys. Rev. Lett., 119:246401, Dec 2017.

[292] W. A. Benalcazar, B. A. Bernevig, and T. L. Hughes. Electric multipole moments, topological multipole moment pumping, and chiral hinge states in crystalline insulators. Phys. Rev. B, 96:245115, Dec 2017.

[293] W. A. Benalcazar, B. A. Bernevig, and T. L. Hughes. Quantized electric multipole insulators. Science, 357(6346):61–66, 2017.

[294] C. Fang and L. Fu. Rotation Anomaly and Topological Crystalline Insulators. arXiv:1709.01929, September 2017.

[295] N. R. Cooper. Rapidly Rotating Atomic Gases. Adv. Phys., 57:539, 2008.

[296] C. Wang and T. Senthil. Time-Reversal Symmetric U(1) Quantum Spin Liquids. Phys. Rev. X, 6:011034, Mar 2016.

[297] C. Xu and T. Senthil. Wave functions of bosonic symmetry protected topological phases. Phys. Rev. B, 87:174412, May 2013.

[298] X.-G. Wen and A. Zee. Topological degeneracy of quantum hall fluids. Phys. Rev. B, 58:15717–15728, Dec 1998.

Appendix A

Observables from BdG solutions

The particle number $\hat{N}$ and OAM $\hat{L}_z$ in the BCS ground state can be found by numerically diagonalizing the BdG Hamiltonian $H^{(l)}$. To obtain a finite spectrum we introduce a cutoff $M \gg 1$ on the radial quantum numbers such that $H^{(l)}$ is a $2M \times 2M$ Hermitian matrix. The eigenstates $(u, v)^T$ of the BdG Hamiltonian satisfy

$$\sum_{n'=1}^{M} H_{n,n'}^{(l)} \begin{pmatrix} u_{n'm}^{(l)} \\ v_{n'm}^{(l)} \end{pmatrix} = E_m^{(l)} \begin{pmatrix} u_{nm}^{(l)} \\ v_{nm}^{(l)} \end{pmatrix}, \tag{A.1}$$

and are normalized as $\sum_{n=1}^{M} \left(|u_{nm}^{(l)}|^2 + |v_{nm}^{(l)}|^2 \right) = 1$. Given these, we obtain

$$\hat{N} = \sum_{l,n,m} |v_{nm}^{(l)}|^2,$$

$$\hat{L}_z = - \sum_{l,n,m} l|v_{nm}^{(l)}|^2, \tag{A.2}$$

where the sum over m is restricted to the positive part of the energy spectrum.

Appendix B

Relation between "magnetic field" $\mathcal{B}^v$ and fermion density n_f

Here we demonstrate that in a superconductor the background vortex "magnetic field" $\mathcal{B}^v = \epsilon^{ij}\partial_i\mathcal{A}_j^v$ is fixed by the density of the elementary fermions n_f. Indeed, in a superconductor the Lagrangian of a single vortex located at position X^i is given by [295]

$$L_v = -\frac{\pi}{2}n_f\epsilon_{ij}X^i\dot{X}^j. \tag{B.1}$$

Alternatively, we can rewrite the same Lagrangian as a minimal coupling of a vortex current to its gauge potential $L_v = -q_v\mathcal{A}_j^v\dot{X}^j$ with $q_v = 1/2$ because in a superconductor the vortex carries only a half of a unit flux quantum of the magnetic field. As a result, we find that the density of elementary fermions fixes the background value of $\mathcal{B}^v$ to be $\mathcal{B}^v = 2\pi n_f$. At the same time the fermion current j_f^i fixes the background value of the "electric field" $\mathcal{E}_j^v$ via the relation $j_f^i = -\frac{1}{2\pi}\epsilon^{ij}\mathcal{E}_j^v$.

Appendix C

Block-diagonal forms of K-matrices of spin-singlet chiral states

It is well-known that different K-matrices can represent the same topological state in the Chern-Simons theory (5.34). Indeed, one is allowed to relabel the statistical gauge fields a^I

$$a^I \to \tilde{a}^I = X_{IJ} a^J, \tag{C.1}$$

where $X \in GL(N, \mathbb{Z})$ is a $N \times N$ matrix of integers with the determinant ± 1. Under such a transformation

$$K \to \tilde{K} = X^T K X,$$
$$l \to \tilde{l} = X^T l, \tag{C.2}$$
$$t \to \tilde{t} = X^T t$$

and the theories defined by (K, l, t) and $(\tilde{K}, \tilde{l}, \tilde{t})$ are *equivalent*.

We demonstrate that the K-matrix of a chiral spin-singlet superconductor paired in the (even) k^{th} partial wave can be put into *block-diagonal* forms. The two distinct block-diagonal forms used in the main text are highlighted here. We start from the K-matrix, l-vectors, and t-vectors that were derived in Sec. 3.5.3 and are given by Eqs. (3.42), (3.43), and (3.44) respectively.

If one chooses now the X-matrix

$$X = \left(\begin{array}{cc|c} 1 & 0 & 0_k \\ 0 & 1 & 0_k \\ \hline -1_k^T & 0_k^T & \mathbb{1}_{k \times k} \end{array} \right), \tag{C.3}$$

one finds

$$\tilde{K}_B = \begin{pmatrix} -k & 2 \\ 2 & 0 \end{pmatrix} \oplus \mathbb{1}_{k \times k}, \tag{C.4}$$

$$\tilde{l}_m^T = (0, 1, 0, \ldots, 0) = l_m^T,$$
$$\tilde{l}_\epsilon^T = (-1, 0, 1, 0, \ldots, 0), \tag{C.5}$$

$$\tilde{t}_s^T = (0, 0, 1, -1, \ldots, 1, -1) = t_s^T,$$
$$\tilde{t}_v^T = (1, 0, \ldots, 0) = t_v^T. \tag{C.6}$$

In Eq. (C.4) the topological order and chirality is encoded in the first and second factor, respectively.

Alternatively, one can find a $GL(N, \mathbb{Z})$ transformation that transforms the K-matrix (3.42) into the Cartan block-diagonal form

$$\tilde{K}_C = A_{k \times k}^{SO(2k)} \oplus \begin{pmatrix} 1 & 0 \\ 0 & -1 \end{pmatrix}, \tag{C.7}$$

where we introduced the *Cartan matrix* of of the Lie algebra SO($2k$)

$$A_{k \times k}^{SO(2k)} = \begin{pmatrix} 2 & -1 & 0 & 0 & \ldots & 0 \\ -1 & 2 & \ddots & \ddots & \ddots & 0 \\ 0 & \ddots & 2 & -1 & 0 & 0 \\ 0 & \ddots & -1 & 2 & -1 & -1 \\ \vdots & \ddots & 0 & -1 & 2 & 0 \\ 0 & 0 & 0 & -1 & 0 & 2 \end{pmatrix}. \tag{C.8}$$

In the form (C.7) both the topological order and chirality are encoded in the first factor, while the second factor is topologically trivial. The X matrix for the $d + id$ ($k = 2$) case is

$$X_{k=2} = \begin{pmatrix} -1 & -1 & 0 & -1 \\ -1 & 0 & 0 & 0 \\ 1 & -1 & 0 & 0 \\ 1 & 1 & 1 & 1 \end{pmatrix}. \tag{C.9}$$

X matrices for higher partial even-waves can also be found. For $k = 4$, $k = 6$, and $k = 8$, for instance, we find

$$X_{k=4} = \begin{pmatrix} -1 & 0 & 0 & 0 & 0 & -1 \\ -1 & 0 & 0 & 1 & 0 & 0 \\ 0 & 0 & 1 & -1 & 0 & 0 \\ 0 & 1 & -1 & -1 & 0 & 0 \\ 1 & -1 & 0 & 0 & 0 & 0 \\ 1 & 0 & 0 & 0 & 1 & 1 \end{pmatrix}, \tag{C.10}$$

$$X_{k=6} = \begin{pmatrix} -1 & 0 & 0 & 0 & 0 & 0 & 0 & -1 \\ -1 & 0 & 0 & 0 & 0 & 1 & 0 & 0 \\ 0 & 0 & 0 & 0 & 1 & -1 & 0 & 0 \\ 0 & 0 & 0 & 1 & -1 & -1 & 0 & 0 \\ 0 & 0 & 1 & -1 & 0 & 0 & 0 & 0 \\ 0 & 1 & -1 & 0 & 0 & 0 & 0 & 0 \\ 1 & -1 & 0 & 0 & 0 & 0 & 0 & 0 \\ 1 & 0 & 0 & 0 & 0 & 0 & 1 & 1 \end{pmatrix}, \tag{C.11}$$

$$X_{k=8} = \begin{pmatrix} -1 & 0 & 0 & 0 & 0 & 0 & 0 & 0 & 0 & -1 \\ -1 & 0 & 0 & 0 & 0 & 0 & 0 & 1 & 0 & 0 \\ 0 & 0 & 0 & 0 & 0 & 0 & 1 & -1 & 0 & 0 \\ 0 & 0 & 0 & 0 & 0 & 1 & -1 & -1 & 0 & 0 \\ 0 & 0 & 0 & 0 & 1 & -1 & 0 & 0 & 0 & 0 \\ 0 & 0 & 0 & 1 & -1 & 0 & 0 & 0 & 0 & 0 \\ 0 & 0 & 1 & -1 & 0 & 0 & 0 & 0 & 0 & 0 \\ 0 & 1 & -1 & 0 & 0 & 0 & 0 & 0 & 0 & 0 \\ 1 & -1 & 0 & 0 & 0 & 0 & 0 & 0 & 0 & 0 \\ 1 & 0 & 0 & 0 & 0 & 0 & 0 & 0 & 1 & 1 \end{pmatrix}. \tag{C.12}$$

While these X matrices are not unique, the ones presented here easily generalize to higher k.

Appendix D

Details on Type I Relaxation Dynamics

Here, we discuss in detail the solutions of the relevant differential equations encountered in the main text. All of the relevant equations can be brought to the form

$$\frac{dy}{dt} = ay^2 e^{\pm\frac{1}{y}}. \tag{D.1}$$

Since this is a separable equation, this is equivalent to

$$\int_{y(0)}^{y(t)} \frac{dz}{z^2} e^{\mp\frac{1}{z}} = at. \tag{D.2}$$

Changing variables to $x = \pm\frac{1}{z}$, we get

$$\mp \int_{\pm 1/y(0)}^{\pm 1/y(t)} e^{-x} = at. \tag{D.3}$$

Thus, the solution is

$$y(t) = \frac{\mp 1}{\log\left(e^{\mp 1/y(0)} \pm at\right)} \tag{D.4}$$

D.1   Equilibration within the bath

First, we consider the dynamics within the bath, ignoring the fractons. As depicted in Fig. 4.4, a composite can decompose into two bosons while remaining on-shell. Being a first order process (in $\Lambda \ll W$), this occurs at a rate $\sim \Lambda n_c$. Similarly, the reverse process where two bosons combine to form a composite occurs at a rate $\sim \Lambda n_b^2$. To leading order, these are the only two processes which contribute to the equilibration between these two sectors, as all other processes require additional

composites/bosons and are suppressed by additional density factors. Considering only the leading

order processes, a detailed balance is established between these two sectors,

$$\frac{dE_c}{dt} = -2W\Lambda(n_c - n_b^2) = -2W\Lambda\left(e^{-\frac{2W}{T_c}} - e^{-\frac{2W}{T_b}}\right)$$

$$\frac{dE_b}{dt} = -2W\Lambda(n_b^2 - n_c) = -2W\Lambda\left(e^{-\frac{2W}{T_b}} - e^{-\frac{2W}{T_c}}\right) \qquad (D.5)$$

Putting in the heat capacities Eq. (4.10), we get

$$\frac{dT_c}{dt} = -\frac{\Lambda}{2W}T_c^2\left(1 - e^{2W\left(\frac{1}{T_c} - \frac{1}{T_b}\right)}\right),$$

$$\frac{dT_b}{dt} = -\frac{2\Lambda}{W}T_b^2\left(1 - e^{2W\left(\frac{1}{T_b} - \frac{1}{T_c}\right)}\right)e^{-\frac{W}{T_b}}. \qquad (D.6)$$

In the regime where $T_b^{(0)} \ll T_c^{(0)}$, the bath is initially comprised primarily of neutral composite

excitations, and in this limit the above equations are approximately

$$\frac{dT_c}{dt} \approx -\frac{\Lambda}{2W}T_c^2\,,$$

$$\frac{dT_b}{dt} \approx \frac{2\Lambda}{W}T_b^2 e^{\frac{W}{T_b}} e^{-\frac{2W}{T_c}}\,. \qquad (D.7)$$

For $T_c(t)$, with initial condition $T_c(0) = T_c^{(0)}$, we find

$$T_c(t) = \frac{2W}{\Lambda t + \frac{2W}{T_c^{(0)}}}. \qquad (D.8)$$

Since we are working in the limit $T_c^{(0)} \ll W$, $T_c(t) \sim T_c^{(0)}$ for a time $t \sim \frac{W}{\Lambda T_c^{(0)}}$. We can hence treat

$T_c(t)$ as a constant over this time scale such that $T_b(t)$ satisfies

$$\frac{dT_b}{dt} \approx \frac{2\Lambda}{W}T_b^2 e^{\frac{W}{T_b}} e^{-\frac{2W}{T_c^{(0)}}}. \qquad (D.9)$$

This is equivalent to Eq. (D.1) with $y = T_b/W$ and $a = 2\Lambda e^{-\frac{2W}{T_c^{(0)}}}$, and hence has the solution

$$T_b(t) = \frac{-W}{\log\left(2\Lambda t + b\right) - \frac{2W}{T_c^{(0)}}}, \qquad (D.10)$$

where $b = e^{\frac{2W}{T_c^{(0)}} - \frac{W}{T_b^{(0)}}}$. This behaviour is expected to hold until the bosons are close to equilibration

$T_b \sim T_c^{(0)}/2$, i.e., over the window

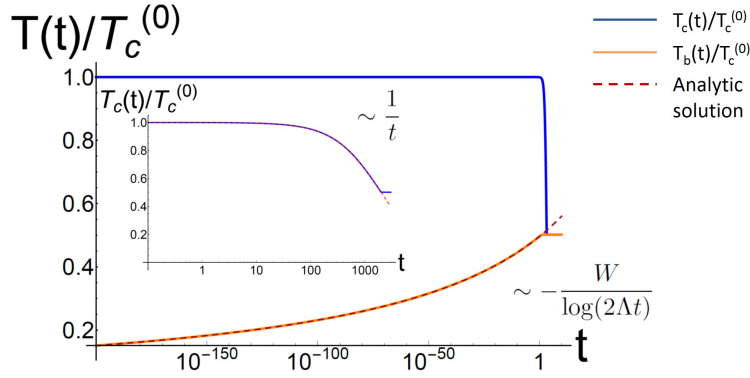$$0 \le t \lesssim \frac{k}{2\Lambda} \qquad (D.11)$$

Figure D.1: The composite sector (blue) cools with power-law behaviour while the bosonic sector (orange) displays a $\log(t)$ behaviour over a short time scale, set by $\sim 1/\Lambda$. The red dashed line, Eq. (D.10), is the approximate analytic solution to Eq. (D.6) in the regime of interest $T_b^{(0)} \ll T_c^{(0)}$, shown here against the numerical solution for $T_b(t)$. The in-set compares the analytic $1/t$ behaviour Eq. (D.8) (red dashed line) with the numerical solution for the composite sector (blue). The parameters here are $W = 1, \Lambda = 10^{-1}, T_c^{(0)} = 10^{-2}$, and $T_b^{(0)} = 0.5 \times 10^{-3}$.

where k is some positive constant.

The bosons thus display logarithmic heating over a time scale $0 \leq t \lesssim \frac{k}{\Lambda}$, for some positive constant k. They reach the equilibrium temperature faster than the neutral composites, which cool down with power-law behaviour over a time scale $0 \leq t \lesssim \frac{k'W}{\Lambda T_c^{(0)}}$ governed by their initial temperature, $T_c^{(0)}$. The equilibration process is depicted in Fig. D.1, where the approximate analytic solutions developed above are shown to be in good agreement with the numerical solutions for Eq. (D.6). In particular, as illustrated in Fig. D.2, the approximate analytic solution Eq. (D.10) fits the numerical solution for Eq. (D.6) quite well, confirming the logarithmic heating of the bosonic sector.

Close to equilibration, we set $T_c = T + \frac{\delta T}{2}$ and $T_b = T - \frac{\delta T}{2}$, such that Eq. (D.6) leads to

$$\frac{d(\delta T)}{dt} \approx -\Lambda T, \tag{D.12}$$

in the limit $\delta T \ll T$ and $T = T_c^{(0)}/2 \ll W$. Thus, close to equilibration the system recovers an exponential relaxation rate since $\delta T(t) = T_c(t) - T_b(t)$ behaves according to Newton's law of cooling: $\delta T(t) \sim e^{-\Lambda t}$.

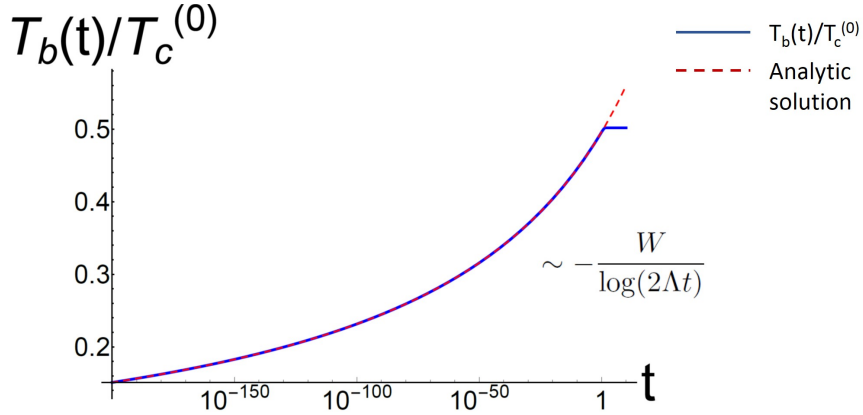The above discussion demonstrates that while we could, in principle, initialize our system

Figure D.2: The bosonic sector displays a $\log(t)$ behaviour over a short time scale, set by $\sim 1/\Lambda$. The red dashed line is the approximate analytic solution, Eq. (D.10), for Eq. (D.6) shown against the numerical solution for $T_b(t)$, in blue. The parameters here are $W = 1, \Lambda = 10^{-1}, T_c^{(0)} = 10^{-2}$, and $T_b^{(0)} = 0.5 \times 10^{-3}$.

without any bosonic excitations, the presence of a finite density bath of neutral composites will quickly establish a finite density of bosons in equilibrium with the composites (see Fig. D.1). Following this discussion, it is easy to show that starting in the opposite limit i.e., with $T_c^{(0)} \ll T_b^{(0)}$ will result in the same equilibrium configuration, except with the dynamics reversed: the bosons will cool with a power law while the composites will display a $\log(t)$ behaviour. When considering the dynamics of the fracton sector, it is therefore reasonable to assume that the composite and bosonic sectors have already equilibrated. Thus, we make this assumption in the main text and consider a heat bath with both the composites and bosons at an initial temperature $T_b^{(0)}$.

D.2 Equilibration between bath and fractons

We now consider equilibration between the charged fractons and the bath (comprised of $e^{(2)}$'s and composites). The equilibration process is governed by Eq. (4.12),

$$\frac{dT_b}{dt} = -\frac{\Lambda^2 T_b^2}{W^2}\left(3n_b + n_f - n_f^2 - \frac{n_f^3}{n_b} - 2\frac{n_f^4}{n_b}\right),$$

$$\frac{dT_f}{dt} = \frac{4\Lambda^2 T_f^2}{W^2}\left(3\frac{n_b^2}{n_f} + n_b - n_b n_f - n_f^2 - 2n_f^3\right). \tag{D.13}$$

In the regime of interest, $T_f^{(0)} \ll T_b^{(0)}$, such that the above equations reduce to

$$\frac{dT_b}{dt} \approx -3\frac{\Lambda^2 T_b^2}{W^2} e^{-\frac{W}{T_b}},$$
$$\frac{dT_f}{dt} \approx 12\frac{\Lambda^2 T_f^2}{W^2} e^{\frac{W}{2T_f}} e^{-\frac{2W}{T_b}}. \tag{D.14}$$

The first equation is equivalent to Eq. (D.1) with $y = T_b/W$ and $a = -3\Lambda^2/W$ and hence has the solution

$$T_b(t) = \frac{W}{\log\left(\frac{3\Lambda^2}{W}t + e^{W/T_b^{(0)}}\right)}, \tag{D.15}$$

establishing the logarithmic cooling displayed by the bath. To understand the heating of the fractons, we first note that the bath temperature stays roughly constant, $T_b(t) \sim T_b^{(0)}$, for an exponentially long period of time $t \sim \frac{W}{3\Lambda^2} e^{W/T_b^{(0)}}$. We can hence treat T_b as a constant, so that the behaviour of the fractons is governed by

$$\frac{dT_f}{dt} \approx 12\frac{\Lambda^2 T_f^2}{W^2} e^{\frac{W}{2T_f}} e^{-\frac{2W}{T_b^{(0)}}}, \tag{D.16}$$

which is again of the form Eq. (D.1) and has the solution

$$T_f(t) = -\frac{W/2}{\log\left(\frac{6\Lambda^2}{W}t + b\right) - \frac{2W}{T_b^{(0)}}}, \tag{D.17}$$

where $b = e^{\frac{2W}{T_b^{(0)}} - \frac{W}{2T_f^{(0)}}}$. Since the bath cools logarithmically over an exponential time scale, this behaviour of the fractons holds until $T_f(t) \sim T_b^{(0)}/2$ i.e., over an exponentially long time scale

$$0 \leq t \lesssim \frac{W}{6\Lambda^2} e^{W/T_b^{(0)}}. \tag{D.18}$$

Thus far, we have only considered processes where two bosons combine to pump energy into the fracton sector, and have neglected processes where a boson and a fracton convert into three fractons. This is no longer accurate once the fracton temperature $T_f \sim T_b^{(0)}/2$. At this time scale $t \sim \frac{W}{6\Lambda^2} e^{W/T_b^{(0)}}$, the fracton density $n_f \sim n_b$, since the temperature of the bath has yet to significantly deviate from its initial temperature $T_b^{(0)}$ while the fracton temperature has almost reached its equilibrium value, $T_b^{(0)}/2$. Once the fractons are close to equilibration, the behaviour of the bath

is hence governed by

$$\frac{dT_b}{dt} \approx -\frac{\Lambda^2 T_b^2}{W^2}(3n_b + n_f), \tag{D.19}$$

where we are dropping terms of $O(n_f^2)$ and higher. The second term on the r.h.s $\sim n_f$ corresponds to channel 3, which is now activated. Treating n_f as a constant (since the fracton sector is close to equilibration), we find that the bath's behaviour is now modified,

$$T_b(t) \sim \frac{W^2}{\Lambda^2 t} e^{W/T_b^{(0)}}. \tag{D.20}$$

To study the behaviour close to equilibration, we set $T_b = T + \frac{\delta T}{2}$ and $T_f = T - \frac{\delta T}{2}$, which leads to

$$\frac{d}{dt}\delta T = -\frac{\Lambda^2}{W} e^{-W/2T} \delta T, \tag{D.21}$$

in the limit $T = T_b^{(0)}/2 \ll W$ and where we are interested in the infinite time i.e, $\delta T \ll T$ behaviour. Here, we recover the standard exponential relaxation expected from Newton's law of cooling

$$\delta T(t) \sim \exp\left(-\frac{\Lambda^2 t}{W} e^{-W/T_b^{(0)}}\right). \tag{D.22}$$

D.3 Equilibration between fractons and external heat bath

Finally, we consider the situation where the fractons are prepared at an initial temperature $T_f^{(0)} \ll T$, where T is the temperature of an external heat bath, to which the temperatures of the composites and dim-2 bosons are pinned. In this scenario, the behaviour of the fractons is governed by Eq. (4.19)

$$\frac{dT_f}{dt} = \frac{4\Lambda^2 T_f^2}{W^2}\left(3\frac{n_b^2}{n_f} + n_b - n_b n_f - n_f^2 - 2n_f^3\right), \tag{D.23}$$

where $n_b = e^{-W/T}$ and $n_f = e^{-W/2T_f}$. As we are interested in the dynamics of fractons prepared in the ground state, in the regime of interest $T_f^{(0)} \ll T$ we find that

$$\frac{dT_f}{dt} \approx \frac{12\Lambda^2 T_f^2}{W^2} e^{-2W/T} e^{W/2T_f}. \tag{D.24}$$

Thus, the fractons display logarithmic heating

$$T_f(t) = -\frac{W/2}{\log\left(\frac{6\Lambda^2}{W}t + b\right) - \frac{2W}{T}}, \tag{D.25}$$

where $b = e^{\frac{2W}{T} - \frac{W}{2T_f^{(0)}}}$. Note that this is the same behaviour encountered in the previous section. However, once $T_f(t) \sim T/2$, we can no longer ignore processes where a boson and a fracton convert into three fractons (channel 3) since $n_b^2 n_f \sim n_b$ at this point. This is in contrast to the previous section, where the fractons had almost equilibrated by the time channel 3 was activated, leading to a logarithmic heating of fractons essentially over the entire equilibration time scale.

Hence, when the composites and dim-2 excitations are coupled to an external heat bath, the logarithmic behaviour of the fractons persists until $T_f(t) \sim T/2$, i.e., over an exponentially long time scale

$$0 \leq t \lesssim \frac{W}{6\Lambda^2} e^{W/T} \tag{D.26}$$

controlled by the temperature of the heat bath, $T \ll W$. Beyond this time scale, however, channel 3 is active, and the dynamics of the fractons are governed by

$$\frac{dT_f}{dt} \approx \frac{4\Lambda^2 T_f^2}{W^2} \left(3\frac{n_b^2}{n_f} + n_b\right), \tag{D.27}$$

with the solution

$$T_f(t) \approx -\frac{W/2}{\frac{2\Lambda^2}{W} e^{-W/T} t + \log\left(3e^{-W/T}\right)}. \tag{D.28}$$

Thus, the fractons first heat up logarithmically slowly, but once a finite density of fractons is established, they display power law heating until they are close to equilibration. Near equilibration, $T_f = T - \delta T$ with $\delta T \ll T$, and the fractons then heat according to

$$\frac{d}{dt}\delta T \approx -\frac{4\Lambda^2}{W} e^{-W/T} \delta T, \tag{D.29}$$

such that the fractons follow the usual Newton's law close to equilibration,

$$\delta T \sim \exp\left(-\frac{4\Lambda^2 t}{W} e^{-W/T}\right). \tag{D.30}$$

Appendix E

Screening in the Dipolar Fermi Gas

We will here treat the different types of screening that occur in the single-species dipolar Fermi gas, adapting the techniques of Ref. [269].

E.1 Dipole-Dipole Screening

We first investigate the ability of the dipoles to screen their interactions with each other. We emphasize that the following is an electrostatic calculation which will not capture e.g. dynamical screening properties of the phase, but an electrostatic calculation of this form is sufficient for our present purposes.

Let us consider a system with an equilibrium density of fermionic dipoles, all with the same orientation p^i, forming a Fermi surface. We then consider adding a static "test dipole" in the p^i direction and seeing how the system responds. In the presence of a perturbing scalar potential ϕ, the potential energy felt by a dipole is $p^i \partial_i \phi$ [81]. Correspondingly, the induced dipole moment density is $-p^j(gp^i\partial_i\phi)$, where g is the density of states of the dipoles at the Fermi surface. Using the form of the potential created by a dipole, $\phi_p(r) = (p \cdot r)/8\pi r$, we can write a self-consistent equation for the potential ϕ as

$$\phi(r) = \phi_{bare}(r) - \int dr' (gp^i\partial_i\phi(r'))\frac{p^j(r_j - r_j')}{8\pi|r - r'|}, \tag{E.1}$$

where $\phi_{bare}(r) = (p \cdot r)/8\pi r$ is the bare potential associated with the test dipole. Integrating by

parts, we obtain

$$\phi(r) = \frac{(p \cdot r)}{8\pi r} - \frac{gp^i p^j}{8\pi} \int dr' \phi(r') \left(\frac{\delta_{ij}}{|r - r'|} - \frac{(r_i - r'_i)(r_j - r'_j)}{|r - r'|^3} \right). \tag{E.2}$$

Taking a Fourier transform, we find

$$\phi(k) = -i\frac{(p \cdot k)}{k^4} - g\phi(k)\frac{(p \cdot k)^2}{k^4}. \tag{E.3}$$

Solving for the potential $\phi(k)$, we have

$$\phi(k) = -i\frac{(p \cdot k)}{k^4 + g(p \cdot k)^2} = -i\frac{pk_p}{k_\perp^4 + gp^2 k_p^2}, \tag{E.4}$$

where k_p is the component of k^i in the p^i direction, and $k_\perp$ is the two-dimensional orthogonal projection. (We drop the k_p^4 term, since it is irrelevant compared to the k_p^2 term at small k.) Converting to the interparticle potential energy for dipoles, $V = p^i \partial_i \phi$, we have

$$V(k) = \frac{(pk_p)^2}{k_\perp^4 + gp^2 k_p^2}. \tag{E.5}$$

We see that, after screening, $V(k)$ remains bounded at $k = 0$, indicating that the long-range interaction has been screened out, leaving only a short-range repulsion between dipoles.

E.2 Screening of Fractons

We now investigate the ability of a Fermi surface of dipoles to screen a fracton, which has a much stronger electric field and potential. The potential of a fracton of charge q takes the form $\phi_q = -qr/8\pi$. The dipoles will still have an induced dipole moment density given by $-p^j(gp^i \partial_i \phi)$, where ϕ is the total potential. Using this information, we can easily modify the self-consistent equation for ϕ from the previous section,

$$\phi(r) = -\frac{qr}{8\pi} - \frac{gp^i p^j}{8\pi} \int dr' \phi(r') \left(\frac{\delta_{ij}}{|r - r'|} - \frac{(r_i - r'_i)(r_j - r'_j)}{|r - r'|^3} \right). \tag{E.6}$$

After a Fourier transform, we obtain

$$\phi(k) = \frac{q}{k^4} - g\phi(k)\frac{(pk_p)^2}{k^4}. \tag{E.7}$$

Solving for the potential $\phi(k)$, we find

$$\phi(k) = \frac{q}{k_\perp^4 + gp^2 k_p^2}, \tag{E.8}$$

where we have once again dropped a k_p^4 term, which is irrelevant at small k. We now reverse the Fourier transform to find the real-space behavior of the potential,

$$\phi(r) = \int \frac{dk_p d^2 k_\perp}{(2\pi)^3} \frac{q}{k_\perp^4 + gp^2 k_p^2} e^{i(k_p r_p + k_\perp \cdot r_\perp)}. \tag{E.9}$$

We first set $r_p = 0$, investigating screening transverse to the dipoles.

$$\begin{aligned}
\phi(r_\perp) &= \int \frac{dk_p d^2 k_\perp}{(2\pi)^3} \frac{q}{k_\perp^4 + gp^2 k_p^2} e^{ik_\perp \cdot r_\perp} \\
&= \frac{q}{2\sqrt{gp^2}} \int \frac{d^2 k_\perp}{(2\pi)^2} \frac{1}{k_\perp^2} e^{ik_\perp \cdot r_\perp} \\
&= \frac{q}{4\pi \sqrt{gp^2}} \log r_\perp.
\end{aligned} \tag{E.10}$$

Similarly, if we set $r_\perp = 0$, studying screening purely along the direction of the dipoles, we obtain

$$\begin{aligned}
\phi(r_p) &= \int \frac{dk_p d^2 k_\perp}{(2\pi)^3} \frac{q}{k_\perp^4 + gp^2 k_p^2} e^{ik_p r_p} \\
&= \frac{q}{8\sqrt{gp^2}} \int \frac{dk_p}{2\pi} \frac{e^{ik_p r_p}}{k_p} \\
&= \frac{q}{16\sqrt{gp^2}} \log r_p.
\end{aligned} \tag{E.11}$$

Directions between $r_\perp$ and r_p will behave similarly, with coefficient interpolating between Eqs. (E.10) and (E.11). In either case, we see that the bare linear potential between fractons has been screened down to a logarithmic interaction (with an anisotropic coefficient). The presence of a dipolar Fermi surface is therefore able to eliminate the issues of "electrostatic confinement" and allow the fractons to be separated much more easily.

Appendix F

Fermi Statistics of Dipoles

In the main text, we have often considered the mobile dipoles of fractons to have fermionic statistics. This is in contrast to some of the simplest lattice models for $U(1)$ fractons [80, 265], in which the dipoles are bosons. However, there is in principle nothing to prevent the dipoles from being fermions. Indeed, some of the previously studied discrete fracton theories featured bound states with fermionic statistics [74].

One can present field theoretic arguments which indicate that fermionic dipoles should be realizable. Furthermore, these arguments will teach us how to go about constructing appropriate lattice models. The primary argument arises from the recently studied "θ terms" which can appear in the action for $U(1)$ tensor gauge theories [272]. These terms have no effect on the gapless gauge mode, but can alter the particle structure of the theory. A θ term will attach electric charge to the magnetic monopoles of the theory. This charge attachment can result in the transmutation of statistics, since electric and magnetic charges pick up phases when moved around each other. As an example of this phenomenon, in Maxwell theory coupled to bosonic charges, adding an appropriate θ term will leave the theory almost invariant, with the exception that the magnetic monopole becomes a fermion [60, 296].

A similar θ term can be added to the scalar charge theory, which has the effect of attaching dipoles to the magnetic monopoles of the theory (which are vector charges) [272]. The dipoles and magnetic monopoles pick up phases when moved around each other, so this attachment procedure can produce the same sort of statistical transformations as in conventional Maxwell theory. By

adding an appropriate θ term, one can convert the dipoles into fermions. (In the discussion of Ref. [272], it was always the monopoles which had their statistics changed. But the electric charge can also have its statistics changed, simply by looking at the problem from the dual perspective.)

At the field theory level, one can conclusively formulate a theory with fermionic dipoles. As mentioned earlier, there has yet to be a concrete lattice model written down with such particles, but the field theory perspective gives an important clue. The θ term in a gauge theory will naturally appear when the charges enter a symmetry protected topological (SPT) phase, protected by time-reversal [60]. In this specific case, the statistics of the dipoles will be transmuted by placing the magnetic vector charges into a bosonic topological insulator phase. By tweaking the dynamics of the "plain-vanilla" lattice models [80, 265], one can drive the monopoles into such a topological insulator state, with the result that the dipoles become fermions.

As an alternative strategy to get fermionic dipoles, one could also consider adapting the strategy of Reference [297]. In conventional Maxwell theory, the ground state wavefunction is written in terms of closed string configurations (*i.e.* a loop gas), and the charges of the gauge field correspond to the endpoints of open strings. In order to modify the statistics of these charges, one can thicken the strings into ribbons. By giving the wavefunction an appropriate sign structure, picking up negative signs for each twist of a ribbon, one can thereby change the charges from bosons to fermions [297]. A similar strategy will likely work for the case of dipoles. By adding extra internal structure to the models, along with an appropriate sign structure, one should be able to turn the dipoles into fermions. Explicitly constructing such a "ribbon"-like wavefunction is left as a task for future work.

Appendix G

Details on Vector Chern-Simons Theories

For completeness, here we review some of the established facts regrading Chern-Simons theories of vector gauge fields before calculating the properties of higher rank Chern-Simons gauge theories.

G.1   Level Quantization

In order to establish the quantization of the level k of the Chern-Simons term (5.30), we consider the thermal partition function

$$\mathcal{Z}[A_\mu] = e^{i\mathcal{S}_{CS}[A_\mu]}, \tag{G.1}$$

by taking time to be Euclidean $\mathbf{S}^1$, parametrized by $\tau \equiv \tau + \beta$, where β is the inverse temperature. As mentioned earlier, the action (5.30) is invariant under $A_\mu \to A_\mu + \partial_\mu \alpha$. Let us consider a large gauge transformation which winds around the circle, with $\alpha = 2\pi\tau/\beta$, under which the temporal part of the gauge field gets shifted by a constant,

$$A_0 \to A_0 + \frac{2\pi}{\beta}. \tag{G.2}$$

Furthermore, we now imagine placing the system on a sphere and placing a magnetic monopole inside the sphere (equivalently, threading a background magnetic flux through the sphere), given by

$$\int_{\mathbf{S}^2} \epsilon^{ij} \partial_i A_j = 2\pi, \tag{G.3}$$

which is the minimum flux allowed by the Dirac quantization condition. Evaluating the Chern-Simons action (5.30) in such a configuration, and with constant $A_0 = a$, we find that

$$\mathcal{S}_{CS} = \frac{k}{2\pi} \int d^3x \, a \left(\epsilon^{ij} \partial_i A_j \right) = ka\beta. \tag{G.4}$$

Hence, under a gauge transformation of the form (G.2), the action transforms as

$$\mathcal{S}_{CS} \to \mathcal{S}_{CS} + 2\pi k, \tag{G.5}$$

and in order for the partition function $\mathcal{Z}[A_\mu]$ to remain gauge invariant, we require that k is quantized to be an integer, $k \in \mathbb{Z}$.

G.2   Ground State Degeneracy on a Torus

Let us consider the Chern-Simons action for the statistical gauge field a

$$\mathcal{S}_{CS} = \frac{m}{4\pi} \int d^3x \, \epsilon^{\mu\nu\lambda} a_u \partial_\nu a_\lambda. \tag{G.6}$$

The equation of motion for the temporal component a_0 (or Gauss' Law) is

$$\epsilon^{ij} \partial_i a_j = 0. \tag{G.7}$$

We now imagine placing this theory on a torus $\mathbf{T}^2 = \mathbf{S}^1 \times \mathbf{S}^1$, with the radii of the two circles R_1 and R_2. On the torus, we can solve the constraint (G.7) by setting

$$a_i = \frac{\tilde{a}_i}{R_i} + \partial_i \Lambda, \tag{G.8}$$

where Λ is periodic on the torus and $\tilde{a}_i$ is spatially constant. Inserting these solutions into the action (G.6), we find that it reduces to

$$\mathcal{S}_{CS} = \frac{m}{4\pi} \int dt \, \epsilon^{ij} \dot{\tilde{a}}_i \tilde{a}_j, \tag{G.9}$$

which identifies $\tilde{a}_i$ as the physical degrees of freedom. The canonical commutation relations follow directly from this action,

$$[\tilde{a}_1, \tilde{a}_2] = \frac{2\pi i}{m}, \tag{G.10}$$

and since the operators $\tilde{a}_i$ are compact, we need to instead consider the algebra of the corresponding gauge-invariant Wilson loop operators,

$$W_i = \exp\left(i \oint_{\gamma_i} dx^j\, \tilde{a}_j \right), \tag{G.11}$$

where γ_i are the two non-contractible loops on the torus. The commutation relations of $\tilde{a}$ imply the algebra

$$W_1 W_2 = e^{2\pi i/m} W_2 W_1, \tag{G.12}$$

the smallest representation of which has dimension m,

$$W_1 \left| n \right\rangle = e^{2\pi i n/m} \left| n \right\rangle, \quad W_2 \left| n \right\rangle = \left| n+1 \right\rangle. \tag{G.13}$$

Thus, the ground state degeneracy of the Chern-Simons action (G.6) on a torus is m.

G.3   Edge Modes of Chern-Simons Theories

Let us consider the Chern-Simons action (5.36) which describes the FQHE state at filling fraction $\nu = 1/m$,

$$\mathcal{S}_{CS} = \frac{m}{4\pi} \int d^3x\, \epsilon^{\mu\nu\lambda} a_\mu \partial_\nu \lambda. \tag{G.14}$$

In order to study the edge excitations of this system, we imagine placing it on a semi-infinite plane with a boundary at $y = 0$ such that the quantum Hall fluid lives at $y < 0$ with vacuum at $y > 0$. Under a gauge transformation $a_\mu \to a_\mu + \partial_\mu \alpha$, the action transforms as

$$\mathcal{S}_{CS} \to \mathcal{S}_{CS} + \frac{m}{4\pi} \int_{y=0} dx dt\, \alpha \left(\partial_t a_x - \partial_x a_t \right), \tag{G.15}$$

i.e., it is gauge-invariant only up to a surface term. Thus, we require additional degrees of freedom living at the edge in order to have a fully gauge-invariant theory.

In order to deduce these additional degrees of freedom, we consider the variation of the action (5.36) in the presence of a boundary,

$$\delta\mathcal{S}_{CS} = \frac{m}{4\pi} \int d^3x\, \epsilon^{\mu\nu\lambda} \left(\delta a_\mu f_{\nu\lambda} + \partial_\mu \left(a_\nu \delta a_\lambda \right) \right), \tag{G.16}$$

where $f_{\mu\nu} = \partial_\mu a_\nu - \partial_\nu a_\mu$. Thus, we see that minimizing the action leads to the required equation of motion $f_{\nu\lambda} = 0$ (equivalently, the zero flux condition) only if we can set the second term to zero. We can achieve this by setting $a_t = 0$ at the boundary $y = 0$.

Now, in order to derive the action for the boundary degrees of freedom, we extend this boundary condition into the bulk i.e., we fix the gauge $a_t = 0$ in the bulk. Then, the constraint imposed by the gauge-fixing condition remains

$$\epsilon^{ij}\partial_i a_j = 0, \tag{G.17}$$

which is solved in terms of a compact scalar field φ by taking $a_i = \partial_i \varphi$. Inserting this into the action $\mathcal{S}_{CS}$, with $a_t = 0$, we obtain the edge action

$$\mathcal{S}_{CS} = \int_{y=0} dx dt\, \partial_t \varphi \partial_x \varphi. \tag{G.18}$$

This is, however, not the most general action we could write down at the edge since we can add energetic terms which respect the shift symmetry $\varphi \to \varphi+$ constant. A mass term $\sim \varphi^2$ term is prohibited (even in the absence of U(1) symmetry) since the field φ is non-local, as evidenced by the commutation relation

$$[\varphi(x), \varphi(x')] = \frac{i\pi}{m}\mathrm{sgn}(x - x'). \tag{G.19}$$

Including the lowest order spatial derivatives, we find the general edge action for a chiral Chern-Simons theory

$$\mathcal{S}_{\mathrm{edge}} = \int_{y=0} dx dt\, \left(\partial_t \varphi \partial_x \varphi - v\partial_x \varphi \partial_x \varphi\right), \tag{G.20}$$

where v is a non-universal velocity which depends on the microscopic details of the edge. The equation of motion satisfied by φ is

$$\partial_t \partial_x \varphi - v\partial_x \partial_x \varphi = 0. \tag{G.21}$$

Re-stated in terms of the field $\rho = 1/(2\pi)\partial_x \varphi$,

$$(\partial_t - v\partial_x)\rho = 0, \tag{G.22}$$

we find the equation governing a chiral density wave propagating along the boundary with velocity v. By coupling the action $\mathcal{S}_{\mathrm{CS}}$, one can show that ρ is indeed the charge density along the edge and that the operator describing electrons at the boundary is

$$\Psi =: e^{im\varphi} : \tag{G.23}$$

where the colons denote normal ordering. We refer the reader to the excellent reviews [23, 147] for a more comprehensive discussion of these boundary CFTs.

Appendix H

Details on Generalized Chern-Simons Theories

Here, we derive some of the technical details regarding higher rank U(1) Chern-Simons theories described by a traceless symmetric rank 2 tensor. The action for such a theory is

$$\mathcal{S}_{gCS}[\tilde{A}_{ij}, \phi] = -\frac{\theta}{4\pi^2} \int d^3x \, \phi \epsilon^{bi} \partial_i \partial_j \tilde{A}_b{}^j + \frac{\theta}{8\pi^2} \int d^3x \, \epsilon^{bi} \dot{\tilde{A}}_{ij} \tilde{A}_b{}^j. \tag{H.1}$$

A remark regarding the dimensions of these fields: in units where $\hbar = c = 1$, $\tilde{A}_{ij}$ has the same units as those of a vector gauge field A_i,

$$[\tilde{A}_{ij}] = [A_i] = L^{-1}, \tag{H.2}$$

where L denotes length. However, while the temporal component of a vector gauge field also has dimensions L^{-1}, the Lagrange multiplier field ϕ has dimension

$$[\phi] = L^0. \tag{H.3}$$

Since under a gauge transformation ϕ transforms as $\phi \to \phi + \dot{\alpha}$, this implies that the gauge parameter α has dimensions of length,

$$[\alpha] = L^1, \tag{H.4}$$

consistent with the gauge transformation and dimension of $\tilde{A}_{ij}$.

H.1   Quantization of θ

Recall that the magnetic flux vector $B^j = \epsilon^{ib} \partial_i \tilde{A}_b{}^j$ in the higher rank theory (5.58) is one-dimensional, moving only transversely i.e., on a square lattice, B^x may only move in the y-direction.

If we now place the system on a sphere, we can imagine threading a flux through this sphere. The minimum such flux allowed by the Dirac quantization condition is

$$\int_{\mathbb{S}^2} B^j = 2\pi \hat{x}^j, \tag{H.5}$$

where $\hat{x}^j$ simply reflects the vector nature of the magnetic flux in this theory.

Generalizing the discussion of level quantization in Appendix G.1, we consider the thermal partition function

$$Z_{gCS}[\tilde{A}_{ij}, \phi] = e^{iS_{gCS}[\tilde{A}_{ij}, \phi]} \tag{H.6}$$

by taking time to be Euclidean $\mathbf{S}^1$, parametrized by $\tau \equiv \tau + \beta$, where β is the inverse temperature. As established earlier, the theory (5.58) is invariant under the gauge transformation $\phi \to \phi + \dot{\alpha}$. Since the field ϕ acts as a Lagrange multiplier and has no dynamics of its own, its role in the theory is analogous to that of A_0, the temporal component of a vector gauge field. However, as mentioned earlier, ϕ is dimensionless and we should instead consider a transformation of $\partial_i\phi$, which has the same dimensions as A_0: $[\partial_i\phi] = L^{-1}$. We hence consider a large gauge transformation

$$\alpha(\vec{x}, t) = \frac{2\pi\tau}{\beta}(x_1 + x_2), \tag{H.7}$$

under which $\partial_i\phi$ transforms as

$$\partial_i\phi \to \partial_i\phi + \frac{2\pi}{\beta}\hat{x}_i. \tag{H.8}$$

Evaluating the generalized Chern-Simons action (5.58) on a configuration specified by the flux threading condition (H.5) and with constant $\partial_i\phi = \Phi\hat{x}_i$, we find

$$S_{gCS} = -\frac{\theta}{4\pi^2}\Phi\hat{x}_j \int B^j = -\frac{\theta}{2\pi}\Phi\beta. \tag{H.9}$$

Under the large gauge transformation specified by Eq. (H.8), the action shifts by a constant

$$S_{gCS} \to S_{gCS} - \theta, \tag{H.10}$$

and hence, in order for the partition function to be gauge-invariant, the coefficient θ must be quantized in units of 2π,

$$\theta = 2\pi k, \quad k \in \mathbb{Z}. \tag{H.11}$$

H.2   Ground State Degeneracy

The generalized Chern-Simons action for an emergent FQH state of dipoles at filling fraction $\nu = 1/m$ is

$$\mathcal{S}_{gCS} = -\frac{m}{2\pi} \int d^3x\, \chi\, \epsilon^{bi} \partial_i \partial_j a_b^{\,j} + \frac{m}{4\pi} \int d^3x\, \epsilon^{ib} \dot{a}_{ij} a_b^{\,j}, \tag{H.12}$$

where a_{ij} is a traceless symmetric tensor. On a closed manifold, S_{gCS} is gauge-invariant under

$$a_{ij} \rightarrow a_{ij} + \left(\partial_i \partial_j - \frac{1}{2}\delta_{ij}\delta^2\right)\alpha, \qquad \chi \rightarrow \chi + \dot{\alpha}, \tag{H.13}$$

for arbitrary gauge parameter $\alpha(\vec{x}, t)$. The Gauss' law constraint for this theory, enforced by the Lagrange multiplies field χ, is

$$-\frac{m}{2\pi}\epsilon^{bi}\partial_i\partial_j a_b^{\,j} = 0. \tag{H.14}$$

We note that the two independent components of a_{ij} are combined into one canonically conjugate pair, with commutation relations

$$[a_{xx}(\vec{x}), a_{xy}(\vec{x}')] = -\frac{i\pi}{m}\delta(\vec{x} - \vec{x}'). \tag{H.15}$$

Due to the Gauss' law constraint on a_{ij}, the theory is fully constrained and there are no local degrees of freedom.

We now imagine placing this system on a torus $\mathbf{T}^2 = \mathbf{S}^1 \times \mathbf{S}^1$, with the radii of the two circles R_1 and R_2. On an $R_1 \times R_2$ torus, we can satisfy the Gauss' law constraint (H.14) by setting the two conjugate variables to

$$a_{xx} = -a_{yy} = \frac{a(t)}{R_1 R_2} + \frac{1}{2}(\partial_x^2 - \partial_y^2)\Lambda, \qquad a_{xy} = a_{yx} = \tilde{a}(t) + \partial_x \partial_y \Lambda, \tag{H.16}$$

where $\Lambda(\vec{x}, t)$ is an arbitrary continuous, periodic function on the torus. Note that a and $\tilde{a}$ only describe the topological contribution to the action, since we have separated them from the gauge-redundant part Λ. Inserting these solutions into the action (H.12), we find

$$\mathcal{S}_{gCS} = \frac{m}{\pi} \int dt\, \dot{a}(t)\tilde{a}(t). \tag{H.17}$$

This theory has a ground state degeneracy [273, 298]

$$\text{GSD} = 2m. \tag{H.18}$$